DEFECTIVE INTERFERING PARTICLES OF PARAINFLUENZA VIRUS SUBTYPE 5 AND INTERFERON INDUCTION

John A. L. Short

A Thesis Submitted for the Degree of PhD
at the
University of St Andrews

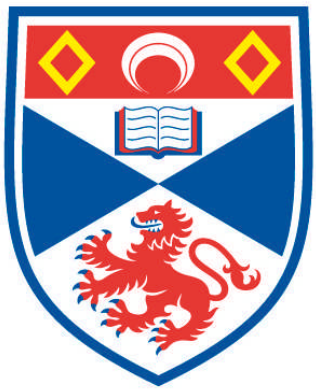

2015

Defective Interfering Particles of Parainfluenza Virus subtype 5 and Interferon Induction

John A L Short

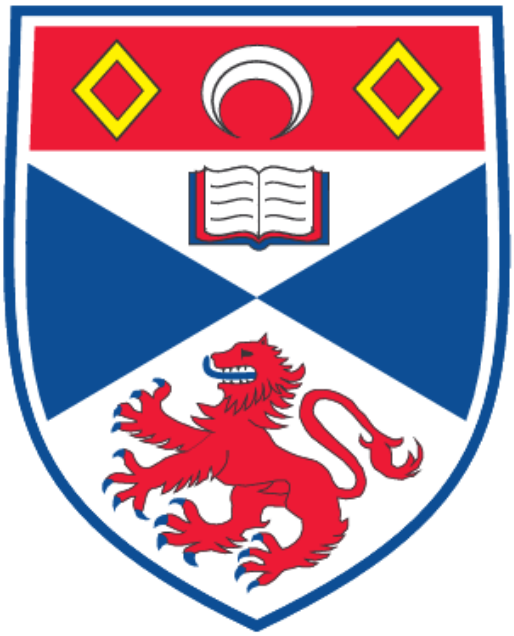

This thesis is submitted for the degree of PhD
at the
University of St Andrews

October 2014

ABSTRACT

The innate immune response is the first line of defence against virus infection. Cells contain a diverse array of pathogen recognition receptors (PRRs) that are able to recognise multiple pathogen associated molecular patterns (PAMPS) that present themselves during virus infection. The RIG-I (Retinoic acid inducible–gene-I) and MDA5 (melanoma differentiation-associated gene 5) PRRs detect specific viral RNA ligands and subsequently induce the expression of the cytokine Interferon-β (IFN-β). IFN-β is secreted, acting on the infected cell and neighbouring uninfected cells to generate an antiviral state that is hostile to virus transcription, replication and dissemination, whilst also orchestrating adaptive immune responses. Given IFN-βs crucial cellular antiviral role, understanding its induction is of great importance to developing future antiviral drugs and vaccine strategies.

Using A549 reporter cells in which GFP expression is under the control of the IFN-β promoter, we show that there is a heterocellular response to parainfluenza virus 5 (PIV5) and infection with other negative sense RNA viruses. Only a limited number of infected cells are responsible for IFN-β induction. Using PIV5 as a model, this thesis addresses the nature of the PAMPs that are responsible for inducing IFN-β following PIV5 infection. The previous work has shown that PIV5 Defective Interfering particle (DI) rich virus preparations acted as a better inducer of IFN-β compared to DI poor stocks. DIs are incomplete virus genomes produced during wild-type virus replication as a result of errors in the viral polymerase. To investigate this further, A549 Naïve, MDA5/RIG-I/LGP2 Knock down reporter cells were infected with PIV5 W3 at a low MOI to examine the inverse correlation of NP and GFP of DIs generated during virus replication and not from the initial infection. GFP+ve cells were cell sorted, and using QPCR it was found that cells that have the IFN-β promoter activated contain large amounts of DIs relative to GFP-ve cells. This data supports the Randall group's findings that DIs generated during errors of wild-type replication by the viral RNA polymerase are the primary PAMPs that induce of IFN-β, as opposed to PAMPs being generated during normal wild-type virus replication.

1. Candidate's declarations:

I, John A L Short hereby certify that this thesis, which is approximately 45,000 words in length, has been written by me, and that it is the record of work carried out by me, or principally by myself in collaboration with others as acknowledged, and that it has not been submitted in any previous application for a higher degree.

I was admitted as a research student in Oct, 2009 and as a candidate for the degree of **Doctor of Philosophy (PhD) in Molecular Virology;** in Oct, 2014; the higher study for which this is a record was carried out in the University of St Andrews between 2009 and 2014.

Date Signature of candidate ..

2. Supervisor's declaration:

I hereby certify that the candidate has fulfilled the conditions of the Resolution and Regulations appropriate for the degree of PhD in the University of St Andrews and that the candidate is qualified to submit this thesis in application for that degree.

Date Signature of supervisor

Prof. R. E. Randall

3. Permission for publication:

In submitting this thesis to the University of St Andrews I understand that I am giving permission for it to be made available for use in accordance with the regulations of the University Library for the time being in force, subject to any copyright vested in the work not being affected thereby. I also understand that the title and the abstract will be published, and that a copy of the work may be made and supplied to any bona fide library or research worker, that my thesis will be electronically accessible for personal or research use unless exempt by award of an embargo as requested below, and that the library has the right to migrate my thesis into new electronic forms as required to ensure continued access to the thesis. I have obtained any third-party copyright permissions that may be required in order to allow such access and migration, or have requested the appropriate embargo. The following is an agreed request by candidate and supervisor regarding the publication of this thesis:

PRINTED COPY

A) No embargo on print copy

ELECTRONIC COPY

A) No embargo on electronic copy

Date Signature of candidate

Date Signature of/supervisor

CONTENTS

ACKNOWLEDGMENTS

Wow, I appear to have submitted! When I started this journey I was naïve, ignorant scientist, and now at this juncture, I'm a slightly less naïve and ignorant scientist. If there is one thing this PhD has taught me, it is of how little I know compared to the gargantuan global interweb of scientific knowledge and understanding. So I first start off by thanking my supervisor, Rick Randall. I've had many ups and downs, a bit like a rollercoaster. Consistency in emotion, stability and output has been hard, but all throughout the good times, but especially through the bad times, Rick has been there. I haven't always been honest with myself or others when it comes to how good or bad things are, but Rick has always enabled me to confront myself and the science. Rick is always cool, calm and collected, able to look at the big picture and past all the weird stuff that is life. I am forever in his debt.

I thank also all those in the Randall group past and present for putting up with me and answering all my daft questions. In particular I thank Lena Andrejeva, Dan Young, Bernie Precious, Dave Jackson, Marian Killip, Claudia Hass, Shu Chen and Hanna Norsted. I thank Fiona Tulloch of the Martin Ryan group and Matt Smith of the David Jackson group for their help with QPCR. I also thank Jean Johnston and Margaret Wilson, always in control as the administrators of the BBSRC programme at the University of St Andrews.

I thank the Goodbourn group at St George's Hospital Medical School, for hosting me for three months. I am indebted in Craig Ross and Steve Goodbourn for their help in acquiring the reagents for RT-QPCR, developing protocols, allowing me to use their cell-sorting machine and for helping me understand the science!

I thank my family, Mum, Dad and Cat and Lizzie, and all the Short's and MacLeish's. I thank them for their continued love and support. They may not always know what I'm talking about, but they are always there for me.

Finally, I thank all those at St Andrews who have made this one of the most fun places to live and enjoy myself as I worked through this PhD. From the Whip Inn Boys 6 aside football team, what amazing times battling people both young or old and experienced and still coming out on top (at least some of the time, and winning the league a few times as well). I thank all those at the BMS past and present, in particular Lee, Andy G., Steve Welch, Ben and Forbes, Beryl, the Richard Elliot group, Andri, Stacy, Rob, Gillian, C David Owen, Claire S. (thanks for reading all of the thesis!), Laura x2, Chris x2 and those outside the BMS, Joe Kenworthy, Myles and everyone else I've missed out.

This work was supported by the BBSRC.

ABBREVIATIONS

%	Percentage
°C	Degrees Celsius
5’-ppp	5’-triphosphate
ADP	Adenosine diphosphate
ATP	Adenosine triphosphate
Bp	Base-pairs
BUNV	Bunyamwera virus
CARDs	Caspase activation and recruitment domains
CBP	CREB-binding protein
CREB	cAMP-responsive-element-binding protein
CTD	C-terminal Domain
DI	Defective interfering particle
DMEM	Dulbecco’s modified Eagle’s medium
DNA	Deoxyribonucleic acid
DNA-AGE	DNA agarose gel electrophoresis
dNTPs	Deoxynucleotide Triphosphates
ds	Double stranded
dsRNA	Double stranded RNA
DTT	Dithiothreitol
ECACC	European Collection of Cell Cultures
ECMV	Encephalomyocarditis virus
EDTA	ethylenediaminetetraacetic acid
eIF2α	Eukaryotic translational initiation factor 2α
F	Fusion protein
FCS	foetal calf serum
G	Guanosine

GAPDH	Glyceraldehyde 3-phosphate dehydrogenase
GAS	Gamma activated sequence
GFP	Green fluorescent Protein
GTP	guanosine triphosphate
HEK	Human embryonic kidney cells
Hel	Helicase
Hep2	Human cervical epithelial cells
HIV	Human immunodeficiency Virus
HN	haemagglutinin-neuraminidase
HSV	Herpes Simplex Virus
IFN	Interferon
IFNAR	Type I IFN receptor
IFNGR	Type II IFN receptor
IkB	Inhibitor of NF-kB
IKK	IκB kinase complex
IPS-1	IFN-β promoter stimulator 1
IRF	IFN regulatory factor
ISG56	Interferon stimulated gene 56
ISGF3	interferon-dependent transcription factor 3
ISGs	Interferon Stimulated Genes
ISRE	IFN stimulated response element
JAK	Janus Kinase
KD	Knock down
L	Large protein
LB	Luria-Bertani
Le	Leader
LGP2	Laboratory of genetics and physiology-2
Lys	Lysine

M	Matrix protein
MAVS	Mitochondrial antiviral signalling protein
MDA5	Melanoma differentiation-associated gene 5
MDCK	Canine Kidney cells
MEFs	Murine embryonic fibroblasts
MeV	Measles virus
MHV	Murine hepatitis virus
MOI	Multiplicity of Infection
mRNA	Messenger RNA
MuV	Mumps virus
NDV	Newcastle Disease Virus
NEMO	(NF-κB essential modulator)
NF-kB	Nuclear factor kappa B
NLR	Nucleotide-binding domain and leucine rich repeat containing family
NNSVs	Negative strand RNA viruses
NOD2	Nucleotide-binding oligomerization domain-containing protein
NP	Nucleoprotein
Nt	Nucleotide
OAS	Oligoadenylate synthetase
P	Phosphoprotein and
p.i.	Post-infection
PAMPs	Pathogen Associated Molecular Patterns
PBS	Phospho-buffered saline
pDCs	Plasmoidal dendritic cells
PE	Phycoerythrin
Pfu	Plaque forming units
PIV2	Parainfluenza virus subtype 2
PIV3	Parainfluenza virus subtype 3

PIV5	Parinfluenza virus subtype 5
PKR	Protein Kinase R
poly(I:C)	Polyinosinic: polycytidylic acid
PPIA	Peptidylprolyl isomerase A
PRRs	Pathogen Recognition Receptors
RIG-I	Retinoic acid inducible–gene I
RNA	Ribonucleic acid
RNase L	Endoribonuclease L
RSV	Respiratory Syncytial Virus
SDHA	Succinate dehydrogenase complex, subunit A
SDS-PAGE	Sodium dodecyl sulphate - polyacrylamide gel electrophoresis
SeV	Sendai virus
SH	small hydrophobic protein
SH2	Src homology 2 domains
shRNA	Short hairpin interfering RNA
siRNA	Small interfering RNA
SOCS	Suppressors of cytokine signalling
ss	Single stranded
SSC	Side scatter
ssRNA	Single Stranded RNA
STAT	Signal Transducers and Activators of Transcription
STING	stimulator of interferon genes
SUMO	Small Ubiquitin-like Modifier
SV5	Simian virus 5
TAK1	Transforming growth factor beta-activated kinase 1
TANK	TRAF family member-associated NF-kappa B activator
TBK	TANK-binding kinase
TLRs	Toll-Like Receptors

PIV5	Parainfluenza virus subtype 5
TNF	Tumour necrosis factor
TPR	Tetratricopeptide repeat
Tr	Trailer
TRAF6	TNF receptor associated factor
TRIM25	Tripartite motif-containing protein 25
Tyk1	Tyrosine kinase 1
VISA	Virus induced signaling adapter
VM	Von Magnus
VSV	Vesticular Stomatitis Virus
Wt	Wild-type
ZVAD	Z-VAD-FMK caspase family inhibitor

1. INTRODUCTION

1.1. Interferon and the Antiviral State

1.1.1. Overview of the importance of Interferon in innate immunity

Innate immunity is the first line of defence to virus infection, consisting of a diverse array of extracellular and intracellular defences. The innate intracellular immune response acts to prevent or slow virus dissemination, and to aid the adaptive response to clear the virus infection. The host cell contains a variety of pathogen recognition receptors (PRRs) that are able to recognise multiple features of the virus, pathogen associated molecular patterns (PAMPs) that are present during infection, and discriminate between host and viral patterns (Janeway, 1989) Two such PRRs which are the main study of this thesis are retinoic acid inducible gene-I (RIG-I) and melanoma differentiation-associated gene 5 **(**MDA5**)**, which recognise viral RNA ligands (**Figure 1**). Upon the sensing of viral PAMPs, the PRRs mediate the rapid induction of interferon (IFN) via the activation of a signal transduction cascade. The signal transduction cascade goes through the signalling platform IFN-β promoter stimulator 1 (IPS-1/MAVS/CARDIF), which subsequently recruits the IFN transcription factors IFN regulatory factor 3 (IRF3) and nuclear factor kappa-light-chain-enhancer of activated B cells (NF-κB). The IFN transcription factors translocate to the nucleus and induce IFN. IFN is secreted by the cell and binds to the IFN receptor of neighbouring uninfected cells. This induces the expression of IFN stimulated genes (ISGs), which target various aspects of virus entry, replication, assembly and egress from the cell. The induction of IFN and the subsequent production of ISGs consequently generates a cellular antiviral state that is hostile to virus infection, transcription, replication and assembly.

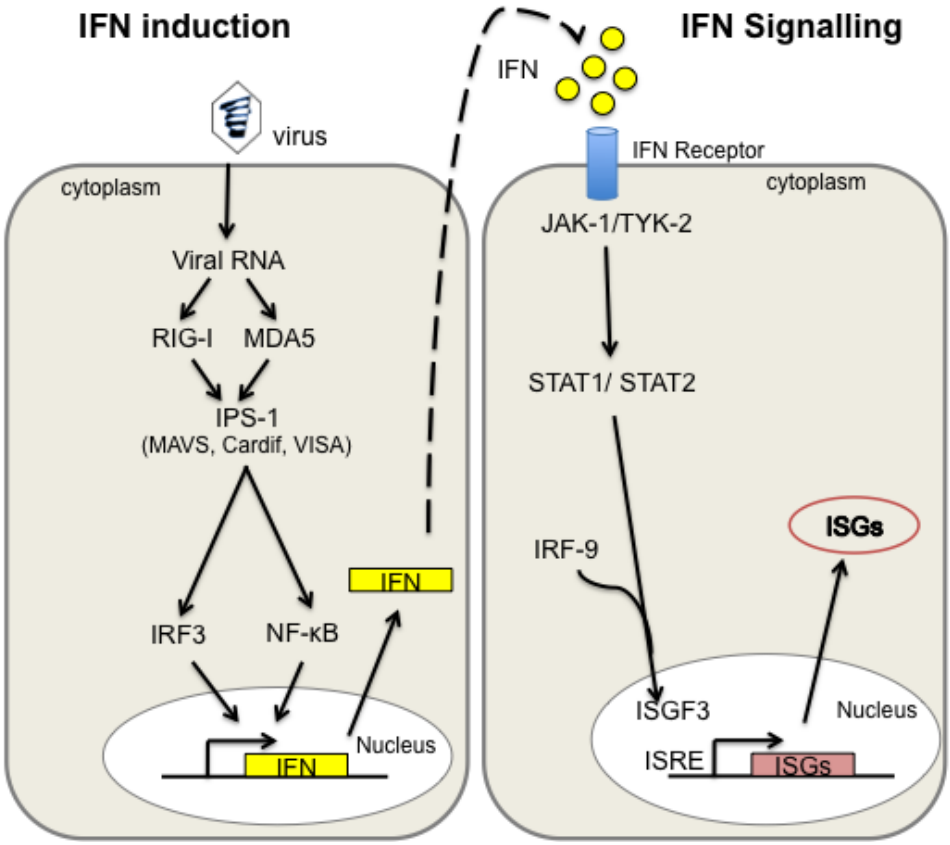

Figure 1. Overview of the IFN system

IFN induction:

Viral RNA, generated in the cytoplasm by uncoating, transcription or replication, activates the RNA helicases MDA5 and RIG-I. MDA5 and RIG-I are both activated by dsRNA, whilst RIG-I can also be activated by RNA molecules with 5'-ppp triphosphates. Both helicases have N-terminal CARD domains that recruit the adaptor IPS-1/CARDIF/VISA/MAVS. This adaptor, in turn, acts as a scaffold to recruit signalling components that feed into either the IRF3 or the NF-kB pathways. Once activated, IRF3 and NF-κB enter the nucleus, forming an enhancesome with other transcription factors. This enhancesome binds to the IFN promoter, leading to the expression of IFN and its subsequent secretion from the cell.

IFN Signalling:

The JAK/STAT IFN signaling pathway is initiated by IFN-α/β binding to the type I IFN receptor. This leads to the activation of the receptor associated tyrosine kinases JAK1 and Tyk2, which phosphorylate STAT1 on tyrosine 701 and STAT2 on tyrosine 690. Phosphorylated STAT1 and STAT2 interact strongly with each other by recognizing SH2 domains, and the stable STAT1/STAT2 heterodimer is translocated into the nucleus, where it interacts with the DNA-binding protein IRF9. The IRF9/STAT1/STAT2 heterotrimer is called ISGF3, and it binds to the ISRE in target promoters, subsequently inducing the expression of ISGs.

See text for details and references.

Figure modified from an original figure provided by Andri Vasou, University of St Andrews.

Types of Interferon

IFNs are a family of cytokines that act as the “gatekeepers” of innate and adaptive immunity, orchestrating intracellular and extracellular antiviral immune responses. Currently, three groups of IFN have been identified, Type I, Type II and Type III (Fontana & Bankamp, 2008; Pestka & Krause, 2004; Randall & Goodbourn, 2008)). Type I IFNs were the first to be identified (Isaacs & Lindenmann, 1957), which include and IFN-α (13 subtypes) and IFN-β (one subtype). IFN-α is produced predominantly in plasmoidal dendritic cells (pDCs) whereas IFN-β, the main study of this thesis, is produced in all nucleated cells. Other less defined Type I IFNs are IFN-ω, -ε, -τ, -δ, –κ and –o. Type II and Type III IFNs are poorly characterized compared to IFN-α/β. Type II IFNs consists of one member, IFN-γ, that is produced by mitogenically activated T-cells or Natural Killer cells (Reviewed in (Schoenborn & Wilson, 2007). Type III IFNs (IFN-λ) in humans include IFN-λ1, -λ2, –λ3 and –λ (Choppin & Stoeckenius, 1964). IFN-λ is produced in a variety of cell types similar to IFN-α/β and acts in concert with IFN-α/β mediated responses. The essential role of IFN-α/β and IFN-γ has been demonstrated by murine *in vivo* studies in which the cell surface receptors, Type I IFN receptor (IFNAR) and Type II IFN receptor (IFNGR) have been knocked down (Broek *et al.*, 1995; Hwang *et al.*, 1995; Kamijo *et al.*, 1993; Van den Broek *et al.*, 1995). These IFNAR and IFNGR deficient mice are highly sensitive to virus infection compared to wild type mice, despite IFNAR and IFNGR deficient mice displaying adaptive immune responses.

1.1.2. The detection of Viral PAMPs by the PRRs

The intracellular innate immune response consists of an array of cell surface, cytosolic and endosomal PRRs that recognise a variety of viral PAMPs that leads to

the subsequent induction of IFN-α/β. It is important to have multiple systems of virus recognition so that the cell can initiate an antiviral response to the different temporal stages and cellular localisations of virus infection, replication and assembly. In addition, multiple mechanisms of PAMP detection enables the host cell to respond to novel virus challenge, caused by the mutation and alteration of viral PAMPs over time. A multisensory approach further confers an advantage to the host cell being able to respond if the virus possesses evasion strategies to a particular IFN-α/β induction pathway, IFN-α/β signalling pathway or to a particular ISG. Viral nucleic acids are the main source of PAMPs that are recognised by intracellular PRRs. Important PRRs that recognise viral nucleic acids are the Toll-Like-Receptors (TLRs) and Nucleotide-binding oligomerization domain-containing protein-2 (NOD2). Other receptors are also important, such as RIG-I-like-receptors and gamma interferon activation site elements, but these are beyond the focus and scope of this thesis.

TLRs are a family of Type I transmembrane glycoproteins that detect a diverse array of pathogens including ssRNA, dsRNA and dsDNA genomic viruses, gram-positive and gram-negative bacteria and fungi. IFN-α/β induction by the TLRs have been extensively reviewed in the literature (Akira *et al.*, 2006; Hornung *et al.*, 2008; Jensen & Thomsen, 2012; Kawai & Akira, 2011; Kumar *et al.*, 2011; Lester & Li, 2014; Mikula & Pastoreková, 2010; O'Neill & Bowie, 2010; Takeda & Akira, 2004; Yamamoto & Takeda, 2010). Many viruses use endosomes to enter the cell and uncoat their genome. Endosomal TLRs such as TLR7, -8, -9 and -3, are important for detecting viral nucleic acids and inducing IFN-α/β, without the need for virus entry and replication in the cytosol of the host cell.

NOD2 is expressed in the cytosol of myeloid derived cells, dendritic cells and intestinal epithelial cells (Gutierrez et al., 2002; Ogura et al., 2001; 2003). NOD2 has previously been associated with the detection of peptidoglycan components from

gram-positive and gram-negative bacteria. NOD2 has recently been shown to bind to viral ssRNA, activating the IRF3-dependent induction of IFN-β following infection by respiratory syncytial virus (RSV), vesticular stomatitis virus (VSV) and influenza A virus (Sabbah et al., 2009). Following recognition of their respective viral PAMPs, the TLRs and NOD2 consequently activate signal transduction pathways that lead to the induction of IFN-α/β and the generation of an antiviral state.

1.1.3. RIG-I, MDA5 and LGP2 mediated induction of IFN

The primary focus of this thesis are the roles of the intracellular PRRs RIG-I, MDA5 and Laboratory of Genetics and Physiology 2 (LGP2) in the detection of negative sense RNA genome viruses. RIG-I and MDA5 are localised in the cytosol of all nucleated cells in humans (Yoneyama *et al.*, 2004; 2005). In unstimulated host cells, RIG-I and MDA5 are expressed at low basal levels to facilitate an immediate response upon the presentation of viral PAMPs. The viral PAMP sensing mechanisms of RIG-I and MDA5 have been extensively reviewed in the literature and will be briefly described (Brennan & Bowie, 2010; Gerlier & Lyles, 2011; Kumar *et al.*, 2011; Luo *et al.*, 2013; Matsumiya *et al.*, 2011; Mogensen, 2009; O'Neill & Bowie, 2010; Onomoto *et al.*, 2010; Randall & Goodbourn, 2008; Wilkins & Gale, 2010). Although RIG-I and MDA5 share a similar domain architecture (**Figure 2**), RIG-I and MDA5 recognize distinct viral RNA structures. RIG-I recognizes short (< 1 kb) double-stranded RNAs (dsRNAs), 5'-triphosphate (5'-ppp) RNAs and RNAs with complex secondary structures (Hornung *et al.*, 2006; Loo *et al.*, 2008). MDA5 detects long dsRNAs (> 1 kb) and "non-self" 2'-O-methylation deficient RNAs (Kato *et al.*, 2006; 2008; Loo *et al.*, 2008; Züst *et al.*, 2011a).

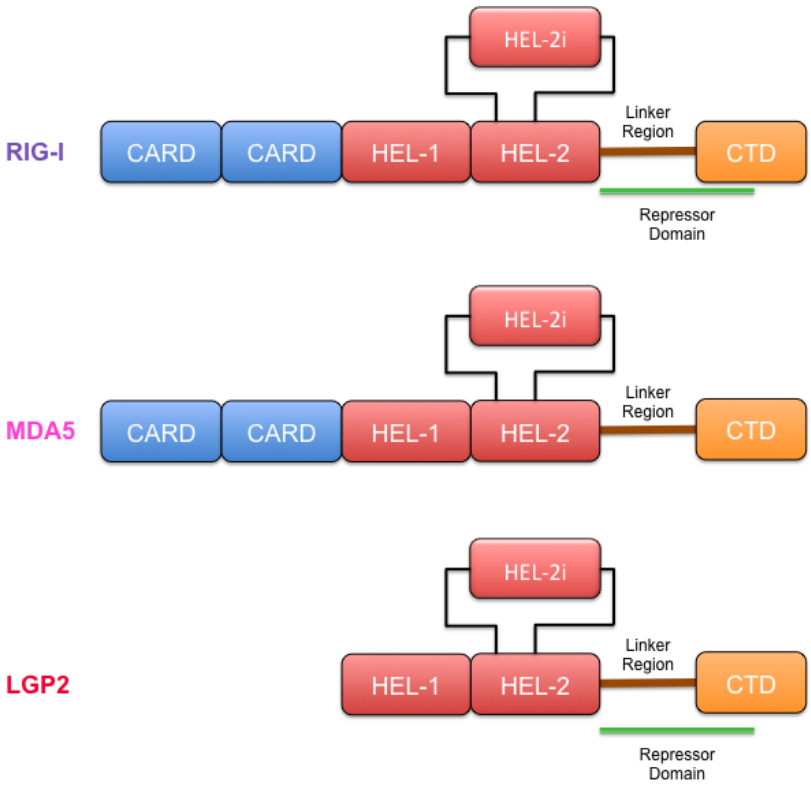

Figure 2. The domain structure of RIG-I, MDA5 and LGP2

RIG-I and MDA5 comprise of two N-terminal caspase activation and recruitment domains (CARDs) fused to a DExD/H-box RNA helicase domain. The RIG-I, MDA5 and LGP2 RNA helicase domain) share a similar architecture, consisting of two subdomains, Hel-1 and Hel-2. Hel-1 and Hel-2 create at their interface an active site for ATP binding and hydrolysis, as well as jointly forming an extended RNA-binding surface. The Hel-2 subdomain contains a family-specific large insertion Hel-2i, which regulates the CARDs of RIG-I and MDA5. A linker region connects the RNA helicase domain to the C-terminal domain (Luo *et al.*, 2011; Saito *et al.*, 2007; Yoneyama *et al.*, 2005). The CTD and linker region of RIG-I and LGP2, but not MDA5, contain a repressor domain (Saito *et al.*, 2007), refer to main text for details. Upon virus infection RIG-I and MDA5 CARDs interact with the downstream CARDs located on the signalling platform IPS-1, leading to the induction of IFN-α/β.

Figure adapted from (Schlee, 2013).

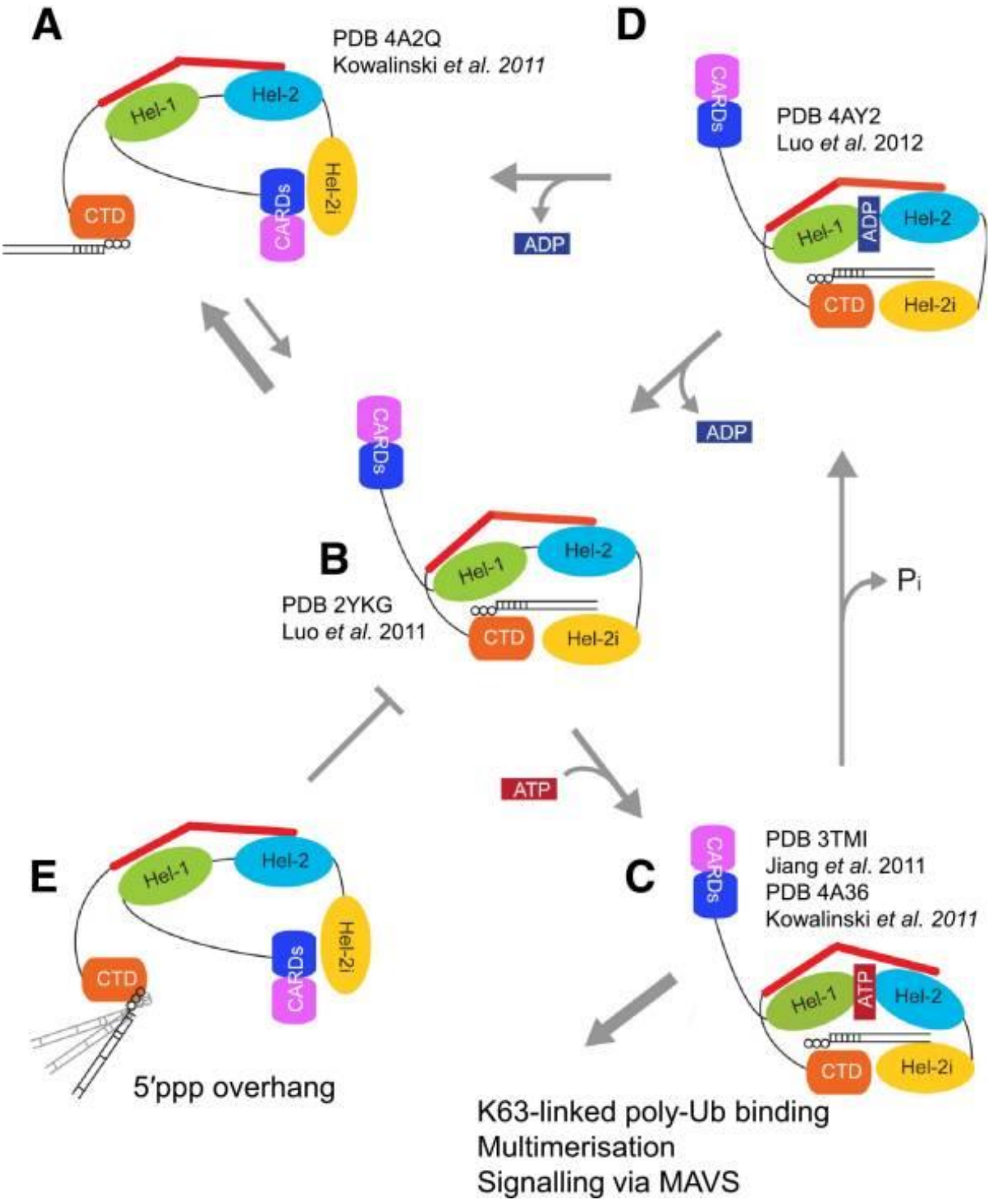

Figure 3. A structure-based model of RIG-I activation.

A. In the autorepressed state, RIG-I CARDs are sequestered by the repressor domain mediating CARD binding to the Hel-2i domain. RIG-I is activated by blunt-ended 5'-ppp dsRNA binding to the CTD (Kowalinski *et al.*, 2011) .

B. The CTD-bound 5'-ppp dsRNA interacts with the helicase domains Hel-1 and Hel-2i, but not Hel-2, leading to displacement of the CARDs bound to Hel-2i. The CARDs are now available for downstream interactions with IPS-1. In the absence of ATP, the RIG-I active state could revert to the autorepressed state (**A**) (Luo *et al.*, 2011).

C. ATP binds at the interface of Hel-1 and Hel-2, stabilizing the RIG-I conformation structure (Jiang *et al.*, 2011; Kowalinski *et al.*, 2011). ATP hydrolysis facilitates the binding of viral dsRNA to the RIG-I helicase domain.

D. Following ATP hydrolysis and phosphate release, RIG-I changes conformation to a viral RNA and ADP bound transition state (Luo *et al.*, 2011). This semi-open conformation is similar to the nucleotide free state **B,** whereupon ADP release, transition state **D** most likely reverts to **B,** rather than immediately reverting to **A**.

Figure adapted from (Kolakofsky et al., 2012).

Upon recognition of their viral PAMPs, RIG-I and MDA5 activate a signal transduction cascade that leads to the induction of IFN-β. Detailed analysis of the specific viral PAMPs that activate RIG-I and MDA5 will be will be discussed later (**1.2.3. The Virus PAMPs of RIG-I, MDA5 and LGP2**).

Both the expression of RIG-I (Yoneyama et al., 2004) and MDA5 (Kang *et al.*, 2004) are strongly induced by IFN-β, creating a positive feedback mechanism for the rapid expression of ISGs upon virus infection. RIG-I and MDA5 contain two N-terminal tandem caspase recruitment domains (CARDs) (**Figure 2**). CARDs are interaction motifs, activated by virus infections that facilitate downstream protein-protein interactions involving antiviral, inflammation and apoptosis pathways. The CARDs of RIG-I and MDA5 interact with the respective CARDs of the signalling platform IPS-1, leading to the induction of IFN-α/β (**Figure 4**). In contrast, LGP2 lacks the CARDs found in RIG-I and MDA5. LGP2 is thus incapable of interacting with IPS-1 and inducing IFN-α/β by itself. This is supported by transient overexpression experiments in which LGP2 does not have an intrinsic ability to activate the IFN-α/β promoter (Rothenfusser *et al.*, 2005). Instead, LGP2 acts as a regulator of RIG-I and MDA5.

The activation of RIG-I

The mechanism of the activation of RIG-I, MDA5 and LGP2 following recognition of their respective viral PAMPs has been obscured by a lack of structural information. It is only recently that four groups independently reported high resolution structures of RIG-I in an unstimulated state and in an active conformation bound to dsRNA, extending previous structural work of RIG-I bound to 5'-ppp dsRNA (Lu *et al.*, 2010; Wang *et al.*, 2010). A number of studies have now been completed using RIG-I from different species. Two studies used human RIG-I (Jiang *et al.*, 2011; Luo *et al.*,

2011) and one mouse RIG-I (Civril *et al.*, 2011), but the most comprehensive results were obtained with duck RIG-I in which the structure of full- length RIG- I in the ligand- free state was obtained (Kowalinski *et al.*, 2011). The model for the structural activation of RIG-I has been comprehensively reviewed (Jiang & Chen, 2012; Kolakofsky *et al.*, 2012; Leung & Amarasinghe, 2012), and will be briefly described here (**Figure 3**).

In unstimulated cells, RIG-I is expressed as a monomer in an autorepressive state (**Figure 3A**). RIG-I CARD activity is inhibited sterically by a repressor domain that is mapped onto the C-terminal domain (CTD) and the linker region that connects the CTD to the helicase domain (Kowalinski *et al.*, 2011; Saito *et al.*, 2007) (**Figure 2**). The linker region forms a V-shaped conformation, forcing the CARDs to bind to the Helicase 2i (Hel-2i) region and sequestering them from interactions with CARDs from the downstream signalling platform IPS-1, inhibiting IFN-β induction (Kowalinski et al., 2011). In addition, *in vitro* studies have determined that the CARDs themselves negatively regulate the ATPase activity of the helicase domain (Gee et al., 2008). ATP hydrolysis is required for the migration of RIG- I along the duplex RNA ligand.

Upon virus infection, virus RNA ligands such as 5'-ppp dsRNA bind to the repressor domain of RIG-I (Lu *et al.*, 2010; Wang *et al.*, 2010). The binding of virus RNA ligands to the repressor domain activates the ATPase activity of the DExD/H-box RNA helicase domain of RIG-I, a process mediated by the linker region (Civril et al., 2011; Gee et al., 2008; Luo et al., 2011) (**Figure 3B**). These actions induce a conformational change in RIG-I, resulting in the virus RNA ligand binding to the helicase domain. The conformational change in RIG-I facilitates the expulsion and exposure of the CARDs from the repressor and Hel-2i domains, whilst facilitating the dimerization of RIG-I (Saito et al., 2007) (Cui *et al.*, 2008; Kowalinski *et al.*, 2011) (Luo et al., 2011) (**Figure 3C**). The exposed CARDs are polyubiquitinated on Lys63

primarily by the E3 ligase TRIM25 (Tripartite motif-containing protein 25) (Gack *et al.*, 2007; Jiang *et al.*, 2012). Polyubiquitination is an absolute requirement for the activation of RIG-I, as dimerised RIG-I with non-ubiquitinated CARDs is unable to induce IFN-β (Zeng *et al.*, 2010). The polyubiquitinated CARDs recruit the IPS-1 signalling platform via CARD-CARD interactions, leading to the induction of IFN-β (**Figure 4**) (Gack *et al.*, 2007; Kawai *et al.*, 2005; Meylan *et al.*, 2005; Seth *et al.*, 2005; Xu *et al.*, 2005). It is important to control the activation of RIG-I (and the other PRRs), as uncontrolled IFN-β induction would result in the production of potentially damaging ISGs and cytokines involved in inflammation, the regulation of host cell transcription, translation, the host cell cycle and apoptosis.

The activation of MDA5

The mechanism of MDA5 activation remains poorly understood compared to RIG-I, with few crystal structures obtained of MDA5 in inactive and active states. This is because MDA5 oligermises when bound to dsRNA, forming filamentous structures which are hard to crystallise (Berke *et al.*, 2013; Peisley *et al.*, 2011; 2012; Wu *et al.*, 2013). It had previously been assumed that MDA5 activation is similar to RIG-I, given that RIG-I and MDA5 share the same structural architecture (Fairman-Williams *et al.*, 2010; Yoneyama *et al.*, 2005) (**Figure 2**). The RIG-I and MDA5 RNA helicase domains are highly conserved, sharing 35% sequence homology (Yoneyama *et al.*, 2008). In addition, previous structural and functional studies have determined that the MDA5 CTD is responsible for binding to blunt end viral dsRNA, using a highly conserved positively charged surface common to RIG-I, MDA5 and LGP2 (Cui *et al.*, 2008; Li *et al.*, 2009b; Pippig *et al.*, 2009; Wang *et al.*, 2010). Comparing the RIG-I linker region to the MDA5 equivalent has revealed important structural differences. The MDA5 linker region is longer and has acidic sequences, and the MDA5 C-

terminus does not appear to contain a repressor domain like that of RIG-I (Saito et al., 2007). RIG-I and MDA5 also diverge in the structure and function of their Hel-2i domains. The Hel2i α2 helix, which in RIG-I interacts with RIG-I CARDs or viral RNA, is shorter in MDA5. A phenylalanine residue essential for binding CARDs in RIG-I is not conserved in MDA5, suggesting that in the absence of RNA, MDA5 CARDs are regulated differently (Berke *et al.*, 2012). Together, these data demonstrate that in contrast to RIG-I, MDA5 has an open and flexible structure in the absence of RNA ligands. These studies raise the question of how MDA5 CARDs are kept inactive if not through steric inhibition like that of RIG-I.

Evidence that MDA5 forms ATP-sensitive oligomer filaments on dsRNA, provides a working model to describe the activation of MDA5 mediated signalling (Berke *et al.*, 2012; Peisley *et al.*, 2011; 2012). MDA5 exists as individual inactive monomers in the cytosol, lacking the necessary structure to activate IPS-1. Upon the presentation of viral RNA ligands, negative-stain electron microscopy showed that MDA5 forms filaments along dsRNA, mediated by the MDA5 CTD. The MDA5 CTD is critical for high-affinity interactions between dsRNA and MDA5, and between MDA5 monomers (Berke *et al.*, 2012; Peisley *et al.*, 2011). The formation of MDA5 filamentous oligomers along the dsRNA activates MDA5 mediated signalling, a process also called positive cooperativity. A recent study further supports this model, in which the crystal structure of MDA5 filamentous oligomers bound to dsRNA was solved (Wu *et al.*, 2013). Following the assembly of MDA5 CARDs, the MDA5 CARDs requires polyubiquitination on Lys63, similar to RIG-I, in order to activate IRF3 (Jiang *et al.*, 2012).

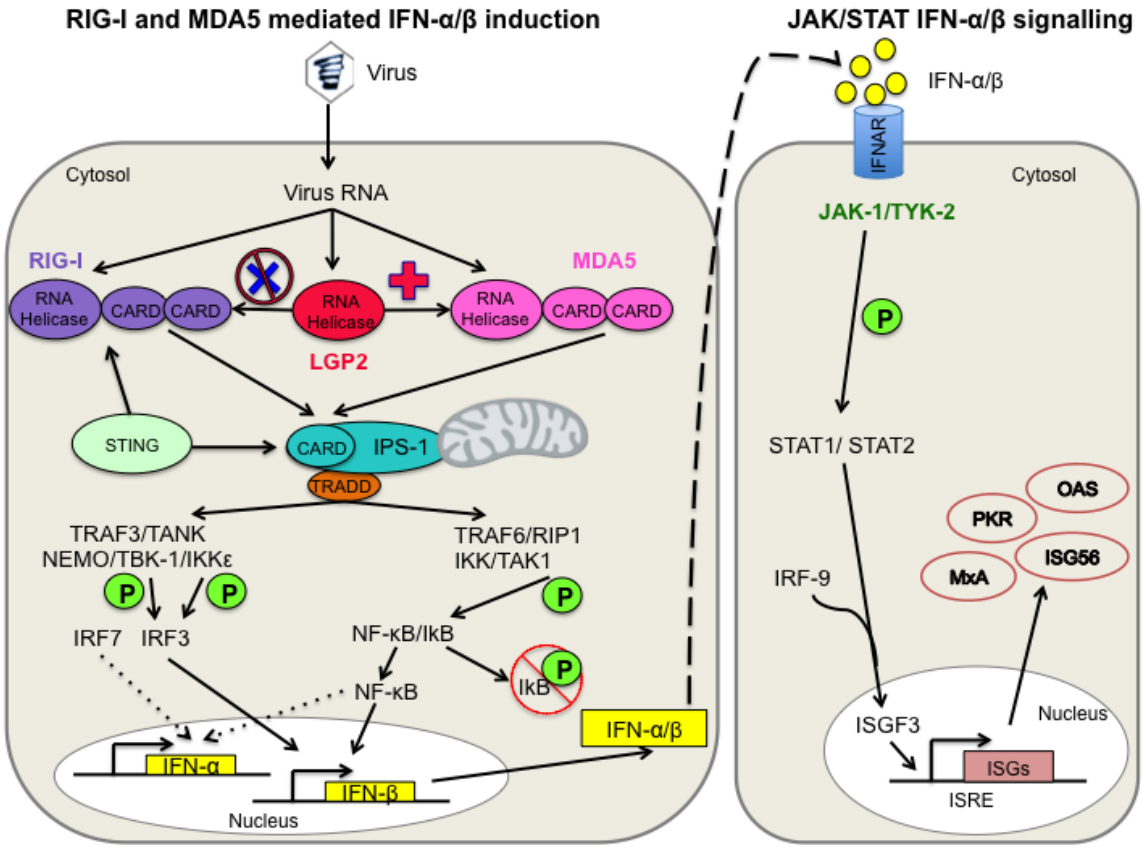

Figure 4. RIG-I and MDA5 mediated induction of IFN-α/β

In unstimulated cells, LGP2 binds to and inhibits RIG-I. Upon virus infection and the binding of virus RNA PAMPs to LGP2,

1) A conformational change in LGP2 leads to the cessation of RIG-I inhibition

2) LGP2 binds to and enhances the activity of MDA5.

Viral RNA PAMPs bind to RIG-I and MDA5, activating their CARDs (refer to main text). The CARDs of RIG-I and MDA5 bind to the downstream CARDs of IPS-1. IPS-1 in turn recruits adaptor proteins that lead to activation of the transcription factors IRF3, IRF7 and NF-κB (refer to main text).

IRF3 and IRF7 activation: TBK-1 and IKKε phosphorylates IRF3. Phosphorylated IRF3 homodimerises and translocates to the nucleus. Some cells (*e.g.* pDCs) express low levels of IRF7, as well as cells in which IFN-β has been induced. TBK-1 and IKKε phosphorylate IRF7. IRF7 as a homodimer or as a heterodimer with IRF3 translocates into the nucleus.

NF-κB Activation: NF-κB is inhibited in unstimulated cells by IκB, which sequesters the NF-κB nuclear localisation signal. Upon stimulation, TRAF6 autoubiquitinates, leading to the polyubiquitination of RIP1 and the subsequent recruitment of the IκB kinase complex (IKK) and TAK1. The IKK comprises of the NEMO scaffolding protein and the catalytic subunits IKKα and IKKβ. TAK1 phosphorylates IKKβ, which subsequently phosphorylates IκB. Phosphorylated IκB dissociates from NF-κB, whereby it is degraded by the proteasome. The NF-κB nuclear localisation signal is unmasked, enabling NF-κB to be translocated to the nucleus.

IFN-α/β Promoter Activation: IRF3 and NF-κB, form an enhancesome together with other transcription factors in the nucleus. The enhancesome then binds to the IFN-β promoter and induces the expression of IFN-β. IRF7 and NF-κB can also form an enhancesome, binding to the IFN-α promoter and inducing IFN-α expression. Following induction, IFN-α/β is secreted from the cell.

IFN-α/β signalling: Secreted IFN-α/β binds to the IFNAR at the cell surface membrane. The IFNAR subsequently activates the receptor-associated tyrosine kinases JAK1 and Tyk2, which phosphorylate STAT1 and STAT2. Phosphorylated STAT1 and STAT2 forms a heterodimer via their SH2 domains. IRF9 binds to STAT1/STAT2, forming the ISGF3 complex. ISGF3 is translocated into the nucleus, binding to the IFN Stimulated Response Element (ISRE) and inducing the expression of ISGs, subsequently generating an antiviral state in the host cell (refer to **1.1.4. IFN-α/β signalling: The JAK/STAT pathway**).

Figure adapted from (Randall & Goodbourn, 2008) and adapted with permission from an original figure by Andri Vasou, University of St Andrews.

The role of LGP2 as a regulator of RIG-I mediated signalling

The role of LGP2 in the induction of IFN has been hotly contested in the literature, acting as a regulator of disputed function for RIG-I and MDA5 (Reviewed in (Zhu *et al.*, 2014) (**Figure 4**). The mechanism of LGP2 regulation of IFN-α/β induction remains unclear, with a lack of structures obtained of full length LGP2 in active and inactive states when bound to either RNA ligands or with RIG-I and MDA5. Like RIG-I and MDA5, LGP2 is strongly induced by IFN-β (Komuro & Horvath, 2006; Satoh *et al.*, 2010; Yoneyama *et al.*, 2005). Initial cell culture experiments suggested that LGP2 acted as a negative regulator of IFN-β induction. The overexpression of LGP2 inhibits the induction of IFN-β, downstream IFN-β signaling and ISG expression upon infection with Sendai virus (SeV), Newcastle disease virus (NDV) or polyinosinic-polycytidylic acid [poly(I:C)], a synthetic dsRNA ligand (Broquet *et al.*, 2011; Komuro & Horvath, 2006; Murali *et al.*, 2008; Rothenfusser *et al.*, 2005; Yoneyama *et al.*, 2005). Like RIG-I, LGP2 contains a C-terminal repressor domain mapped onto the CTD and linker region (**Figure 2).** The LGP2 repressor domain is responsible for binding to both dsRNA and ssRNA in a 5'-ppp independent manner with a greater affinity than RIG-I, in which the LGP2/dsRNA interaction has been crystallised (Li *et al.*, 2009a; Pippig *et al.*, 2009). Hence it was proposed that LGP2 negatively regulates IFN-β induction by sequestering PAMPs from RIG-I and MDA5 (Rothenfusser *et al.*, 2005; Yoneyama *et al.*, 2005).

The exact mechanism of LGP2 mediated RIG-I inhibition remains unclear. Several studies indicate that LGP2 functions as an inhibitor of RIG-I by the LGP2 repressor domain directly binding to RIG-I in a dsRNA ligand independent manner, inhibiting RIG-I dimerisation and subsequent interacts with IPS-1 and the induction of IFN-β (Murali *et al.*, 2008; Saito *et al.*, 2007). Mutations in the dsRNA binding activity of LGP2 did not abolish its inhibitory capacity of RIG-I (Li *et al.*, 2009a), and further

mutagenesis studies revealed that the LGP2 helicase ATPase functionality is essential for LGP2 inhibition of IFN-β induction. A recent paper supports the model of LGP2 inhibition of RIG-I, utilising the PIV5 V protein, discussed later (Childs *et al.*, 2012a). The PIV5 V protein is able to bind to MDA5 and LGP2, but the V protein is unable to bind to RIG-I (Childs *et al.*, 2007; 2012a; Parisien *et al.*, 2009). HEK293 cells were transiently transfected to express the PIV5 V protein, and then the cells were stimulated by RIG-I specific ligands (Childs *et al.*, 2012a). The PIV5 V protein exploits the inhibitory capacity of LGP2, by the V protein forming a complex between LGP2 and RIG-I and antagonising the induction of IFN-β. However, the same authors found that for inhibition of RIG-I to occur under poly(I:C) stimulation, high levels of LGP2 were required, at a greater amount than required for LGP2 activation of MDA5 (Childs *et al.*, 2013). This indicates that under infections *in vivo*, LGP2 may have to be in excess or induced at significantly high levels in order to exert an inhibitory effect on RIG-I. Further highlighting the complex nature of LGP2 regulation of RIG-I, LGP2 may play a role in stimulating RIG-I activity, depending on the infecting virus and cell type (Satoh *et al.*, 2010). Bone marrow-derived dendritic cells from LGP2 knock out mice were found to produce less IFN-β, not just in response to EMCV, but also to RIG-I specific viruses such as VSV, SeV and, Japanese encephalitis. This effect was also seen in the same study where LGP2 appears to stimulate RIG-I mediated IFN-β induction in Mouse Embryonic Fibroblasts, but to suppress IFN-β induction in HEK293 cells.

The role of LGP2 in the regulation of MDA5 mediated signalling

In contrast to RIG-I, LGP2 appears to act as an enhancer of MDA5 mediated signalling. Initial *in vivo* experiments with LGP2 knockout mice revealed that LGP2 has a more complex role in the regulation of MDA5 and RIG-I mediated responses

(Venkataraman *et al.*, 2007). Consistent with a negative regulatory role, LGP2 deficient mouse embryonic fibroblasts (MEFs) showed increased levels of IFN-β mRNA in response to poly(I:C) and vesicular stomatits virus (VSV) infection, and the LGP2 knock out mice were more resistant to VSV infection than wild-type mice. However, LGP2 deficient macrophages made less IFN-β in response to EMCV than wild-type cells, virus titres were higher, and the LGP2 knock out mice were more sensitive to EMCV infection. This data suggests that LGP2 acts as a negative regulator of IFN-α/β induction with viruses that are recognized by RIG-I (VSV), and as a positive regulator with viruses that are recognized by MDA5 (EMCV) (**Figure 3**). The role of LGP2 acting as an enhancer of MDA5 activity, is supported in a study where IFN-β promoter activity was rescued in LGP2 deficient cells by infection with a LGP2 expressing retrovirus, prior to infection with EMCV (Satoh *et al.*, 2010). In addition, a recent study found that LGP2 enhances IFN-β induction in response to limited levels of poly(I:C) stimulation of HEK293 cells {Childs:2013im). The authors showed that LGP2 stimulation by poly(I:C) is dependent upon endogenous MDA5, whereby HEK293 cells in the presence of siRNA to MDA5 were unable to induce IFN-α/β . These findings are in contrast to previous studies that used high levels of poly(I:C) in which IFN-β induction was inhibited (Kato *et al.*, 2008). Co-immunoprecipitation studies revealed that LGP2 interacts with MDA5 in a dsRNA dependent manner (Childs *et al.*, 2013). Furthermore, *in vitro* mutagenesis studies have determined that full length LGP2 is needed to activate MDA5 (Pippig et al., 2009). LGP2 can only form a dimer in response to dsRNA, suggesting that dsRNA is LGP2s unique ligand, and that LGP2 is activated in a similar way to RIG-I (Saito et al., 2007). Clearly, the role of LGP2 as a regulator of RIG-I and enhancer of MDA5 and its role in the induction of IFN-β is complex and needs to be further elucidated.

STING Mediated signalling

An additional adaptor for RIG-I, but not MDA5 mediated signalling is the Stimulator of interferon genes protein (STING) (Ishikawa & Barber, 2008) (**Figure 4**). STING (also called MITA, MYPS and ERIS) is localised in the membrane of the endoplasmic reticulum. Co-immunoprecipitation and transient transfection studies revealed that STING interacts and enhances the interaction between IPS-1, RIG-I TBK-1 and IRF3 (Ishikawa & Barber, 2008; Zhong *et al.*, 2008). STING can also be phosphorylated by TBK-1, facilitating the activation of IRF3 (Li *et al.*, 2009c). These studies suggest that STING acts as a molecular scaffold for the interaction of RIG-I and downstream adaptors, creating a ready state for the recruitment and activation of IRF3 in response to virus infection.

IPS-1 mediated signalling

Upon binding of their respective ligands, RIG-I and MDA5 undergo conformational changes (as described previously) that enables their respective CARDs to interact with the downstream CARDs located on IPS-1 (also known as MAVS, CARDIF, or VISA) (**Figure 4**). IPS-1 functions as the central signalling platform for the RIG-I and MDA5 mediated induction of IFN-α/β (Boga *et al.*, 2013; Jacobs & Coyne, 2013; Kawai *et al.*, 2005; Xing-Xing & Kai, 2013). IPS-1 contains a transmembrane domain that localises IPS-1 to the outer membrane of mitochondria. Following the binding of the CARDs of RIG-I or MDA5 to IPS-1, IPS-1 recruits the tumour necrosis factor receptor (TNFR1)- associated death domain (TRADD) protein. TRADD in turn mediates the formation of complexes that mediate the activation of the transcription factors IFN regulatory factor 3 (IRF3) and Nuclear Factor kappa B (NF-kB). NF-κB and IRF3 are localized in the cell cytosol in an inactive state, enabling their

immediate activation and induction of IFN-β in response to virus infection, without the need for *de novo* protein synthesis

Activation of the IFN-β Promoter by NF-κB and IRF3

NF-κB is inhibited by the Inhibitor of NF-kB (IkB), which sequesters the nuclear localisation signal located on the NF-κB p65 subunit (DiDonato *et al.*, 1997; Mercurio *et al.*, 1997; Rothwarf *et al.*, 1998; Yamaoka *et al.*, 1998). Following virus infection and the activation of IPS-1, TRADD recruits TRAF6 (TNF receptor-associated factor 6) and RIP1 (Receptor Interacting Protein 1) (Cusson-Hermance *et al.*, 2005; Jiang *et al.*, 2004; Meylan *et al.*, 2004; Michallet *et al.*, 2008; Yamamoto *et al.*, 2003). Upon the recruitment of TRAF6 to TRADD, TRAF6 auto-polyubiquitinates and then also polyubiquitinates RIP1. The polyubiquitinated RIP1, forms a scaffold for the recruitment of the IκB kinase complex and the TAK1 (transforming growth factor β-activated kinase 1) binding proteins 2 and 3, that in turn recruit TAK1 (reviewed by Chen, 2005; Deng *et al.*, 2000; Kanayama *et al.*, 2004; Wang *et al.*, 2001). The IκB kinase complex consists of the NF-κB Essential Modulator (NEMO) scaffolding protein and the catalytic subunits IKKα and IKKβ. TAK1 directly phosphorylates the IKKβ subunit (Wang *et al.*, 2001). The phosphorylated IKKβ subunit in turn phosphorylates IκB. Phosphorylated IκB is dissociates from NF-κB, whereby phosphorylated IκB is then degraded by the proteasome. The nuclear localisation signal is consequently unmasked from the newly free NF-κB, allowing NF-κB to be translocated to the nucleus.

In contrast to NF-κB, IRF3 is constitutively expressed in cells as a monomer in an inactive state (Au *et al.*, 1995). Upon stimulation, TRAF3 is recruited to the TRADD/IPS-1 complex (Häcker *et al.*, 2006; Michallet *et al.*, 2008; Oganesyan *et al.*,

2006). TRAF3 in turn recruits TANK (TRAF family member-associated NF-κB activator) (Balachandran *et al.*, 2004; Hoebe, 2006; Li *et al.*, 2002; Michallet *et al.*, 2008; Xu *et al.*, 2005). NEMO interacts with TANK to enable the recruitment of TBK-1 and IKKε (Pomerantz & Baltimore, 1999; Yamamoto *et al.*, 2003; Zhao *et al.*, 2007). TBK-1 and IKKε phosphorylate Serine/threonine residues in the IRF3 C-terminus. Phosphorylated IRF3 homodimerises, causing a conformational change in IRF3 that reveals a nuclear localization signal (Fitzgerald *et al.*, 2003; Sharma *et al.*, 2003). The phosphorylated IRF3 homodimer then translocates into the nucleus.

In the nucleus, phosphorylated IRF3 homodimers and NF-κB interact, forming a IFN-β transcription factor complex called the enhancesome. The enhancesome comprises of other important transcription factors such as activator protein 1 (AP-1, formed of the subunits ATF-2 and c-Jun) (Wathelet et al., 1998) and high mobility group proteins. Following the formation of the enhancesome complex, the enhancesome recruits the co-activator cAMP-responsive-element binding protein (CREB)-binding protein and p300, whereby the enhancesome complex binds to the IFN-β promoter and subsequently initiates IFN-β transcription (Munshi et al., 1998). IFN-β is subsequently secreted by the cell.

Activation of the IFN-α promoter by IRF7 and NF-κB

In addition to phosphorylating IRF3, TBK1 and IKKε phosphorylate and activate a second IFN transcription factor, IRF7. The majority of cell types have undetectable or very low basal levels of expression of IRF7 (Au *et al.*, 1995; Erlandsson *et al.*, 1998; Génin *et al.*, 2009; Marié *et al.*, 1998; Sato *et al.*, 1998; Yeow *et al.*, 2000) (Wathelet *et al.*, 1998; Yang *et al.*, 2004). IRF7 is required for the rapid induction of IFN-α in immune cells such as pDCs (Prakash, 2005; Raftopoulou, 2005). Upon the

phosphorylation of IRF7 by TBK1 and IKKε, IRF7 homodimerises or heterodimerises with IRF3 to reveal the IRF7 nuclear localization signal. Once translocated to the nucleus, IRF7 interacts with NF-κB and the enhancesome, activating the IFN-α promoter. Unlike IRF3, IRF7 is IFN-β inducible. Hence in cells where the IFN-β induction cascade has been activated, IRF7 is induced which subsequently induces IFN-α. This aids the host cell to rapidly express ISGs and to generate the antiviral state.

1.1.4. IFN-α/β signalling: The JAK/STAT pathway

The JAK/STAT pathway is the key classical signalling pathway activated by IFN-α/β that leads to the induction of ISGs and the generation of an antiviral state. Upon induction and secretion from cells, IFN-α/β acts in a paracrine and autocrine manner, binding to the IFN-α/β receptor (IFNAR) (**Figure 3**). The IFNAR is composed of two subunits, IFNAR1 and IFNAR2 (Abramovich *et al.*, 1994; Novick *et al.*, 1994). Prior to activation by IFN-α/β, the tyrosine kinase Tyk2 is constitutively expressed and associated with IFNAR1, whilst JAK1 is constitutively expressed and associated with IFNAR2 (Abramovich et al., 1994; Colamonici et al., 1994; Müller et al., 1993; Novick et al., 1994). Prior to activation by IFN-α/β, STAT2 is associated with IFNAR2, and STAT1 is weakly associated with STAT2 (Precious *et al.*, 2005; Stancato *et al.*, 1996). IFN-α/β binds to the IFNAR, inducing IFNAR dimerization and causing a conformational change in which Tyk2 is able to phosphorylate tyrosine 466 on IFNAR1. The phosphorylation of IFNAR1 forms a docking site that allows STAT2 to strongly associate with IFNAR1 via their corresponding Src homology 2 (SH2) domains, permitting STAT2 phosphorylation on Tyrosine 690 by Tyk2 (Stahl et al., 1995). Phosphorylation of STAT2 enables the JAK1 mediated phosphorylation of STAT1 at Tyrosine 701, consequently enabling the formation of a stable heterodimer

between STAT1 and STAT2 (Leung *et al.*, 1995). Formation of the heterodimer permits binding of IRF9 to STAT1/STAT2, forming the Interferon-stimulated gene factor 3 (ISGF3) transcription factor complex. The formation of the ISGF3 complex exposes a nuclear localization signal that promotes ISGF3 translocation to the nucleus (Fagerlund *et al.*, 2002; Melen *et al.*, 2003). ISGF3 subsequently binds to the *cis* element IFN-stimulated response element (ISRE) contained in the promoter of certain ISGs and induces ISG transcription (Darnell, 1997; Levy & Darnell, 2002). The ISGF3 complex is eventually broken down via the dephosphorylation of the STAT1/STAT2 heterodimer, exposing the nucleus export signals and subsequent translocation to the cytosol (Banninger, 2004; McBride & McDonald, 2000). The JAK/STAT pathway is tightly regulated given its critical role in the expression of ISGs following the induction of IFN-α/β. This has been extensively reviewed in the literature and beyond the scope of this thesis (Dalpke *et al.*, 2008; HAQUE & SHARMA, 2006; Kohanbash & Okada, 2012; Krämer & Heinzel, 2010; Najjar & Fagard, 2010; Platanias, 2005). There are other mechanisms of ISG induction independent of the JAK/STAT pathway such as gamma activated sequence (GAS) elements, but these are beyond the scope of this thesis.

1.1.5. The Generation of the Antiviral state by IFN-α/β

IFN-α/β upregulates the expression of over 380 ISGs which are able to establish an antiviral state in the infected cell and neighbouring uninfected cells, directly inhibiting further virus infection, replication, transcription, assembly and dissemination (Schoggins *et al.*, 2011; Yoneyama *et al.*, 2005). IFN-α/β also upregulates the expression of components involved in IFN-α/β induction and the JAK/STAT pathway, priming uninfected cells to illicit a rapid, thorough antiviral response upon infection. There have been many comprehensive reviews in the literature of ISGs that inhibit

RNA viruses, and those that have been well characterised are summarised in **Table 1** (reviewed in (Liu *et al.*, 2011; Randall & Goodbourn, 2008; Sadler & Williams, 2008). The primary ISGs examined in this project are MxA and ISG56, utilised as markers for the induction of IFN-α/β and are the main focus of this section. IFN-α/β also upregulates genes involved in cell cycle arrest, apoptosis and the immunomodulation of innate and adaptive immune cells. Together, these responses act in concert to create a hostile environment against the infecting virus before the other arms of the immune system are able to respond.

Mx GTPases

The Mx family of genes encode large GTPases which are involved in the inhibition of viral ribonucleocapsids (Reviewed in (Verhelst *et al.*, 2013). Human MxA is localised in the cytosol, recognizing and binding to the viral ribonucleocapsids of a large range of viruses, including orthomyxoviruses, paramyxoviruses, rhabdoviruses, togaviruses, bunyaviruses, hepatitis B virus and Coxsackie virus (Chieux *et al.*, 2001; Gordien *et al.*, 2001; Haller *et al.*, 2007; Landis *et al.*, 1998). It is not known how Mx proteins can suppress such a diverse range of viruses lacking an obvious common molecular pattern. Although its antiviral mechanism has not been fully elucidated, MxA appears to oligomerize to form rings around the ribonucleocapsids, blocking early viral replication events (Andersson *et al.*, 2004; Kochs, 1999; Kochs *et al.*, 2002; Malsburg *et al.*, 2011; Weber & Haller, 2000). Furthering this, Xiao *et al* determined that human MxA inhibits the early stages of influenza A virus infection by retaining the incoming viral genome in the cytosol (Xiao *et al.*, 2013). Supporting this are structural studies of MxA, which revealed intra- and inter-molecular interactions required for their antiviral activity, consistent with the proposed ring model of inhibition of viral replication (Gao, n.d.; Sadler & Williams, 2011).

Table 1. Summary of well characterised ISGs that inhibit negative strand RNA viruses.

ISG	Target	Viruses affected	Mechanism of action
Protein Kinase R	Viral dsRNA	ECMV, Vaccinia Virus, HIV-1, VSV. HSV-1 (Herpes Simplex Virus) (Adelson *et al.*, 1999; Balachandran *et al.*, 2000; Lee & Esteban, 1993; Meurs *et al.*, 1992; Tallóczy *et al.*, 2006).	PKR is a serine threonine kinase that binds to viral dsRNA, inducing a conformational change in which PKR homodimerises and autophosphorylates (Gale *et al.*, 1998; Nanduri *et al.*, 2000; Taylor *et al.*, 1996). Activated PKR phosphorylates eukaryotic translational initiation factor 2α (eIF2α), preventing eIF2α recycling and thus inhibiting the initiation of ribosomal virus translation and recycling of IKKβ for NF-κB activation. eIF2α phosphorylation also induces cellular autophagy (Balachandran *et al.*, 1998; Tallóczy *et al.*, 2002).
2'-5' Oligoadenylate Synthetase (2-5OAS)/ RNase L	Viral dsRNA	ssRNA viruses including *Picornaviridae, Reoviridae*, *Togaviridae*,*Paramyxoviridae*, Orthomyxoviridae, *Flaviviridae* and *Retroviridae* (Hovanessian, 2007) (Lin *et al.*, 2009; Silverman, 2007)	2-5' OAS catalyses the synthesis of 2'-5' adenosine phosphodiester bond linked oligomers from ATP, which in turn activate endoribonuclease L (RNase L) (Slattery & Ghosh, 1979; Zhou *et al.*, 1993). RNase L degrades cellular and viral ssRNA and mRNA, inhibiting viral protein translation and inducing cellular apoptosis (Silverman, 2007; Zhou *et al.*, 1998)
ISG15	Cellular and virus protein machinery involved in	Influenza, Sindbis Virus, HSV1, Chikungunya Virus, Lymphocytic choriomeningitis Virus, Hepatitis C virus (HCV), Human Papilloma Virus, HIV-1 (Okumura *et al.*,	ISG15 is a ubiquitin homologue that is conjugated to cellular proteins following virus infection (Loeb & Haas, 1992), including IRF3, STAT1, Jak1, PKR and MxA (Malakhova *et al.*, 2003; Shi *et al.*, 2010; Zhao *et al.*, 2005). The addition of ISG15 to cellular proteins

	virus release	2006) (Lenschow et al., 2007) (Chen & Li, 2011; Ritchie *et al.*, 2004; Werneke *et al.*, 2011) (Lenschow et al., 2005)	(SGylation), enhances protein translocation (Loeb & Haas, 1994) and stabilization (Lu *et al.*, 2006). ISG15 inhibits multiple stages of HIV-1 release from the cell, preventing virion budding (Pincetic *et al.*, 2010). This could be the mechanism that ISG15 affects other viruses.
Viperin	Host cell Lipid Rafts	Human cytomegalovirus, HCV, influenza, HIV-1 (Chin & Cresswell, 2001; Jiang *et al.*, 2008; Wang *et al.*, 2007)	Viperin is associated with the endoplasmic reticulum membrane. Viperin disrupts cell surface membrane and lipid raft integrity, preventing virus budding and release e.g. during Influenza A infection (Wang *et al.*, 2007), or the release of viruses from lipid droplets that use them as a site for replication e.g. HCV (Jiang *et al.*, 2008; Miyanari *et al.*, 2007).

Table Modified from (Liu *et al.*, 2011)***.***

ISG56

ISG56 (also known as Interferon Induced protein with tetratricopeptide protein repeats 1, IFIT1) belongs to the *ISG56* family of genes that are evolutionary conserved in humans, mice, birds, fish and amphibians (Fensterl & Sen, 2011). Most cell types do not express detectable levels of ISG56 in the absence of viral stimuli. Upon virus infection, ISG56 is rapidly induced following the induction of IFN-α/β (Der *et al.*, 1998; Kusari & Sen, 1986; Terenzi *et al.*, 2008). Furthermore, the ISG56 promoter can be activated independently of the IFN-α/β and the JAK/STAT signalling pathway. The ISG56 promoter contains an IRF3 binding cis-element (Nakaya et al., 2001), enabling IRF3 to directly induce ISG56 (Grandvaux *et al.*, 2002; Nakaya *et al.*, 2001; Peters *et al.*, 2002).

ISG56 is composed of a single structural motif, the tetratricopeptide repeat (TPR). The TPRs form scaffolds that allows ISG56 to interact and modulate the activities of a wide range of cellular and viral proteins involved in viral translation, such as eIF3 (eukaryotic initiation factor 3) (D'Andrea, 2003; Lamb *et al.*, 1995). eIF3 is a large protein complex made up of 13 subunits (a-m). eIF3 controls the assembly of the 48S translation initiation complex on mRNA that have a 5' cap or an Internal Ribosomal Entry Site. eIF3 prevents binding of the 60S ribosomal subunit to the 40S subunit until the translation initiation complex has been formed. The 48S translation initiation complex is formed by eIF3 acting as a scaffold for the recruitment of the 40S ribosome, the ternary complex (eIF2-GTP-Met-tRNA), eIF4F and mRNA (Guo *et al.*, 2000; Hinnebusch, 2006). ISG56 inhibits the ternary complex formation step of translation initiation by binding to the eIF3e subunit of eIF3, leading to the inhibition of protein synthesis (Hui *et al.*, 2003; Terenzi *et al.*, 2006).

A recent study showed that for West Nile virus, ISG56 can restrict the replication of

mutant viruses deficient for 2'-*O* methyltransferase activity. 2'-0 methyltransferase methylates the 2'-hydroxyl group of ribose sugars in the 5'-cap viral mRNA. The wildtype and mutant viruses induced similar levels of IFN-β, but the mutant viral mRNAs were extremely sensitive to ISG56 compared to the wildtype virus. This indicates that viral mRNA or virus RNAs lacking 2'-*O* methylated sites are ligands for ISG56. In comparison, two recent studies have shown that for PIV5, the viral mRNAs are methylated at the 5'-cap, but this feature does not reduce ISG56 activity ('ISG56/IFIT1 is primarily responsible for interferon-induced changes to patterns of parainfluenza virus type 5 transcription and protein synthesis', 2013; Killip *et al.*, 2012a). Instead, ISG56 was shown to be the primarily ISG responsible for in the inhibition of translation of viral mRNAs, independent of whether the 5'-cap was methylated or not. The mechanism of action of ISG56 remains to be fully elucidated.

IFN-α/β mediated regulation of the Cell cycle and Apoptosis

In addition to the regulation of ISGs, IFN-α/β also upregulates genes involved in cell cycle arrest. IFN-α/β modulates cell cycle progression through the upregulation of cyclin-dependent kinase inhibitors (Sangfelt et al.,1999, Sangfelt et al., 1997b, Mandal et al., 1998, Mandal et al., 1998) and the p200 family of proteins (reviewed in (Lengyel, 2008). Treatment with IFN-α/β delays and inhibits cell growth, forcing the cell to remain longer in the G1, S and G2 phases, whilst also promoting cellular apoptosis (Balkwill & Taylor-Papadimitriou, 1978). As certain viruses use host cell machinery for viral transcription and translation, upregulating genes that cause cell cycle arrest would reduce viral transcription and translation of some viruses.

The establishment of a pro-apoptotic state in cells by IFN-β mediates the clearance of those cells that have been overwhelmed by virus infection, before completed virus

assembly and egress from the cell can be achieved (reviewed in (Clemens, 2003). IFN-β upregulates pro-apoptotic ISGs including PKR, PML nuclear bodies and the OAS/RNase L (Tanaka et al., 1998, Sedger et al., 1999).

IFN-α/β mediated immunomodulation of innate and adaptive immunity

IFN-α/β upregulates Major Histocompatibility Complex (MHC) Class I machinery involved in cytotoxic T-cell (CD8+ T-cells) antigen presentation including MHC class I molecules, proteasome subunits and transporters (Der et al., 1998a, Schroder et al., 2004, Epperson et al., 1992). The upregulation of MHC Class I components counters the virus specific downregulation of MHC class I expression (Der et al., 1998a). Furthermore, IFN-α/β can sustain the proliferation of antigen specific cytotoxic T cells and upregulate their effector mechanisms (Tough et al., 1996, Marrack et al., 1999, Kolumam et al., 2005). In addition, IFN-α/β promotes dendritic and natural killer cell maturation (Le Bon et al., 2003). Together, these features act to aid the immediate proliferation and enhance the activity of innate and adaptive immune cells, leading to the rapid clearance of virus-infected cells.

1.2. The interplay between PIV5, IFN and the antiviral state

To study the mechanisms behind the induction of IFN, we use parainfluenza virus subtype 5 (PIV5) as a model virus, acting as the stimulator of the PRRs RIG-I, MDA5 and LGP2. PIV5 has been used as a model to study the fundamental properties of the *Paramyxoviridae* and the host cell response since it's discovery and characterisation in the 1950s and 1960s (Chanock, 1956; Choppin & Stoeckenius, 1964; Hull & Minner, 1957). PIV5 was first originally isolated in rhesus monkey kidney cells and was therefore named simian virus 5 (SV5). It has since been recovered from several species, such as dogs and humans (Goswami *et al.*, 1984; Gur & Acar, n.d.; McCandlish *et al.*, 1978) and it was therefore suggested that it should be re-named parainfluenza virus 5 (Chatziandreou *et al.*, 2004). The International Committee on Taxonomy of Viruses has accepted this change in nomenclature. PIV5 infects a range of epithelial cell types including human A549 cells (adenocarcinomic human alveolar basal epithelial cells) and primary human cells (Arimilli *et al.*, 2006; Chatziandreou *et al.*, 2004). Indeed, there has been no report of a cell line that is resistant to PIV5 infection In the following section PIV5 structure, life cycle and replication will be described in the context of detection by the PRRs and the consequent induction of IFN.

1.2.1. Introducing PIV5 and the Paramyxoviruses

PIV5 is a prototypic member of the *Paramyxoviridae* family of non-segmented negative strand RNA viruses (NNSVs) (**Figure 5**; reviewed in (Samal, 2011)

Paramyxoviruses infect a diverse range of hosts, capable of causing significant morbidity and mortality to humans and other mammals, poultry and fish. Some of the human pathogens include measles virus (MeV), mumps virus (MuV), and metapneumoviruses, which can cause severe respiratory infections in children and infants (Black, 1991). A recent epidemiological study estimated that 199,000 children under 5 years of age died globally from respiratory syncytial virus (RSV) (Nair *et al.*, 2013). The same study revealed the morbidity of RSV infections, in which 3.4 million children were admitted to hospital. There are also important animal pathogens such as rinderpest virus, bovine respiratory syncytial virus and Newcastle disease virus (NDV), which cause serious economic impact on farmers.

Paramyxoviruses usually have a narrow host range with no cross species transmission. However, paramyxoviruses have been identified in various types of bat, across Africa, Australia, Asia and South America, and also in European fruit bats (Chua *et al.*, 2000; Drexler *et al.*, 2012; Kurth *et al.*, 2012). Recently, two new zoonotic paramyxoviruses emerged, Nipah and Hendra viruses, with high mortality in humans and animals (Eaton *et al.*, 2006; Vigant & Lee, 2011). Alarmingly, these new findings suggest a potential risk of emerging zoonotic paramyxoviruses. (Aljofan, 2013; Virtue *et al.*, 2009). Clearly, it is important to find out how these viruses interact with host immune responses with the objective to developing vaccines against these pathogens.

1.2.2. The structure of PIV5

Like other paramyxoviruses, PIV5 has a host-derived lipid membrane that envelops the virion (**Figure 6**). The lipid envelope contains two integral membrane proteins, haemagglutinin-neuraminidase (HN) and fusion (F).

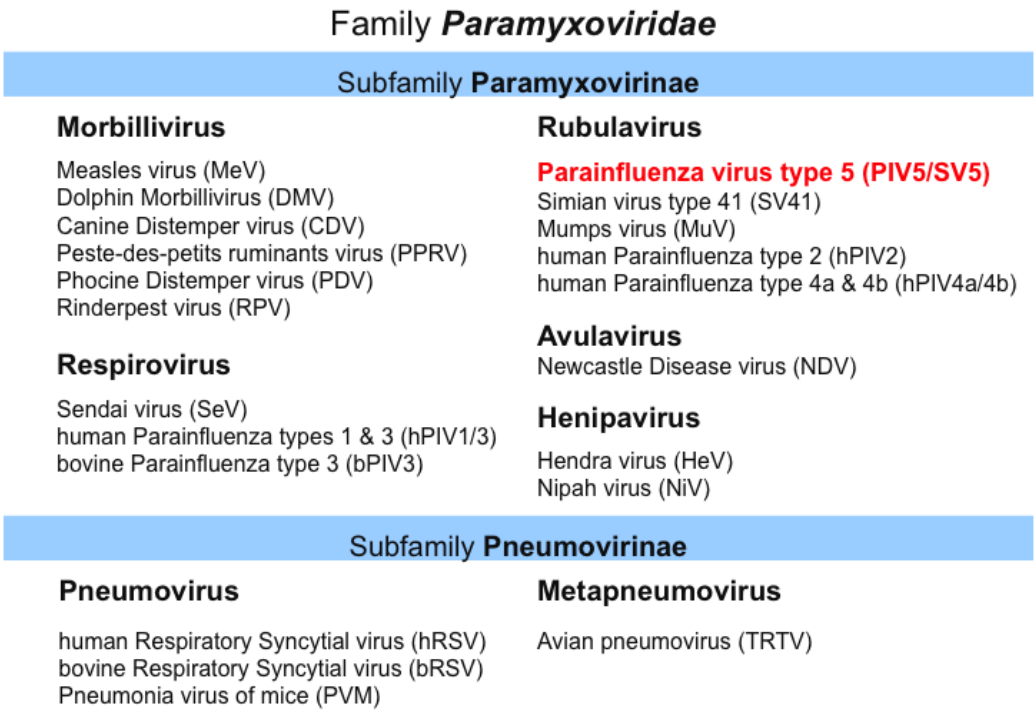

Figure 5. Classification of the *Paramyxoviridae* Family of viruses

The family *Paramyxoviridae* is classified into two subfamilies: the *Paramyxovirinae* and the *Pneumovirinae*. The *Paramyxovirinae* contains five genera: *Respirovirus*, *Rubulavirus*, *Avulavirus*, *Morbillivirus*, and *Henipavirus*. The *Pneumovirinae* contains two genera *Pneumovirus* and *Metapneumovirus*. The classification is based on morphologic criteria, the organization of the genome, the biological activities of the proteins, and the sequence relationship of the encoded proteins now that the genome sequences have been obtained.

Figure adapted from (Samal, 2011).

HN is required for cell attachment whilst F is required for fusion of the lipid envelop to the host cell membrane. Associated with the lipid envelop is the SH (small hydrophobic) protein (Hiebert *et al.*, 1985). The SH protein has been implicated in the inhibition of apoptosis of the host cell (He *et al.*, 2001; Lin *et al.*, 2003; Wilson *et al.*, 2006). Lining the lipid envelope is the Matrix (M) which plays a role in virus assembly. PIV5 has ssRNA genome that is helically encapisidated by the nucleoprotein (NP). Found in association with NP are the V protein and the viral RNA polymerase components, the phosphoprotein (P) and large (L) proteins.

The PIV5 V protein is multifunctional, playing key roles as an IFN antagonist, in viral RNA encapsidation (Precious *et al.*, 1995; Randall & Bermingham, 1996), viral RNA synthesis (Gainey *et al.*, 2008; Lin *et al.*, 2005) and cell cycle regulation (Lin & Lamb, 2000).

1.2.3. The Life cycle of PIV5

In order to investigate the mechanisms by which potential virus PAMPs are generated during virus replication, it is important to understand the life cycle of PIV5. The lifecycle of PIV5 has been extensively reviewed and will be briefly described (Knipe *et al.*, 2013; Samal, 2011). Upon infection, the viral lipid envelope localized HN and F proteins mediate the attachment and fusion of the viral lipid envelope to the host cell plasma membrane (**Figure 7**).

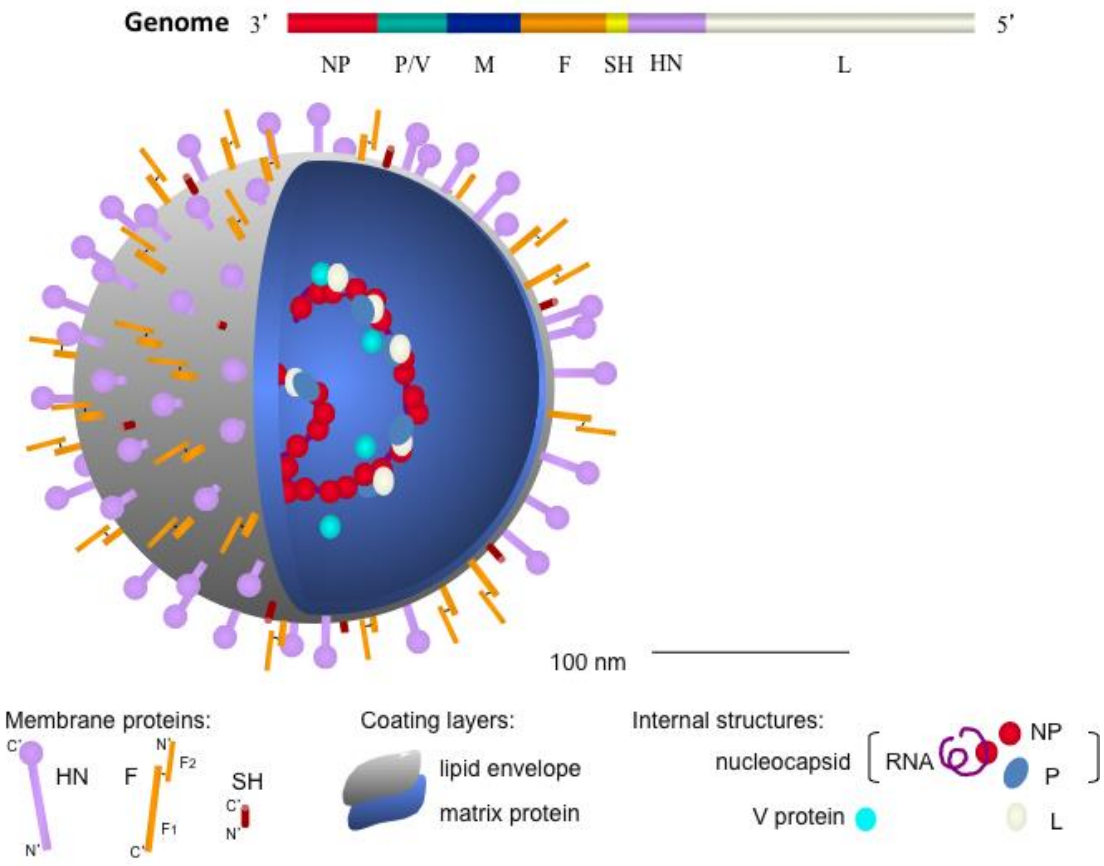

Figure 6. The structure of PIV5

The PIV5 virion consists of a lipid bilayer derived from the host cell plasma membrane. Two glycoproteins are embedded in the lipid envelope: the haemagglutinin-neuraminidase (HN) protein and the fusion (F) protein. The matrix (M) protein lines the inside of the membrane. Inside the virion is the single-stranded negative-sense RNA genome encapsidated by the nucleocapsid (NP) protein and associated with the phosphoprotein (P) and the large (L) protein as well as the V protein. Embedded in the membrane is also the small hydrophobic (SH) protein.

Figure courtesy of Dr. N. Chatziandreou.

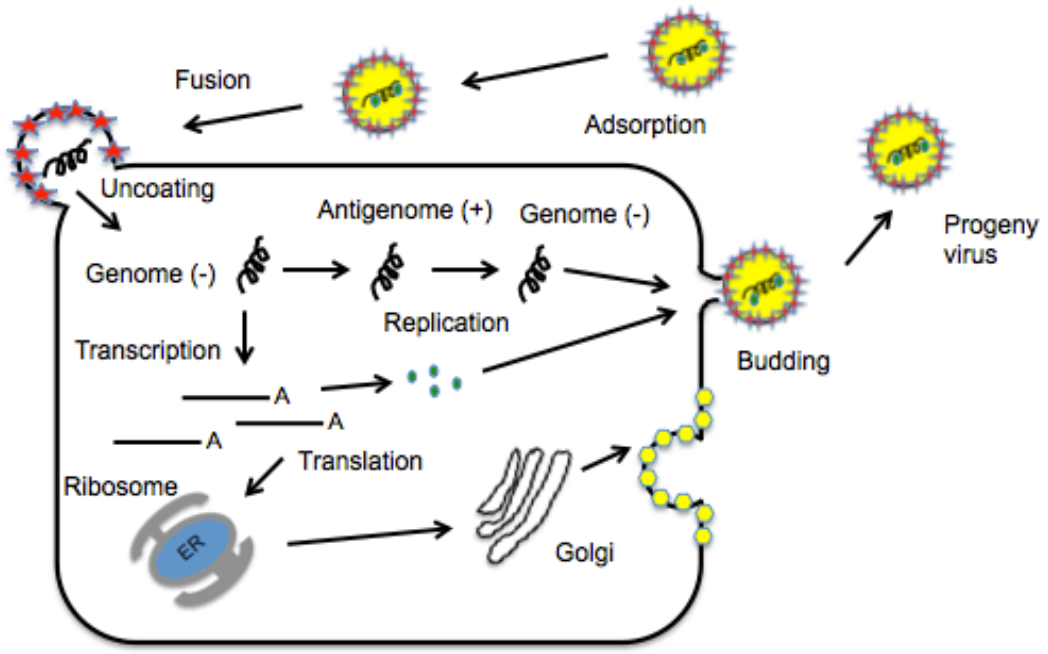

Figure 7. Life cycle of PIV5

The HN glycoprotein facilitates the attachment of virions to the host cell surface. The F protein mediates the fusion of the viral envelope with the cell surface plasma membrane of the infected cell. The virus is then uncoated and the nucleocapsid is released into the cytosol, where viral RNA synthesis occurs. Negative sense genomes are first transcribed into capped and polyadenylated mRNAs, which are translated into viral proteins. When levels of NP have increased, the viral polymerase switches from transcription to replication to produce full-length antigenomes (positive sense). These antigenomes are used to synthesise further viral progeny genomes and together, the antigenomes and genomes are encapsidated by NP. Correctly folded viral proteins are then transported to the Golgi apparatus, where proteins are packaged and then assembled at the cell membrane where the M protein directs the assembly and budding of virions.

Figure courtesy of Hannah Norsted, University of St Andrews.

The HN glycoprotein attaches to sialic acid receptors on the cell surface membrane, whilst the F protein initiates infection through pH-independent fusion of the virion lipid bilayer with the host cell plasma membrane. The virus genome is absorbed into the cytosol of the cell. The encapsidated genome (but not NP) is uncoated, and viral RNA synthesis takes place in the cytosol. Potentially, PAMPs that are sensed by RIG-I, MDA5 and LGP2 could be generated when the genome is uncoated and also at the RNA synthesis step. Following RNA synthesis, the Golgi apparatus sends viral proteins to the cell surface membrane. The M protein facilitates virion assembly and budding. At later stages of infection, the F protein facilitates fusion between infected cells and neighbouring uninfected cells. The F proteins are inactive when synthesized and have to be cleaved by a host cell protease to become biologically activated.

1.2.4. PIV5 RNA synthesis

PIV5 RNA synthesis takes place in the cytosol of the cell using the virus RNA polymerase. Potentially, it is at this level of the virus life cycle that could generate RNA PAMPs that could be detected by MDA5, RIG-I and LGP2. The genome of PIV5 for isolate W3A is 15,246 nucleotides (nt) in length and contains seven genes that encode eight known viral proteins NP, P and V, M, F, SH, HN and L (Paterson 1984b). The PIV5 genome contains a terminal noncoding 55nt leader (Le) and 31nt trailer (Tr) sequences at its 3′ and 5′ ends of the genome. The Le and Tr sequences act as bipartite promoters inducing viral transcription and replication (Murphy & Parks, 1997) (**Figure 8**). The P and L proteins form the viral RNA polymerase, which mediates virus transcription and replication.

PIV5 Transcription

Early in infection, the 3′ Le genomic promoter directs synthesis of both viral mRNAs and the replication of genomic RNA to produce positive sense antigenomes (the full-length complement of the genome) (**Figure 8**) (Knipe *et al.*, 2013; Samal, 2011; Whelan *et al.*, 2004). The viral polymerase can only attach to the template at a single site at the 3' genome terminus. PIV5 transcription occurs in a 3' to 5' direction, directed by the cis-acting regions of the gene junctions. PIV5 employs the same stop-start mechanism that is shared among NNSVs. The first gene transcribed is NP, followed by P/V, M, F, SH, HN and L. Each gene terminus contains a sequence of several U residues that serve as the template for polyadenylation, followed by signals that are recognized by the viral polymerase to terminate transcription.

The polymerase stays attached to the template while it reads along the intergenic region until it reaches the start of the downstream gene, which contains signals for reinitiation of transcription and the addition of a methylated 5' guanine cap to the mRNA (Lamb & Parks, 2006; Whelan et al., 2004). Viral mRNA is 5' capped and 3' polyadenylated to sequester it from cellular RNAses that would destroy foreign RNAs. Sometimes the polymerase fails to reinitiate transcription and disengages from the template. Measurement of the amount of virus mRNAs demonstrated that viral transcription of PIV5 (and other paramyxoviruses) occurs in a transcriptional gradient, with decreasing transcription of the genes the further away from the 3' Le (Cattaneo et al., 1987a, b;Villarreal et al., 1976).

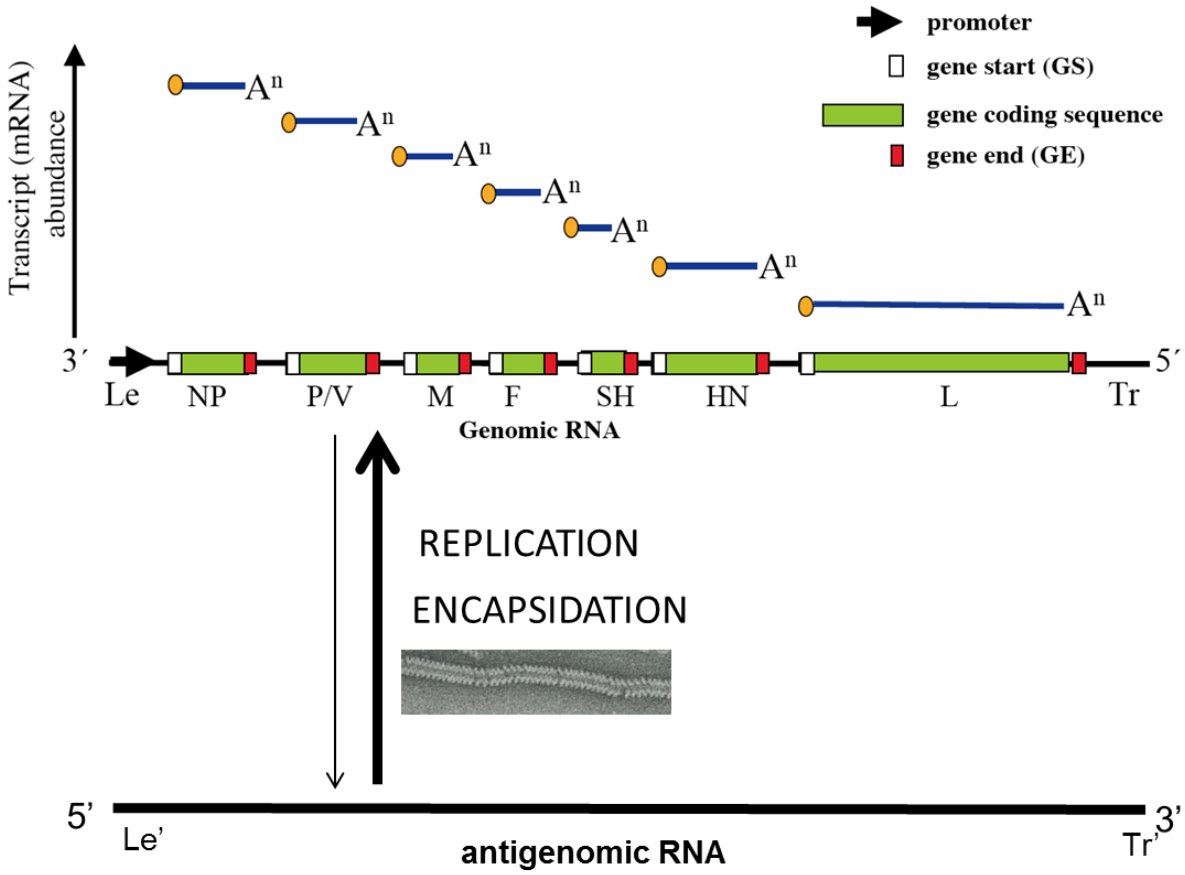

Figure 8. PIV5 RNA Synthesis

The viral polymerase (P-L) transcribes the genome template, starting at its 3’ Le terminus, to generate the successive capped 5’ capped and polyadenylated (A^n) mRNAs. The Viral RNA polymerase stops and restarts at each gene junction, whereby the polymerase can “drop off” ceasing transcription. The NP, P/V, M F, SH, HN and L genes are thus transcribed along a transcriptional gradient. Once these primary transcripts have generated sufficient viral proteins, unassembled NP (as a P-N complex) begins to assemble the nascent leader chain. Encaspidation of the nascent chain by NP causes the viral RNA polymerase to ignore the junctions, yielding the positive sense antigenomic RNA (bottom). The 3’ antigenomic promoter directs the viral RNA polymerase to produce genomic RNA that is immediately encapsidated by NP. See text for details.

Figure courtesy of Rick Randall, University of St Andrews.

The V protein is a faithful transcript of the P/V gene however, both the V and P proteins are transcribed from the P/V gene, as the open reading frames of V/P gene are overlapping resulting in two different gene products. The P gene mRNA is generated by RNA editing, which was first described for PIV5 and is common to other paramyxoviruses (Thomas *et al.*, 1988). RNA editing is the pseudotemplated addition of nucleotides at the open reading frame of mRNAs derived from the gene encoding both the P and V proteins. The addition of two G residues results in a frame shift in the translational open reading frames downstream of the insertion site.

PIV5 Replication

Firstly, during PIV5 replication an antigenomic template is generated. The antigenomic 3' Tr directs replication by the viral polymerase of the template antigenomic RNA to produce progeny negative sense genomes (**Figure 8**). The 3' Tr antigenomic promoter is stronger than the genomic promoter, reflecting the requirement of the virus to generate greater numbers of genomes than antigenomes (Le Mercier *et al.*, 2002). Associated with the viral polymerase P protein is a soluble form of NP, NP0 (Precious *et al.*, 1995). PIV5 replication follows the "rule of 6", in which the genome size is a multiple of six for efficient replication by the viral RNA polymerase (Calain & Roux, 1993). PIV5 replication is most efficient when it follows the "rule of 6", but this has been shown to not be a strict requisite (Murphy & Parks, 1997). During PIV5 replication, nascent viral RNA is immediately encapsidated with firstly NP0 at the 5' terminus as it emerges from the polymerase complex, in order to resist degradation by cellular RNAses. Each NP associates with 6 nucleotides as the full length genome is replicated, which also stops the formation of dsRNA.

1.2.4. The Induction of IFN by PIV5: The Viral PAMPs of RIG-I, MDA5 and LGP2

The critical importance of RIG-I and MDA5 in the detection of paramyxoviruses, using Newcastle Disease virus (NDV) and VSV as a model has been demonstrated using *in vivo* studies (Kato *et al.*, 2006) Infections of RIG-I and MDA5 knock-out mice confirmed the essential roles of these PRRs in the induction of antiviral immune responses. Further *in vivo* and *in vitro* studies demonstrated that RIG-I and MDA5 sense different sets of RNA viruses summarised in **Figure 9**. Our current understanding of the recognition of synthetic and potential viral RNA structures by RIG-I, MDA5 and LGP2 has been comprehensively reviewed in (Schlee, 2013). The following sections will discuss our current understanding of the nature of potential viral PAMPs generated during infection by negative-sense RNA viruses, how these PAMPs are potentially detected by the host cell and induce IFN, and finally how the IFN antagonist function of the V protein may or may not point to a different source of PAMPs generated by PIV5 other than that of the wildtype virus.

RIG-I and MDA5 recognition of PAMPs based on the length of dsRNA

Viral dsRNA is a PAMP that is presented by dsRNA genome viruses such as reoviruses, or potentially generated as intermediates during virus replication of negative sense and positive sense RNA viruses. DsRNA is not produced by host cells and hence supports discrimination of host cellular and viral patterns. Whilst the *in vivo* viral dsRNA ligands have not been identified, many studies have used the synthetic poly(I:C) dsRNA analogue to tease apart the potential ligands for RIG-I and MDA5. Cellular *in vitro* studies revealed that both RIG-I and MDA5 are able to

signal in response to transfected poly (I:C) (Marques *et al.*, 2006) (Kawai *et al.*, 2005).

MDA5 has been shown to have a greater role than RIG-I in the induction of IFN-β in poly(I:C) infected mice, macrophages, poly(I:C) transfected embryo-derived fibroblasts (Kato *et al.*, 2006) and poly (I:C) treated dendritic cells (Gitlin *et al.*, 2010). RIG-I recognises short poly(I:C) structures whereas MDA5 can detect longer poly (I:C) structures. RIG-I, but not MDA5 recognises short blunt ended dsRNA, between 24bp-200bp in length (Kato *et al.*, 2008; Li *et al.*, 2009b; Loo *et al.*, 2008; Lu *et al.*, 2010; Marques *et al.*, 2006; Schlee *et al.*, 2009; Schmidt *et al.*, 2011). Using next generation sequencing it has been shown that RIG-I preferably binds to short viral RNA in infected cells (Baum *et al.*, 2010).

In contrast to RIG-I, MDA5 is able to detect long dsRNA greater than 1kbp (Gitlin *et al.*, 2010; Kato *et al.*, 2006; 2008; Pichlmair *et al.*, 2009). The MDA5 CTD binds to blunt-ended dsRNA (Li *et al.*, 2009b; Wu *et al.*, 2013). MDA5 can recognise RNA complexes formed from ssRNA and dsRNA (Pichlmair *et al.*, 2009). Further evidence for this is displayed when poly(I:C) is converted from a longer structure to a shorter structure. When long poly(I:C) dsRNA is digested with RNase III, this transforms poly(I:C), from a ligand that is able to induce MDA5 into a ligand that induces RIG-I, which suggests that MDA5 recognizes long dsRNA, whereas RIG-I recognizes short dsRNA (Kato, 2008).

RIG-I Recognition of 5'-ppp RNA

A substrate difference between RIG-I and MDA5 in the detection of negative sense RNA viruses, is the recognition by RIG-I, but not by MDA5, of 5'-triphosphate (5'-ppp)

groups that are present on viral genomic ssRNA of certain viruses (Hornung *et al.*, 2006; Pichlmair *et al.*, 2006). DNA template dependent RNA transcription occurs primer independently from the 5′- to the 3′- terminus (Banerjee, 1980). Hence, in the host cell nucleus, cellular RNA primary transcripts initially contain a 5'-ppp group. Before host cell mRNA is exported to the cytosol it undergoes processing to remove this potential molecular PAMP, including CAP ligation, 5' terminus removal or the 5'-ppp modification of ribosomal RNA. Viral mRNAs generated by certain viruses where transcription is localised in the cytosol have a 5'-ppp group. The 5'-ppp group present on viral ssRNAs allows RIG-I to discriminate between viral and host RNA, as host cell ssRNAs in the cytosol do not contain a 5'-ppp group. It has been repeatedly shown that the 5' terminus of 5'-ppp ssRNA detected by RIG-I contains a dsRNA sequence at least 10-19bp in length (Lu *et al.*, 2010; Schlee *et al.*, 2009; Schmidt *et al.*, 2009; Wang *et al.*, 2010) (Kolakofsky *et al.*, 2012)

Unsurprisingly, certain viruses that have viral transcription localised in the cytosol have developed evasion strategies to RIG-I sensing of 5'-ppp mRNAs (Fechter, 2005). Influenza virus steals a 5' cap from host cell mRNA to be used as primers for initiating synthesis of their viral mRNA. Other negative sense viruses such as paramyxoviruses (including PIV5) avoid RIG-I recognition of viral 5'-ppp ssRNAs by placing a 5' cap on viral mRNA via their respective RNA viral polymerases.

RIG-I dominates the immune response to many negative sense ssRNA viruses (Cardenas et al. 2006; Habjan et al. 2008; Hornung et al. 2006; Kato et al. 2005, 2006; Loo et al. 2008; Plumet et al. 2007; Yoneyama et al. 2005). An additional study revealed that Influenza RIG-I activation occurs exclusively by the genomic RNA and not mRNA of Influenza (Rehwinkel et al. 2010). Analysis of RIG-I-bound viral RNA from Influenza infected cells revealed that only 5'-ppp viral genomic RNA

coprecipitated with RIG-I. RIG-I (and MDA5) is also important in the detection of dsRNA genomic viruses and positive ssRNA genomic viruses, that also generate cytosolic dsRNA species, such as replicative dsRNA intermediates during their replication (Feng et al. 2012; Targett-Adams et al. 2008; Triantafilou et al. 2012; Weber et al. 2006). Together with 5'-ppp, such RNA species represent ideal RIG-I target structures.

Picornaviruses do not activate RIG-I during infection (Gitlin *et al.*, 2006; Kato *et al.*, 2006) because instead of a 5′-ppp group, their RNA genomes possess a Vpg peptide linked via a tyrosine residue to a 5′monophosphate (Lee *et al.*, 1977). In line with these findings, Feng *et al.* observed that purified picornavirus RNA did not stimulate RIG-I, but instead stimulated MDA5 (Feng *et al.*, 2012).

MDA5 recognition of 2'-O deficient 5' cap mRNA structures

Recent studies have uncovered an additional potential feature for MDA5 recognition of viral mRNA based on the 2'-*O* methylation status of RNA, that is analogous to RIG-I sensing of 5'-ppp RNA (García-Sastre, 2011). Host cell mRNA has a 5' cap which prevents recognition by RIG-I and 5' exonucleases (as well as promoting mRNA stability and RNA translation by ribosomes). The 5' cap structure is methylated at the N7 position of the capping guanosine residue (cap 0), the ribose-2′-*O* position of the 5′ penultimate residue (cap 1) and sometimes at adjoining residues (cap 2). Whilst the physiological function of 2'-O methylation unknown, many virus families including *Flaviviridae*, *Coronaviridae* and *Poxviridae* encode not only N7-methyltransferases, but also 2′-*O* methyltransferases that modify the 5′ end of their viral mRNAs.

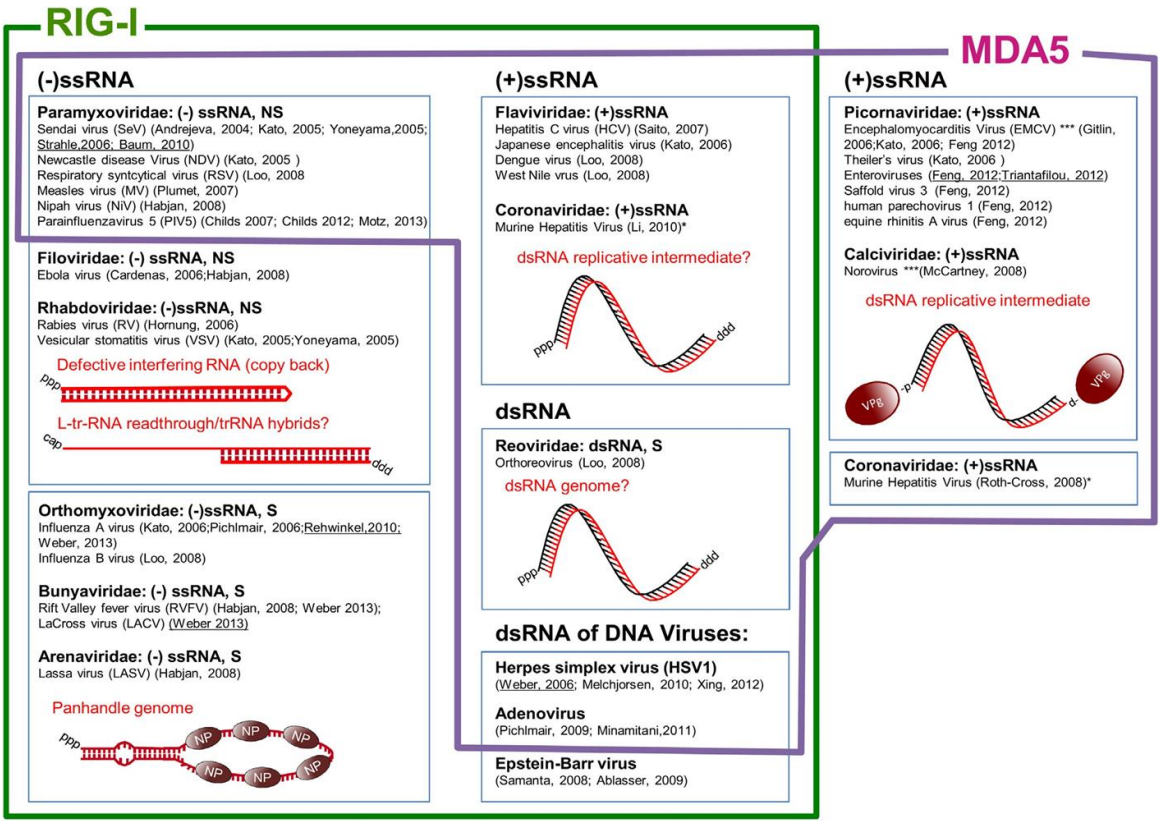

Figure 9. Viruses recognized by RIG-I and MDA5

S: segmented, NS: non-segmented, ssRNA: single-stranded RNA, dsRNA: double-stranded RNA, (+): positives sense genome, (−): negative sense genome.

See text for details.

Figure adapted from (Schlee, 2013).

.

A recent study showed that deficiency of the viral cap N-terminal 2'-O-methyltransferase by murine hepatitis virus (MHV) provoked recognition by MDA5 and TLR7 (Züst *et al.*, 2011b). This study suggested MDA5 mediated 5' dependent RNA recognition. This finding contrasts with studies by Luthra et al., in which MDA5 stimulatory mRNA was expressed from promoter that supported normal capping including N-terminal 2'-O-methylation (Luthra *et al.*, 2011). Later studies on a N-terminal 2′ O-methyltransferase-lacking West Nile virus did not reveal a role for MDA5 in the recognition of non-methylated cap structures (Szretter *et al.*, 2012), suggesting that N terminal 2'-O-methylation does not generally impair MDA5 engagement.

Viral RNA PAMPs generated by ISGs

Interestingly, it has been reported that RIG-I and MDA5 are activated by RNA products produced by the RNase L system (Malathi *et al.*, 2007). RNase L, an ISG, is an endonuclease that degrades both cellular and viral RNAses and generates short fragments with 3' monophosphates (see section **1.1.5. The generation of the Antiviral State by IFN-α/β**). Malathi *et al* found that both MDA5 and RIG-I induced IFN-β upon RNase L activation, dependant on the presence of the 3' monophosphate groups generated by RNase L. A further study by the authors identified that RNase L products produced during HCV infection were able to bind to RIG-I and induce IFN-β (Malathi et al., 2010). Luthra et al. discovered an mRNA fragment from PIV5 that activated type-I IFN expression in a MDA5-dependent manner (Luthra *et al.*, 2011). Since type I IFN induction by this RNA required RNase L, the authors concluded that RNase L recognises and processes viral mRNA into a MDA5 activating structure.

Viral PAMPs of LGP2

The viral PAMPs that activate LGP2 have yet to be fully characterized. As mentioned previously, the CTD of the RIG-I inhibiting helicase LGP2 is closely related to the RIG-I CTD (Li *et al.*, 2009b; Pippig *et al.*, 2009). Similar to RIG-I, LGP2 was reported to preferentially bind to blunt ended dsRNA (Li *et al.*, 2009b; Murali *et al.*, 2008; Pippig *et al.*, 2009), in a 5′-ppp independent manner. Amino acids mediating the interaction with the 5′ terminal base pair and the ribose backbone are conserved or at least functionally related between the RIG-I and the LGP2 CTD, while triphosphate-interacting amino acids were found to be involved in dsRNA binding of the LGP2 CTD. Mutation of lyseine amino acids in the LGP2 CTD led to a loss of RNA binding but did not impair LGP2-mediated inhibition of RIG-I activation, suggesting a ligand-independent RIG-I inhibiting mechanism by LGP2 (Li *et al.*, 2009b)

1.2.5. PIV5 Inhibition of IFN mediated responses

To survive in nature all viruses appear to require a strategy to circumvent the IFN response. The evasion strategies can be classified as (i) generally inhibiting cellular transcription and/or protein synthesis, (ii) specifically inhibiting components of the IFN induction or IFN signalling pathways, or (iii) inhibiting IFN-induced factors that have antiviral activity (Randall & Goodbourn, 2008). PIV5 primarily follows the second strategy of inhibiting IFN induction and signalling (**Figure 10**). It has previously been shown that during PIV5 infection of cells in an IFN-induced antiviral state, there are significant changes to the localisation and pattern of virus protein synthesis and cytoplasmic bodies containing the NP, P and L proteins (Carlos *et al.*, 2005) and virus genomes (Carlos *et al.*, 2009).

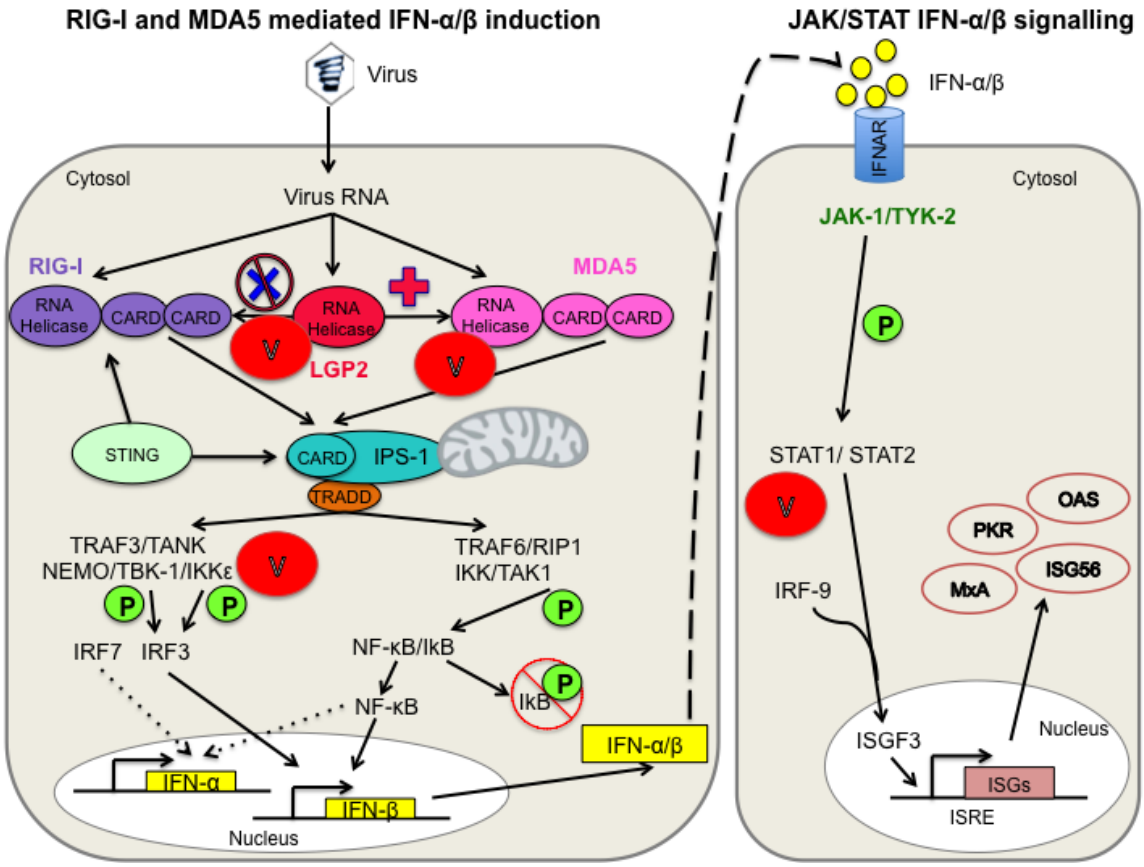

Figure 10. RIG-I and MDA5 mediated induction of IFN-α/β

PIV5 V protein inhibition of IFN induction:

The PIV5 V protein is able to bind to MDA5, inhibiting its activity. The V protein acts as a competitive inhibitor against MDA5s substrate, viral dsRNA. The V protein also binds to LGP2 and RIG-I, forming a trimeric complex. As LGP2 is a natural inhibitor of RIG-I, the PIV5 V protein mediated trimeric complex leads to the inhibition of RIG-I mediated signalling.

PIV5 V protein inhibition of IFN signalling:

The PIV5 V protein binds to STAT1, targeting it for proteasomal mediated degradation.

Figure adapted with permission from an original figure by Andri Vasou, University of St Andrews.

Under these conditions the virus continues to slowly spread from cell-to-cell despite inducing limited amounts of IFN. The IFN induced antiviral state is extremely effective at reducing virus replication. However, PIV5 is not eliminated from these cells, whereby PIV5 is localised in cytosolic bodies whilst the V protein dismantles the antiviral state by the V protein targeting STAT1 for proteolytic degradation (Andrejeva *et al.*, 2002; Didcock *et al.*, 1999; Precious *et al.*, 2007; Young *et al.*, 2000). Destruction of STAT1 leads to the absence of continuous IFN signalling, in which the cell cannot maintain its anti-viral state indefinitely, and eventually normal virus replication is established. Nevertheless, the potential of IFN to significantly slow virus spread presents a formidable obstacle, and thus the V protein has evolved to antagonise IFN induction as acting as a competitive inhibitor of TBK-1 (Lu *et al.*, 2008) and via inhibition of the PRRs.

PIV5 V protein inhibition of MDA5 mediated signalling

The PIV5 V protein (as well as those of other paramyxoviruses) can limit IFN induction by competitively competing with MDA5 ligands and directly binding to MDA5, inhibiting its activity (Andrejeva *et al.*, 2004; He *et al.*, 2002; Poole *et al.*, 2002). The V protein only directly binds to MDA5 and not to RIG-I, whereby MDA5 mediated activation of the IFN-β promoter was inhibited (Childs et al., 2007; Yoneyama et al., 2005) . The mechanism of action of V inhibition of MDA5 has been proposed to involve the inhibition of MDA5 homo-oligomerisation. As mentioned previously, activation of MDA5 by dsRNA requires homo-oligomerisation through its helicase domain. Since the V-binding site of MDA5 has been mapped to a stretch of residues in its C-terminal helicase domain, the V protein competes with dsRNA ligands for MDA5 binding, to inhibit MDA5 oligomerisation (Childs *et al.*, 2007; 2009).

PIV5 V protein inhibition of RIG-I mediated signalling

The PIV5 protein inhibits RIG-I mediated induction of IFN by binding to LGP2.

The PIV5 V protein (as well as those of other paramyxoviruses) interacts directly with LGP2 (Parisien et al., 2009). Yeast hybridization studies and co-immunoprecipitation studies (Childs *et al.*, 2012b) showed that a complex is formed between V and LGP2, and between RIG-I, LGP2 and V, but not between RIG-I and V confirming previous results (Childs *et al.*, 2007). LGP2 and the V protein were shown to co-operatively inhibit IFN induction via luciferase assays following influenza A infection and with induction by artificial RIG-I RNA ligands. The V protein exploits the LGP2 mediated inhibition of RIG-I to impede the induction of IFN.

Observations on the Induction of IFN by PIV5 and interference by the PIV5 V protein

The current model of IFN induction holds that viruses generate viral RNA PAMPs during their normal replication cycle. Seminal studies by Marcus and colleagues in the 1970s and 1980s generated a paradigm in which both RNA and DNA viruses induced IFN by the production of viral dsRNA (Marcus & Sekellick, 1977; Sekellick & Marcus, 1985). Thus, negative-sense RNA viruses were proposed to generate a dsRNA molecule dependent upon transcription, positive-stranded RNA viruses to generate a dsRNA molecule via replication, and even DNA viruses were proposed to generate dsRNA as a result of convergent transcription that induced IFN.

Further developing this model, it is assumed that the IFN inducing PAMPs generated during PIV5 wild-type replication are effectively suppressed by the V protein IFN antagonist. This is supported by the observations that PIV5 has been found to establish highly productive long term persistent infections in many tissue culture cell

lines with only minimal activation of host cell antiviral responses (Choppin, 1964; Hsiung, 1972; Young *et al.*, 2007). In epithelial cells, PIV5 is a poor inducer of IFN, where infected cells display very low levels of Type I IFNs and other proinflammatory cytokines such as IL-6 (Didcock *et al.*, 1999; He *et al.*, 2002; Poole *et al.*, 2002; Wansley & Parks, 2002). This has further been displayed in primary cultures of human epithelial cells (Young & Parks, 2003) and monocyte-derived dendritic cells (Arimilli *et al.*, 2006). In addition, further studies were carried out using a PIV5 recombinant virus called PIV5 VΔC. PIV5 VΔC makes a non-functional C-terminally truncated V fragment. PIV5 VΔC thus lacks a functional V protein and therefore it does not have a functional IFN antagonist. Infection of cells with PIV5 VΔC generated severely reduced plaques compared to the wildtype virus (He *et al.*, 2002; Poole *et al.*, 2002). Molecular studies showed that PIV5 VΔC is extremely sensitive to the IFN system, being unable to either block IFN signalling or limit IFN production. Complicating this picture is that the limited induction of IFN generated during wild-type virus infections can still exert an antiviral effect that limits viral replication. PIV5 produces larger plaques on cells that have been engineered to either fail to produce or respond to IFN than they do on unmodified IFN-competent cells (Young *et al.*, 2003). The apparent incomplete block to the IFN system suggests that the PAMPs of the PRRs are being produced during virus infection and inducing IFN, and that this is a dynamic and complex process.

However, the interactions between wild-type virus PAMPs and the PRRs have not been characterised and the corresponding structures have not been reported in the literature. To confirm that PIV5 PAMPs were generated from wild-type virus replication, the Randall group studied the induction of IFN by PIV5 at the single-cell level. A549 cells expressing GFP under the control of the IFN-β promoter were infected with PIV5 VΔC (Killip *et al.*, 2011). They demonstrated that infection of these reporter cells with PIV5 VΔC, strikingly, does not activate the IFN-β promoter in

the majority of infected cells, despite the absence of the IFN antagonist. This indicates that the viral PAMPs capable of activating the IFN induction cascade are not produced or exposed during the normal replication cycle of PIV5, and these results suggest instead that another source, such as defective interfering viruses generated during virus replication, are primarily responsible for inducing IFN during PIV5 infection.

1.2.6. Defective Interfering Particles as potential primary inducers of Interferon

Defective interfering Particles (DIs) are incomplete copies of the wild type virus spontaneously generated during wild type virus replication, due to errors in the viral polymerase (Reviewed in (López, 2014). DIs of negative sense RNA viruses were first described for influenza virus in the late 1940s (Magnus, 1947) , and were first identified in paramyxoviruses over 30 years ago for SeV and VSV (Kolakofsky, 1976; Lazzarini *et al.*, 1981; Leppert, 1977; Perrault, 1981). It has since been found that DIs are generated during replication of other paramyxoviruses. These DIs are subgenomic and contain deletions (often extensive) that render the virus unable to complete a full replication cycle by themselves in the absence of co-infecting, wild type non-defective, “helper” viruses. Just as for their respective wild type genomes, SeV and VSV DI genomic replication follows the “rule of six”, whereby for efficient replication the genome length is a multiple of 6 (Calain & Roux, 1993; Pattnaik *et al.*, 1992). For PIV5 DIs, the rule of six is optimal but not essential for efficient DI replication (Murphy & Parks, 1997). The replicated DI RNAs were shown to assemble into virus particles.

DIs efficiently inhibit the replication of non-defective genomes due to the replicative advantage conferred by their smaller genome size, or through successful competition for viral or host factors that are required for genome replication. DI genomes have therefore the ability to successfully compete with their helper non-defective genomes for the viral replication substrates provided by the latter; hence, they are also "interfering" (Kolakofsky, 1979; Lazzarini *et al.*, 1981; Leppert, 1977; Perrault, 1981; Wu *et al.*, 1986) Further to this, a characteristic feature of DI particles is their emergence and outgrowth during high multiplicities of infection (MOI), where numerous copies of the wild type non-defective virus infect each host cell. Ecological models of predator-prey behaviour have been proposed and examined to describe the kinetics of paramyxoviruses and influenza A virus DI particle populations in relation to non-defective virus genomes (Bangham, 1990; Thompson & Yin, 2010) (Kirkwood & Bangham, 1994; Frank, 2000; Frensing *et al.*, 2013; Nelson & Perelson, 1995; Szathmáry, 1992; 1993). Under such conditions "predator" DI particles can productively utilize the resources such as NP and viral RNA polymerase of "prey" non-defective viruses. DI genomes invariably accumulate in the cell, whereby the DI levels reach a tipping point whereby no viral substrates are available due to the lack of non-defective virus being replicated. As a result DI levels rapidly decrease or "crash" until enough non-defective virus genomes have been replicated, whereby the cycle repeats itself.

Four potential DI genomes can be generated for PIV5 and paramyxoviruses from either or both from the genome strand or the antigenome strand during replication (**Figure 11, Figure 12**). Firstly, DI genomes are generated that have extensive internal deletions between the 5' and 3' terminus (**Figure 11i**). Internal deletion DIs are essentially truncated versions of the wild type virus genome that usually share the 3' and 5' termini with the wild type virus. They retain the leader and trailer sequences of the genome and therefore possess transcription and replication signals

and have been shown to generate viral translation products (Hsu *et al.*, 1985) (Re & Kingsbury, 1986). Internal deletion DIs are generated when the viral polymerase falls off the original template and reattaches further downstream, resulting in a genomic deletion. A second form of the internal deletion DIs comprises an authentic 5′ terminus and an inverted repeat of the same terminus at the 3' end (**Figure 11ii**).

Copyback DIs (**Figure 11iii, iv**) comprise of a segment of the viral genome flanked by reverse complementary versions of its 5' terminus. Copybacks occur when the viral polymerase detaches from the template and reattaches to the newly synthesizing strand, copying back the 5' terminus end of the genome. In the absence of nucleoproteins that would prevent base pairing, the copyback DI RNA can form a panhandle structure, formed by the authentic 5' terminus complementary binding to the corresponding bases of the inverted 3' terminus (**Figure 11iv**). The panhandle structure thus consists of a short complementary stem region and a loop region. 5' leader copyback DIs are formed during replication from the genomic strand, with complementary $5'–3'$ ends. Similarly, a 3' trailer copyback DI can be generated from the antigenomic strand as well. Given the prevalence of DIs that are generated during wild type virus replication, it is unsurprising that it has been found that DIs interact and influence the host innate immune response.

DIs and the induction of IFN-β

Various groups have characterised some of the interactions between DIs and the induction of IFN-β. Strahle *et al* infected HEK293 IFN-β promoter reporter cells with SeV stocks containing DI copybacks, and found that the presence of DI copybacks correlated with that of the activation of the IFN-β promoter (Strahle *et al.*, 2006).

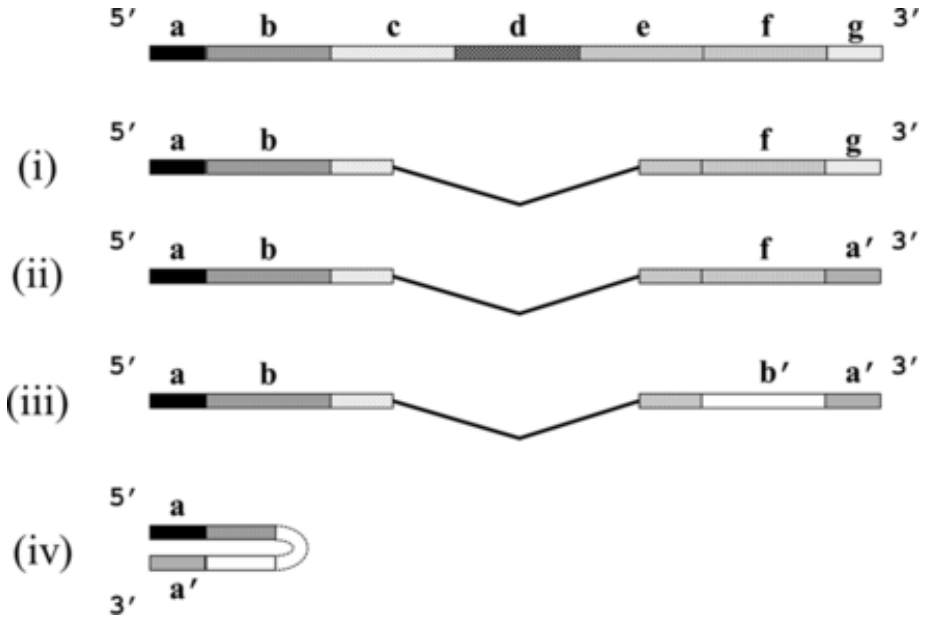

Figure 11. Schematic of the different types of DI RNA (not to scale).

The virus genome is shown at the top with terminal sequences containing the replication signals labelled at the 5′ terminus (a) and at the 3′ terminus (g). The remainder of the genome is arbitrarily divided into sections to indicate the possible origin of some of the DI RNA sequences.

Section (i): Internal Deletion

Section (ii): Internal Deletion with inverted repeat (a') of the 5' (a) sequence.

Section (iii): Copyback DIs

Section (iv): Copyback DI with panhandle "loop" structure

See text for details of sections i to iv.

Figure taken from (Dimmock and Easton, 2014)

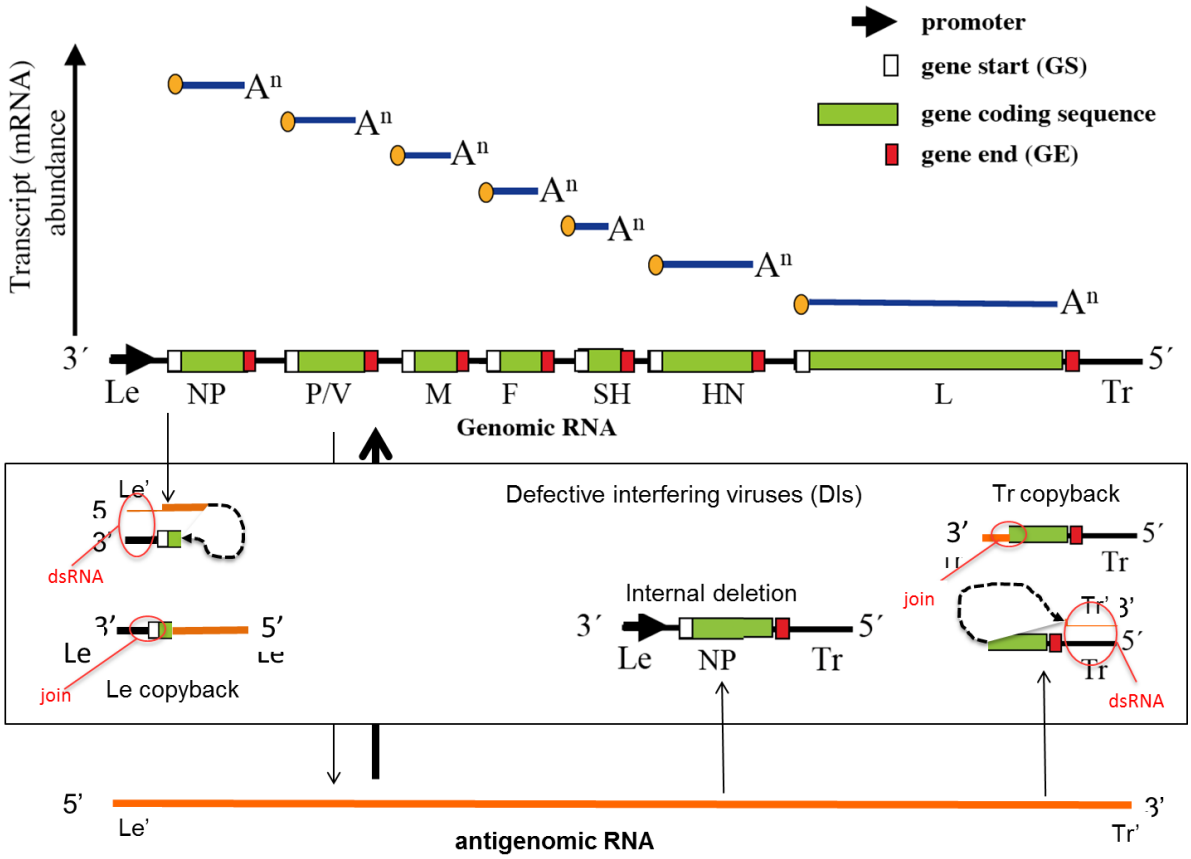

Figure 12. PIV5 potential DIs

Le copybacks, Tr copybacks and internal deletion DIs are spontaneously generated during wild type virus replication due to errors by the viral polymerase. PIV5 DIs can potentially be generated from either or both from the genome strand and the antigenomic strand. See text for details.

Figure modified from an original figure supplied generously by Rick Randall, University of St Andrews.

The level of IFN-β activation was found to be proportional to that of DI genome replication and to the ratio of DI to non-defective genomes during infection. Another group showed this using the same system for infections with DI rich stocks of VSV (Panda *et al.*, 2010). It was found that DI rich stocks not only upregulated the induction of IFN-β, but also upregulated IFN-β signalling via the ISRE promoter. Further studies by Strahle *et al.* have correlated Sendai virus (SeV) induced RIG-I activation with the occurrence of copyback DI genomes (Strahle *et al.*, 2007). The copybacks that are generated during infection are not always encapsidated, and are thus able to form the snapback panhandle structures in infected cells. In concordance with this data, by applying a deep sequencing approach after purification of RNA attached to RIG-I from SeV infected cells, Baum *et al*. determined preferred binding of DI genomes to RIG-I (Baum *et al.*, 2010). Similarly to RIG-I, Yount *et al.* has demonstrated that MDA5 can detect SeV DI particles *in vitro.* The authors created a dendritic cell line which constitutively expresses the SeV V protein (DC2.4), a viral antagonist that inhibits MDA5 (but does not inhibit RIG-I). Using QPCR to detect levels of IFN-β, it was found that infection of DC2.4 and of dendritic MDA5 knockout cells with a SeV DI enriched stock, displayed decreased levels of IFN-β compared to naïve dendritic cells. In all of the studies mentioned previously, it was found that the DIs normally generated during wild-type virus replication for VSV and SeV were copyback DIs. Furthermore, infection with stocks enriched for copyback DIs were found to be far greater inducers of IFN-β than infection with internal deletion DI enriched stocks. Clearly, there is an interplay between copyback DIs, the PRRs and the induction of IFN-β, which remains to be fully elucidated.

Characterizing PIV5 DIs

This project uses PIV5 as a model for other paramyxovirus infections. In order to investigate the mechanisms by which DIs interact with the PRRs and induce IFN-β, it is first necessary to characterise the specific types of DIs generated during PIV5 (wt) replication. PIV5 has the potential to generate leader copybacks, trailer copybacks and internal deletion DIs during virus replication (**Figure 12**). Killip *et al.* investigated the types of DIs produced during high MOI passages of PIV5 (wt) and of PIV5 VΔC (Killip *et al.*, 2013). Sequential high MOI passages are referred to as VM1, VM2, etc., after Von Magnus (Magnus, 1947). PIV5 VΔC DI rich preparations (PIV5 VΔC VM2) are utilised as they have been previously been shown to be efficient inducers of IFN-β (Chen *et al.*, 2010; Killip *et al.*, 2011). Furthermore, PIV5 VΔC VM2 DIs can be readily detected as opposed to infections with non-DI enriched stocks of PIV5 VΔC VM0 and PIV5 (wt) VM0. Preparations of PIV5 that are enriched for DIs are generated by high multiplicity passage in Vero cells (that do not produce IFN) in order to accumulate DI genomes. Nucleocapsid RNA from these virus preparations was extracted and subjected to deep sequencing. Sequencing data were analysed using methods designed to detect internal deletion and copyback DIs, in order to identify and determine which species of DIs were most abundant (**Figure 13**).

Deep sequencing analysis of RNA extracted from PIV5 (wt) VM12 infected cells showed that the vast majority of DIs generated during high MOI passaging at VM12 are trailer copybacks (**Figure 13B**). For PIV5 VΔC, the generation of DI enriched preparations was much quicker, at VM2 (**Figure 13A**).

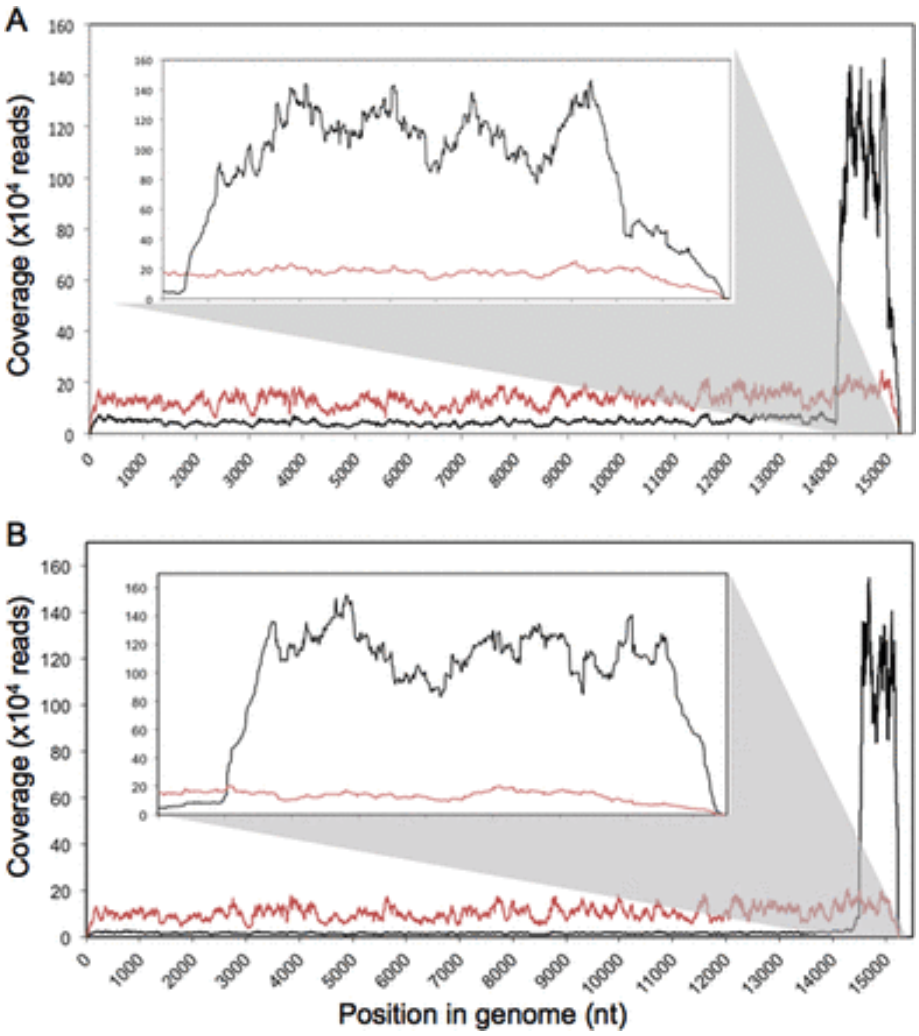

Figure 13. Deep sequencing analyses of RNA isolated from Vero cells infected with PIV5 DI enriched preparations.

Viral RNPs were extracted from Vero cells infected with PIV5 VΔC VM0 and VM2. Associated RNA was subjected to deep sequencing using the Illumina GA2x platform, and sequencing reads were mapped to the PIV5 VΔC (A) or the PIV5 (wt) reference genome. The frequency of reads at each nucleotide is shown in red for VM0 virus preparations and in black for the DI rich virus preparations PIV5 VΔC VM2 (**A**) and PIV5 (wt) VM12 (**B**). Coverage from nt 14000 to 15246 is shown as an inset in order to highlight the peaks at the 5′ end of the genome. See text for details.

Figure taken from (Killip *et al.*, 2013).

The V protein itself may play a role in regulating DI generation, leading to PIV5 VΔC accumulating DIs at a higher rate than PIV5 (wt). Like PIV5 (wt) VM12, the vast majority of PIV5 VΔC VM2 DIs are trailer copybacks. That the majority of DIs found are trailer copybacks reflects the need for the 3' antigenomic promoter to be stronger than the 3' genomic promoter (which directs antigenome synthesis and transcription), reflecting the requirement of the virus to generate greater numbers of genomes for virus assembly than antigenomes.

Killip *et al.* identified a range of distinct trailer copybacks, and these varied considerably in the site of the copyback error, the length of the predicted dsRNA stem, and the size of the DI genome. Furthermore, no major trailer copyback species were detected that were present in both PIV5 (wt) and PIV5 VΔC DI rich preparations.

The lack of conserved copyback points suggested that there is no particular part of the trailer in which a template switching error is substantially more likely to occur. In addition, during PIV5 (wt) VM12 infections, and during co-infections of PIV5 (wt) vM0 and DI rich virus preparations it was found that interference from co-infecting DI trailer copybacks impaired the replication of non-defective PIV5 (wt), consistent with previous findings for SeV, Influenza A and VSV as mentioned previously. These previous studies have been conducted with virus preparations at high MOI infections. The disadvantage of this method is that even with infection with stocks not enriched for DIs, it is still possible for DIs to be present in these stocks and co-infect with wild type viruses during a high MOI infection. In order to determine the impact of DIs generated exclusively during infection and replication, a low MOI infection needs to be carried out in which the initial infection is only by a wild type non-defective virus.

Features of the PIV5 Trailer copyback DI

The PIV5 trailer copyback is generated due to template switching of the viral RNA polymerase from the antigenome to the nascent strand during synthesis of genomic RNA (**Figure 14**). The viral RNA polymerase thus uses the nascent genomic strand as the template for further RNA synthesis. The 3′- genomic promoter in trailer copyback DI genome has been replaced by a sequence complementary to the 5′ antigenomic promoter of the termini of the DI trailer copyback. These complementary sequences are able to bind together and form a dsRNA stem-loop structure when SDS treatment is used to dissociate the RNA genomes from encapsidating NP protein (Kolakofsky, 1976). It is this structure that is thought to be responsible for the ability of DI trailer copybacks to act as potent inducers of IFN (Baum *et al.*, 2010; Killip *et al.*, 2011; Shingai *et al.*, 2007; Strahle *et al.*, 2006). The substitution of the weak genomic promoter for the stronger antigenomic promoter in DI trailer copyback genomes additionally confers a significant replicative advantage over non-defective virus genomes, and this leads to their accumulation in virus stocks that are generated at high multiplicity.

1.2.7. Investigating PIV5 DIs: The A549 pr/(IFN-β).GFP Reporter cell line

To enable examination of IFN-β promoter activation by PIV5 DI rich and non-DI rich preparations, we can use the A549 pr/(IFN-β).GFP reporter cell line that was developed and characterised by Shu Chen to follow the dynamics of IFN induction (**Figure 15A**). A549 pr/(IFN-β).GFP reporter cells express green fluorescent protein (GFP) under the control of the IFN-β promoter. A549 naïve cells were infected with a lentivrus containing the pdl′pIFNβ′GFP plasmid, and subsequently underwent selection.

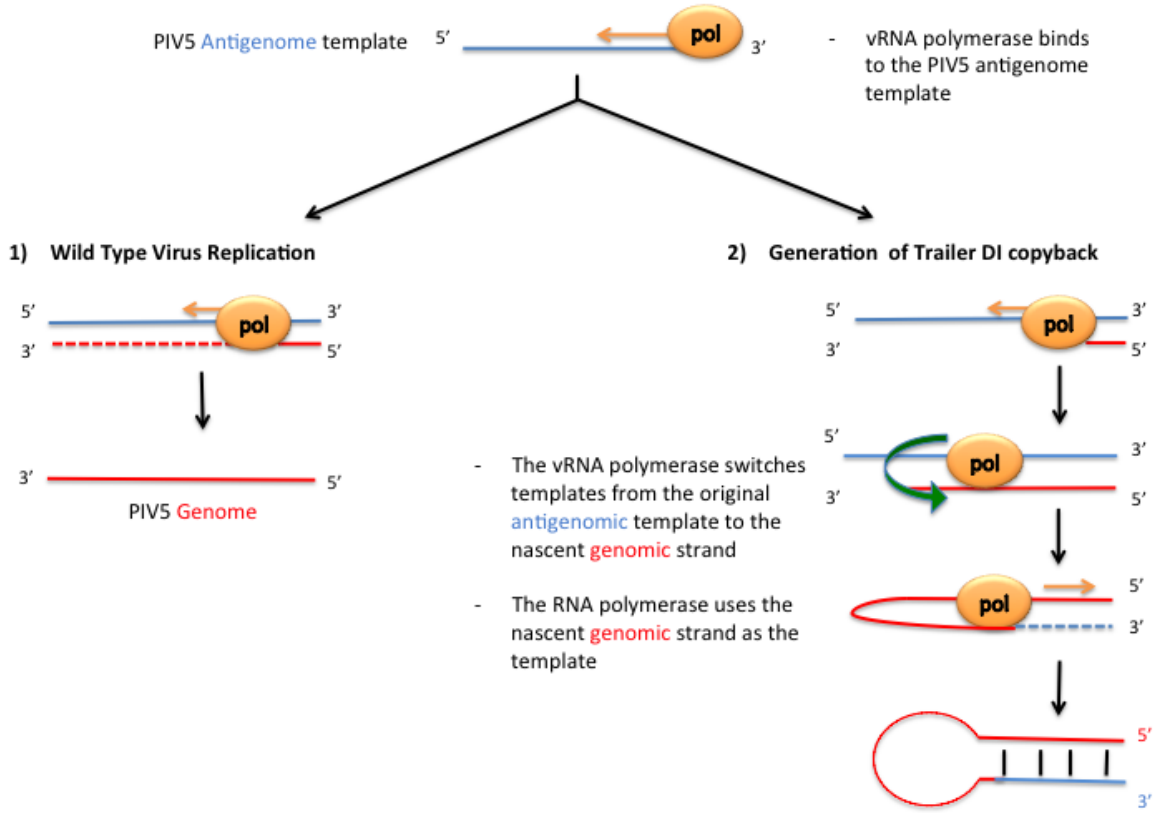

Figure 14. Generation of the PIV5 Trailer copyback DI.

1) Wild Type Replication

- Replication occurs normally by the viral RNA polymerase
- Full length Genomic strand is generated from the antigenomic template

2) Generation of PIV5 Trailer copyback DI

- The vRNA polymerase switches templates from the original antigenomic template to the nascent formed genomic strand
- The vRNA polymerase uses the nascent genomic strand as the template
- An antigenomic sequence that is complementary to the genomic template is generated. The antigenomic sequence binds to the corresponding nts on the genomic sequence forming a stem structure and a loop.

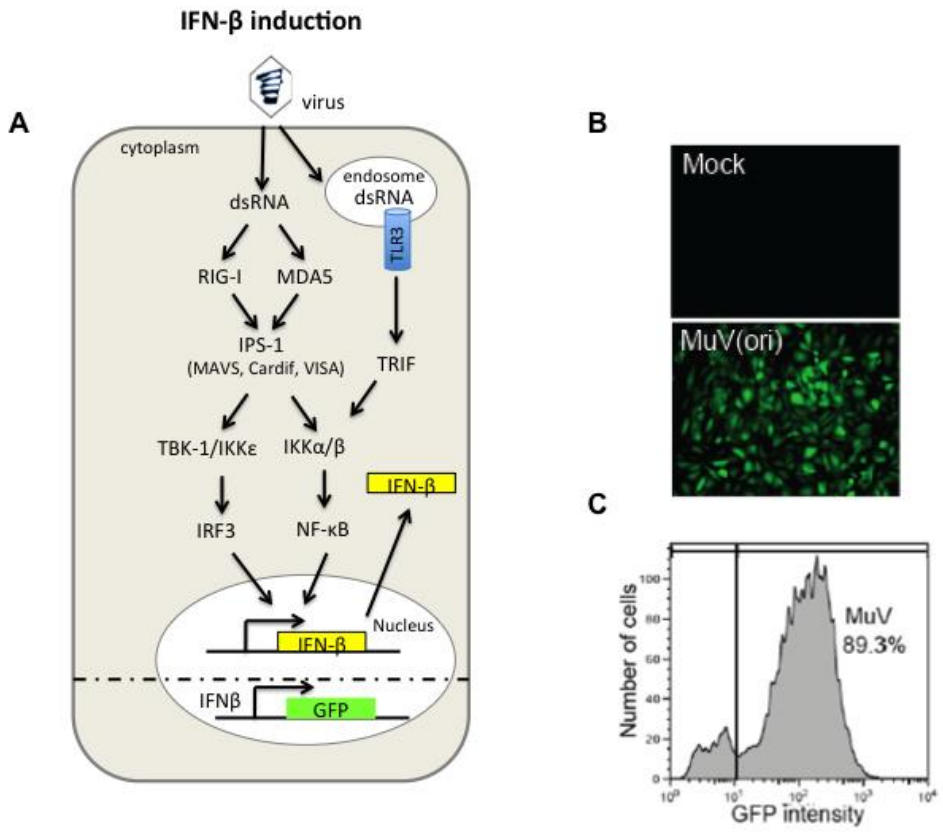

Figure 15. The A549 pr/(IFN-β).GFP reporter cell line

A) In the A549/pr(IFN-β).GFP reporter cell line (Naïve reporter cells), GFP expression is under the control of the IFN-β promoter

B) Confluent monolayers of Naive reporter cells were grown in 60 mm dishes that contained coverslips and infected at MOI 10 with MuV(ori). At 8hrs p.i. the coverslips were fixed and those cells expressing GFP visualised using a Nikon Microphot-FXA fluorescence microscope.

C) Naive reporter cells were infected with MuV (Ori) at MOI 10. At 8hrs p.i. cells were trypsinised to a single cell suspension and the percentage of GFP+ve cells estimated by flow cytometry analysis.

See text for details.

Figure modified from (Chen *et al.*, 2010)

The resulting cells were screened for their ability to express GFP following infection with a stock of MuV that contains a high number of DIs that is a good inducer of IFN-β (**Figure 15B**). At 8 hours p.i. 90% of the cells were strongly positive for GFP, indicating that the vast majority of cells were able to respond to the presence of a PAMP. Flow cytometry analysis of MuV infected cells showed that a discrete population of cells were strongly positive for GFP expression, as opposed to there being a gradient of GFP expression. This suggests that the IFN-β promoter is either **'**on**'** or **'**off**'** in infected cells (**Figure 15C**). In conclusion, the expression of GFP under the control of the IFN-β promoter in the A549 pr/(IFN-β).GFP reporter cell line (referred to as naïve reporter cells from now on), is a reliable marker to identify cells that are positive for activation of IFN-β induction and it has been shown that these cells faithfully report activation of the IFN-β induction cascade (Chen *et al.*, 2010; Killip *et al.*, 2011).

1.3. Aims

This thesis firstly investigates the nature of the host cellular IFN-β response to virus challenge by negative strand viruses. Secondly, the roles of the PRRs RIG-I, MDA5 and LGP2 in the induction of IFN-β following infection with negative strand viruses are investigated. Thirdly, PIV5 DIs generated during virus replication are investigated in their role as potential PAMPs of the cytosol PRRs RIG-I, MDA5 and LGP2, and the subsequent activation of the IFN-β promoter and induction of IFN-β.

2. MATERIALS and METHODS

2.1. Mammalian Cells and Tissue Culture

2.1.1. Cell lines used in this Study

A549 cells

A549 cells are human lung carcinoma cells routinely used to study paramyxovirus and Influenza A virus infection of the respiratory tract (European Collection of Cell Cultures (ECACC)).

A549 Npro cells

A549 cells expressing the Npro protein of BVDV.

A549/pr(IFN-β).GFP reporter cell line

With the A549/pr(IFN-β).GFP reporter cell line (Naïve reporter cells), GFP expression is under the control of the IFN-β promoter. Cell line originally generated by Shu Chen, University of St Andrews.

A549 pr/(IFN-β).GFP RIG-I Knock Down cell line

A549 pr/(IFN-β).GFP RIG-I Knock Down cell line (RIG-I KD reporter cells) expresses shRNA that knocks down RIG-I. Cell line originally generated by Shu Chen, University of St Andrews.

A549 pr/(IFN-β).GFP MDA5 Knock Down cell line

A549 pr/(IFN-β).GFP MDA5 Knock Down cell line (MDA5 KD reporter cells) expresses shRNA that knocks down MDA5. Cell line originally generated by Shu Chen, University of St Andrews.

A549 pr/(IFN-β).GFP LGP2 Knock Down cell line

A549 pr/(IFN-β).GFP LGP2 Knock Down cell line (LGP2 KD reporter cells) expresses shRNA that knocks down MDA5. Cell line generated by the author.

A549 pr/(IFN-β).GFP ISG56 Knock Down cell line

A549 pr/(IFN-β).GFP ISG56 Knock Down cell line (ISG56 KD reporter cells) expresses shRNA that knocks down MDA5. Provided by Lena Andrejeva, University of St Andrews.

HEK293T:

A highly transfectable derivative of the human embryonic kidney 293
Cell line, constitutively expressing the SV40 large T-antigen. Provided by Prof. R. Iggo, University of St Andrews.

MDCK

Canine kidney cells (ECACC).

Vero

Fibroblast-like cells established from the kidney of an African Green monkey (ICN Pharmaceuticals Ltd.).

2.1.2. Cell Maintenance

Cell monolayers were maintained in 25cm^2 or 75cm^2 tissue culture flasks (Greiner) in Dulbecco's modified Eagle's medium (DMEM; Invitrogen) supplemented with 10% (v/v) heat-inactivated foetal calf serum (FCS; Biowest) and incubated at 37^{o}C/ 5% CO_2. Cells were routinely passaged using trypsin/ethylenediaminetetraacetic acid (EDTA; Becton Dickinson Ltd.), and passed every 3-5 days as appropriate.

2.1.3. Cell line stock storage and resuscitation

Adherent cells were trypsinised, resuspended in DMEM/10% FCS, and centrifuged at 1000rpm for 5mins. Pelleted cells were resuspended in DMEM supplemented with 20% FCS and 10% (v/v) dimethyl sulfoxide (DMSO) and aliquoted into cryovials. Cell stocks were frozen at -70^{o}C, to slow down the temperature decrease, before long-term storage in liquid nitrogen. For resuscitation of cells, cryovials were thawed at 37^{o}C before centrifugation at 1000rpm. Pelleted cells were then resuspended and grown in DMEM/10% FCS at 37^{o}C/ 5% CO_2. Medium was replaced after 24 hours in order to remove traces of DMSO.

2.1.4. Treatment of cells

IFN treatment

Cells were treated overnight (at least 16 hours, unless where otherwise stated) with media supplemented with Roferon A recombinant human IFN-α-2a (Roche Diagnostics) at a concentration of 1000 units/ml in DMEM/10% FCS.

Z-VAD-FMK

Samples were treated with with Z-VAD-FMK Caspase family inhibitor (Enzo Life Sciences) at 100μM final concentration per sample. This was carried out at the same time as the infection of cells.

Transfections with plasmid DNA

Transfection of cells with plasmid DNA was carried out using FuGENE 6 transfection reagent (Roche) according to the manufacturer's instructions.

2.2. Viruses and virus infections

2.2.1. Viruses used in this study

PIV5 (wt)

Two original PIV5 isolates were isolated from rhesus and cynomolgus monkey kidney cell cultures and are referred to as WR and W3A (or W3) as wild-type (wt) viruses.

PIV5 VΔC

A mutant strain of PIV5 wt (W3A) has been isolated from a recombinant PIV5 (rSV5) which has deletions at the V protein specific C-terminal cysteine-rich domain (VΔC). This virus is unable to block IFN production or signalling.

PIV5 VΔC VM2 and defective interfering particles

PIV5 VΔC VM2 was generated from the original PIV5 VΔC stock by passaging PIV5 VΔC twice at a high MOI in confluent Vero cells This was performed in order to increase the ratio of defective interfering particles to non-defective virus within the virus population. Virus stocks kindly supplied by Dan Young (University of St Andrews, UK).

PIV2 (wt)

Parainfluenza virus 2 wild-type strain.

PIV3 (rwt)

Parainfluenza virus 3 recombinant wild-type strain.

Influenza A (Udorn)

Recombinant wild-type influenza A virus (A/Udorn/72; H3N2), provided by David Jackson (University of St Andrews, UK).

Bunyamwera Virus (wt)

Wild-type strain kindly provided by Richard Elliott.

2.2.2. Preparation of Virus stocks

PIV5 (wt), PIV3 (rwt), PIV2 (wt)

Vero cells at 90% confluency were infected with the virus master stock (prepared by Dan Young) and incubated at 37°C and 5% CO_2 until the

cytopathic effect was visible in the monolayer. Subsequently, the supernatant was harvested and centrifuged at 2000rpm for 5 minutes to remove cellular debris. The supernatant was then used to infect larger monolayers grown in roller bottles. Cells were incubated with the virus inoculum on a rolling platform for 1-2 hours at 37^{o}C before it was replaced with fresh DMEM supplemented with 2% FCS. When fusion could be detected in the cell monolayer (approximately two days later), the supernatant was harvested and centrifuged to precipitate cell debris, aliquoted into cryovials and stored at -70^{o}C.

Other Virus stocks

Stocks of PIV5 VΔC VM0 and PIV5 VΔC VM2 were maintained and kindly provided by Dan Young (University of St Andrews, UK).

Stocks of BUNV (wt) were maintained and kindly provided by Richard Elliott.

2.2.3. Virus infection

To infect with paramyxovirus isolates, monolayers were inoculated with virus diluted in DMEM supplemented with 2% FCS (with the exception of PIV3 (rwt) with no FCS) at an appropriate multiplicity of infection (MOI), or DMEM only (for mock infections). For virus infections in 6-well plates, cells were inoculated in a volume of 1ml per well and placed on a rocking platform at 37°C for an adsorption period of 1-2 hours. Inoculations in 96-well plates were carried out without rocking in a volume of 50µl per well. Virus inoculum was then removed and replaced with DMEM/ 2% FCS. Cells were incubated at 37°C/ 5% CO_2 until harvested.

Influenza A (Udorn) infections were carried out in serum-free DMEM. Monolayers were washed in DMEM prior to infection to remove all traces of serum. Cell monolayers were infected with 400µl virus (per well of a 6-well plate) diluted in serum-free DMEM at an appropriate MOI (or DMEM only for mock infections). Cells were incubated for 1hr at 37°C, with gentle agitation at regular intervals. Inoculations in 96-well plate were carried out as for paramyxoviruses (see above). Virus inoculum was removed and replaced with serum-free DMEM. Cells were incubated at 37°C/ 5% CO_2 until harvested.

2.2.4. Virus Titration

To titrate paramyxovirus isolates, Vero cells were grown in 6-well plates (Greiner, UK) until 80-90% confluent. Cells were incubated with 10-fold dilutions of virus and DMEM containing 2% FCS (1 ml/well). After 1 hour on a rocking platform at 37ºC the inoculum was removed and 5-7 ml of medium overlay (0.5% Methicel; Sigma-Aldrich) was added to each well. Cells were incubated at 37ºC and 5% CO_2 for 10-12 days until plaques had formed in the monolayer. The overlay was then aspirated and plaques were fixed with 5% formaldehyde in PBS for 10-15 minutes. Plaques were stained with crystal violet (0.1% crystal violet, 3.6% formaldehyde, 1% methanol, 20% ethanol in H_2O). Virus titres were then estimated in pfu/ml, taking into account the original dilutions made.

Titration of influenza A (Udorn) was carried out on confluent MDCK monolayers in 6-well plates. Cells were washed twice in serum-free DMEM in order to remove all traces of serum. Virus preparations were serially diluted 10-fold in serum-free DMEM, and cells were inoculated with 400µl of each virus dilution per well. Cells were incubated at 37°C/ 5% CO_2 and plates were agitated every 10 minutes to

ensure even adsorption of the virus. During this period, 2x overlay medium (13.4g DMEM/3.7g $NaHCO_3$ per 485ml water supplemented with 4µg/ml NAT) was incubated at 37°C. 2% agarose in water was melted and placed in a 55°C water bath until required. After an adsorption period of 1 hour, virus inoculum was removed, the 2x overlay medium and the 2% agarose (Biogene Ltd.) were mixed in a 1:1 ratio, and 2ml of this was added to each well. After the overlay had set, plates were inverted and incubated at 37°C/5% CO_2 until distinct plaques had formed (~3 days). Cells were fixed by adding 2ml PBS/5% formaldehyde/ 2% sucrose on top of the agarose plugs, and the monolayers were left to fix overnight. Agarose plugs were then removed and plaques were stained with crystal violet.

2.3. Plasmid DNAs

2.3.1. Plasmids used in this study

pJET-PIV5-A1/C

This plasmid encodes the PIV5 VΔC VM2 Large DI, present at the highest proportion of total DIs following detection by deep sequencing of high MOI passages of PIV5 VΔC (Killip *et al.*, 2013). The Large DI A1/C primer PCR product is 965bps in size. The plasmid was generated by Craig Ross, Goodbourn group, St George's Hospital. Medical School.

pJET-PIV5-A3/C

This plasmid encodes the Small DI, present as the second highest proportion of DIs following detection by deep sequencing of high MOI passages of PIV5 VΔC (Killip *et al.*, 2013). The Small DI A3/C PCR product is 220bp in size. The plasmid was generated by Craig Ross, Goodbourn group, St George's Hospital. Medical School.

pCAGGS-PIV5-NP

The pCAGG-PIV5-NP plasmid encodes the full length NP of PIV5. This plasmid was kindly donated by Dr. Lena Andrejeva, University of St Andrews.

pCMVR8.91

Plasmid expressing the gag/pol, tat and rev genes of HIV-1 (used in lentivirus production, provided by Y.-H. Chen).

pMD-G

Plasmid expressing the vesicular stomatitis virus glycoprotein (VSV-G) gene (used in lentivirus production, provided by Y.-H.Chen).

pdlNOTI MCS R-IRF3

IRF3 is under the control and driven by the SFFV promoter.

p.LKO.1-puro shRNA LGP2

LKO.1-puro plasmid expressing a shRNA against human LGP2 kindly provided by Prof. Steve Goodbourn, originally purchased from Sigma-Aldrich.

2.3.2. Generation of plasmid stocks

E. coli DH5α cells were grown in Luria-Bertani (LB) medium (10g/l bacto-tryptone, 5g/l yeast extract, 10mM NaCl, pH 7.5), or plated on solid LB medium supplemented with 1.5% (w/v) agar and 10mM $MgSO_4$. As appropriate, media was supplemented with ampicillin (100 µg/ml) for selection.

Transformation of competent cells

1µg plasmid was added directly to 100µl of thawed, competent cells (Invitrogen). After incubation on ice for 1h, cells were transferred to a 42^{o}C water bath for 2mins before being immediately returned to ice for a further 2mins. Cells were resuspended in 1ml LB broth and incubated at 37^{o}C for 1h. The cell suspension was plated out onto LB-agar plates supplemented with ampicillin (90 mm-diameter Petri dishes;

Scientific Laboratory Supplies Ltd., U.K.). Plates were inverted and incubated at 37°C overnight. Mini-cultures were prepared from selected colonies.

Preparation of plasmid DNA

To produce large scale plasmid DNA preparations, 100ml of bacterial culture was grown overnight in a 37°C shaking incubator. DNA was extracted from cells using the QIAfilter Plasmid Maxi-Prep Kit (according to the manufacturer's instructions; QIAGEN).

2.3.3. Measurement of Plasmid concentration

The concentration of plasmid DNA was quantified by measurement of Abs_{260} using a NanoDrop ND-1000 spectrophotometer (Thermo Scientific). DNA purity was estimated by calculating the Abs_{260}/Abs_{280} ratio. Ratios greater than 1.8 were considered acceptable.

2.4. Lentivirus generation of transient cell lines

The pdINOTI MCS R-IRF3 plasmid was transfected using FuGENE 6 transfection reagent following the standard Promega protocol. Mock cells were transfected with an empty vector. 48 hours post-transfection, cells were trypsinised and fixed with 5% formaldehyde/ PBS in suspension, before resuspension in suspension solution (5% FCS/ PBS). Cells were then analysed by flow cytometry for GFP expression.

2.5. Lentivirus generation of stable cell lines

Lentivirus Production

To generate recombinant lentivirus, a 75 cm^2 tissue culture flask HEK293T cells (70% confluent) was co-transfected with three plasmids: 3µg pCMVR8.91, 3µg pMD-G, and 5µg of the pdl vector containing the construct of interest. Supernatants were harvested at 48 hours and 72 hours post-transfection and pooled. Cellular debris was removed by centrifugation at 3,000x*g* for 10mins and filtering through 0.45µm Tuffryn membrane filters (Invitrogen). Virus aliquots were stored at -70^oC until required.

Transduction

30% confluent target cell monolayers (25cm^2 flask) were infected with the harvested lentivirus supernatant (estimated MOI of 1 pfu/cell) in the presence of polybrene (8µg/ml; Sigma-Aldrich). 48 hour post-infection, transformed cells were selected by resistance to puromycin (Invivogen); MRC5 cells, 1µg/ml; A549 cells 2µg/ml. Puromycin-containing medium was replaced every four days until control naïve cells were dead. Cells were kept under continuous selection with puromycin.

Subcloning

Subcloning was required to generate LGP2 KD reporter cell line. Cells were trypsinised, counted using a haemocytometer, and diluted to around 1 cell/100µl in DMEM (10%FCS), and plated into 96-well microtitre plates (Greiner Bio-One, UK).

To compensate for mis-counting, cells were also diluted to 3 cells/100µl, and 1 cell/ 300µl, and plated into 96-well microtitre plates. Cells were normally cultured, replacing growth medium every 3-7 days, and observed under the microscope to pick single cell colonies growing in single wells. The cells from selected wells were trypsinised, and passed into either a 24-well microtitre plate (Nunc A/S, Denmark) or 25cm^2 tissue culture flask according to the growth rate and cell number. When enough cells were obtained from single cell colonies, candidate was tested via endpoint PCR for LGP2 mRNA expression. Colonies which showed most knock down of LGP2 were then frozen in DMEM (30% FCS, 10% DMSO) at either -70°C, or in liquid nitrogen for long-term storage.

2.6. Antibodies

2.6.1. Primary antibodies

Mouse Monoclonals

PIV5-NP-a; PIV5 NP; (Randall *et al.*, 1987)

PIV5-HN-4a; PIB5 HN; (Randall *et al.*, 1987)

PIV2; NP; Dan Young, University of St Andrews

PIV3: NP; Dan Young , University of St Andrews

MxA; a kind gift from Otto Haller, University of Freiburg, Germany,

β-actin; Sigma-Aldrich

Other Antibodies

Bun 592; Rabbit polyclonal Ab; Bun N; Kindly provided by Prof. Richard Elliott (University of St. Andrews)

α-X31 (H3N2, Udorn); Sheep Polyclonal Ab*;* A kind gift from A. Douglas, National (Institute for Medical Research, London)

2.6.2. Secondary antibodies

Anti-mouse, rabbit and sheep IgG Texas Red were from Oxford Biotechnology.

Phycoerythrin (PE) and Cy5 were supplied by Abcam.

Horseradish peroxidase (HRP)-conjugated anti-mouse IgG was supplied by Sigma-Aldrich.

2.7. Protein analysis

2.7.1. SDS-polyacrylamide gel electrophoresis

Mammalian cells were lysed by adding disruption buffer (6M Urea, 4% (w/v) SDS, 2M β-mercaptoethanol coloured with bromophenol blue).
Lysates were sonicated (15 seconds) to reduce viscosity and proteins were separated on 4-12% NuPAGE polyacrylamide gradient gels (Invitrogen) by

electrophoresis at 170V, 1 hour in MOPS [3-(N-morpholino) propanesulphonic acid] buffer (Invitrogen).

2.7.2. Immunoblotting

Proteins were separated by SDS-PAGE as described above and transferred to a polyvinylidene difluoride (PVDF) membrane using the XCell II Blot Module according to the manufacturer's instructions (Invitrogen). The membranes were then incubated for 30 minutes in blocking buffer (5% (w/v) skimmed milk powder 0.1% Tween 20 in PBS), followed by a further incubation for 1 hour to overnight with primary antibody diluted in blocking buffer. After three washes with 0.1% Tween 20 in PBS, membranes were incubated with secondary antibody conjugated with HRP for 1 to 3 hours. This was followed by washing again with 0.1% Tween 20 in PBS before proteins were detected using ECL Plus Western Blotting Detection Reagents (GE Healthcare). Membranes were then exposed to Kodak XOmat film.

2.8. Cell/virus Visualisation techniques

2.8.1. Immunofluorescence Microscopy

Cells were grown on 10mm coverslips and were fixed for 10mins in 5% formaldehyde/ 2% sucrose/ PBS then permeabilised with 0.5% NP-40/10% sucrose/PBS. Non-specific binding sites were blocked for at least 30 min with PBS/ 1% FCS/ 0.1% sodium azide, then monolayers were incubated with appropriately diluted primary antibody for 1 hour (10%FCS/PBS). Unbound antibody was washed

away with PBS, and cells were incubated for 1 hour with Texas Red (routine Nikon Microscopy) or PE conjugated secondary antibody (confocal microscopy) (Oxford Biotechnology Ltd., U.K.) in 10%FCS/ PBS solution.

If staining of the nucleus was required, the DNA-binding fluorochrome 4', 6-diamidino-2-phenylindole (DAPI; 0.5 µg/ml; Sigma Aldrich) was also added to this solution at 1/500. Coverslips were washed in PBS, fixed again in 5% formaldehyde/ 2% sucrose/ PBS and mounted on slides using Citifluor AF-1 mounting solution (Nikon microscopy) or Prolong Gold; Fermentas (confocal microscopy). All reactions were performed at room temperature in a humidified chamber. Immunofluorescence was visualised using a Nikon Microphot-FXA microscope or Zeiss Pascal Meta 510 Confocal Imaging system.

2.8.2. Immunostaining of Viral Plaque Assays

Fixed monolayers were permeabilised (0.5% IGEPAL, 10% sucrose/ 0.1% sodium azide in PBS) for 15 min, and then incubated in PBS supplemented with 1% FCS for 1 hour. Monolayers were incubated for 1 hour at room-temperature with 500µl/well of diluted (1/2000) primary antisera; diluted in PBS/10% FCS. Cells were washed with PBS/0.1% TWEEN, and monolayers were subsequently incubated for 1h at room-temperature with 500µl/well of the appropriate diluted (1/2000) secondary IgG alkaline phosphatase (AP)-conjugated antibody. Monolayers were subsequently washed with PBS/0.1% TWEEN, and incubated with 500µl/well of alkaline phosphatase substrate (as per manufacturer's instructions; Sigma-Aldrich) until plaques were easily visualised. Monolayers were rinsed with water in order to stop the reaction.

2.9. Flow cytometry analysis

2.9.1. Monostaining reporter cells

Following treatment/infection in a T25cm^2 flask, cells were trypsinised to a single cell suspension, fixed and permeabilised as for immunofluorescence, and immunostained with the mAbs. Viral NP was secondary stained with PE. Following immunostaining, cells were resuspended in 2% FCS/ PBS in BD Falcon 5ml polystyrene round bottom tubes. The percentage of fluorescent cells, and intensity of their fluorescence in 10,000 events was determined by using the LYSYS programme on a Becton Dickinson FACScan. Analysis of flow cytometry data was performed using the FlowJo programme

2.9.2. Live Cell sorting via flow cytometry

Following treatment/infection in a T25cm^2 flask, cells were trypsinised to a single cell suspension and resuspended in 2% FCS/ PBS. At all intermediate steps the cells are kept on ice. In order to determine the minimum number cells required for DI detection, an initial flow cytometry analysis was performed. GFP intensity was measured against side scatter (SSC). Cells were initially gated into two separate distinct populations, “true” GFP+ve and “true” GFP-ve cells. The middle population containing a mixture of GFP+ve and GFP-ve cells was discarded. Subsequently, cells were live sorted into discrete GFP+ve and GFP-ve populations into two collecting vials respectively. The cell sorter machine used was the Beckman Couture MOFLO (cytomation).

2.10. Nucleic acid analysis

2.10.1. Total cellular RNA extraction

Infected/treated cells were lysed using TRIzol (Invitrogen) with 2 ml per 25cm^2 flask. Cell lysates were incubated at room temperature for approximately 30 min before being transferred to 1 ml Eppendorf tubes and RNA was extracted according to the manufacturer's instructions.

Determination of RNA concentration

RNA concentration was determined using the same method as for DNA concentration as previously described.

RNA reverse transcription

Complementary DNA was generated in a two-step reaction using reagents from Promega, as described below. Samples were normalised based on the RNA used in the reaction, at 1µg. For housekeeping genes such as β-actin, the Oligo(dT) primer was used in the reverse transcription reaction.

RNA (1µg) X µl

Reverse primer (5µM) 1µl

H_2O up to 10µl

- Incubate for 10 min at 72°C in a thermocycler.

- Add the following:

dNTPs (10 mM each); 2µl

DTT (0.1 mM); 2µl

5x M-MLV buffer; 4µl

M-MLV (reverse transcriptase); 1µl

RNasin; 1µl

- Incubate for 1 hour at 42°C in a thermocycler.

2.10.2. Endpoint PCR

All PCR reactions were performed with the GoTaq DNA polymerase (Promega). Samples were transferred using pre-sterilised filter tips (Axygen). The reactions were prepared using 0.5 ml thin-walled tubes and analysed with a thermocycler, according to the parameters described below:

Standard PCR protocol using GoTaq DNA polymerase

5x reaction buffer 10µl

dNTPs (10 mM each) 1µl

DNA template x µl

Forward primer (2 µM) 1µl

Reverse primer (2 µM) 1µl

GoTaq polymerase (5U/ml) 0.25µl

ddH2O (up to 50 µl) x µl

PCR programme for GoTaq DNA polymerase

Polymerase activation; 95°C; 2min

Denaturation: 95°C; 30 sec

Annealing: 55°C; 30 sec } 25 cycles

Elongation; 72°C; 1 min

Final extension; 72°C; 10 min

2.10.3. Real-Time Quantitative PCR

Total cellular RNA was extracted using TRIzol as described above and 1µg of RNA was then used in a reverse transcription PCR reaction (total volume 20µl). The cDNA produced was subsequently used in the real-time quantitative PCR reaction, which was performed using a SYBR Green-based master mix (MESA Blue MasterMix Plus for SYBR Assay; Low ROX, Eurogentec). Primer concentrations were optimised for each primer pair. Reactions were prepared in 96-well flat deck thermofast real-time QPCR plates (Thermo-Scientific). The wells were sealed with a Thermaseal RTS (VWR) plastic seal followed by centrifugation of the plate at 1000 rpm for 2 minutes. The RT-QPCR reaction reagents are described below:

cDNA; 2.5µl

Forward primer (final concentration 100-300nM) 2.5µl

Reverse primer (final concentration 100-300nM) 2.5µl

MESA Blue MasterMix Plus, Low ROX; 12.5µl

RNase free ddH_2O; 5µl

Total reaction mix volume: 25µl

Real-time quantitative PCR programme:

Activates polymerase 5min, 95°C; 1 Cycle

Denaturation; 0.15min, 95°C; 1 min } 40 Cycles

Annealing/extension; 1 min, 60°C

Final step: meltcurve/dissociation curve 60°C-95°C

Real-time quantitative PCR was analysed using a Stratagene Mx3005p thermocycler.

Negative controls included Non-primer control (NPC), Non-template control (NTC), reaction master mix (-SYBR) and minus Reverse transcription enzyme (-RT). The positive control was respective plasmid encoding NP, the Small DI or the Large DI. Samples were performed in triplicate unless otherwise stated.

2.10.4. Visualisation of PCR products by Agarose gel electrophoresis

DNA was separated using 1% (w/v) agarose/TAE buffer. Four µg/ml of ethidium bromide was added to the agarose before the gels were covered in 1x TAE buffer (40 mM Tris-acetate, 1 mM EDTA). Samples were mixed together with loading dye and separated by electrophoresis at 100V. The gels were analysed by UV light.

3. RESULTS

The results chapter is split into three parts. The first part concerns the heterocellular induction of IFN-β in A549 cells by paramyxoviruses and Influenza A virus (Udorn). Secondly, the identification of the primary PRR(s) responsible for IFN-β induction and signalling is studied, by examining viral plaque development and activation of the IFN-β promoter in Naïve reporter cells by immunofluorescence and FACs analysis. The third part concerns the role of DIs as inducers of IFN-β, as detected by RT-QPCR from cell-sorted GFP+ve cells following PIV5 (wt) infection.

3.1.1. The Heterocellular induction of IFN-β by negative sense RNA viruses

IFN-β is induced and secreted by cells upon virus infection, subsequently inducing the expression of ISGs that generate an antiviral state by inhibiting further infection and virus replication. This was visualized via a simple plaque assay whereby A549 cells (referred to as Naïve cells from now on) and A549 BVDV Npro cells were infected with PIV5 (wt) at an MOI of 0.001 pfu/cell. A549 BVDV Npro cells express the BVDV Npro protease, in which Npro targets IRF3 for proteasomal mediated degradation. As a result, A549 BVDV Npro cells lack a functional IFN-β induction pathway and do not express IFN-β. At five days post infection (p.i.), cells were fixed and ELISA stained for PIV5 NP. At five days p.i. a significant increase in plaque size can be seen in the infected A549 BVDV Npro cells compared to A549 naïve cells (**Figure 16A**). Thus, despite the existence of potent virus-encoded antagonists of the IFN-β system, IFN can still exert an antiviral effect that limits PIV5 (wt) virus

replication before PIV5 is able to dismantle the antiviral state. This raises the question of whether in a given cell population under virus challenge, all the cells express IFN or whether it is only a minority of cells that express IFN.

To determine if the antiviral response of cells to virus infection is homo- or heterogenous in the developing plaque, Naïve cells were grown as a monolayer and infected at an MOI of 0.001 pfu/cell with PIV5 (wt). At two days p.i. cells were fixed and stained for PIV5 NP and for MxA, an ISG used as a marker for the production of IFN-β (**Figure 16B**). Cells were subsequently stained with the NP secondary antibody, Texas Red and MxA secondary antibody, Cy5 for visualisation by confocal fluorescence microscopy. At two days p.i., viral plaques consisting of 10–30 cells expressing viral antigen were seen, indicative of viral replication and spread. Surprisingly, only some of the developing plaques were surrounded by cells that were positive for MxA expression. From these observations it can be concluded that although some of the cells must have produced and secreted IFN, leading to the induction of MxA expression, this was not the case for all infected cells in which no MxA expression could be seen surrounding the developing plaque. Clearly, this shows that there is a heterogeneous cellular response to virus infection.

In order to address the question of the nature of the cellular response to virus infection, we generated an A549 reporter cell line in which IFN-β induction was monitored by placing the eGFP gene under the control of the IFN-β promoter (**1.2.7. Investigating PIV5 DIs: The A549 pr/(IFN-β).GFP Reporter cell line**). With the development of the A549/pr(IFN-β).GFP reporter cell line (referred to from now on as Naive reporter cells), the activation of the IFN-β promoter can be examined in a population of cells following virus infection. Naive reporter cells were grown as a monolayer in 60 mm dishes that contained coverslips.

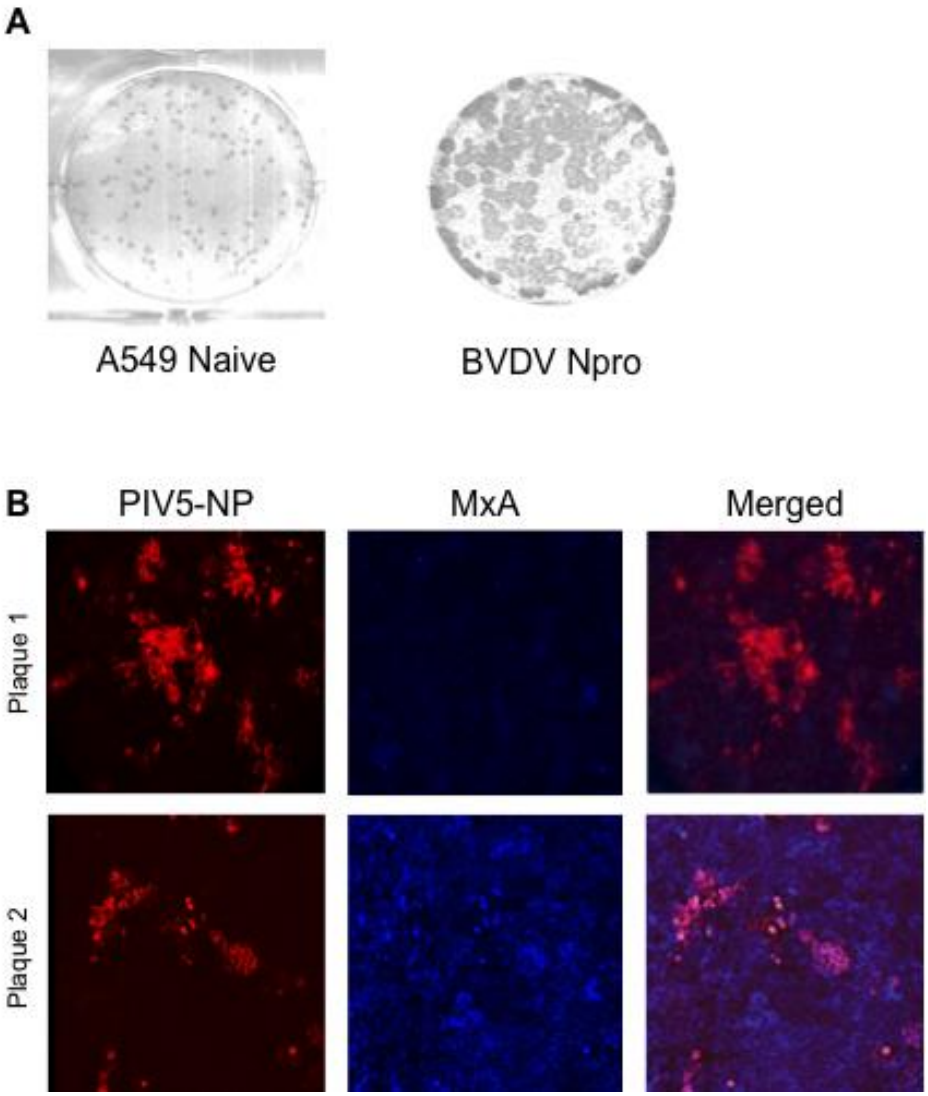

Figure 16. Response of Naïve cells to PIV5 (wt) infection

A) Naïve cells and A549 BVDV Npro cells were grown as monolayers and infected at a low MOI of 0.001 in 60mm dishes. At 5 days p.i. cells were fixed and ELISA stained to PIV5 NP.

B) Naïve cells were grown as a monolayer on coverslips and infected with PIV5 wt at low MOI of 0.001. At 2 days p.i.,cells were fixed and co-stained with antibodies for PIV5 NP with Phycoerythrin secondary; MxA with Cy5 secondary. Cells were visualised by confocal microscopy. Plaque 1 = viral plaque surrounded by cells negative for MxA expression. Plaque 2 = viral plaques surrounded by cells positive for MxA expression.

The Heterocellular induction of IFN-β in response to infection

Monolayers were infected at a low MOI of 0.001 with PIV5 (wt) (**Figure 17A**), PIV3 (rwt) (**Figure 17B**), PIV2 (wt) **(Figure 17C**), BUNV (wt) (**Figure 17D**) and influenza A (Udorn) (**Figure 17E**). At two days p.i. cells were fixed. Cells infected with influenza A (Udorn wt) which was fixed at one day p.i. Cells were subsequently stained for virus NP with Texas Red secondary antibody, and co-stained for MxA and Cy5 secondary antibody for visualization by confocal immunofluorescence microscopy.

In addition, a positive control was generated by treating a cell monolayer with IFN-α (Roferon A, Roche) at 1000 U/ml for 12 hours before fixation and staining (**Figure 17A**). The cell monolayer of the positive control at 12 hours post-treatment was 100% for MxA expression. This showed that the Naïve reporter cells could all respond to IFN. Following infection with PIV5 (wt), at two days p.i. plaques could be readily visualized (**Figure 17B).** Some developing plaques were visualized that contained no GFP+ve cells, suggesting that IFN-β had not been produced by any of the infected cells within these plaques. Supporting this, the layer of cells surrounding these plaques which were negative for GFP expression and were also negative for MxA expression. This is unsurprising, as without the induction and secretion of IFN, the expression of ISGs such as MxA is not induced following virus infection.

However**,** following PIV5 infection, some plaques were visualized in which they contained by one to three GFP+ve cells and were surrounded by a layer of cells expressing MxA (**Figure 17B Plaque 2**). These GFP+ve cells strongly suggest that the IFN-β promoter has been activated and IFN-β subsequently expressed and secreted by the cell. The secreted IFN subsequently diffuses through the cell monolayer, activating the JAK/STAT pathway in neighbouring uninfected cells and inducing the expression of MxA expression (and other ISGs) that is observed.

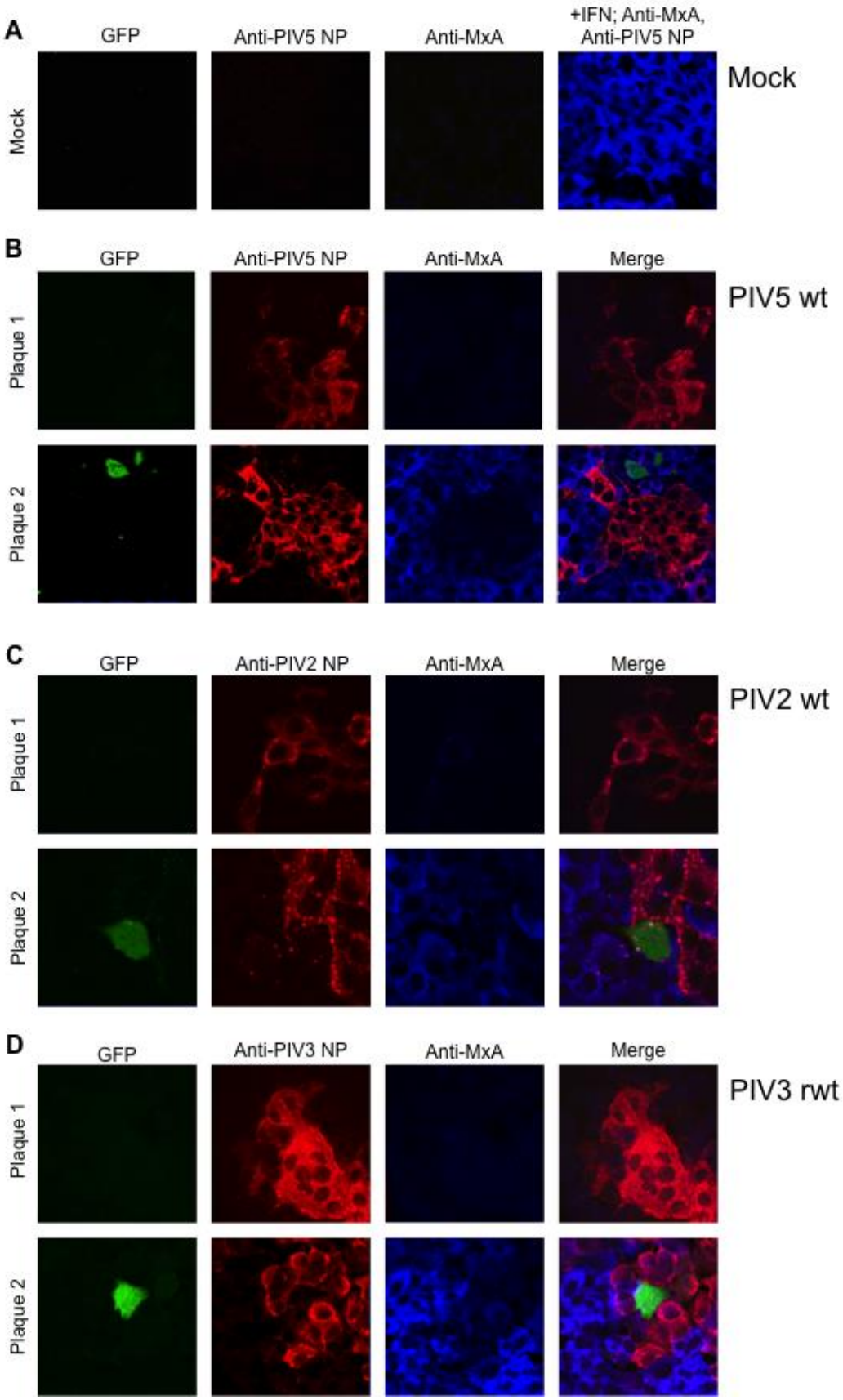
A
GFP
Anti-PIV5 NP
Anti-MxA
+IFN; Anti-MxA, Anti-PIV5 NP
Mock
Mock
B
GFP
Anti-PIV5 NP
Anti-MxA
Merge
PIV5 wt
Plaque 1
Plaque 2
C
GFP
Anti-PIV2 NP
Anti-MxA
Merge
PIV2 wt
Plaque 1
Plaque 2
D
GFP
Anti-PIV3 NP
Anti-MxA
Merge
PIV3 rwt
Plaque 1
Plaque 2

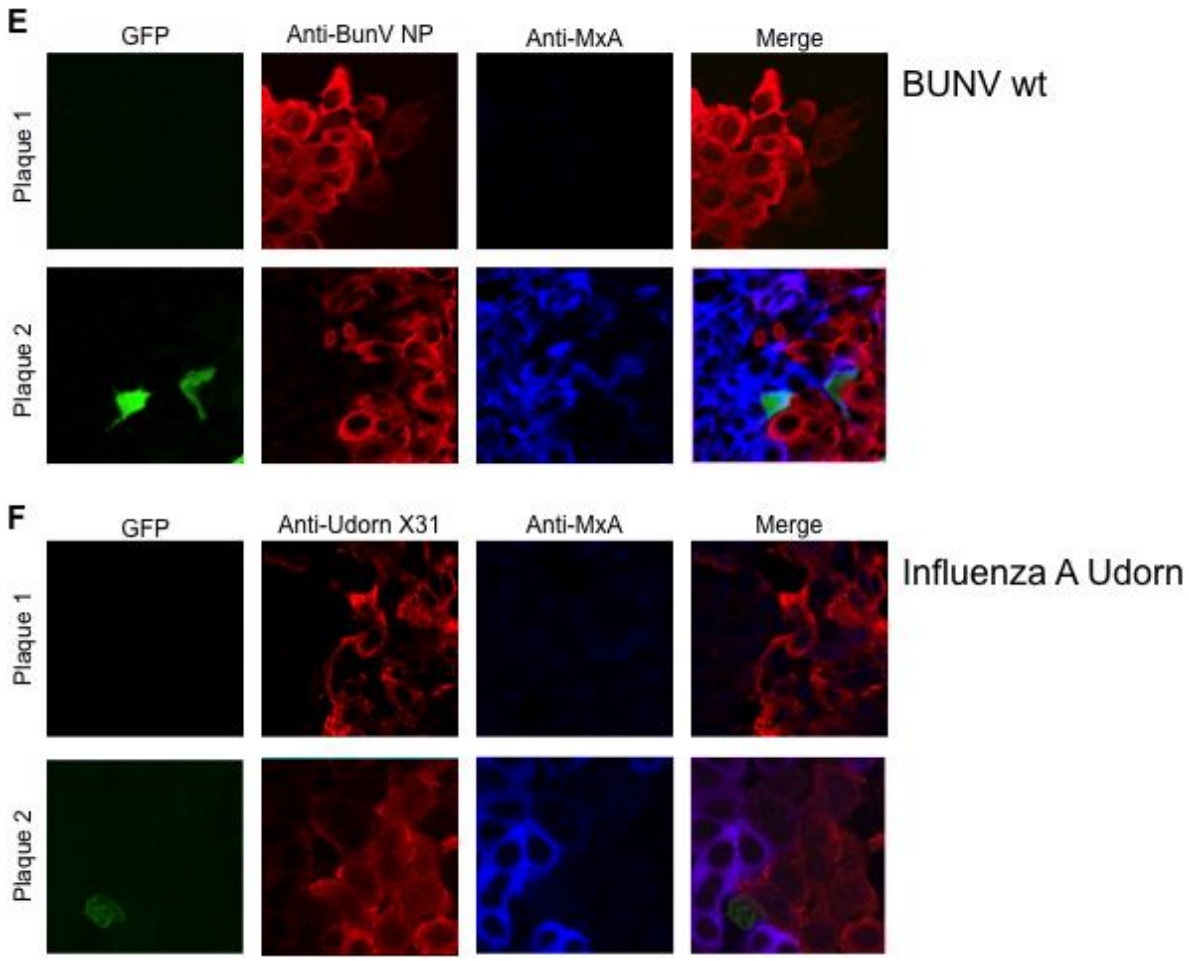

Figure 17. The Heterocellular induction of IFN-β in Naive reporter cells

Naïve reporter cell monolayers were infected with PIV5 (wt) (**B**), PIV3 (rwt) (**C**), PIV2 (wt) (**D**), BUNV (wt) (**E**) and Influenza A (Udorn wt) (**F**) at low MOI 0.001 pfu/cell. At 2 days p.i. cells were fixed and co-stained for virus NP and for MxA, with the secondary antibodies phycoerythrin and Cy5 respectively. **Plaque 1** = plaque surrounded by cells negative for GFP expressing cells and negative for MxA expression. **Plaque 2** = plaque surrounded by cells positive for GFP expression and positive for MxA expression. **Green cells** = cells which have the IFN-β promoter activated and the subsequent expression of GFP (The GFP gene is under the control of the IFN-β promoter). A positive control was generated in which Naïve reporter cells were treated with IFN-α (Roferan A) at 1000U/ml for 12 hours before fixation and staining. Cells were visualised on a Zeiss LSM 5 Exciter confocal microscope.

Therefore the expression of MxA is directly correlated with the presence of a GFP+ve cell within the developing plaques. From these observations, it is clear that there is a heterocellular response to infection, in which only a minority of infected cells has IFN been induced in. This heterocellular response was observed with infection by wild type strains of PIV3 (**Figure 17C**), PIV2 (**Figure 17D**), BUNV (**Figure 17E**) and influenza A (Udorn) (**Figure 17F**). This suggests that the heterocellular response observed is a general feature of negative strand viruses. The vast majority of infected cells are negative for GFP expression. These results strongly suggest that only a few cells within developing plaques of negative strand viruses produce the IFN-β that is responsible for generating the antiviral state in the surrounding uninfected cells.

3.1.2. Heterocellular Induction of IFN-β in reporter cells by PIV5 lacking a functional IFN antagonist

The heterocellular response of Naïve reporter cells to low MOI infections of negative sense RNA viruses indicates that the PAMPs that induce IFN are generated during PIV5 infection. However, what is not known is whether the PAMPs generated are sourced as a feature of normal wild-type non-defective virus replication. To answer this, the % of GFP+ve cells can be measured in response to infection by a virus lacking a functional IFN antagonist. If the sources of PAMPs are generated during normal wildtype virus replication, then following infection of the Naïve reporter cell line with a virus lacking an IFN antagonist, it would be expected that the majority of the infected cells would be positive for GFP expression and thus positive for activation of the IFN-β promoter.

As mentioned previously, PIV5 encodes a potent IFN antagonist, the V protein, which targets the establishment of an antiviral state at multiple levels (see **1.2.5. PIV5 Inhibition of IFN mediated responses**). The PIV5 VΔC virus encodes a C-terminally truncated version of the V protein which cannot interact with MDA5 or target STAT1 for proteasome-mediated degradation, and is consequently impaired in its ability to inhibit IFN-β induction and IFN-β signalling. We examined whether the heterocellular activation of the IFN-β promoter observed in response to PIV5 (wt) infection in Naive reporter cells is observed for infection with PIV5 VΔC. Cell monolayers of Naïve reporter cells was grown and infected with PIV5 VΔC VM0 at a low MOI of 0.001 pfu/cell. At two days p.i., cells were fixed and then co-stained for PIV5 NP and for MxA, and stained with secondary antibodies for phycoerythrin and Cy5 respectively for confocal fluorescence microscopy (**Figure 18A**). Furthermore, a second set of Naïve reporter cell monolayers were grown and infected at an MOI of 0.001 pfu/cell with PIV5 VΔC VM0 (**Figure 3B**). At two days p.i. cells were trypsinised, fixed in suspension and then resuspended in suspension solution (PBS; 5% FCS, 0.01% sodium azide). These cells were then analysed by flow cytometry for GFP expressing cells.

PIV5 VΔC is extremely sensitive to the effects of IFN, and so only forms small plaques in Naive reporter cells; nevertheless, plaque development can be followed at 2 days p.i. before enough IFN is produced to prevent further plaque development (**Figure 18A**). As seen for infection with PIV5 (wt) (**Figure 17B**), it is observed with infection by PIV5 VΔC that only a minority of infected cells are positive for GFP expression and thus in only a minority cells has the IFN-β promoter been activated. As expected, the uninfected cells surrounding plaques containing a GFP+ve cell were positive for MxA expression. The observation that only a minority of cells are positive for GFP expression is supported by the flow cytometry analysis of PIV5 VΔC

infected Naïve reporter cells. Only 14.7% of cells were positive for GFP expression (**Figure 18B**).

However, plaques could also be seen that contained no GFP+ve cells, indicating that the IFN-β promoter had not been activated within these developing plaques (**Figure 18A)**. Furthermore, an antiviral state had not been established in the uninfected cells surrounding these plaques, as demonstrated by a lack of MxA expression, indicating that no endogenous IFN-β had been secreted by any of the infected cells in the plaque.

These results confirm that the IFN-β promoter is only activated in a minority of cells infected with PIV5 VΔC VM0, and that there is a heterocellular response to infection to a virus with a non-functional IFN antagonist. The significance of this was that the loss of the PIV5 IFN antagonist did not lead to IFN-β promoter activation in all of the PIV5 VΔC VM0 infected cells. If the loss of a functional V protein were the primary reason for IFN induction in infected cells, then it would be expected that infection with PIV5 VΔC would activate the IFN-β promoter in all infected cells. However, as the IFN-β promoter is not activated in the majority of cells infected with PIV5 VΔC this demonstrates that the PAMPs capable of inducing IFN are not generated during PIV5 VΔC transcription and replication processes.

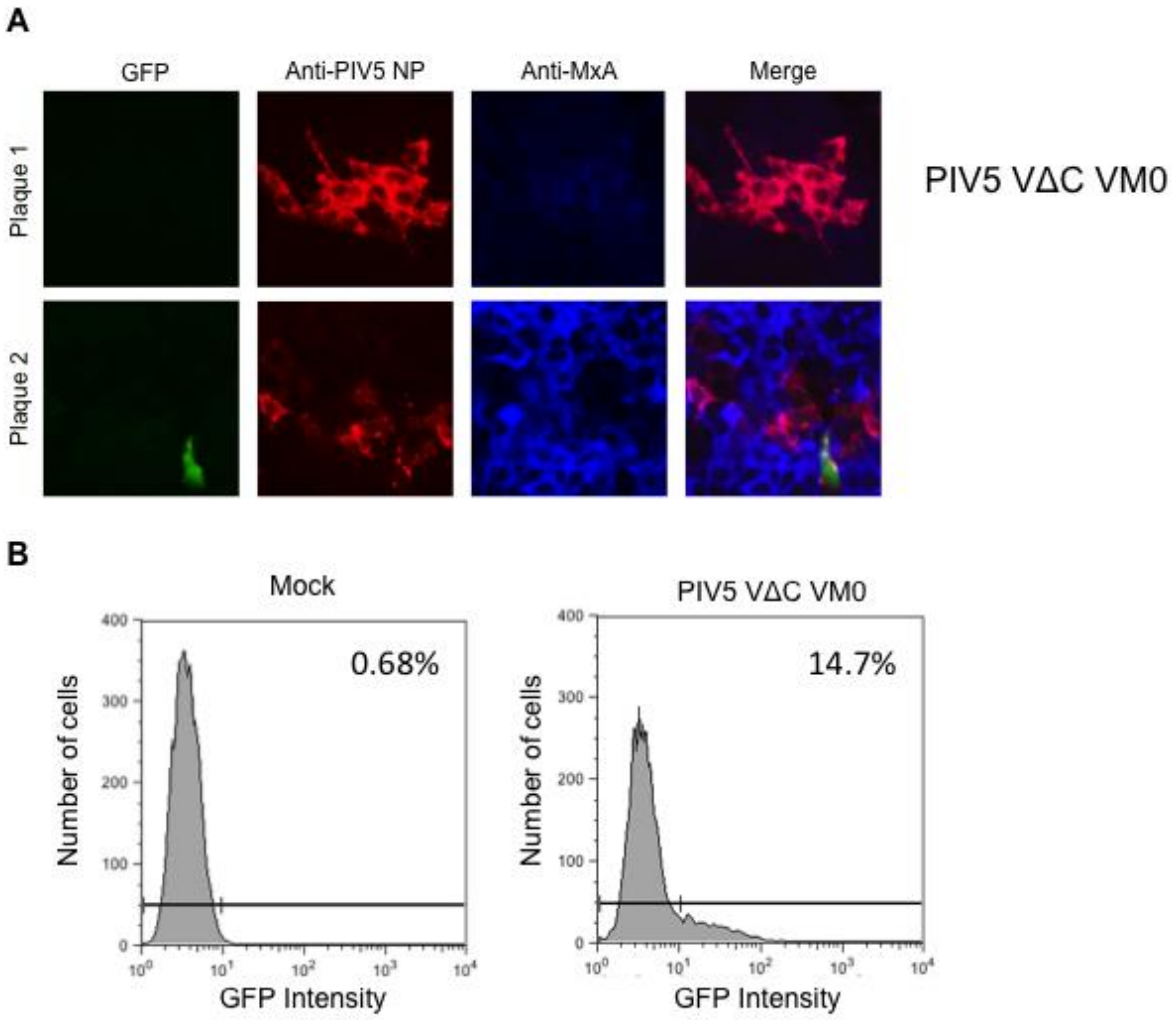

Figure 18. The Heterocellular induction of IFN-β following infection with PIV5 lacking an IFN-β antagonist

Naïve reporter cell monolayers were infected with PIV5 VΔC VM0 at an MOI of 0.001 pfu/cell.

(A) At 2 days p.i. cells were fixed and co-stained for PIV5 NP and for MxA, with the secondary antibodies phycoerythrin and Cy5 respectively for immunofluorescence confocal microscopy.

(B) Plaque 1 = viral plaque surrounded by cells negative for GFP expression and negative for MxA expression.

Plaque 2 = viral plaque surrounded by cells positive for GFP expression and positive for MxA expression.

(C) At 2 days p.i. cells were trypsinised and fixed in suspension. Cells were then resuspended in suspension solution and subsequently subjected to flow cytometry analysis to determine GFP expression. The percentage of cells considered to be GFP+ve (based on the line gate indicated) is given in the top right hand of each panel.

3.1.3. Section Summary

We investigated the activation of the IFN-β promoter by the PAMPs generated during plaque development following a low MOI infection of reporter cells infected with negative sense RNA viruses. Infecting at a low MOI ensures that the cells at the initial site of infection are infected with wild-type virus, and not by any PAMPs present in the viral stock. It was clear from the immunofluorescence and flow cytometry of infected samples, that during plaque development only a minority of cells were positive for the expression of GFP and hence only a minority of reporter cells have activation of the IFN-β promoter and are responsible for the induction of IFN during an infection.

We also found that only a small minority of Naïve reporter cells expressed GFP when infected with PIV5 VΔC when analysed by flow cytometry and by immunofluorescence. The most striking result of this study was that the loss of the PIV5 IFN antagonist did not lead to IFN-β promoter activation in all PIV5 VΔC-infected cells. The data presented here, challenges the notion that paramyxoviruses generate PAMPs capable of activating the IFN response during their normal replication cycle, and we suggest that these PAMPs are not generated during normal non-defective PIV5 (wt) replication.

Our data indicate that the loss of this fine control of transcription and replication via the V protein, does not affect the level of activation of the IFN-β promoter during infection, since we do not see IFN-β promoter activation in the majority of PIV5 VΔC (VM0) infected cells. These results suggest that, in this reporter system, DI viruses, generated due to errors in the viral polymerase, are primarily responsible for IFN induction during infection with PIV5, and will be discussed in the next section.

3.2. Determining the PRRs involved in the induction of IFN following Paramyxovirus infection

Both RIG-I and MDA5 have the capacity to induce IFN following infection with PIV5 (wt). To determine which PRR is the primary sensor that subsequently induces IFN following infection with paramyxoviruses, reporter cell lines in which the RIG-I and MDA5 sensors had been knocked down were utilised in subsequent experiments. These were created using a lentivirus shRNA strategy, and cells that were knocked down for the respective sensors were subsequently subcloned (cell lines generated by Shu Chen, University of St Andrews). The PRR knock down reporter cell lines generated were the A549 pr/(IFN-β).GFP RIG-I Knock Down cell line and the A549 pr/(IFN-β). GFP MDA5 Knock Down cell lines (referred to as the RIG-I KD reporter cells and the MDA5 KD reporter cell line from now on). All infections (as in the previous section) are performed at a low MOI. This is so that the impact of PAMPs generated during virus replication and dissemination throughout the cell monolayer, and not PAMPs present in the virus stock at the site of the initial infection, can be examined in their ability to induce the activation of the IFN-β promoter.

3.2.1. Characterising the RIG-I KD and MDA5 KD reporter cell lines for RIG-I and MDA5 expression and for IFN-β promoter activation

Before utilizing the RIG-I and MDA5 KD reporter cell lines for future studies, it was first needed to characterize them to confirm that they had reduced levels of RIG-I and MDA5 expression respectively. As RIG-I and MDA5 are IFN inducible, a simple

test of their expression is to treat a cell monolayer with IFN and probe for RIG-I and MDA5 expression. RIG-I KD and MDA5 KD reporter cells were grown as a cell monolayer and stimulated with Roferon A for 16 hours. Post-incubation, cells were lysed and samples loaded onto an SDS-PAGE gel. Samples were immunoblotted for RIG-I, MDA5 and actin (**Figure 19**). Following stimulation with IFN, RIG-I KD reporter cells express MDA5 equivalent to Naïve reporter cells. In contrast, the RIG-I KD cells have severely reduced RIG-I expression compared to Naive reporter cells. In contrast following stimulation with IFN, MDA5 KD reporter cells express RIG-I similarly to Naïve reporter cells, but MDA5 KD reporter cells contain little MDA5 compared to Naïve reporter cells. In conclusion RIG-I and MDA5 have been successfully knocked down in their respective cell lines.

For future studies, it is important to test if the RIG-I KD and MDA5 KD reporter cell lines have consistent GFP expression which correlates with IFN-β promoter activation compared to Naïve reporter cells. To determine this, a transient transfection of the Naïve, RIG-I KD and MDA5 KD reporter cell lines was carried out with a plasmid encoding IRF3, pdlNOTI MCS R-IRF3. In pdlNOTI MCS R-IRF3, the gene of interest, IRF3 is transiently expressed under the control and driven by the SFFV promoter. As IRF3 is downstream of RIG-I and MDA5, the transient expression of IRF3 would activate the IFN-β promoter and thus GFP expression in the reporter cell lines. The pdlNOTI MCS R-IRF3 plasmid was transfected using FuGENE 6 transfection reagent following the standard Promega protocol. Mock cells were also transfected with an empty vector. Following incubation of 48 hours post-transfection, cells were trypsinised and fixed in suspension, before resuspension in suspension solution. Cells were then analysed by flow cytometry for GFP expression (**Figure 20**).

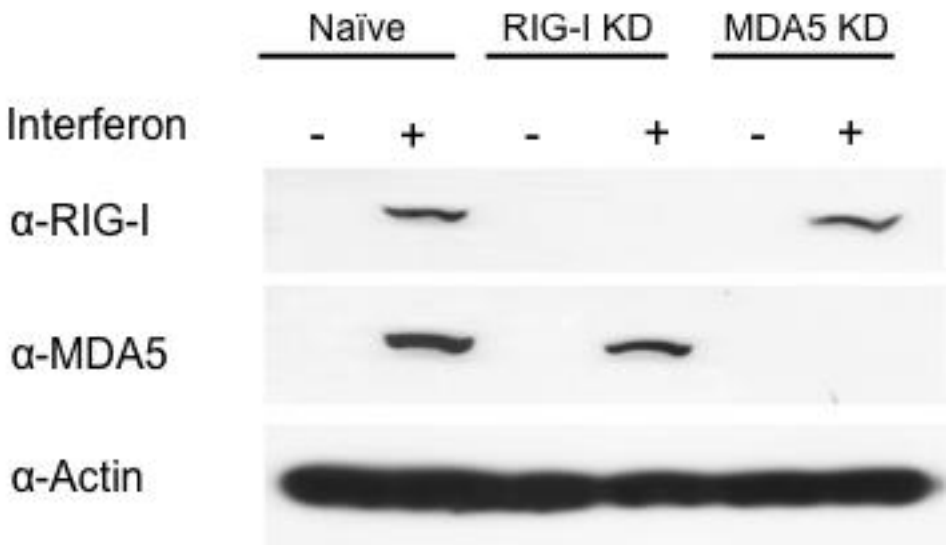

Figure 19. Characterising the Reporter cell lines for RIG-I and MDA5 expression

Naïve, RIG-I KD and MDA5 KD reporter cell lines were stimulated with Roferon A for 16 hours before cells were lysed and samples put onto an SDS-PAGE gel. Samples were immunoblotted for RIG-I, MDA5 and actin.

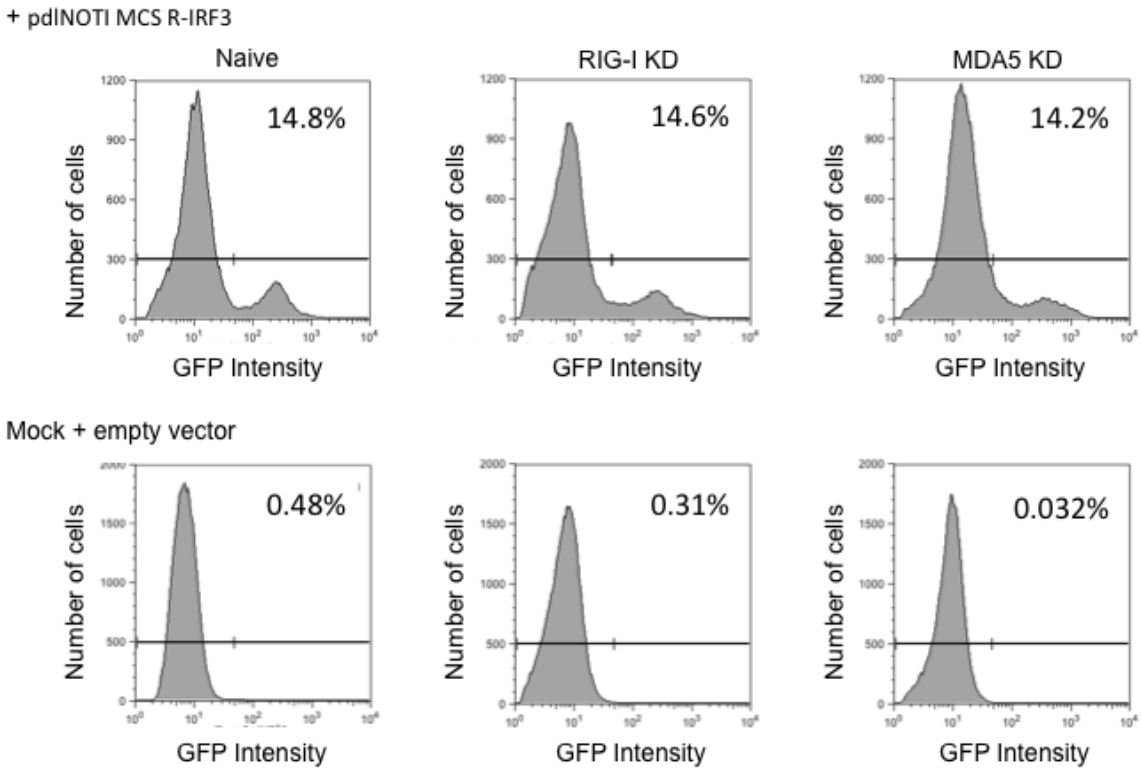

Figure 20. The reporter cell lines display similar levels of IFN-β promoter activation following the transient expression of IRF3

Naïve, RIG-I KD and MDA5 KD reporter cell lines were transfected with an expression plasmid for the transient expression of IRF3 (pdINOTI MCS R-IRF3). Following transfection, cells were trypsinised and fixed and then subsequently resuspended in cell suspension solution. Cells then underwent flow cytometry analysis measuring for the number of GFP expressing cells. The percentage of cells considered to be GFP+ve (based on the line gate indicated) is given in the top right hand of each panel.

Following transfection with the IRF3 encoding plasmid, Naïve, RIG-I KD and MDA5 KD reporter cell lines display similar % of GFP+ve cells as a proportion of total cells, within 0.6% of each other. Although these values are ~14%, a minority of total cells, this is due to the poor transfection efficiency of the A549 cell line. Furthermore, there are clearly defined discrete peaks of GFP+ve and GFP-ve cells , indicating that the IFN-β promoter is either “on” or “off” in the absence or presence of stimuli. The RIG-I KD and MDA5 KD reporter cell lines are thus consistent in their GFP expression in their response to activation of the IFN-β promoter compared to Naive reporter cells.

3.2.2. Measuring paramyxovirus virus spread in the reporter cell lines lacking a PRR

To study the effect of removing a PRR sensor on virus infection and spread in a cell monolayer, plaque assays were performed using the reporter cell lines. Naïve, RIG-I KD and MDA5 KD reporter cell lines were grown to 90% confluence in 60mm plates and infected with PIV5 (wt) (**Figure 21A**), PIV3 (rwt) (**Figure 21B**) and PIV2 (wt) (**Figure 21C**) at an MOI of 0.001 pfu/cell. As a positive control, A549 BVDV Npro cells were also infected. At 5 days p.i. when plaques had developed to a suitable size and observed via a Nikon microscope, cells were fixed. Cells were ELISA stained for PIV5, PIV3 and PIV2 NP. Plaques sizes were then measured and averaged for each reporter cell line.

Firstly, comparing plaque sizes following PIV5 (wt) infection of Naïve reporter cells to A549 BVDV Npro cells, it can be observed that there are significant differences between the two (**Figure 21A**).

A

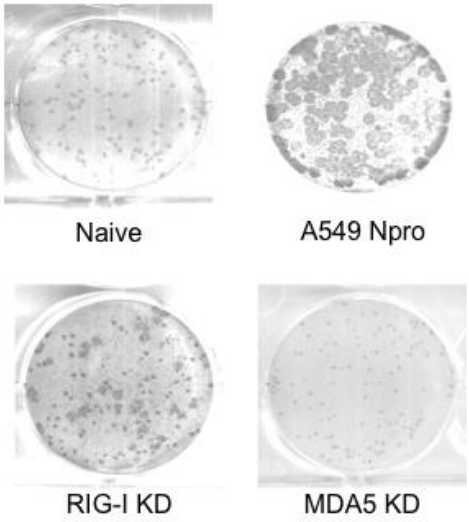
Naive
A549 Npro
RIG-I KD
MDA5 KD

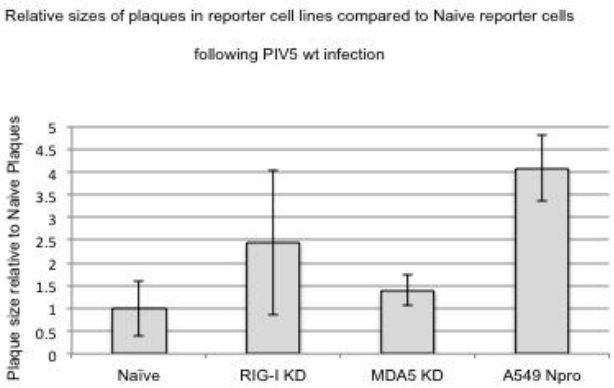
Relative sizes of plaques in reporter cell lines compared to Naive reporter cells
following PIV5 wt infection
Plaque size relative to Naive Plaques
5
4.5
4
3.5
3
2.5
2
1.5
1
0.5
0
Naïve
RIG-I KD
MDA5 KD
A549 Npro

B

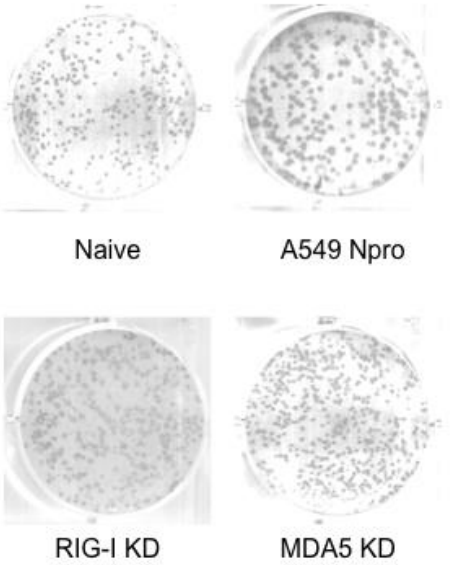
Naive
A549 Npro
RIG-I KD
MDA5 KD

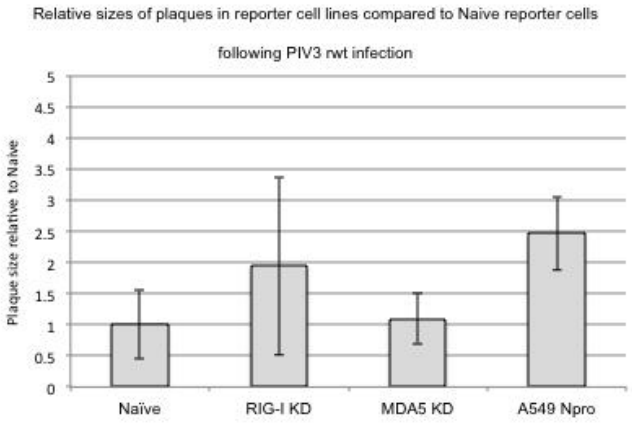
Relative sizes of plaques in reporter cell lines compared to Naive reporter cells
following PIV3 rwt infection
Plaque size relative to Naive
5
4.5
4
3.5
3
2.5
2
1.5
1
0.5
0
Naïve
RIG-I KD
MDA5 KD
A549 Npro

C

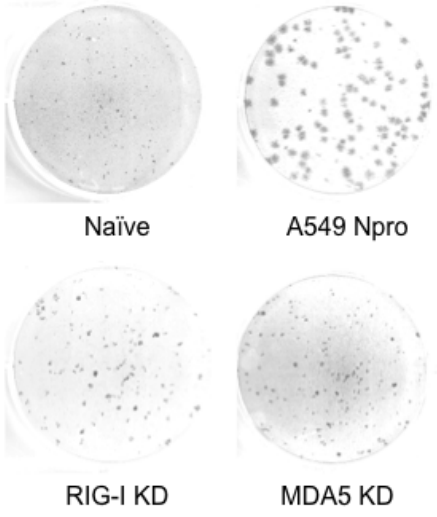
Naïve
A549 Npro
RIG-I KD
MDA5 KD

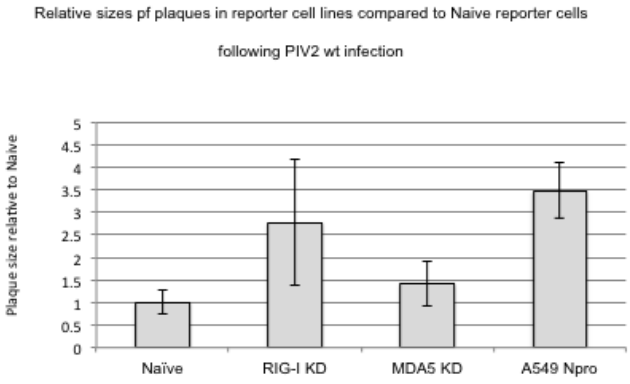
Relative sizes pf plaques in reporter cell lines compared to Naive reporter cells
following PIV2 wt infection
Plaque size relative to Naive
5
4.5
4
3.5
3
2.5
2
1.5
1
0.5
0
Naïve
RIG-I KD
MDA5 KD
A549 Npro

Figure 21. Comparison of viral plaques generated from infecting reporter cell lines with paramyxoviruses

A549 Naive, RIG-KD, MDA5 KD reporter cells and BVDV Npro cells were infected with (**A**) PIV5 (wt); (**B**) PIV3 (rwt); (**C**) PIV2 (wt) at an MOI of 0.001 pfu/cell. At 5 days p.i. for PIV5 and PIV2 infections, and at 3 days for PIV3 infections when the developing plaques were visible using a Nikon microscope, cells were fixed. Following fixation, plaques were ELISA stained for NP of PIV5, PIV3 and PIV2. Plaques sizes were measured and averaged. Error bars indicate the standard deviation of plaque sizes in each data set.

As expected, the plaque sizes are far larger in the cell population that lack a functional IFN induction signalling pathway, the A549 BVDV Npro cells, than those observed in Naïve reporter cells in which IFN can be induced. As a result, virus replication and dissemination in the cell monolayer is reduced compared to cells that are unable to induce IFN. However, the largest plaques of PIV5 infected RIG-I KD reporter cells are comparable, albeit slightly smaller to those found in infections of A549 BVDV Npro cells. This suggests that knocking down RIG-I expression severely limits the sensing of viral PAMPs generated during virus infection. Supporting this, the RIG-I KD plaques are significantly larger than those found in infections of Naïve reporter cells. This indicates that cells lacking the RIG-I sensor are significantly less able to induce IFN in response to infection where the virus is better able to replicate and spread increasing the size of the plaques in RIG- KD reporter cells compared to Naïve reporter cells.

In contrast, following infection of MDA5 KD reporter cells with PIV5, the plaques observed were of a similar, being slightly larger size to those observed in infections of Naïve reporter cells, and MDA5 KD reporter cell plaques were far smaller than that of those plaques observed in A549 BVDV Npro cells. This suggests that cells that primarily possess the RIG-I sensor are able to respond to virus infection and sense the PAMPs generated, leading to the induction of IFN and the generation of an antiviral state. Supporting this, the plaque size of MDA5 KD reporter cells were around 50% smaller than that of plaques found in RIG-I KD reporter cells, indicating that the removal of the RIG-I sensor led to increased virus spread within the cell population than the removal of the MDA5 sensor.

As the plaque sizes for RIG-I KD cells are smaller than those visualised for A549 Npro cells, this suggests that virus PAMPs are being generated during infection that are able to activate MDA5 mediated induction of IFN. This is supported by the plaque

sizes of MDA5 KD reporter cells being slightly larger than Naïve reporter cells, which indicates that some PAMPs are generated during infection that activate MDA5 mediated induction of IFN.

Furthermore, infections of RIG-I KD reporter cells generated a mixed population of plaque sizes, where some were as small as Naïve reporter cells, whilst others were far larger comparable to those observed in A549 BVDV Npro cells. This could be due to the presence of a mixed population of RIG-I KD reporter cells, where only some of the cells are knocked down for RIG-I expression, or that there are differing levels of shRNA expression of RIG-I being expressed in the cell population. It is possible that not all the cells could be knocked down for RIG-I expression uniformly. A second possible explanation is that during PIV5 replication, MDA5 PAMPs are generated at a relatively slow rate compared to RIG-I activating PAMPs. A way to test this is that if the IFN inducing PAMPs can be identified, then if the PAMPs being generated during virus infection activate MDA5, then it would be possible to detect these PAMPs via RT-QPCR in GFP+ve RIG-I KD reporter cells that had been cell sorted from GFP-ve cells.

The plaque assay patterns detected for PIV5 infections can also be observed for infections of the reporter cells with PIV2 (wt) (**Figure 21B**). This data suggests that RIG-I is the primary sensor for the PAMPs generated during virus replication for PIV5 (wt) and PIV2 (wt). However, for infection with PIV3 (rwt) (**Figure 21C**), the patterns observed appear to be less pronounced that for infections with PIV5 (wt) or PIV2 (wt). The relative plaque sizes observed of PIV3 (rwt) infected Naïve and MDA5 KD reporter cells are comparable to PIV5 (wt) and PIV2 (wt), suggesting that RIG-I appears to be the primary sensor as explained earlier for inducing IFN. However, the plaques observed in PIV3 (rwt) infected RIG-I-KD and A549 Npro cells, although still

larger than that in MDA5 and Naive reporter cells, are relatively smaller in difference that that found between PIV5 and PIV2 infected cells. This suggests that perhaps another pathway other than IFN is important for inhibiting PIV3 (rwt) infection.

3.2.3. Immunofluorescence of developing viral plaques in reporter cell lines

The heterocellular induction of IFN observed in response to virus infections, means that one or both of the PRRs, RIG-I and MDA5, are being activated by the PAMPs generated during virus infection and replication. In order to determine the PRRs responsible for inducing IFN-β, the percentage of cells that are GFP+ve and thus have activation of the IFN promoter, can be measured following infection of the reporter cell lines that lack either RIG-I or MDA5. Naïve, RIG-I KD and MDA5 KD reporter cells were grown as a monolayer and infected with PIV5 (wt) (**Figure 22A**), PIV3 (rwt) (**Figure 22B**) and PIV2 (wt) (**Figure 22C**) at an of MOI 0.001. Cells were infected at a low MOI with a DI poor prep of virus in order to reduce the chances of large numbers of DIs in the initial infection.

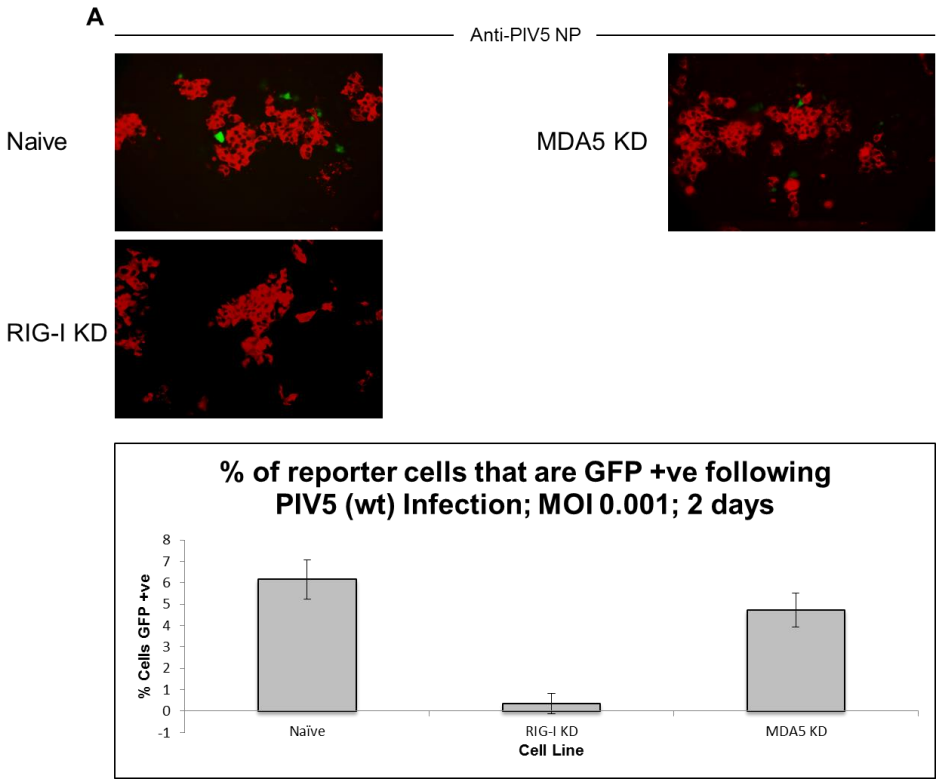
A
Anti-PIV5 NP
Naive
MDA5 KD
RIG-I KD
% of reporter cells that are GFP +ve following
PIV5 (wt) Infection; MOI 0.001; 2 days
% Cells GFP +ve
8
7
6
5
4
3
2
1
0
-1
Naïve
RIG-I KD
MDA5 KD
Cell Line

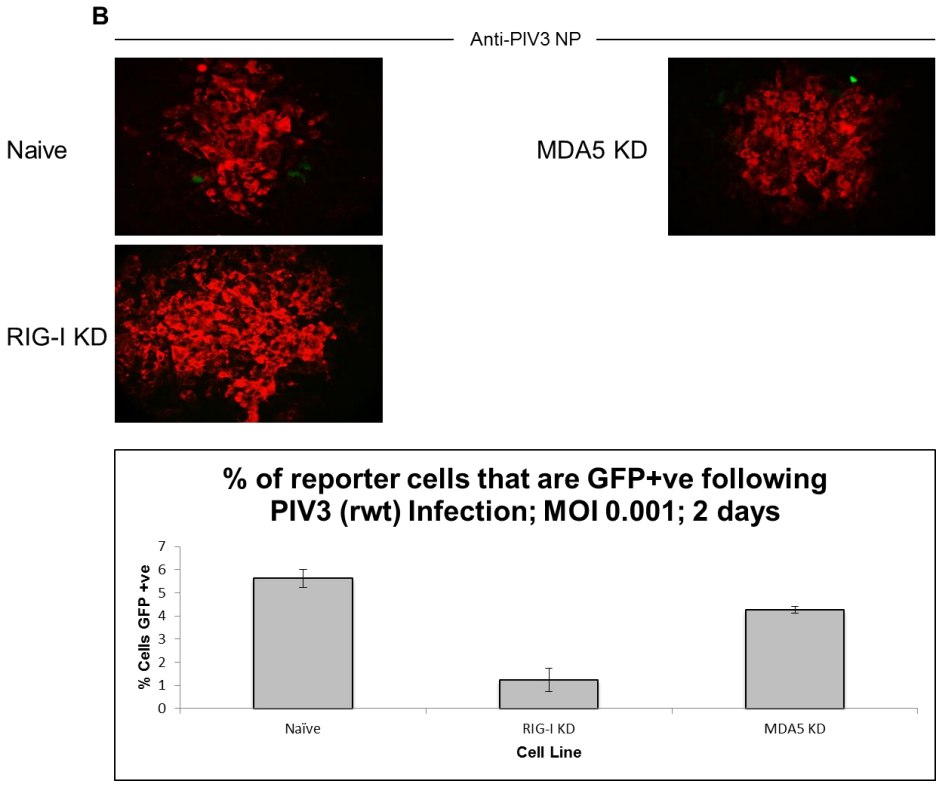
B
Anti-PIV3 NP
Naive
MDA5 KD
RIG-I KD
% of reporter cells that are GFP+ve following
PIV3 (rwt) Infection; MOI 0.001; 2 days
% Cells GFP +ve
7
6
5
4
3
2
1
0
Naïve
RIG-I KD
MDA5 KD
Cell Line

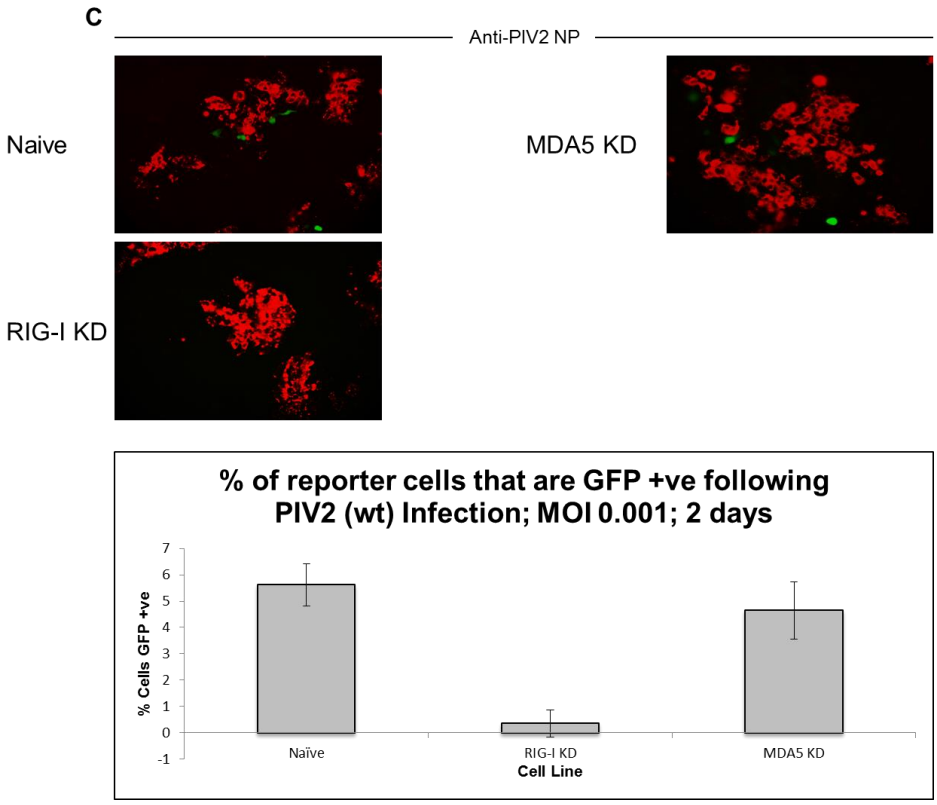

Figure 22. Immunofluorescence of developing plaques in reporter cell lines

Naïve, MDA5 KD and RIG-I KD reporter cells were grown as a monolayer and infected with (**A**) PIV5 (wt), (**B**) PIV3 (rwt) and (**C**) PIV2 (wt) at an MOI of 0.001 pfu/cell. Cells were fixed at 2 days p.i and were stained for NP, with secondary antibody conjugated to Texas Red. Developing plaques were then observed via the Nikon microscope. Error bars indicate the standard deviation of each data set.

Cells were fixed at 2 days p.i. where cells were stained for virus NP, with the secondary antibody conjugated to Texas Red for immunofluorescence microscopy. The number of infected cells and the number of cells that were GFP+ve were counted from 10 fields of vision and averaged (**Figure 22**). It was observed that following infection with PIV5 (wt), PIV3 (rwt) and PIV2 (wt), Naïve and MDA5 KD reporter cells both had at least 5% of cells that were GFP+ve found at the developing plaque. There were fewer GFP+ve cells observed at the developing plaque for infections of RIG-I KD reporter cells than for infections of Naïve and MDA5 KD reporter cells. Thus, by removing the RIG-I sensor, fewer cells are able to respond to virus infection. This supports the previous plaque assay data (**Figure 21**), as larger plaque sizes are observed of infections of the RIG-I KD reporter cell line compared to Naïve and MDA5 KD reporter cells. This suggests that RIG-I is the primary sensor for recognizing virus PAMPs generated by PIV5 (wt), PIV3 (rwt) and PIV2 (wt).

3.2.4. Creating the A549 pr/(IFN-β).GFP LGP2 KD cell line

During this investigation it became apparent from the literature that LGP2 could have a role in the induction of IFN-β following virus infection. As mentioned previously, LGP2 is incapable of inducing IFN itself, but instead inhibits RIG-I in the absence of viral RNA PAMPs and is an enhancer of MDA5 is the presence of viral RNA PAMPs. In order to study the role of LGP2, a stable cell line was created in which LGP2 expression was knocked down by shRNA. The A549/pr(IFN-B).GFP LGP2 Knock Down reporter cell line (referred to as the LGP2 KD reporter cell line from now on) was created using a shRNA lentivirus strategy (**Figure 23**). A lentivirus plasmid expressing shRNA against LGP2 (pBCK shRNA LGP2 KD) was supplied by the

Goodbourn group. To produce the desired recombinant lentivirus, the pBCK shRNA LGP2 KD plasmid (also encoding the puromycin gene) and packaging plasmids pCMVR8.91 and pVSV-G were co-transfected into HEK293T cells using FUGENE 6 transfection reagent. The harvested recombinant lentiviruses were then used to infect Naïve reporter cells. At 48 hours p.i. cells underwent puromycin selection. The LGP2 KD reporter cell line was then subcloned. As expected, the LGP2 KD reporter cell line expresses both RIG-I and MDA5 following IFN treatment (**Figure 24A**). As LGP2 could not be detected by Western Blot, primers were designed to detect the expression of LGP2 by PCR. As LGP2 is IFN inducible, expression levels of LGP2 mRNA in the LGP2 KD reporter cells was tested compared to Naïve reporter cells. Naïve and LGP2 KD reporter cells were grown as monolayers and then treated with +/IFN for 16 hours. Following treatment, RNA was extracted and analysed for LGP2 mRNA expression by PCR (**Figure 24B**). It was found that the Naïve reporter cells expressed LGP2 after IFN treatment, but the subclone of the LGP2 KD reporter cell line did not express detectable levels +/- IFN by PCR.

In addition, the LGP2 KD reporter cell line was tested for the % of cells that express GFP compared to Naïve reporter cells. Naive and LGP2 KD reporter cells were transiently transfected with pdINOTI MCS R-IRF3 in order for the cells to transiently express IRF3 in the cell. Following transfection, cells were trypsinised, fixed, and then underwent flow cytometry analysis measuring for the number of GFP expressing cells. It was found that similar levels of GFP+ve cells could be detected between LGP2 KD reporter cells and Naïve reporter cells that transiently expressed IRF3 (**Figure 24C**). In light of this, the LGP2 KD reporter cell line can be used in future studies as LGP2 has successfully been knocked down and that the cell line has equivalent levels of GFP responsiveness and activation of the IFN-β promoter to Naïve reporter cells.

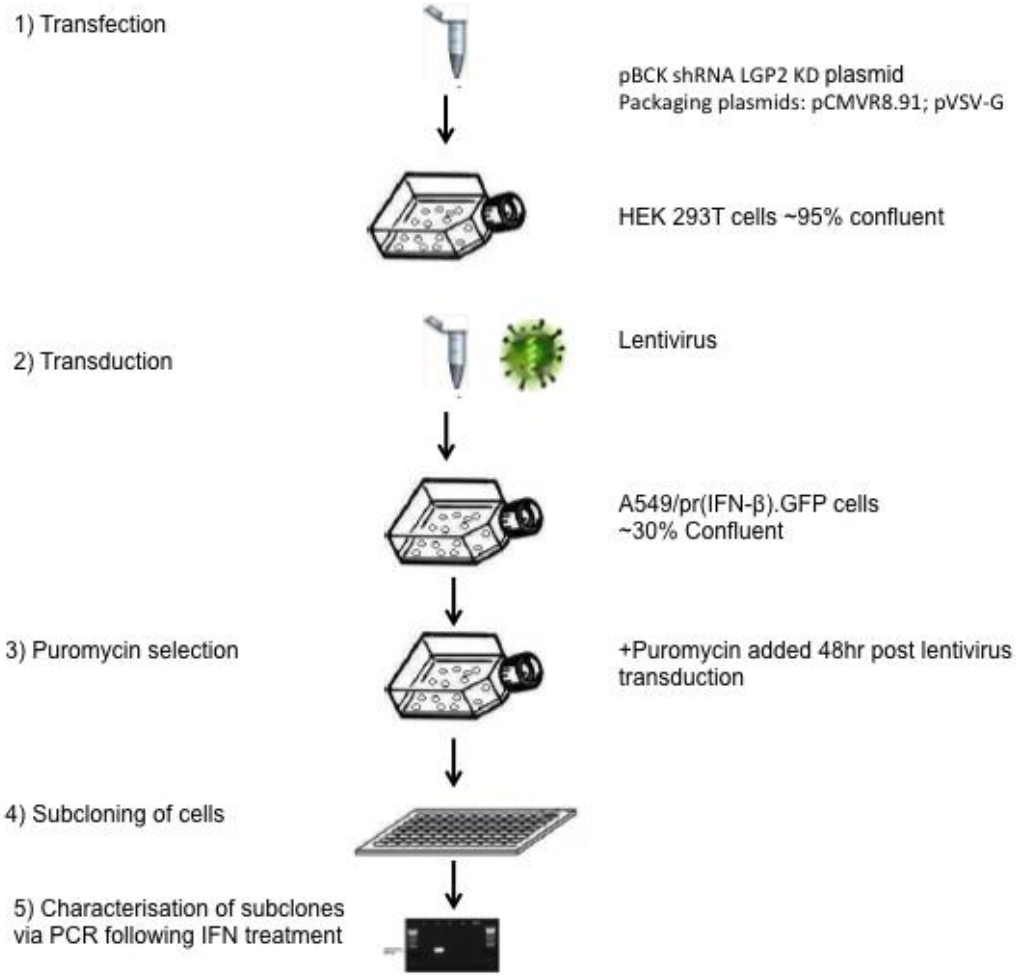

Figure 23. Generation of the A549/pr(IFN-β).GFP/KD.LGP2 KD cell line

Step 1: The lentivirus plasmid expressing shRNA to LGP2 were co-transfected into HEK 293T cells with packaging plasmids pCMVR8.91 and pVSV-G. The lentivirus supernatant was harvested at 72hr p.i. The supernatant was centrifuged to remove cell debris.

Step 2: The lentivirus supernatant was used to infect A549/pr(IFN-β).GFP cells.

Step 3: Lentivirus transduced cells were selected using puromycin at 48hr p.i.

Step 4. The lentivirus transduced cells were then subcloned.

Step 5. Subclones were further characterized for inhibition of LGP2 expression

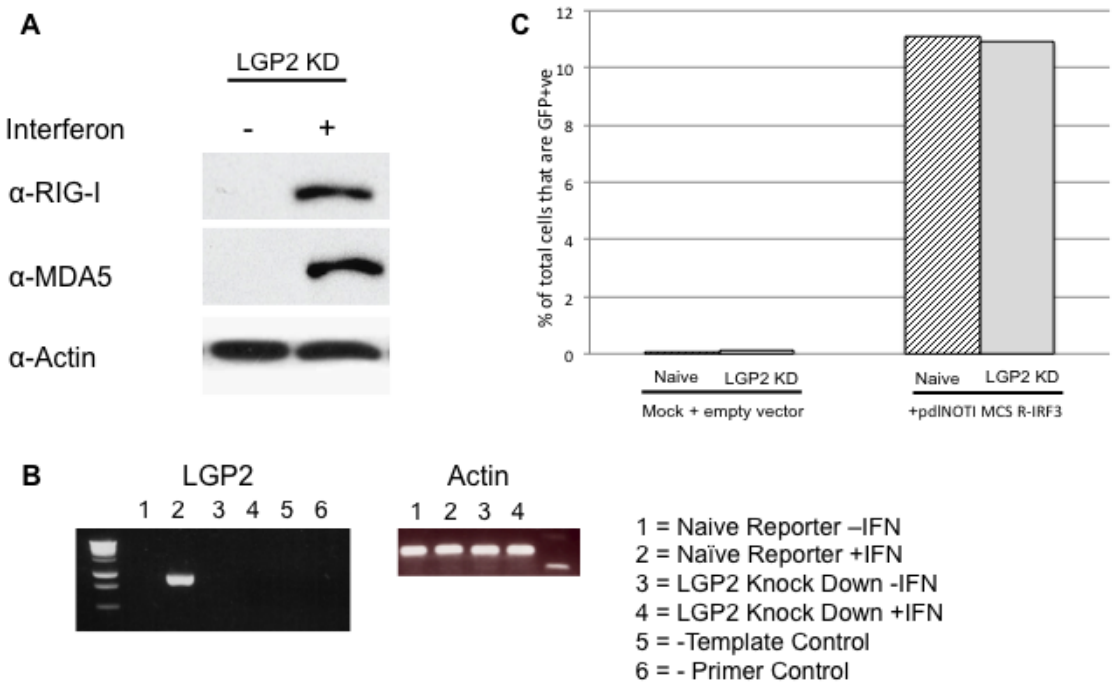

Figure 24. Characterising the A549/pr(IFN-β).GFP LGP2 KD cell line

(A) A549 pr/(IFN-β).GFP LGP2 KD cells express MDA5 and RIG-I following IFN treatment

- A549 pr/(IFN-β).GFP LGP2 KD cells (referred to as LGP2 KD cells) were stimulated +/-IFN for 16 hours before cells were lysed and samples put onto an SDS-PAGE gel. Samples were probed for RIG-I and MDA5, analysed by immunoblotting

(B) Following IFN treatment, LGP2 KD cells do not express detectable levels of LGP2 by PCR compared to Naïve cells.

Cells were treated +/-IFN for 16 hours before TRIzol RNA extraction and endpoint PCR. The LGP2 KD cells were found not to contain LGP2 when probed compared to the Naïve cells.

(C) Naïve and LGP2 KD reporter cells display similar levels of GFP+ve cells following transient transfection with pdINOTI MCS R-IRF3, for transiently expressing IRF3 in the cell. See text for details.

3.2.5. Flow cytometry analysis of virus infected reporter cells

The previous plaque assay and immunofluorescence data suggests that RIG-I is the primary sensor that detects PAMPs generated during virus infection, resulting in the induction of IFN. In order to examine this more quantitatively, the levels of GFP expressing reporter cells in which the IFN-β promoter has been activated as % total of cells was analysed by flow cytometry. Cell monolayers of Naïve, RIG-I KD, MDA5 KD and LGP2 KD reporter cell lines were grown and infected at an MOI of 0.001 pfu/cell with infections of PIV5 (wt), PIV3 (rwt) and PIV2 (wt). At 2 days p.i. cells were trypsinised and fixed in suspension. Cells were then stained for virus NP and with secondary antibody conjugated to phycoerythrin (PE) for analysis by flow cytometry. Cells expressing (NP-PE) and GFP were counted in a total viable cell population of 10,000 cells. Cell populations were gated based on analysis of mock infected cells that were negative for GFP and NP-PE.

Analysing the flow cytometry data for infections of the reporter cell lines with PIV5 (wt) (**Figure 25A**), it is important to note that the majority of cells are negative for NP (and GFP expression) at the time of fixation. This means that not all of the cells had detectable levels of NP expression caused by virus infection and viral protein transcription. This allows us to study IFN induction generated in the cell monolayer during the development of the viral plaque, before all of the cells are infected. Several discrete cell populations can be detected when analysing infected Naïve reporter cells there is a cell population that is positive only for GFP expression. In GFP+ve/ NP-ve cells, the IFN-β promoter has been activated due to the infection/uptake of a viral PAMP that has been sensed by the PRR(s). This has occurred in the absence of a co-infection with a non-defective wild-type virus, as NP expression is not detected in this cell population.

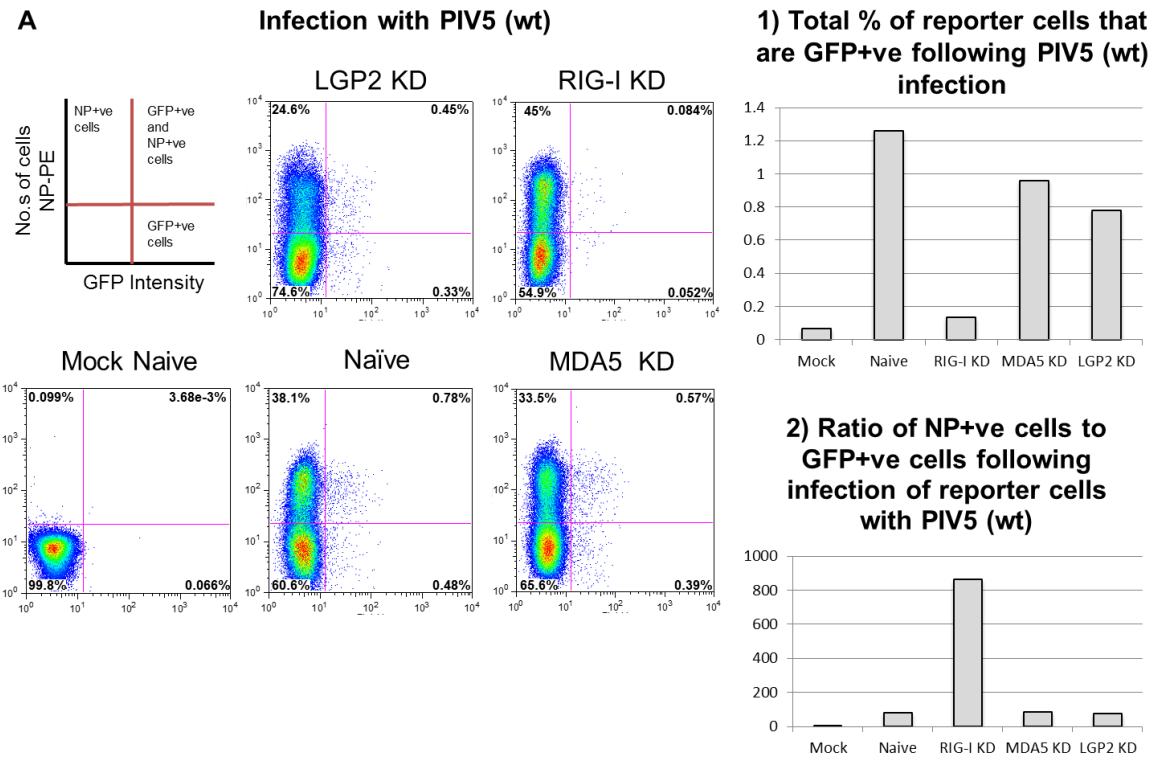
A
Infection with PIV5 (wt)
LGP2 KD
RIG-I KD
NP+ve cells
GFP+ve and NP+ve cells
GFP+ve cells
No.s of cells NP-PE
GFP Intensity
24.6%
0.45%
74.6%
0.33%
45%
0.084%
54.9%
0.052%
Mock Naive
Naïve
MDA5 KD
0.099%
3.68e-3%
99.8%
0.066%
38.1%
0.78%
60.6%
0.48%
33.5%
0.57%
65.6%
0.39%
1) Total % of reporter cells that are GFP+ve following PIV5 (wt) infection
1.4
1.2
1
0.8
0.6
0.4
0.2
0
Mock
Naive
RIG-I KD
MDA5 KD
LGP2 KD
2) Ratio of NP+ve cells to GFP+ve cells following infection of reporter cells with PIV5 (wt)
1000
800
600
400
200
0
Mock
Naive
RIG-I KD
MDA5 KD
LGP2 KD

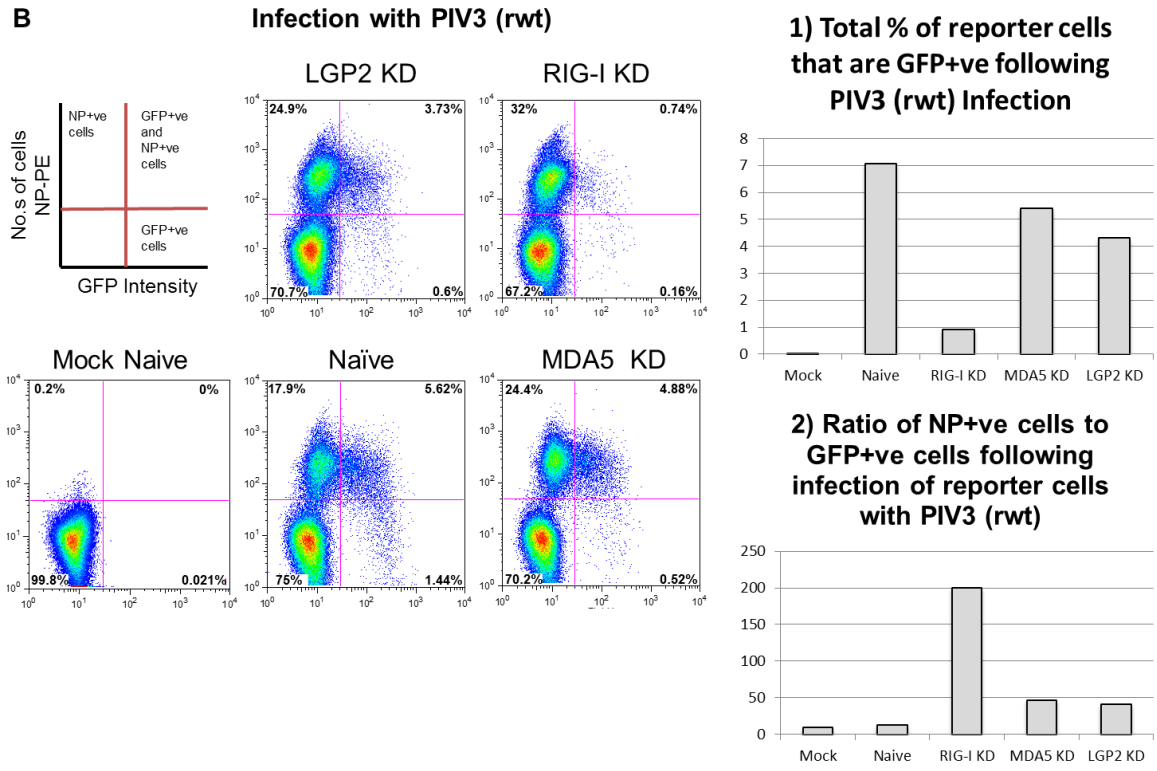
B
Infection with PIV3 (rwt)
LGP2 KD
RIG-I KD
NP+ve cells
GFP+ve and NP+ve cells
GFP+ve cells
No.s of cells NP-PE
GFP Intensity
24.9%
3.73%
70.7%
0.6%
32%
0.74%
67.2%
0.16%
Mock Naive
Naïve
MDA5 KD
0.2%
0%
99.8%
0.021%
17.9%
5.62%
75%
1.44%
24.4%
4.88%
70.2%
0.52%
1) Total % of reporter cells that are GFP+ve following PIV3 (rwt) Infection
8
7
6
5
4
3
2
1
0
Mock
Naive
RIG-I KD
MDA5 KD
LGP2 KD
2) Ratio of NP+ve cells to GFP+ve cells following infection of reporter cells with PIV3 (rwt)
250
200
150
100
50
0
Mock
Naive
RIG-I KD
MDA5 KD
LGP2 KD

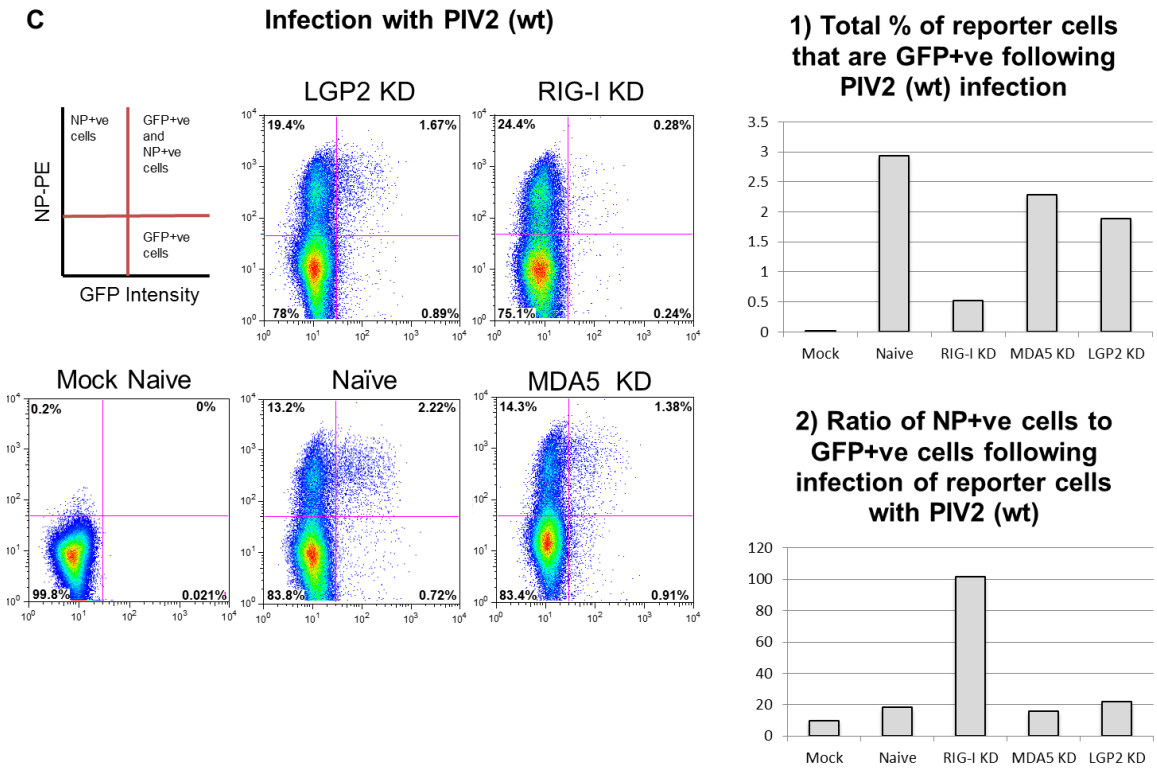

Figure 25. Flow cytometry analysis of reporter cells following infection.

Naïve, RIG-I KD, MDA5 KD and LGP2 KD reporter cell monolayers were infected at an MOI of 0.001 pfu/cell with (**A**) PIV5 (wt), (**B**) PIV3 (rwt) and (**C**) PIV2 (wt). At 2 days p.i cells were trypsinised and fixed in suspension. Cells were then stained for virus NP and then with secondary antibody conjugated to phycoerythrin (PE) for analysis by flow cytometry. Cells expressing NP-PE and GFP were counted in a given total cell population of 10,000 cells. Cell populations were gated based on analysis of mock infected cells that were negative for GFP and NP-PE.

Graph 1) The total numbers of cells that were GFP+ve, i.e. total number of cells that were positive GFP for expression (+/- for the expression of NP) were counted for each infected cell line and plotted.

Graph 2) The ratio of NP+ve cells to GFP+ve cells was taken by the sum of total NP+ve cells (+/- for the expression of GFP) divided by the sum of total GFP+ve cells (+/- for the expression of NP) and plotted for each infected cell line.

Secondly, there is a cell population that is exclusively strongly positive for NP expression. This due to the wild-type non-defective virus infecting the cell, and subsequently viral transcription and replication has occurred without the uptake or generation of a PRR activating PAMP. Thirdly, there is a population of cells that are positive for both NP and GFP expression. This indicates that successful non-defective wild-type virus infection of the cell has taken place due to positive NP expression. During virus infection or replication, a viral PAMP has been produced or has been taken up by the cell that has been sensed by one or more of the PRRs and led to the induction of activation of the IFN-β promoter and hence the expression of GFP. As mentioned before, the previous results (**3.1.2. Heterocellular Induction of IFN-β in reporter cells by PIV5 lacking a functional antagonist**) point to a source of PAMPs such as DIs that are potentially the primary inducers of IFN. As the reporter cells were infected at low MOI, this data suggests that the cells positive for NP and GFP expression are infected with a wild-type virus and that a DI(s) that has been generated during wild-type virus replication. This DI(s) has triggered one or more of the PRRs and led to the activation of the IFN-β promoter and the subsequent induction of IFN in these GFP+ve cells. These findings above were again found for PIV3 (rwt) (**Figure 25B**) and PIV2 (wt) (**Figure 25C**) infections. The co-infection of a GFP+ve cell with a wildtype virus and a DI that has induced the activation of the IFN-β promoter needs to be characterised, and will be examined in the next section of the results (**3.3. Investigating Defective Interfering Particles as the primary inducers of IFN**).

Several patterns can be observed when studying the total % GFP+ve cells generated following infections of the Naïve and PRR knock down reporter cell lines (**Figure 25A Graph 1**). Supporting the previous findings, PIV5 (wt) infection of Naïve reporter cells generates a heterocellular antiviral response. Only a small minority of cells are positive for GFP expression, at 1.26%, and thus only a minority of cells have IFN induced by a viral PAMP generated during virus infection and replication.

Compared to the other reporter cell lines that have reduced expression of the PRRs, Naïve reporter cells have the highest % GFP+ve cells as a proportion of the total cell population. This is unsurprising, as Naive reporter cells possess the full complement of PRRs that are able to sense viral PAMPs generated during viral infection and replication and subsequently induce the activation of the IFN-β promoter and the subsequent expression of GFP.

Clear important differences emerge between infections of the reporter cell lines depending on which PRR has been knocked down. PIV5 (wt) infections of the RIG-I KD reporter cell line generates far fewer GFP+ve cells, at 0.15% of total cells, a reduction of 88% compared to Naïve reporter cells. The level of RIG-I KD reporter GFP+ve cells observed is closer to that found in Mock infected reporter cells. In contrast, the % of total cells that are GFP+ve in MDA5 KD reporter cells at 0.96%, is much closer to that observed for Naïve reporter cells, a reduction of 23%. In the absence of RIG-I expression, this results in significantly fewer cells that are able to respond and have the IFN-β promoter activated following infection, compared to the Naïve and MDA5 KD reporter cell populations. The RIG-I KD reporter cells are thus severely reduced in their ability to recognise viraL PAMPs generated during infection. Supporting this, despite the fully functional expression of MDA5 in RIG-KD reporter cells, IFN-β promoter activation is negligible compared to Naïve reporter cells. Furthermore, MDA5 KD reporter cells have fully functional expression of RIG-I and

shRNA inhibited expression of MDA5, and it is clear that these cells are able to respond to the virus PAMPs generated during virus infection. That there is some reduction in the total % of GFP+ve cells observed for MDA5 KD reporter cells compared to Naïve reporter cells, suggests that some viral PAMPs are generated during virus infection and replication that activate MDA5 mediated signalling. However, this is a rarer event, possibly due to selection pressure by the V protein that inhibits MDA5 mediated signalling.

The flow cytometry data from the PIV5 (wt) infection of LGP2 KD reporter cells (**Figure 25A**) supports the above conclusion that RIG-I is the primary IFN inducing sensor for PIV5 infections. As LGP2 is an enhancer of MDA5 mediated signalling, if MDA5 has been a primary or a significant sensor of PIV5 viral PAMPs, then with the removal of LGP2 expression, the % of GFP+ve cells observed would have been severely reduced compared to Naïve reporter cells and comparable to that observed in RIG-I KD cells. However, this is not the case as it can be observed that the % total LGP2 KD reporter GFP+ve cells is at a similar level to that found in MDA5 KD reporter cells, and is 5.7 times greater than that observed in RIG-I KD reporter cells. However, that there is a reduction of 38% of GFP+ve cells found in LGP2 KD reporter cells compared to Naïve reporter cells, suggesting that LGP2 may have a role as an enhancer of other PRRs or be involved as an adaptor in the IFN induction signalling pathway.

Further supporting the conclusion that RIG-I is the primary sensor that detects PIV5 virus PAMPs, is when the flow cytometry data is analysed for the ratio of NP expressing cells to GFP expressing cells (Figure 25A Graph 2). It is clear from **Graph 2** that for PIV5 (wt) infection of Naïve, MDA5 KD and LGP2 KD reporter cells, they display equivalent low NP+ve:GFP+ve cell ratios in comparison to the NP+ve:GFP+ve cell ratio of the RIG-I KD reporter cells. The RIG-I KD reporter cell

NP+ve:GFP+ve ratio is 5.7 times greater than the ratios found in the other reporter cell lines. This strongly indicates that viral dissemination throughout the monolayer of the Naive, MDA5 KD and LGP2 KD reporter cells is being inhibited by the sensing of virus PAMPs by the fully functionally expressing RIG-I, subsequently inducing IFN and the generation of the antiviral state. Removal of RIG-I means that the cells have a severely reduced response to the virus PAMPs generated during infection, thus resulting in increased virus infection replication and spread throughout the monolayer, observed by the high NP+ve:GFP+ve cell ratio observed in PIV5 (wt) infection of RIG-I KD reporter cells. The results and conclusions observed for PIV5 (wt) infections of the reporter cell lines are replicated for infections with PIV3 (rwt) (**Figure 25B**) and PIV2 (wt) (**Figure 25C**). This indicates that the results observed could be true for other paramyxoviruses.

3.2.6. Section Summary

It has been demonstrated in this thesis via immunofluorescence, plaque assays, flow cytometry that RIG-I is the primary sensor for the detection of the DI PAMPs generated during PIV5 replication. Reporter cells that are knocked down for RIG-I have larger plaques developed over the course of infection. Furthermore, far fewer GFP+ve RIG-I KD reporter cells are detected compared to Naïve, MDA5 and LGP2 KD reporter cells following infection with PIV5 (wt). By removing the RIG-I sensor, reporter cells are significantly reduced in their ability to recognize the DI PAMPs generated during PIV5 infection, and consequently far fewer cells do not have activation of the IFN-β promoter when compared to Naïve, MDA5 KD and LGP2 KD cells.

The data also points to a role of MDA5 and LGP2 in the induction of IFN. Firstly, viral plaques in MDA5 KD reporter cells infected with PIV5 (wt) were not the same size, but were smaller than those found for Naïve reporter cells. Furthermore, flow cytometry analysis of PIV5 (wt) infected MDA5 KD reporter cells showed decreased numbers of GFP+ve cells when compared to Naïve reporter cells. This demonstrates that DI PAMPs containing ligands unique to detection by MDA5 are being generated, as removal of the MDA5 sensor does reduce the % of total cells that are GFP+ve when compared to Naïve reporter cells. The role of LGP2 as an enhancer of MDA5 is supported by the flow cytometry data. The % of cells that are GFP+ve is reduced when LGP2 is knocked down in reporter cells infected with PIV5 (wt).

3.3. Investigating Defective Interfering Particles as the primary inducers of IFN

This section concerns the investigation of PIV5 DIs as the primary inducers of IFN. To investigate the role of DIs in the induction of IFN, a strategy was devised to detect DIs from PIV5 (wt) infected reporter cells. Following infection of reporter cells with PIV5 (wt), Naïve reporter cells would be cell sorted into two discrete populations, GFP+ve and GFP-ve cells. These two distinct populations, following RNA extraction and reverse transcription, would be probed for DIs via real time-Quantitative PCR (RT-QCR). The amount of DIs and viral genomic NP detected in the samples would be analysed via relative quantification compared to housekeeping genes with stable expression. Relative quantification allows the comparison of samples probed under different experimental conditions. If DIs are the primary inducers of IFN, then they would only be detected in cells that have the IFN-β promoter has been activated. *i.e.* GFP+ve cells. Complementing this, GFP-ve cells would be expected not to contain DIs. In addition, by infecting the PRR KD reporter cell lines and probing for the presence of DIs and a reduction in NP expression in GFP+ve cells, the primary PRR that recognises the DIs generated during PIV5 infection can be determined.

3.3.1. Detection of the Large and Small DIs from Control Plasmids

As mentioned previously, it is relatively easy to generate DI rich virus stocks by passaging PIV5 VΔC at high multiplicity, where DIs can readily be detected at passage VM2. Two DI sequences that were present at most abundance following high MOI passaging of PIV5 VΔC were the Large DI trailer copyback (copyback junction at nt position 14043/4-15023/4) and the Small DI trailer copyback (copyback

junction at nt position 14827-15157) (Killip *et al.*, 2013). The Large DI is 1427nt in size and the Small DI is 510nt in size. Plasmids encoding the Large DI and the Small DI for use as positive controls for subsequent experiments and primers used for detecting DIs were developed and supplied by the Goodbourn group, St Georges Medical School. Both of the Forward Primers for the large DI and small DI, primer A1 and A3 respectively, bind to the loop of the DI structure (**Figure 26A**). Furthermore, the Large DI and Small DI Forward primers bind to loop sequences present in DI species for PIV5 (wt) found by deep sequencing. The Large DI and Small DI share the Reverse primer C, which binds to the stem structure of the DI, as both the Large DI and small DI share a common stem trailer sequence (this is true for other species of trailer copyback DIs) (**Figure 26B**). Primer combinations A1/C and A3/C are located on the same antigenomic strand. They thus only produce PCR products if template switching of strands has taken place such as when a Trailer copyback DI is generated. In comparison, the B1/C PIV5 genomic primers are located in opposing orientations, and thus permit amplification of any PIV5 genomic RNA generated by authentic replication. To determine if the primers could successfully probe for the respective DIs for QPCR, the Large and Small DI plasmids were diluted in concentration. The Large and Small DIs were successfully detected by endpoint PCR using the Promega GoTAQ kit (**Figure 26C**). The Large DI A1/C primer PCR product is 965bps in size, and the Small DI A3/C PCR product is 220bp in size. The lowest concentration that the DI can be visualised was used as the initial concentration of the plasmid for QPCR. The Large DI plasmid at ~2.5ng/µl is the initial concentration for QPCR. The Small DI plasmid at ~$1x10^{-4}$ ng/µl is the initial concentration to be utilised for QPCR.

A

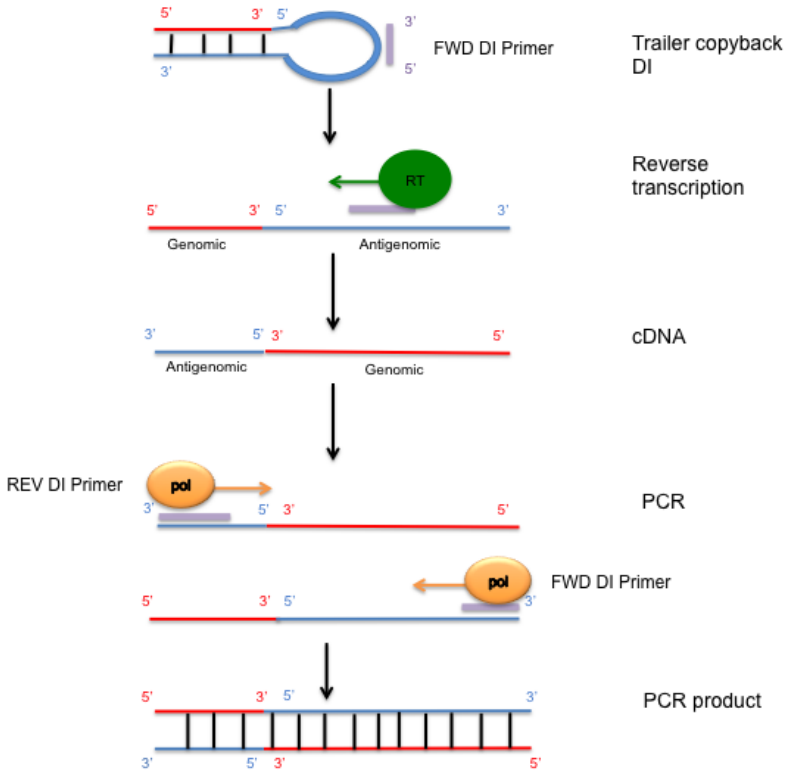

B

Large DI Primers			
Primer Name	Primer Sequence	Primer binding site	PCR product Size
A1	5'- CCAAGAAGACCTAAATTGTAAGGAG – 3' Forward	Loop of DI	900bps
C	5'- CCAAGGGGAAAACCAAGATTAATCCTC – 3' Reverse	Stem of DI	
Small DI primers			
A3	5'- TTTGGAGAAAGCTTCAGGAACC-3' Forward	Loop of DI	220bps
C	5'-CCAAGGGGAAAACCAAGATTAATCCTC – 3' Reverse	Stem of DI	

PIV5 Genomic RNA (vRNA) Primers			
B1	5'- CTCCTTACAATTTAGGTCTTCTTGG-3’ Forward	-	500bps
C	5’-CCAAGGGGAAAACCAAGATTAATCCTC-3’ Reverse	-	

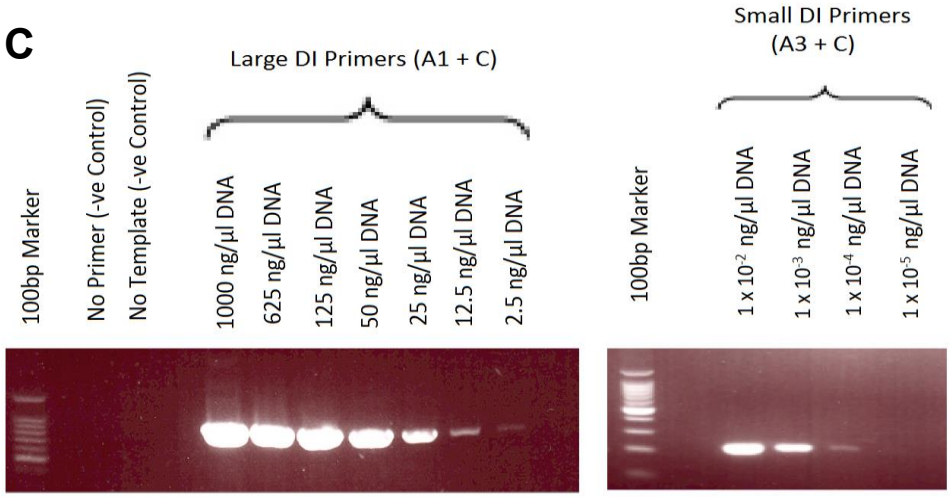

Figure 26. Detecting DIs from Control plasmids by Endpoint PCR

A. Primer Binding Strategy

The Forward primer for reverse transcription and the detection of DIs bind to sequences located in the loop section of the DI structure.

B. Primer combinations for the Large DI, Small DI and PIV5 genomic wild type RNA

C. Detecting large and small DIs from Control Plasmids using Endpoint PCR

Control Plasmids supplied by Goodbourn group. Primers were ordered from Sigma-Aldrich. The DI plasmids were detected by Endpoint PCR, 40 Cycles on a Biometra T Gradient Thermocycler, using the Promega GoTAQ kit.

3.3.2. Detection of DIs from cells following virus infection

The next stage was to detect the Large and Small DIs from Naïve reporter cells infected with PIV5 (wt), PIV5 VΔC VM0 and PIV5 VΔC VM2. Naive reporter cells were infected for 18 hours at a high MOI of 10pfu/cell. Cells were then probed with primers for detection by endpoint PCR (40 cycles) for virus genomic RNA (vRNA), the large DI and small DI (**Figure 27**). Firstly, for all infections PIV5 virus genomic RNA was detected, indicating that there was a successful infection. Secondly, the large and small DIs were detected following infection of Naïve reporter cells with PIV5 VΔC VM2. In contrast, DIs were not detected following infection with DI poor virus preparations of PIV5 (wt) or PIV5 VΔC VM0. This could be due to the absence of DIs present within the DI poor virus preparations of PIV5 (wt) and PIV5 VΔC VM0. This is extremely unlikely as previously, by deep sequencing analysis of the virus preparations, they were found to contain DIs {Killip:2013cbb}. This leads to the second more probable explanation, whereby endpoint PCR is too insensitive a technique for detecting DIs following infection with DI-poor virus preparations. This highlights the need for using the far more sensitive technique of RT-QPCR for detecting DIs in the low numbers of GFP+ve cells generated following infection at a low MOI with PIV5 (wt).

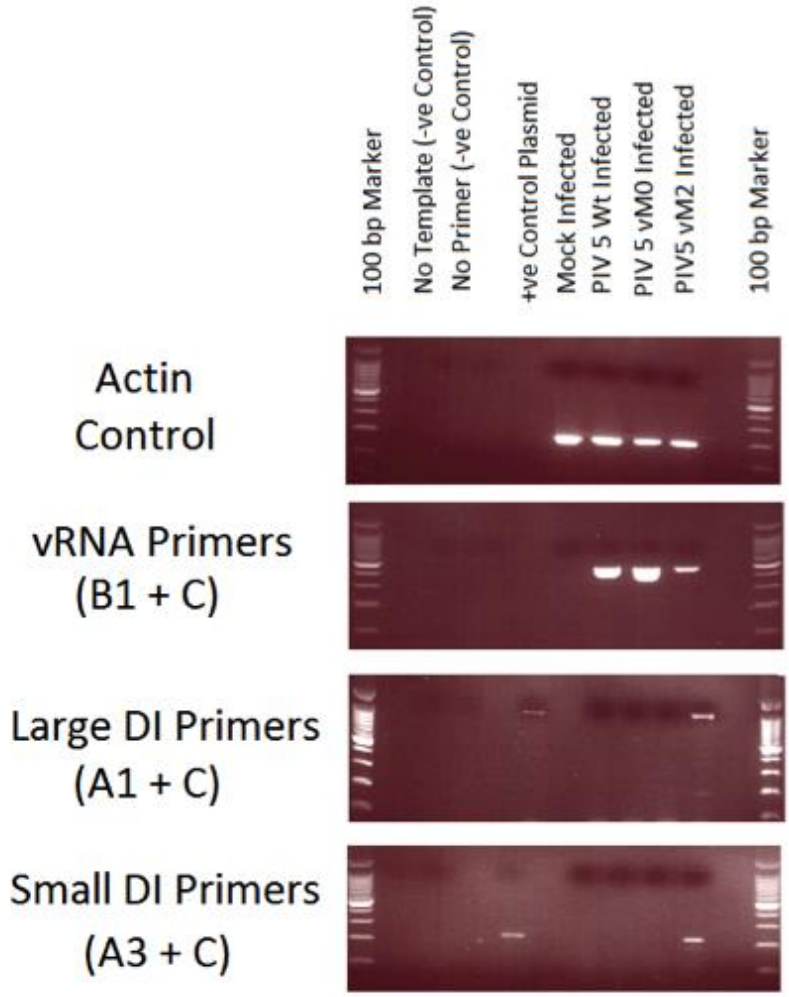

Figure 27. Detection of DIs from infected Naive Reporter cells

Naïve Reporter cells were infected with PIV5 (wt), PIV5 VΔC VM0 and PIV5 VΔC VM2 at a high MOI of 10pfu/cell for 18hrs. RNA was extracted from samples and analysed by endpoint PCR using the Promega GoTAQ kit.

3.3.3. Detection of DIs from cells post-fixation

As mentioned previously, in order to determine if DIs are the primary inducers of IFN following infection, cell sorted reporter cells that are GFP+ve and thus have the IFN-β promoter activated would be probed for the Large and Small DIs in comparison to GFP-ve cells. There are two routes by which reporter cells can be cell sorted following infection and trypsinisation. Firstly, cells could be fixed and then samples sent to a cell sorting facility. The potential advantage is that following fixation there would be little degradation of viral DI RNAs, and cell degradation is reduced. Secondly, infections could take place on site by a cell sorting facility. Immediately after infection, live cell sorting could take place. There are a number of problems that can occur with fixing cells prior to cell sorting. The use of formaldehyde in fixation solutions can crosslink RNA, preventing its purification and extraction using TRIzol. Secondly, alcohol fixatives can destroy some of the cells in suspension prior to cell sorting. In order to determine if cells could be fixed prior to sorting, a range of fixation conditions was tested (**Table 2**). Trypsin contains EDTA, which is superior to DPEC for inhibiting RNAses. Sucrose was tested, as this acts as a "cushion" for cells, increasing osmolarity and stabilizing the integrity of cell membranes. During fixation everything was kept on ice to minimize RNA degradation. Cells were fixed in 5mls of solution, where by fixing in larger volumes, cell "clumpage" and degradation can be reduced.

Naïve reporter cells were infected with PIV5 VΔC VM2 and cells fixed using several different fixation methods (**Table 2**). It was found that following fixation with all of the different methods, the Large DI and Small DI could not be detected by endpoint PCR following RNA extraction (**Figure 28**). As a result, the investigation methodology was altered to use to live cell sorting of samples following infection with the Goodbourn group, St Georges Medical School.

Table 2. Fixation conditions for Naïve reporter cells infected with PIV5 VΔC VM2.

Fixation solution	Fixation conditions
1% Formaldehyde (2% Sucrose) PBS	10mins on ice
1% Formaldehyde (2% Sucrose) PBS Complexes were eluted and cross-links attempted to be reversed by the addition of 300 µl of elution buffer (50 mM Tris–HCl, pH 6.8, 200 mM NaCl, 1 mM EDTA, 1% SDS) and incubation at 65 °C for 12 h. (Chan *et al.*, 2006)	10mins on ice
75% Ethanol in PBS at -20°C	15mins on ice
75% Ethanol in PBS 2% Sucrose at -20°C	15mins on ice
95% Ethanol/ 5% Acetic Acid at -20°C	15mins at -20°C
Methanol, 10% Polyethylene glycols -20°C	15mins on ice
Methanol, 10% Polyethylene glycols -20°C, 2% Sucrose	15mins on ice
70% Methanol PBS -20°C,	15mins on ice
70% Methanol PBS -20°C, 2% sucrose	15mins on ice
Carnoy's solution (60% ethanol, 30% chloroform and 10% glacial acetic acid) (best for keeping RNA intact) -20°C,	15mins on ice
Carnoy's Solution (60% ethanol, 30% chloroform and 10% glacial acetic acid) 2% sucrose	15mins on ice

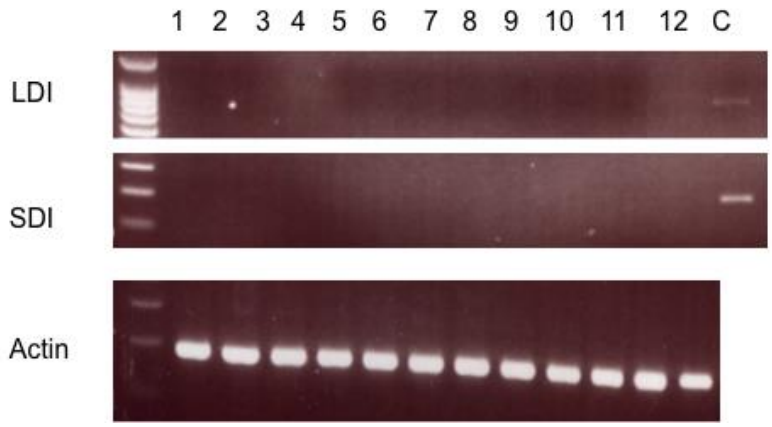

Figure 28. Endpoint PCR of Naïve report cells following infection and fixation.

Naïve reporter cells were infected with PIV5 VΔC VM2 at a high MOI of 10 for 18hrs. Cells were then fixed using the below fixation solutions prior to Endpoint PCR, 40 cycles.

1) 1% Formaldehyde (2% Sucrose) PBS
2) 1% Formaldehyde (2% Sucrose) PBS, plus additional RNA crosslinking reversal step.
3) 75% Ethanol, PBS
4) 75% Ethanol, PBS, 2% Sucrose
5) 95% Ethanol/ 5% Acetic Acid
6) 95%/ 5% Acetic Acid, 2% Sucrose
7) 90% Methanol, 10% Polyethylene glycols
8) 90% Methanol, 10% Polyethylene glycols, 2% Sucrose
9) 70% Methanol, PBS
10) 70% Methanol PBS, 2% sucrose
11) Carnoy's solution (60% ethanol, 30% chloroform and 10% acetic acid)
12) Carnoy's Solution, 2% sucrose,

C = Large DI/ Small DI plasmid Control

3.3.4. Investigating the minimum number of cells required for DI detection by PCR following infection

Following infection and live cell sorting of GFP+ve and GFP-ve cells, RNA would be extracted using TRIzol and probed via RT-QPCR for DIs.. A potential problem that can arise with infecting cell at a low MOI with PIV5 (wt), is that there could be too few GFP+ve cells generated during infection to live cell sort and then subsequently detect DIs by RT-QPCR. At each step in the process, samples containing low numbers of cells cells can easily be degraded by the environment and by the cell sort itself. This was illustrated earlier in the results section where only a tiny minority of cells were GFP+ve following a low MOI infection with PIV5 (wt) (**3.2.5. Flow cytometry analysis of virus infected reporter cells**). To counter this, future infections will take place on cells seeded in a T25 flask to minimise losses during infection, trypsinisation and cell sorting. Naïve reporter cells were infected at a high MOI of 10pfu/cell with PIV5 VΔC VM2 for 24hrs. Cells were then trypsinised and resuspended in 2% FCS/PBS and counted using a SLS HAE 2118 (improved Neubauer) haemocytometer. Samples were then 10 fold serial diluted from 10k cells/100µl to ~10cells/100µl. RNA was extracted from the samples and the Large and Small DIs probed by RT-PCR (**Figure 29**). Encouragingly from the data, it was found that from a population of cells that had not been FACs sorted, the Large and Small DIs could be detected in samples containing ~10 cells.

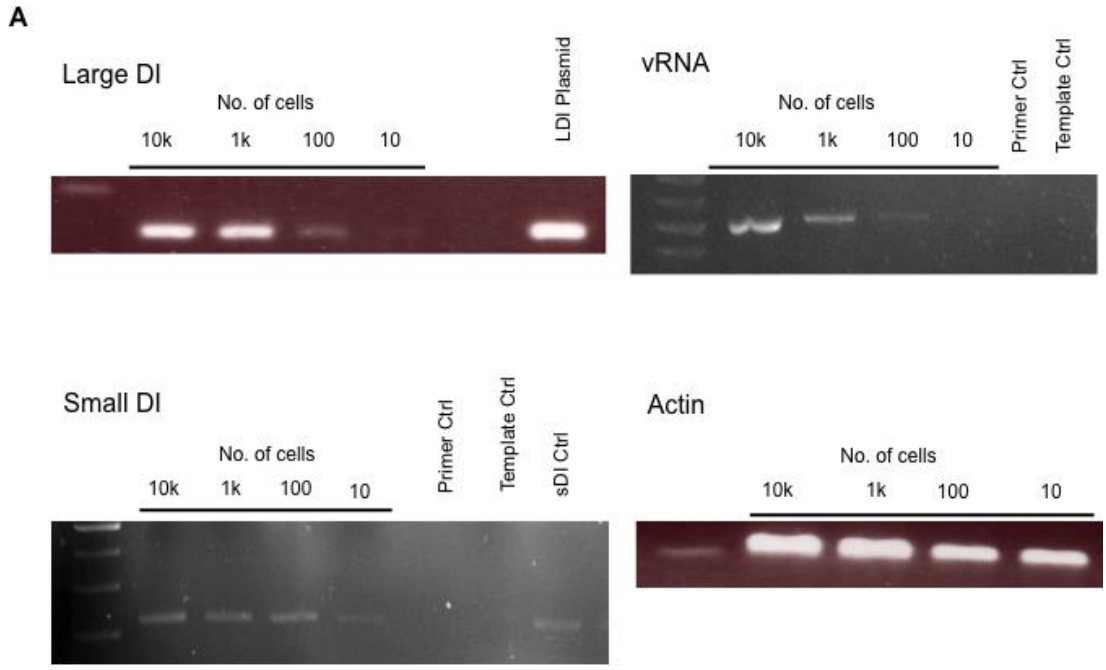

Figure 29. Detection of DIs following dilution of Naïve Reporter cells after infection.

Naïve reporter cells were infected at a high MOI of 10 with PIV5 VΔC VM2 for 24hrs. Cells were then trypsinised and resuspended in 2% Foetal Calf serum (PBS, 0.01% Sodium Azide) and counted using a Haemocytometer. Samples were then 10 fold serial diluted from 10k cells/100µl to ~10cells/100µl. RNA was extracted from the samples and the Large and Small DIs probed by RT-PCR, 40 cycles.

3.3.5. RT-QPCR Detection of DIs from samples following PIV5 infection

The RT-QPCR protocol utilized is a two-step process, beginning with a reverse transcription step, where cDNA is synthesised from the total RNA extracted from infected samples and then used as a template for the RT-QPCR reaction. The levels of RNA are measured in real-time as it is amplified. For this study, SYBR Green (Eurogentec) was used, which is a double stranded intercalating dye that fluoresces when it binds to DNA. SYBR Green binds to any double-stranded DNA, including non-specific DNA and primer-dimer products. It is therefore important to include a dissociation curve (melt curve) in the PCR program that enables one to measure the specificity of the amplified product. If the amplified product is valid, it shows a single, sharp peak.

To detect DIs via QPCR, gene specific primers were generated for the Large and Small DIs using DNA Strider (**Table 3**). For QPCR, products must be below 250bps in size, and the primers products for the Large DI and Small DI are 150bps and 162bps in size respectively. NP is used as a representation of genomic virus RNA. During the Reverse transcription step, the NP reverse primer is used as this will enable the detection of genomic RNA and not messenger RNA for NP, which would be the case if Oligo dT was used instead. In addition, primers were manufactured to a HPLC standard in order to provide sufficient purity/ stringency for the QPCR reaction, by reducing the occurrence of primer-dimer and non-specific products being generated due to errors in the primer sequences.

To test the identification of DIs by QPCR using the HPLC primers, Naïve Reporter cells were infected with PIV5 VΔC VM2 at a high MOI of 10 for 24hrs.

Table 3. HPLC Primers used for probing the Large DI, Small DI and NP during QPCR

Large DI HPLC Primers			
Primer Name	Primer Sequence	Primer Binding on DI	QPCR product Size
LDI HPLC FWD	5'- CAAGCTTGCACTTGATTCCA– 3' Forward	Loop of DI	150bps
LDI HPLC REV	5'- GGATAGGTCTGGTTGGATCG– 3' Reverse	Stem of DI	
Small DI HPLC primers			
SDI HPLC FWD	5'- ATCAGAATTGAGGATGGAAG-3' Forward	Loop of DI	162bps
SDI HPLC REV	5'- GATATGTTTAGATTTCCTCGC– 3' Reverse	Stem of DI	
NP (Genomic RNA) HPLC Primers			
NP HPLC FWD	5'- AGGGTAGAGATCGATGGCT-3' Forward	-	254bps
NP HPLC REV	5'- GCTACATTAGGAAATTGATTGAGGGG -3' Reverse	-	

Primers were ordered from Sigma-Aldrich.

RNA was extracted from cells using TRIzol (Invitrogen) and the RNA concentration measured using the Nanodrop ND-100 Spectrophotometer. Input RNA for all samples for the reverse transcription reaction were standardised at 1µg.

The reverse transcription reaction was carried out using the Promega M-MLV-H RNase H Minus kit. A 2.5µl volume of cDNA was then used in a 25µl reaction using the Eurogentec MESA Blue QPCR Mastermix Plus SYBR Green (low ROX) on the Stratagene Mx3005p QPCR thermocycler (**Figure 30**). ROX is a reference dye used as an internal control that normalises against any fluctuations in the volume or concentration of the mastermix. This gives a higher reproducibility of the PCR assay. A low ROX concentration was used as high concentrations of ROX creates an oversaturated signal on the ROX channel and results in the normalized data containing more noise than the non-normalized data. The QPCR protocol is displayed in **Figure 30**. Initial primer concentrations used were 100µM. Samples initially were performed in duplicate.

Analysing the QPCR results, a strong signal was detected for the Large DI and the Small DI, as well as for the Large DI and Small DI control plasmids as expected. (**Figure 31A, Figure 31B**). This indicates that the Large DI and the Small DI were present in the infected cells and the virus preparation. In comparison, no Large DI or Small DI signal was detected for Mock infected cells. Furthermore, for both the Large DI and the Small DI primer products, the melting curves only showed one large peak, whereby the results are thus valid as only one product had been generated.

For further analysis of the QPCR products, the samples were visualised by DNA-AGE (**Figure 32**). QPCR samples were compared to Endpoint PCR samples, generated using the same cDNA used for QPCR from the previous reverse transcription reaction.

A

Component	Volume (µl)
2x Reaction Buffer	12.5
Forward Primer	2.5
Reverse Primer	2.5
Water	5
Input Material	2.5

B **Eurogentec QPCR Protocol**

Step 1	Meteor *Taq* Activation	5mins	95°C
Step 2	40 Cycles	15 sec	95°C
		1min	60°C
Step 3	Perform Melt curve		

Figure 30. Eurogentec QPCR Protocol

A. QPCR component volumes

B. Eurogentec Mesa Blue QPCR protocol. The initial concentrations of the primers in the reaction mix were at 100µM.

A

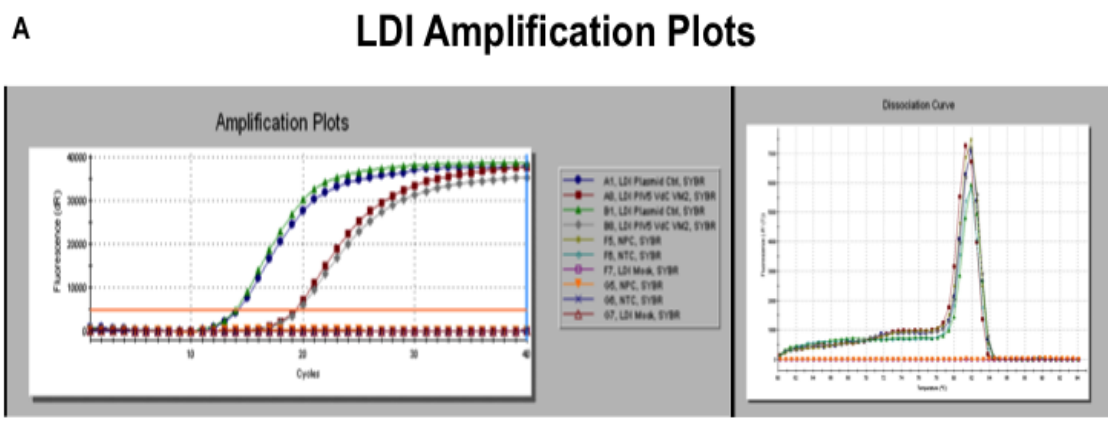

B

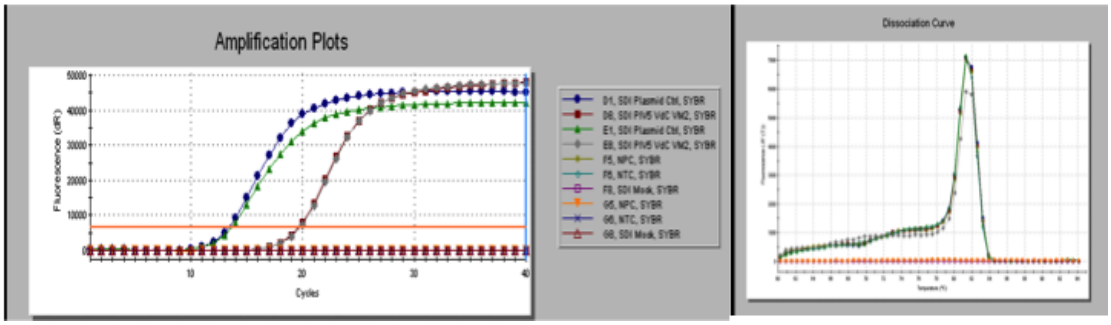

Figure 31. Large DI and Small DI QPCR analysis following infection with PIV5 VΔC VM2

Naïve Reporter cells were infected with PIV5 VΔC VM2 at high MOI of 10 for 24hrs. RNA was extracted and samples analysed by RT-QPCR.

A. QPCR analysis for the Large DI, including dissociation curve

B. QPCR analysis for the Small DI, including dissociation curve

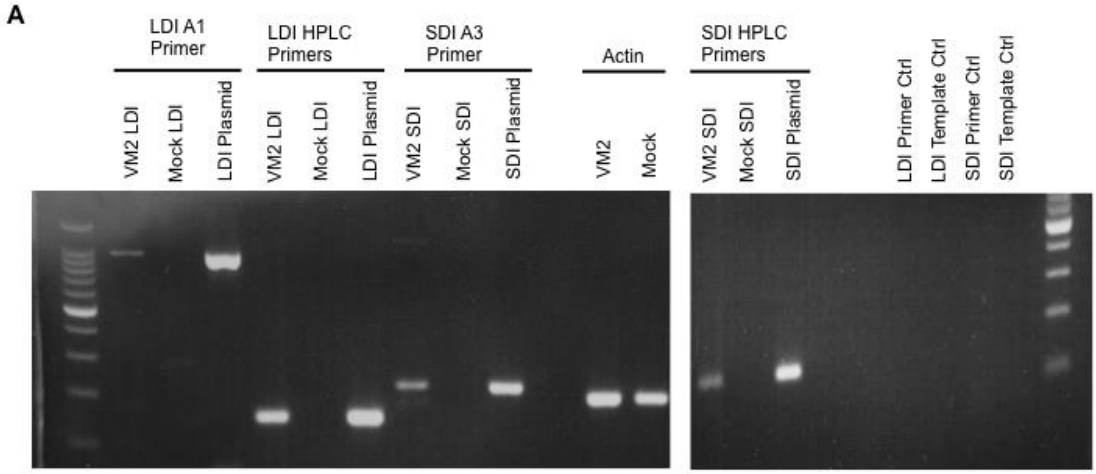

Figure 32. Comparison of QPCR (HPLC primers) and Endpoint PCR samples generated from Naïve reporter cells infected with PIV5 VΔC VM2.

Naïve reporter cells had been infected with PIV5 VΔC CM2 at high MOI of 10 for 24hrs. RNA was extracted, and samples analysed by QPCR and by Endpoint PCR.

The Small DI and Large DI products generated by QPCR can be easily visualised. Samples generated by QPCR have a stronger signal than Endpoint PCR samples, illustrating the high sensitivity and appropriateness of the QPCR assay for DI detection from potentially low numbers of cells.

3.3.6. Optimisation of QPCR Input DNA Plasmid control concentration

It is important to optimise the concentration of the input DNA for the Large DI and Small DI and NP control plasmids. Using the initial concentration found previously of $1x10^{-1}$ng/µl, ((**3.3.1.Detection of the Large and Small DIs from Control Plasmids**) 10-fold serial dilutions were made of the plasmids and tested by QPCR (**Figure 33**). It was found that the optimal concentrations for the Large and Small DI plasmids were $1x10^{-2}$ ng/µl. The dissociation curves also gave rise to a single peak for all of the control plasmids, which indicated that no primer dimers were made during the reaction and that the primers did not bind non-specifically.

3.3.7. Optimisation of LDI, SDI and NP Primer concentration

The Ct values for each primer pair from the real-time quantitative PCR assay were plotted as a standard curve (**Figure 34**). The slope of this curve gives the efficiency of the PCR reaction by the following equation (Pfaffl, 2001):

Efficiency = 10(-1/slope) – 1.

A

Sample name	Ct	Mean Ct	Std.Dev. Ct
LDI 1x10-1ng/µl	10.26	10.23	0.11
	10.12		
	10.32		
LDI 1x10-2ng/µl	13.26	13.52	0.28
	13.48		
	13.82		
LDI 1x10-3ng/µl	15.32	16.58	1.09
	17.17		
	17.24		
LDI 1x10-4ng/µl	20.97	20.85	0.18
	20.94		
	20.65		
LDI 1x10-5ng/µl	24.59	24.87	0.38
	25.3		
	24.72		
LDI 1x10-6ng/µl	27.53	27.3	0.28
	26.99		
	27.37		
LDI 1x10-7ng/µl	29.88	29.99	0.1
	30.09		
	29.98		
LDI -primer Control	No Ct		
	No Ct		
	No Ct		
LDI NTC	32.9	32.39	1.07
	33.11		
	31.17		

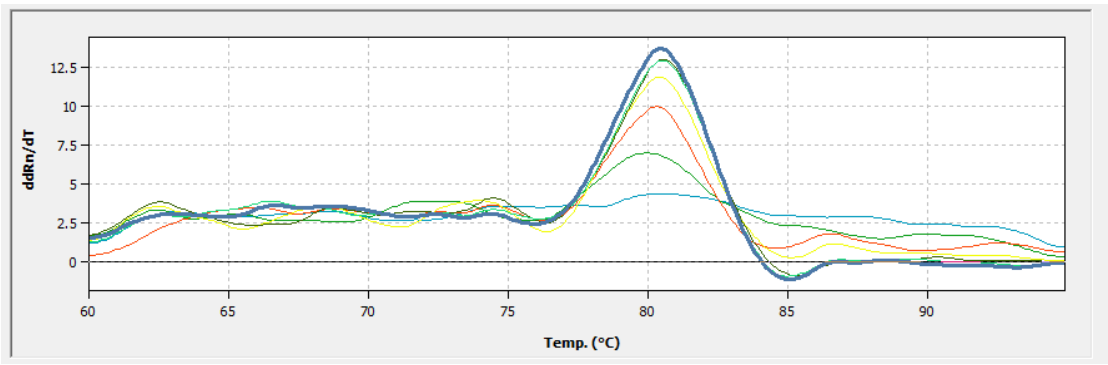

B

Sample name	Ct	Mean Ct	Std.Dev. Ct
SDI 1x10-1ng/µl	No Ct	9.77	0.09
	9.71		
	9.83		
SDI 1x10-2ng/µl	13.23	13.46	0.22
	13.48		
	13.66		
SDI 1x10-3ng/µl	16.59	16.96	0.4
	16.91		
	17.39		
SDI 1x10-4ng/µl	21.48	21.48	0.39
	21.1		
	21.87		
SDI 1x10-5ng/µl	24.5	23.65	1.31
	24.31		
	22.14		
SDI 1x10-6ng/µl	28.44	27.7	0.99
	26.57		
	28.07		
SDI 1x10-7ng/µl	32.48	32.36	0.22
	32.49		
	32.1		
SDI -primer Control	No Ct		
	No Ct		
	No Ct		
SDI NTC	34.03	34.59	0.79
	No Ct		
	35.15		

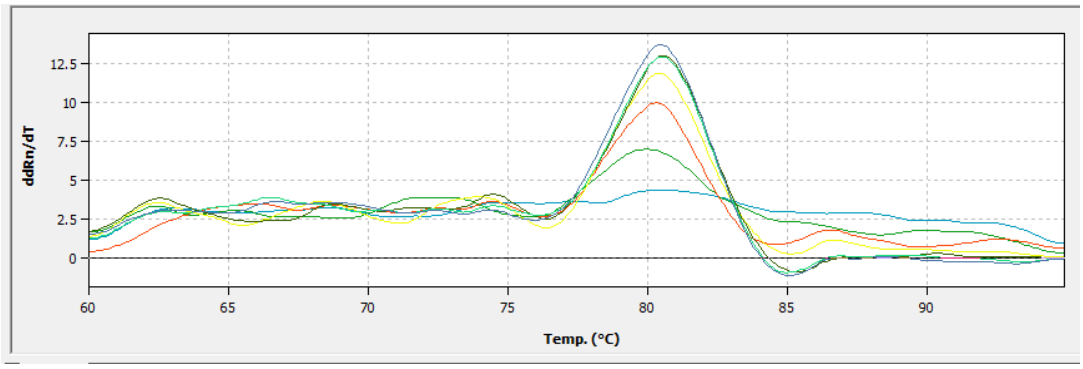

C

Sample name	Ct	Mean Ct	Std.Dev. Ct
NP 1x10-1ng/µl	No Ct		
	No Ct		
	No Ct		
NP 1x10-2ng/µl	9.79	9.48	0.31
	9.46		
	9.18		
NP 1x10-3ng/µl	12.85	12.47	0.42
	12.55		
	12.02		
NP 1x10-4ng/µl	16.1	10.55	0.47
	15.56		
	15.16		
NP 1x10-5ng/µl	19.69	12.99	0.40
	19.29		
	18.89		
NP -primer Control	No Ct		
	No Ct		
	No Ct		
NP NTC	No Ct		
	No Ct		
	No Ct		

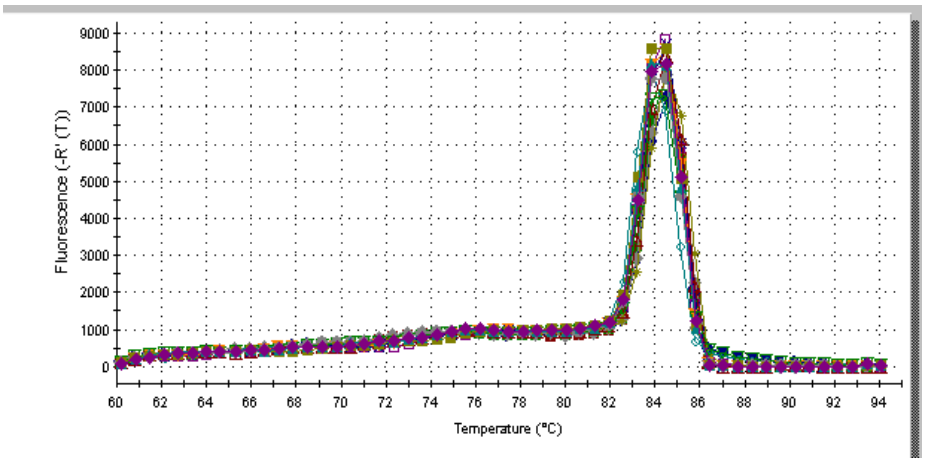

Figure 33. Optimisation of DI and NP control Plasmids

A = Optimisation of Large DI control Plasmid by QPCR and dissociation curve

B = Optimisation of Small DI Control Plasmid by QPCR and dissociation curve

C = Optimisation of NP Control Plasmid by QPCR and dissociation curve

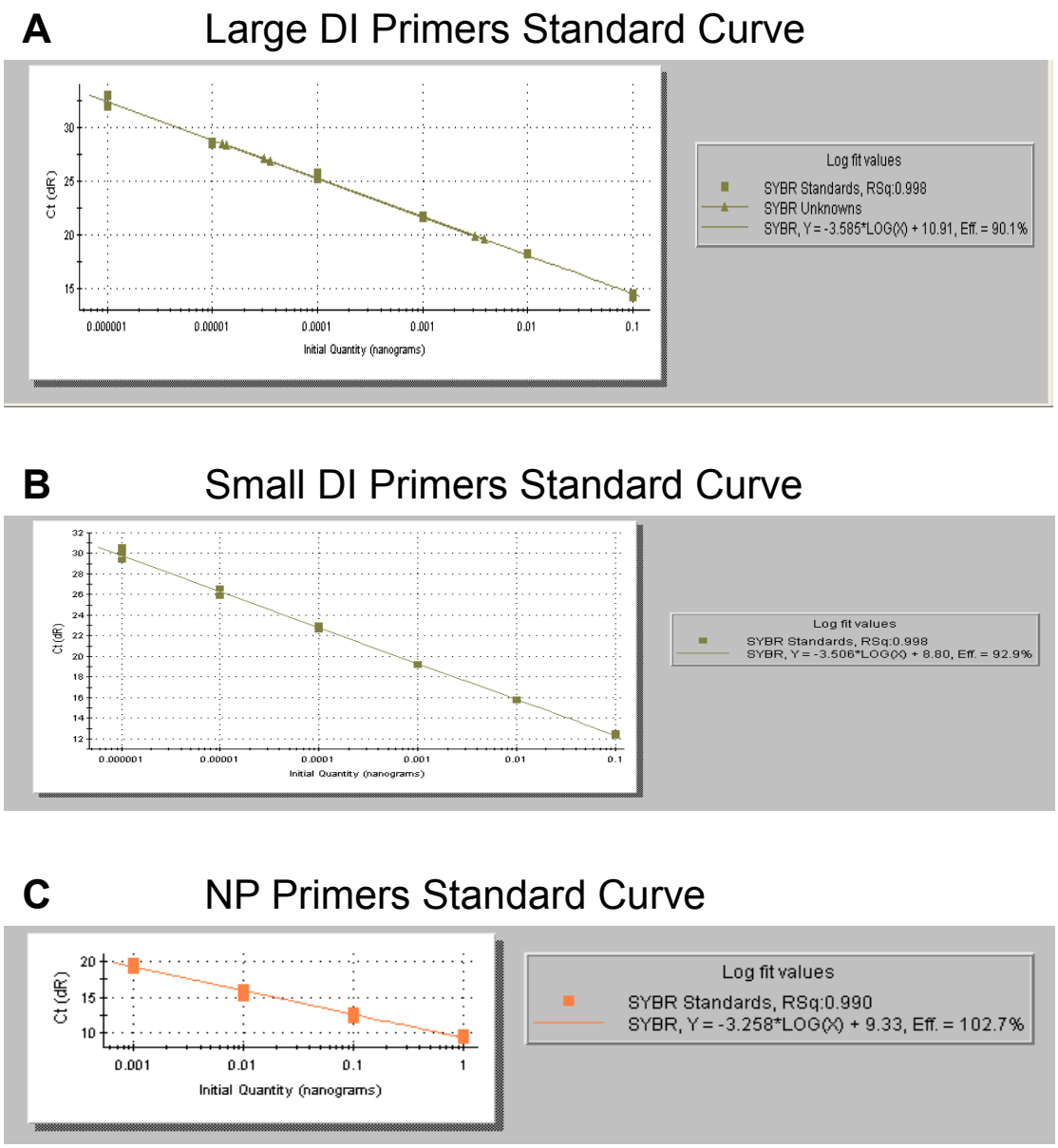

Figure 34. Standard curves obtained for each primer

To calculate the efficiency, the formula Efficiency = 10(-1/slope) – 1 was used.

A = Large DI primers standard curve

B = Small DI Primers standard curve

C = NP Primers standard curve

3.3.8. Optimisation of the QPCR Reference Gene set

When the slope of the standard curve is -3.32, the primer efficiency is 100%. Acceptable PCR efficiency is 100% **±**10%. The Primer slope efficiency obtained from the machine software was 90.1% for the LDI primers; 92.9% for the SDI primers; 102.7% for the NP primers. All the primer combinations were in the acceptable range for PCR efficiency, and thus no further optimization is required. All Forward and Reverse Primer concentrations for the Large DI, Small DI and NP will remain at 100µM.

In order to quantify the amount of DIs in infected samples, two different quantification methods are available, Absolute and Relative Quantification. Absolute quantification requires a standard curve to plot the cycle threshold (Ct) values obtained from the PCR against known amounts of template, whereas relative quantification does not need a standard curve and instead shows the RNA levels of the gene of interest relative to a reference gene or untreated samples. For this study, as we are answering the question "how much are DIs expressed in one sample to another?" i.e. measuring the fold difference in the expression of DIs between two different samples, Relative Quantification is the best method. The relative values were quantified using the comparative Livak Ct method (Cikos et al., 2007; Livak &Schmittgen, 2001):

Step 1

Normalize the Ct of the sample target to that of the sample reference gene (ref) gene for both the test sample and the calibrator sample (i.e. Mock Naïve sample):

ΔCt = Ct test sample target – Ct sample reference

Step 2

Normalize the ΔCt of the test sample to the ΔCt of the calibrator:

ΔΔCt = ΔCt test sample target – ΔCt calibrator

Step 3

Calculate the expression fold difference:

$2^{-\Delta\Delta Ct}$ = normalized expression ratio

The result is the fold difference of the target gene in the test sample to the calibrator sample, normalized to the expression of the reference gene. Normalizing the expression of the target gene to that of the reference gene compensates for any difference in the amount of sample tissue.

However, there are many reference genes available in the cell, where for some reference genes their expression levels may be altered by virus infection. In the Literature, the accepted method is to compare the samples to three housekeeping reference genes that do not vary in their expression levels when testing different experimental conditions such as virus infection. In the literature, a combination of six reference genes have been identified for infections of cells, Glyceraldehyde 3-phosphate dehydrogenase (GAPDH), Tubulin, peptidylprolyl isomerase A (PPIA), Actin, Succinate dehydrogenase complex, subunit A (SDHA) and TATA Binding Protein (Aleksandar Radonić et al. 2005; Watson et al. 2007; Mijatovic-Rustempasic S et al. 2013; Wilson WC et al. 2013; Fuller CM. 2010). The reference gene HPLC primers are outlined in **Table 4**. In order to test for the correct combination of reference genes, Naive reporter cells were infected with PIV5 (wt), PIV5 VΔC VM0, PIV5 VΔC VM2 and Mock infected for 18hrs at high MOI of 10pfu/cell.

Table 4. Housekeeping gene HPLC primers used in QPC

Housekeeping gene	Primers
GAPDH	Forward 5'-ATGACATCAAGAAGGTGGTG-3' Reverse 5'-CATACCAGGAAATGAGCTTG-3'
Tubulin	Forward 5'-TCGTGGAATGGATCCCCAAC-3' Reverse 5'-CTCCATCTCGTCCATGCCC-3'
PPIA	Forward 5'-CCTGGTGGTGCATGCCTAGT-3' Reverse 5'-CTCACTCTAGGCTCAAGCAATCC-3'
β-Actin	Forward 5'-ACTCTTCCAGCCTTCCTTC-3' Reverse 5'-ATCTCCTTCTGCATCCTGTC-3'
SDHA	Forward 5'-TGGGAACAAGAGGGCATCTG-3' Reverse 5'-CCACCACTGCATCAAATTCATG-3'
TATA Box BP	Forward 5'-TGCACAGGAGCCAAGAGTGAA-3' Reverse 5'-CACATCACAGCTCCCCACCA-3'

Primers were ordered from Sigma-Aldrich

Using the Mesa Blue Eurogentec protocol, samples were reverse transcribed and subjected to RT-QPCR following RNA extraction. From the raw Ct values (**Figure 35A**), fold differences in expression levels compared to Mock infected cells were calculated (**Figure 35B**). From **Figure 35B** it can be seen that for all of the reference genes, their relative expression levels in PIV5 VΔC VM0, PIV5 VΔC VM2 and PIV5 (wt) infected cells compared to that of Mock are remarkably similar. All of the reference gene expression levels from infected cells are within +/- 0.2 fold of Mock infected cells.

In addition to examining whether the reference gene expression levels in A549 reporter are altered by infection, it is important to determine if the reference gene expression levels are altered by the expression of Interferon during virus infection. In order to determine this, A549 Reporter cells were Roferon A +/- for 16hrs reference gene expression level subsequently analysed by RT-QPCR (**Figure 36**).
As shown in Figure 13, there was little difference in expression levels of the reference genes between cells treated +/- Interferon. The three reference genes that will be used in future studies will be β-Actin, GAPDH and PPIA.

3.3.9. Optimisation of the Reverse Transcription method

There are three different methods for performing the reverse transcription step. The first method involves separate reverse transcription reactions in different tubes for the Large DI, the Small DI, NP and the reference genes (**Figure 37A**). Whilst this would prevent any interference between the different reverse transcription reactions, the disadvantage with this method is that Reference genes are being reverse transcribed in a separate reaction and tube to the sample targets (Large DI, Small DI and NP).

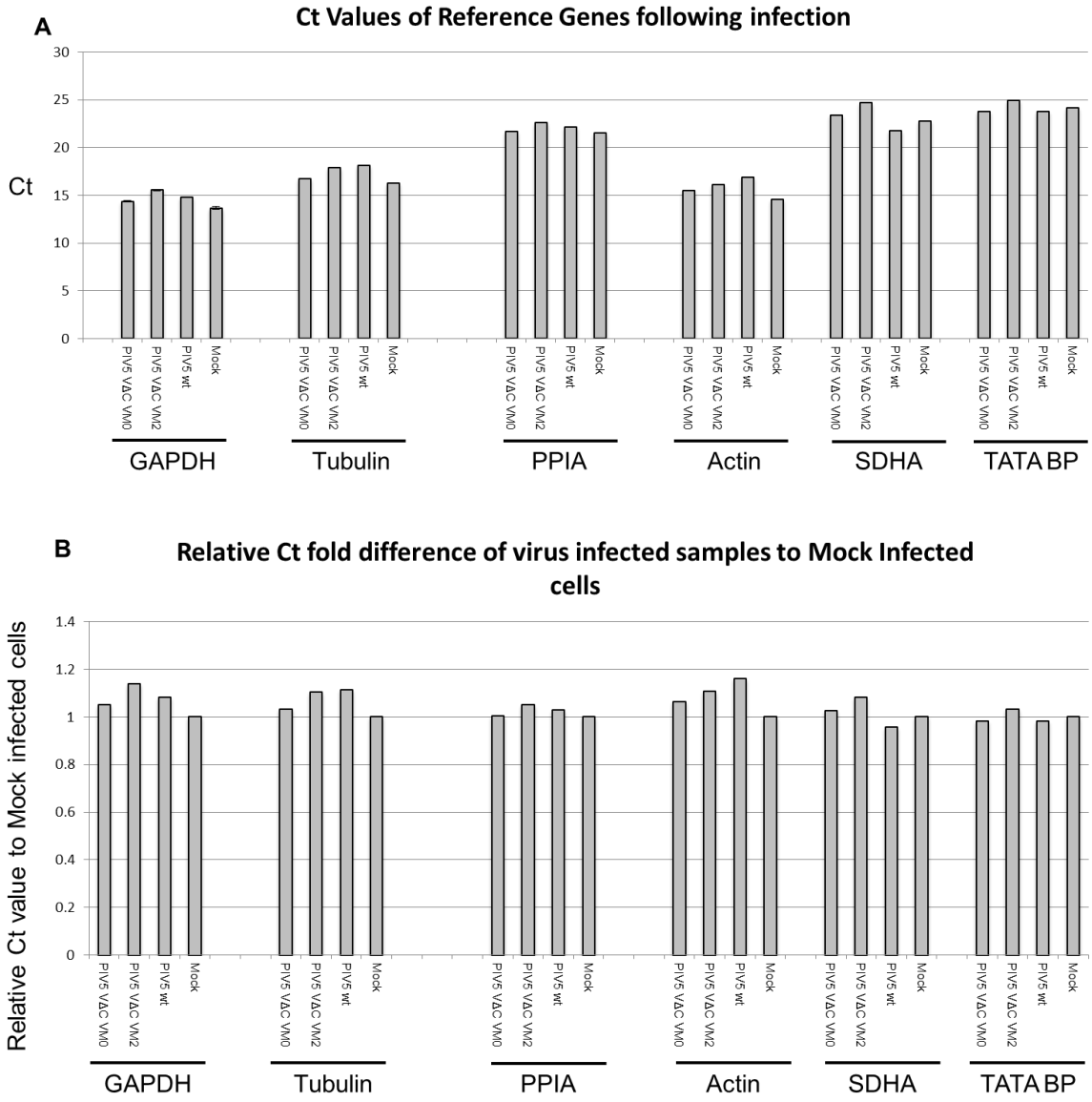

Figure 35. Comparing expression levels of housekeeping genes following infection

A = Graph of raw Ct values of reference gene expression levels from infected A549 reporter cells. Cells were infected with PIV5 (wt), PIV5 VΔC VM0, PIV5 VΔC VM2 and Mock infected at a high MOI of 10pfu/cell for 18hrs prior to TRIzol RNA extraction. Reverse transcription: Oligo (dT).

B = Graph of Relative fold difference of reference gene expression levels to Mock infected cells following infection.

Samples were performed in triplicate. Error bars indicate the standard deviation of each data set.

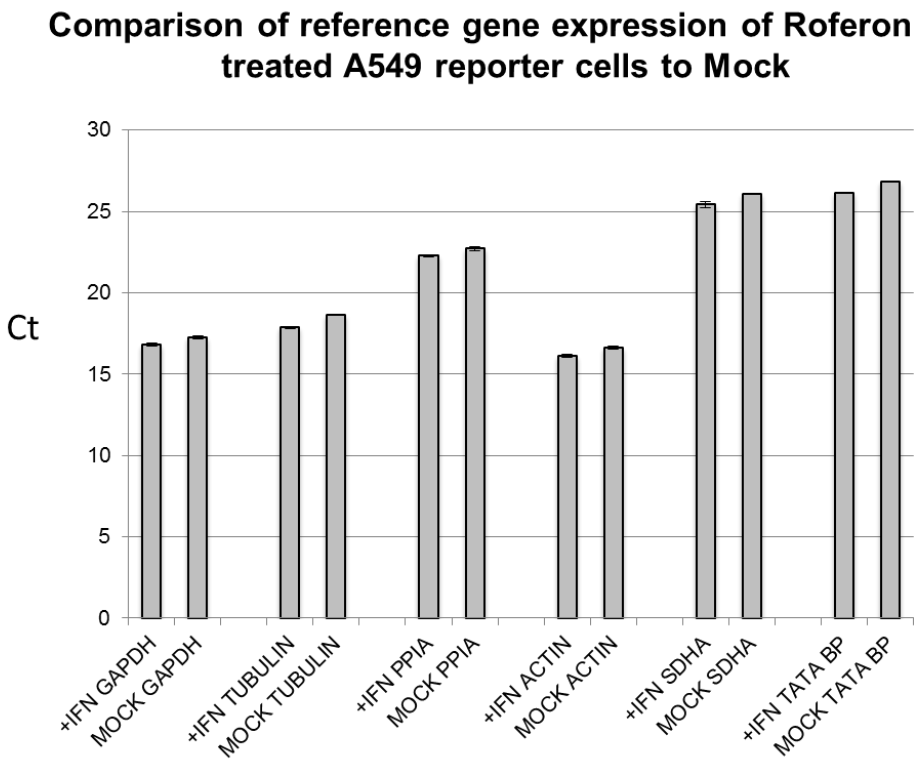

Figure 36. Expression levels of reference genes do not significantly alter between samples treated +/- Interferon.

Naive reporter cells were treated with+/- Roferon A at 1000U per ml, 16hrs before RNA Trizol extraction. Reverse transcription with with olgio (dT). QPCR probing for: GAPDH; Tubulin; PPIA; Actin; SDHA; TATA box Binding protein. Samples were performed in triplicate. Error bars indicate the standard deviation of each data set.

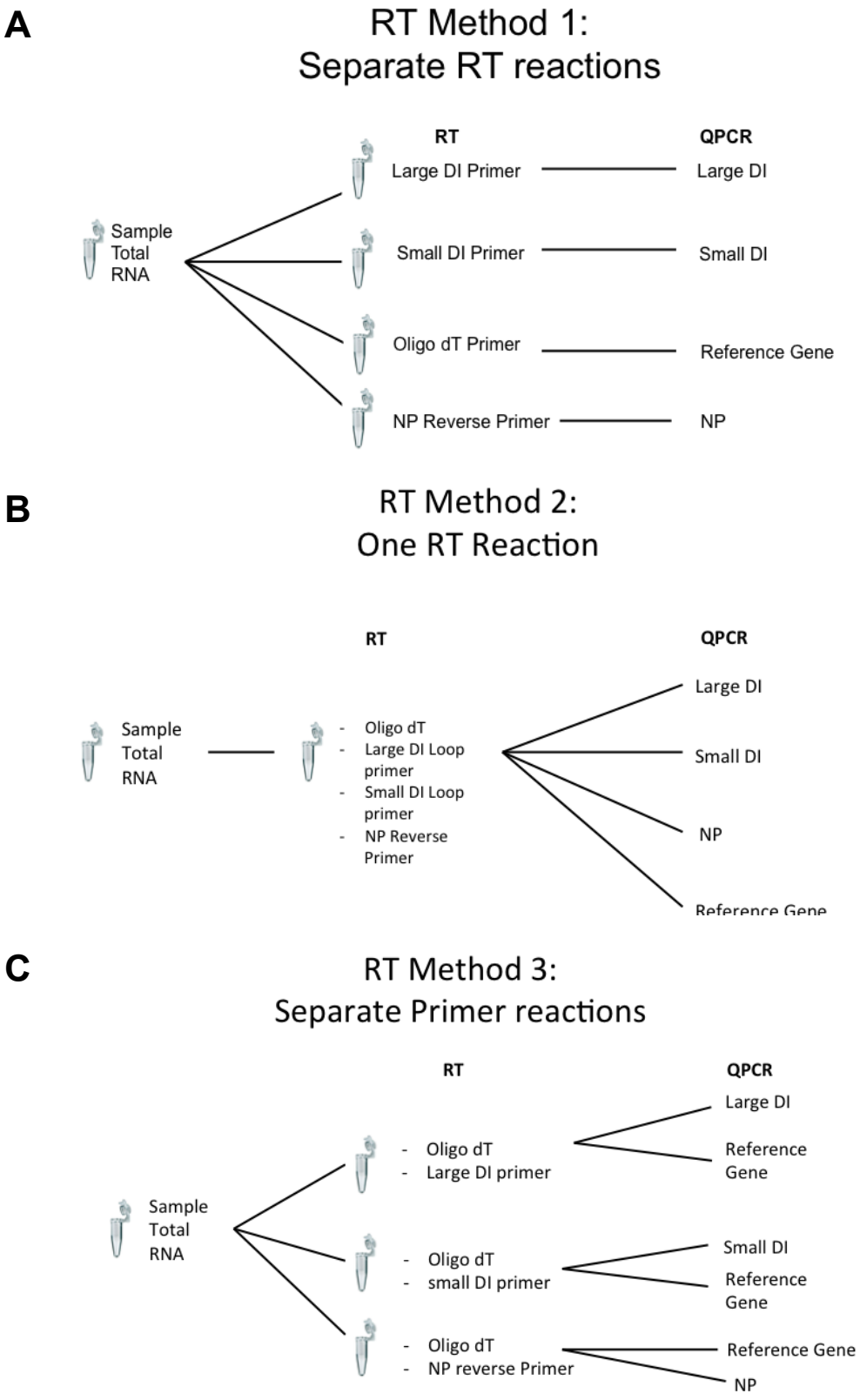

Figure 37. Three different Reverse Transcription methods for RT-QPCR of samples.

See text for details.

By performing separate RT reactions, this means that reference gene cDNA products generated in relation to the target and subsequent QPCR analysis may be unrepresentative. The second method is combining all the primers and reverse transcription reactions into one tube (**Figure 37B**). The advantage of this method is that the cDNA products generated for the reference genes, NP, Large DI and Small DI are representative of each other and a direct stringent comparison can be made following QPCR. A possible disadvantage of this method is that there could be interference between the primers for the Large DI and the Small DI. This is because in theory in a mixed tube for method 2, the Small DI primer could bind to Large DI RNA, generating a product. However, this has not been visualised in the products generated by endpoint PCR in previous reactions. The third method is a compromise, where if interference is detected between the Large DI and Small DI primers for Method 2, the Small DI and Large DI reverse transcription reactions can take place in separate tubes but have the reference gene primers combined with them respectively to give more of a representative result compared to Method 1 (**Figure 37C**).

To test the different reverse transcription methods, Naive reporter cells were infected with PIV5 VΔC VM0 for 18hrs at a high MOI of 10pfu/cell. QPCR analysis of the different RT methods showed that there was minimal variation between LDI products generated and also minimal variation between SDI products generated (**Figure 38**). In conclusion Reverse Transcription Method 2, where the different RT reactions are combined into one tube and performed at the same time will be the method used, as it is the most representative of sample expression levels.

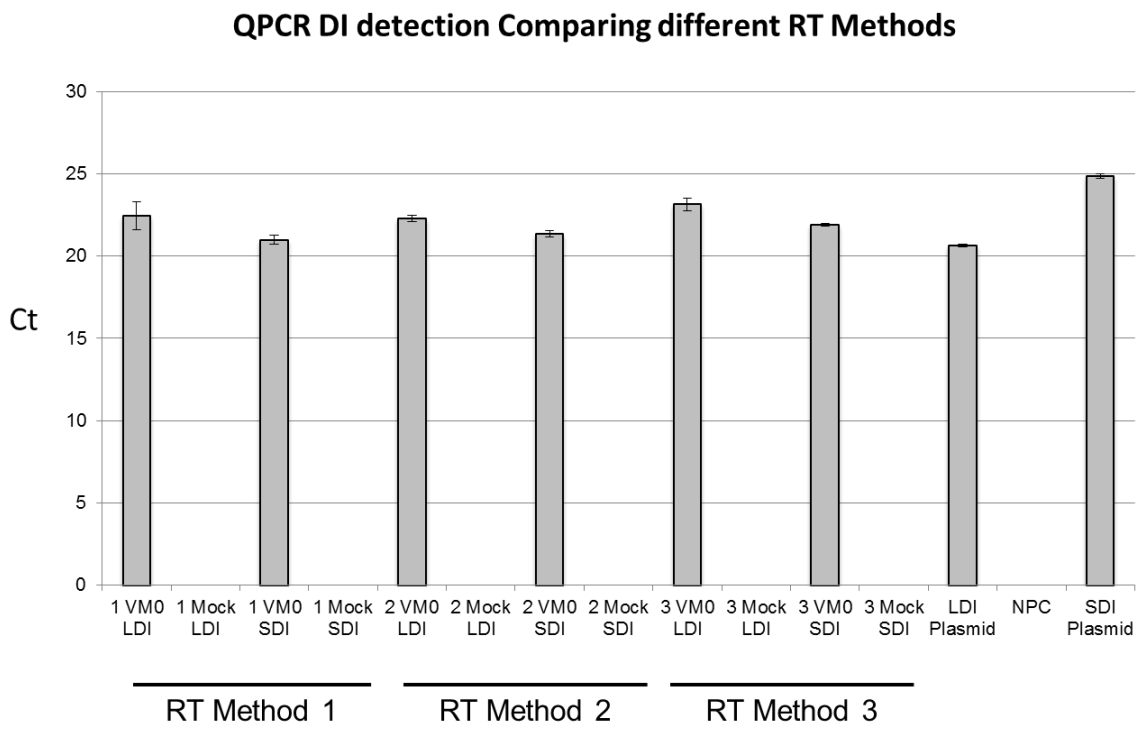

Figure 38. QPCR analysis of DI expression levels between the three different Reverse Transcription methods

Naïve reporter cells were infected with PIV5 VΔC VM0 at a high MOI of 10pfu/cell for 18hrs. RNA was extracted and reverse transcription carried out, evaluating the three different reverse transcription methods identified (**Figure 37**). cDNA was analysed by RT-QPCR of the samples, probing for the Large DI and the Small DI. Samples were performed in triplicate. Error bars indicate the standard deviation of each data set.

3.3.10. Flow cytometry gating optimisation for cell sorting

Prior to cell sorting and collection, it is necessary to gate the populations of cells that are either GFP+ve or GFP-ve following infection. As an example, Naïve reporter cells were +/- infected with PIV5 (wt) at a low MOI of 0.0001 pfu/cell for 4 days. After incubation, cells were trpsinised and resuspended in 2% FCS/PBS (suspension solution). Immediate flow cytometry analysis of these cells displays that there is a spectrum of cell populations displaying a gradient of GFP intensity of infected cells compared to mock cells (**Figure 39**). Mock cells display a discrete population of cells that are GFP-ve. Using mock cell analysis as a base line, infected cells can be divided into a "true" GFP-ve population. However, it is necessary to gate GFP+ve cells further up in the GFP intensity scale, in order to collect a "true" discrete population of GFP+ve cells that are not mixed with GFP-ve cells. If a mixture of GFP-ve and GFP+ve cells were collected, this would invalidate subsequent QPCR analysis for the abundance of DIs. As a consequence, prior to each sample being cell sorted for GFP+ve and GFP-ve cells, a preliminary flow cytometry analysis was conducted in order to determine the appropriate gates using mock cells as a base line, as shown in **Figure 39**. The "middle" mixed population of GFP+ve and GFP-ve cells was discarded.

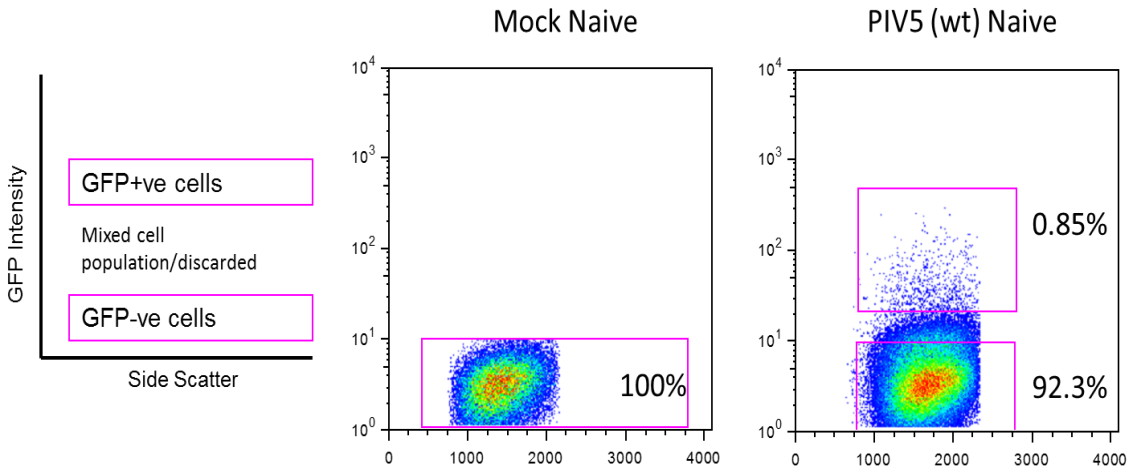

Figure 39. Example of Gating of GFP+ve and GFP-ve cell populations, prior to cell sorting and collection following infection with PIV5 (wt)

Naïve reporter cells were +/- infected with PIV5 (wt) for 4 days at an MOI of 0.0001pfu/cell. Cells were trpsinised and resuspended in 2% FCS/PBS. Live Cells were analysed by the Beckman Coutoure MOFLO (Cytomation) cell sorter. Infected cells were analysed compared to Mock at a collection of 10,000 cells. Infected cells were gated for GFP+ve and GFP-ve populations in comparison to mock (in pink gates, gated cells as a % of total cells shown next to each gate). Following gating, GFP+ve cells and GFP-ve cells were collected separately at the same time by the cell sorter machine. Collected cells were immediately spun down and RNA TRIzol extraction taken place, prior to RT-QPCR.

3.3.11. RT-QPCR Analysis of reporter cells following infection with PIV5 (wt)

Flow Cytometry Analysis of reporter cells infected with PIV5 (wt)

As the methods of cell sorting, reverse transcription and the RT-QPCR protocols for probing for DIs have been optimised, we can proceed to study the relative abundances of DIs present in GFP+ve and GFP-ve cell sorted samples following PIV5 (wt) infection. Naïve, RIG-I KD, MDA5 KD and LGP2 KD reporter cells were infected with PIV5 (wt) at a low MOI of 0.0001pfu/cell for 4 days incubation. A low MOI infection enables the analysis of DIs generated only during plaque development to be analysed. In addition, a Naïve reporter cell set of samples were treated with the Z-VAD-FMK caspase family inhibitor (ZVAD; Enzo Life Sciences) at 100μM final concentration per sample. This was performed as ZVAD is an inhibitor of apoptosis, and it was important to test for potential future experiments whether the addition of this chemical could enhance cell survival for subsequent analysis by RT-QPCR. In addition, a Naïve reporter cell sample was also treated with Roferon A for 12hrs, before analysis by flow cytometry.

Following infection/treatment, cells were trypsinised and resuspended in 2% FCS/PBS solution. Samples were analysed by flow cytometry to decide the appropriate gates for sorting the cells into the respective GFP+ve and GFP-ve populations by comparing the infected sample to the mock sample as a base line. In addition, the population distribution of GFP+ve cells as a % of total cells was recorded for each sample (**Figure 40**). Analysing the flow cytometry data it is interesting to note that the results observed are comparable to those found previously (**3.2.5. Flow cytometry analysis of virus infected reporter cells).**

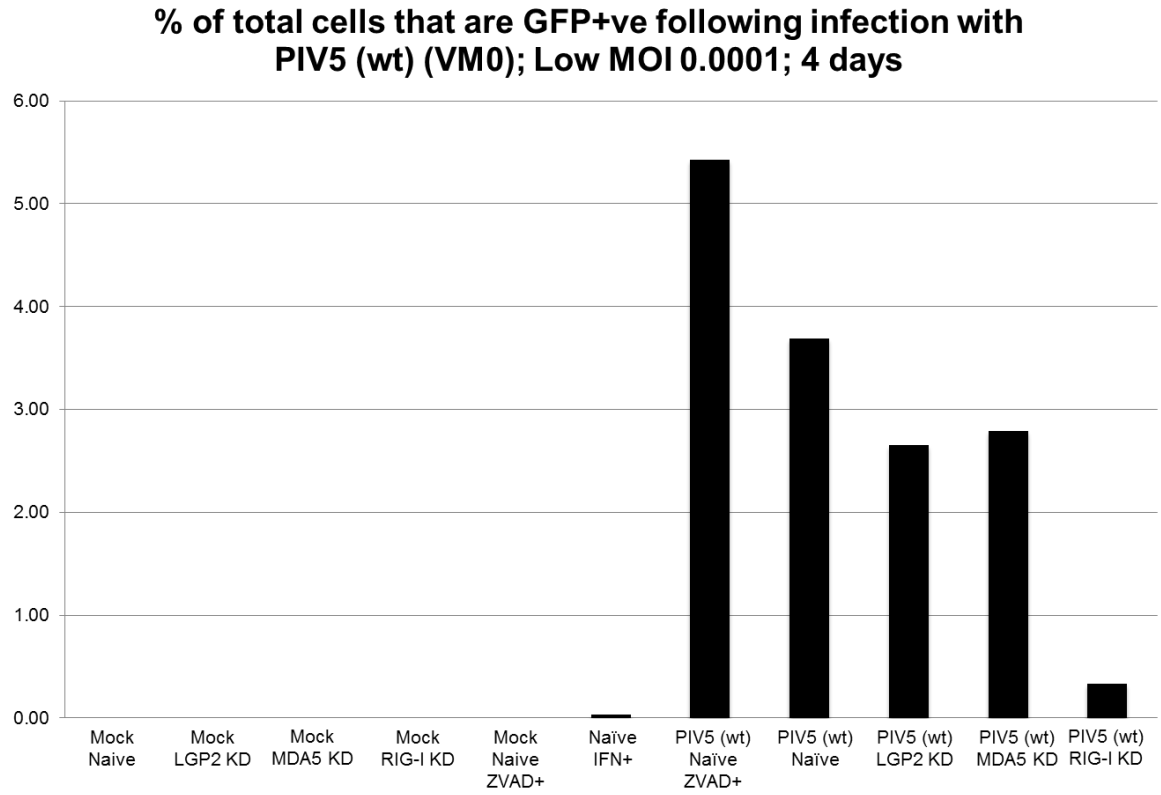

Figure 40. Flow cytometry analysis of reporter cells infected with PIV5 (wt)

Naïve, RIG-I KD, MDA5 KD and LGP2 KD reporter cells were +/- infected with PIV5 (wt) for 4 days at an MOI of 0.0001pfu/cell. Naïve reporter cells also +/- treated with 100μM ZVAD during infection. A Naïve reporter cell sample was also treated with Roferon A for 16hrs. Cells were trpsinised and resuspended in 2% FCS/PBS. Live Cells were analysed by the Beckman Coutoure MOFLO (Cytomation) cell sorter.

Supporting the previous data (**Figure 25A Graph 1**), similar levels of GFP+ve cells as a % of total cells can be observed when studying the total % GFP+ve cells generated following infections of the Naïve and PRR knock down reporter cell lines with PIV5 (wt) (**Figure 40**). Supporting the previous findings, PIV5 (wt) infection of Naïve reporter cells generates a heterocellular antiviral response. Only a minority of Naive reporter cells are positive for GFP expression, at 3.69%, and thus only a minority of cells have IFN induced by a viral PAMP generated during virus infection and replication. In accordance with expectations, Naïve reporter cells treated with ZVAD during infection had a greater survival rate compared to untreated cells, in which 5.43% cells were positive for GFP expression.

Compared to the other reporter cell lines that are knocked down for the PRRs, Naïve reporter cells have the highest % GFP+ve cells as a proportion of the total cell population. This is unsurprising, as Naive reporter cells possess the full complement of PRRs that are able to sense viral PAMPs generated during viral infection and replication and subsequently induce the activation of the IFN-β promoter and the expression of GFP.

PIV5 (wt) infections of the RIG-I KD reporter cell line generates far fewer GFP+ve cells compared to Naïve reporter cells. In contrast, the % of total cells that are GFP+ve in MDA5 KD and LGP2 KD reporter cells are similar in level to each other and are greater than the levels observed for RIG-I KD cells. It can be concluded that in the absence of RIG-I expression, this has caused in far fewer instances RIG-I KD reporter cells that are able to recognise and respond to DI PAMPs generated during infection when compared to the higher levels of GFP+ve cells detected for the Naïve, MDA5 KD and LGP2 KD reporter cell populations. The RIG-I KD reporter cells, despite having a fully functional MDA5 sensor, are severely reduced in their ability to sense the viral PAMPs generated during PIV5 (wt) plaque

development and thus have negligible activation of the IFN-β promoter when compared to Naïve, MDA5 and LGP2 KD reporter cells that possess a RIG-I sensor. This data suggests that the majority of the DI PAMP populations generated during viral plaque development activate primarily RIG-I. As there is some reduction in the % of GFP+ve cells observed for MDA5 KD and LGP2 KD reporter cells as a proportion of total cells when compared to the GFP+ve level observed for Naïve reporter cells, this suggests that some viral PAMPs are generated during viral plaque development that are capable of activating MDA5 mediated signalling, albeit that are generated at a far reduced rate compared to the generation of RIG-I sensed DI PAMPs.

RT-QPCR of cell sorted GFP+ve and GFP-ve reporter cells

Following flow cytometry analysis and gating of the samples, samples were then cell sorted into discrete populations of GFP+ve and GFP-ve cells. GFP+ve and GFP-ve cells were collected in separate collection vials at the same time on ice. Following the cell sorting procedure, cells were spun down and immediately RNA was TRIzol extracted. RNA concentrations were measured and normalised between samples to allow comparison whereby 1µg of extracted RNA was used in the reverse transcription reaction. Reverse transcription was carried out using the appropriate primers for detecting housekeeping genes (Oligo (dT)), PIV5 genomic NP (NP reverse primer), Primer A1 (LDI) and Primer A3 (SDI) by combining the reverse transcription reactions into the same tube by "Method 2" as described previously (**3.3.8. Optimisation of the Reverse Transcription method**). The DI primers used in the detection of the Large DI and Small DI of PIV5 VΔC VM2 can be used to

detect the DIs generated during PIV5 (wt) infection. The DIs generated during PIV5 (wt) infection will be a mixed population and different to those generated by PIV5 VΔC (as shown in (Killip *et al.*, 2013)), The PIV5 (wt) DIs subsequently detected using the Large DI and Small DI primers will be referred to as the LDI primer product and the SDI primer product respectively.

Following the reverse transcription step, samples were then subjected to RT-QPCR using the Mesa Blue Eurogentec protocol. Samples were probed for the LDI primer product, the SDI primer product, PIV5 genomic NP and the housekeeping genes PPIA, β-Actin and GAPDH. Negative controls included non-primer control (NPC), non-template control (NTC), minus Mesa Blue (-SYBR) and minus Reverse transcription enzyme (-RT). The positive control was the respective plasmid encoding the PIV5 VΔC Large DI, the PIV5 VΔC Small DI or PIV5 NP. The Ct values generated were then analysed using the Livak Ct method for the relative quantification of LDI primer products, SDI primer products and PIV5 genomic NP to the housekeeping genes.

Analysing the data for the Large DI primer product relative to the housekeeping genes (**Figure 41),** as expected, Mock infected reporter cells and mock infected Naïve reporter cells treated with IFN did not contain any DIs. It is striking to note that when comparing the relative abundance of DIs present in GFP+ve cells compared to the abundance of DIs present in GFP-ve cells, it is clear that DI products can be detected by RT-QPCR in GFP+ve cells, and this is observed when comparing Large DI primer product relative fold difference to β-Actin (**Figure 41A**), PPIA (**Figure 41B**) and GAPDH (**Figure 41C**). In comparison, the relative fold difference of DI abundancy in GFP-ve reporter cells was vastly reduced when compared to DIs present in GFP+ve reporter cells.

A

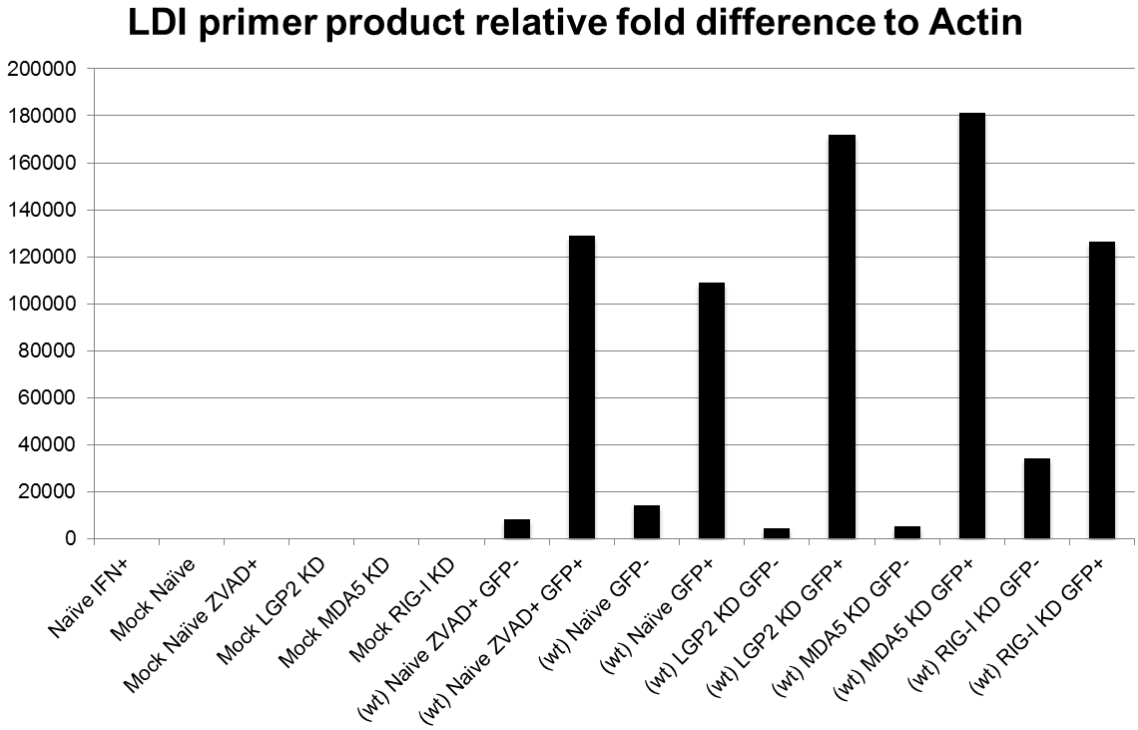
LDI primer product relative fold difference to Actin
200000
180000
160000
140000
120000
100000
80000
60000
40000
20000
0
Naïve IFN+
Mock Naïve
Mock Naïve ZVAD+
Mock LGP2 KD
Mock MDA5 KD
Mock RIG-I KD
(wt) Naive ZVAD+ GFP-
(wt) Naive ZVAD+ GFP+
(wt) Naïve GFP-
(wt) Naïve GFP+
(wt) LGP2 KD GFP-
(wt) LGP2 KD GFP+
(wt) MDA5 KD GFP-
(wt) MDA5 KD GFP+
(wt) RIG-I KD GFP-
(wt) RIG-I KD GFP+

B

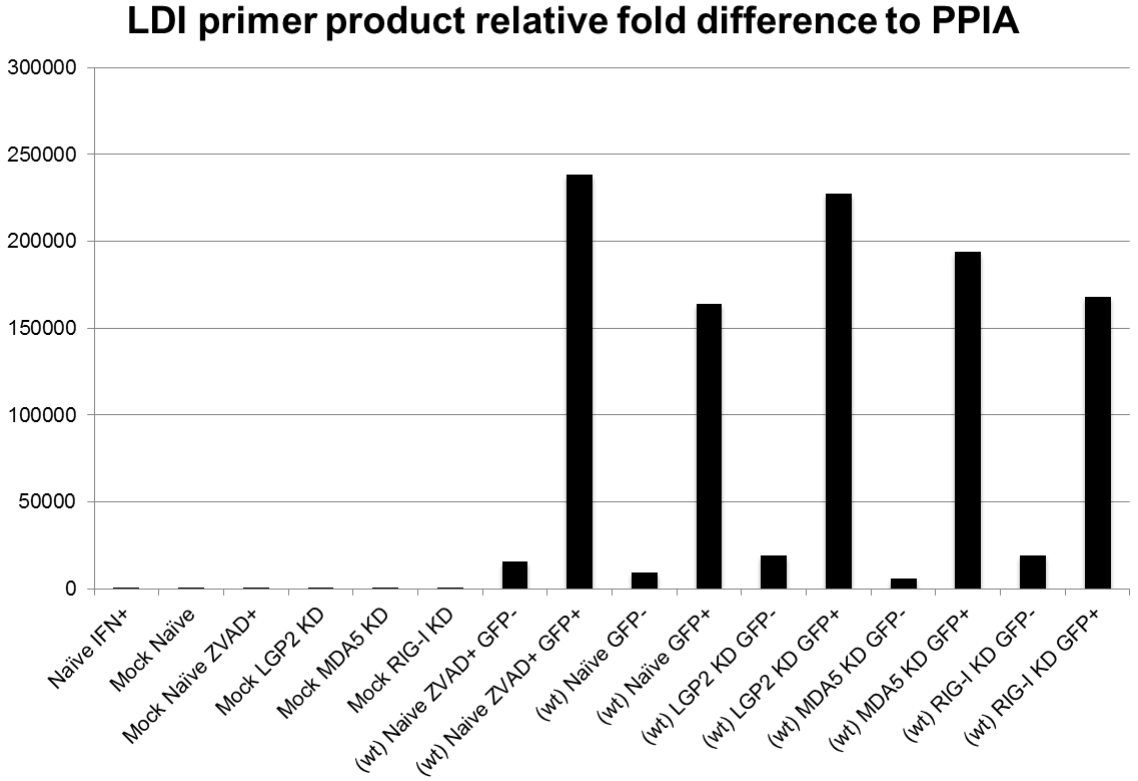
LDI primer product relative fold difference to PPIA
300000
250000
200000
150000
100000
50000
0
Naïve IFN+
Mock Naïve
Mock Naïve ZVAD+
Mock LGP2 KD
Mock MDA5 KD
Mock RIG-I KD
(wt) Naive ZVAD+ GFP-
(wt) Naive ZVAD+ GFP+
(wt) Naïve GFP-
(wt) Naïve GFP+
(wt) LGP2 KD GFP-
(wt) LGP2 KD GFP+
(wt) MDA5 KD GFP-
(wt) MDA5 KD GFP+
(wt) RIG-I KD GFP-
(wt) RIG-I KD GFP+

C

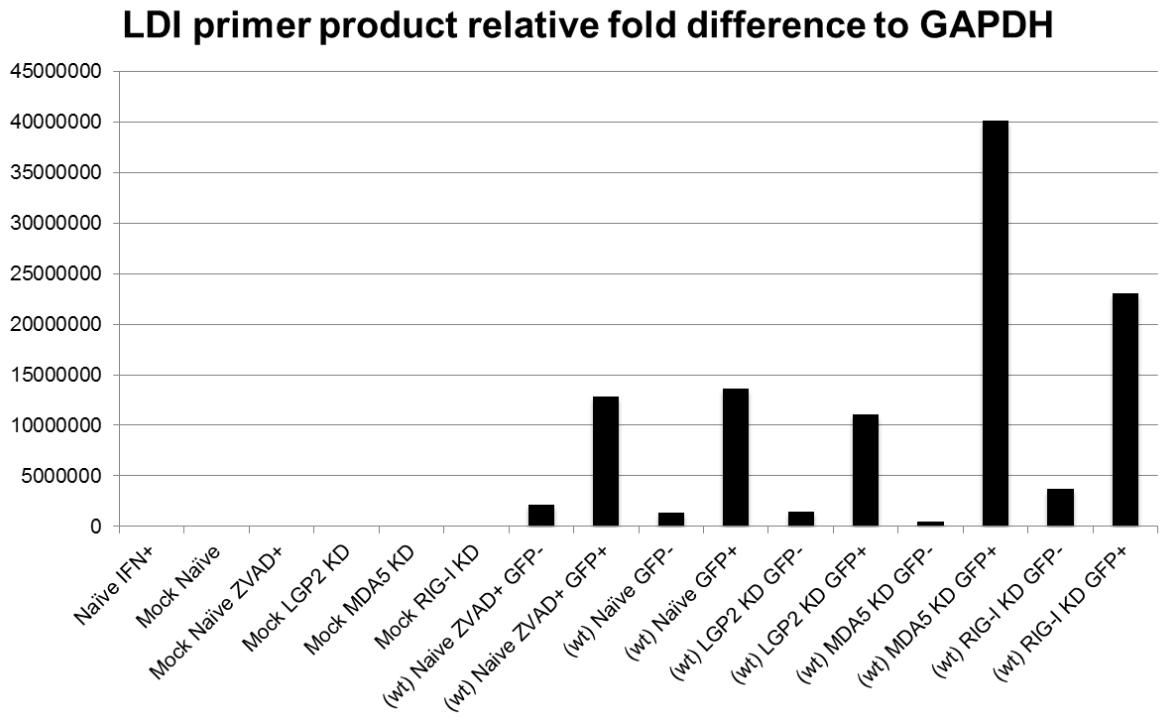

Figure 41. Relative quantification of LDI primer products to housekeeping genes following cell sorting of GFP+ve and GFP-ve cells.

Reporter cells had previously been infected with PIV5 (wt) at a low MOI of 0.0001pfu/cell for 4 days. Following incubation, GFP+ve and GFP-ve cells were cell sorted using the Beckman Coutoure MOFLO (Cytomation) cell sorter. RNA was TRIzol extracted and reverse transcribed. RT-QPCR was performed, probing for the Large DI primer product. Samples were performed in triplicate. The Ct values generated were then analysed using the Livak Ct method for the relative quantification of LDI primer product, to the housekeeping genes β-Actin (**A**), PPIA (**B**) and GAPDH (**C**).

For example, the fold difference between the Large DI primer product between Naïve reporter GFP+ve cells and GFP-ve cells is 6 fold. There is a clear correlation between the presence of DIs and the generation of GFP+ve cells during viral plaque development in which there is activation of the IFN-β promoter. That this pattern was replicated across all reporter cell samples, and the observation confirmed between three different housekeeping genes, gives credence to conclusion that DIs are the primary inducers of IFN.

Furthermore, DIs were detected in GFP+ve RIG-I KD reporter cells. Previous flow cytometry data suggested that PAMPs were generated that activated MDA5 during viral plaque development (**Figure 25**, **Figure 40**). GFP+ve cells observed for MDA5 and LGP2 KD reporter cells as a % of total cells were lower than levels of GFP+ve cells observed for Naïve reporter cells. As DIs were detected for GFP+ve RIG-I KD reporter cells, this supports the notion that a minority subset of DI populations that are generated during viral plaque development are capable of being recognised by MDA5, and subsequently inducing IFN.

The above conclusions are firmly supported by the same patterns being observed when analysing the SDI primer product relative fold differences between GFP+ve and GFP-ve cells (**Figure 42**). When analysing the SDI primer product abundance levels observed when compared to all three of the housekeeping genes, high levels of DIs were only detected in GFP+ve cells, and only low DI abundance levels were detected in GFP-ve cells. This correlation between high DI levels and GFP+ve cells in which the IFN-β promoter has been activated, supports the conclusion that it is the DI PAMPs generated by errors in the replication of non-defective virus by the RNA polymerase during viral plaque development, that are recognised by the PRRs and subsequently leads to the PRR mediated activation of the IFN-β promoter and the subsequent induction of IFN.

A

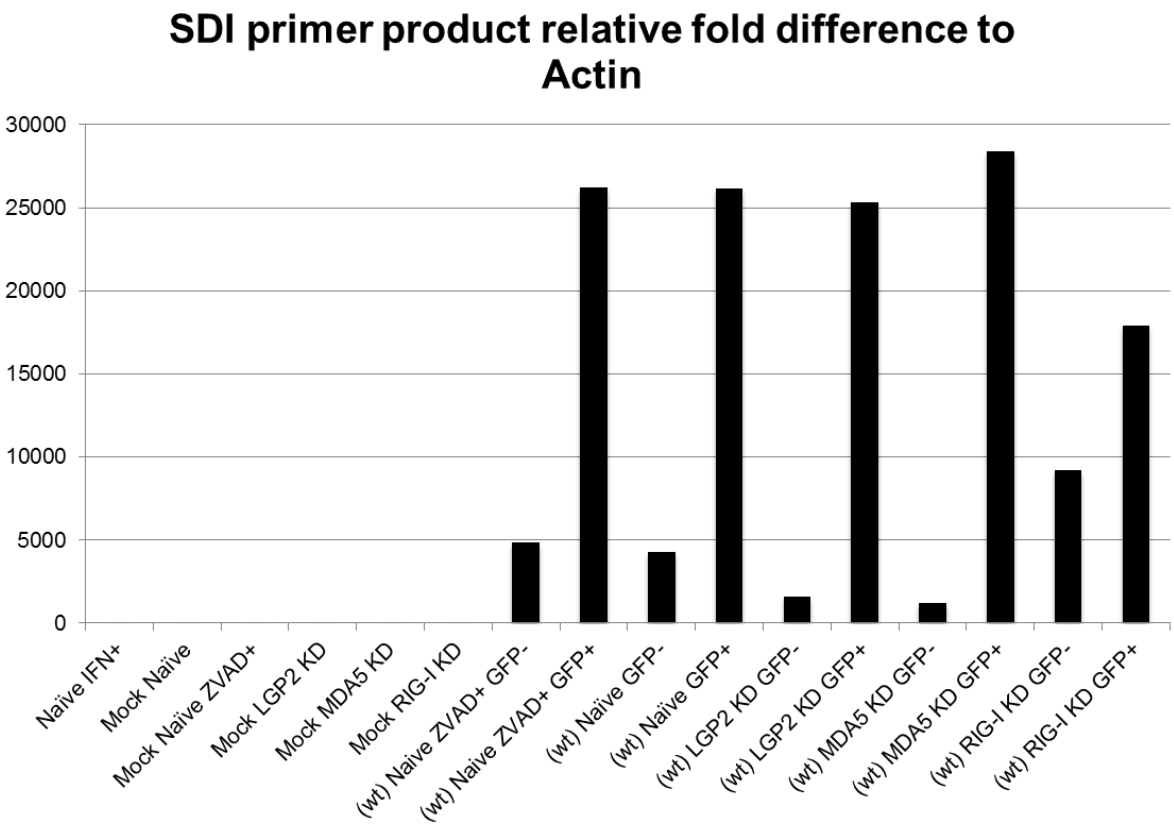
SDI primer product relative fold difference to Actin
30000
25000
20000
15000
10000
5000
0
Naïve IFN+
Mock Naïve
Mock Naïve ZVAD+
Mock LGP2 KD
Mock MDA5 KD
Mock RIG-I KD
(wt) Naïve ZVAD+ GFP-
(wt) Naïve ZVAD+ GFP+
(wt) Naïve GFP-
(wt) Naïve GFP+
(wt) LGP2 KD GFP-
(wt) LGP2 KD GFP+
(wt) MDA5 KD GFP-
(wt) MDA5 KD GFP+
(wt) RIG-I KD GFP-
(wt) RIG-I KD GFP+

B

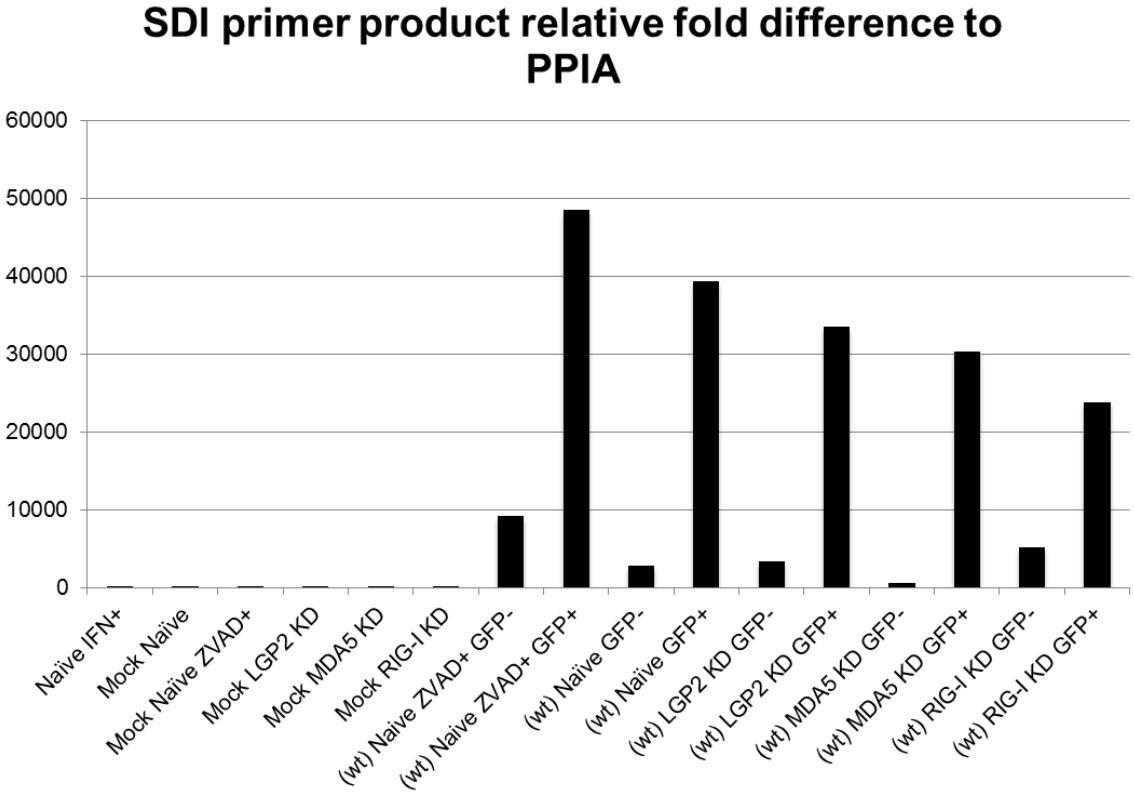
SDI primer product relative fold difference to PPIA
60000
50000
40000
30000
20000
10000
0
Naïve IFN+
Mock Naïve
Mock Naïve ZVAD+
Mock LGP2 KD
Mock MDA5 KD
Mock RIG-I KD
(wt) Naïve ZVAD+ GFP-
(wt) Naïve ZVAD+ GFP+
(wt) Naïve GFP-
(wt) Naïve GFP+
(wt) LGP2 KD GFP-
(wt) LGP2 KD GFP+
(wt) MDA5 KD GFP-
(wt) MDA5 KD GFP+
(wt) RIG-I KD GFP-
(wt) RIG-I KD GFP+

C

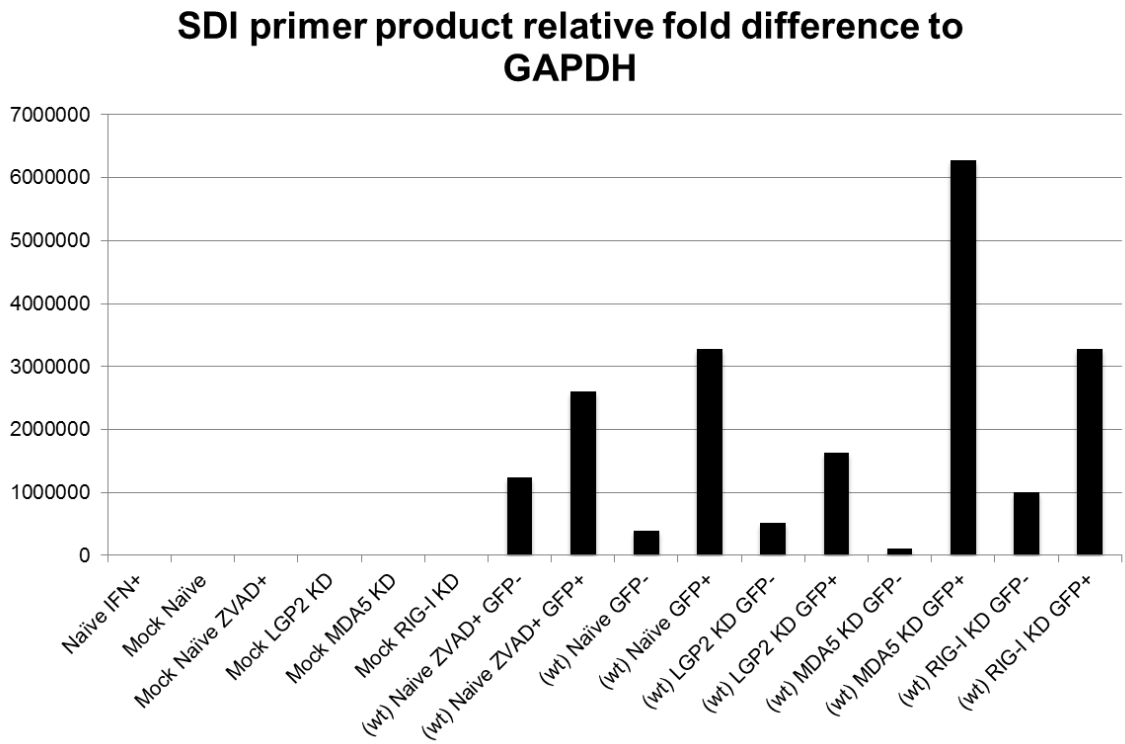

Figure 42. Relative quantification of SDI primer product to housekeeping genes following cell sorting of GFP+ve and GFP-ve cells.

Reporter cells had previously been infected with PIV5 (wt) at a low MOI of 0.0001pfu/cell for 4 days. Following incubation, GFP+ve and GFP-ve cells were cell sorted using the Beckman Coutoure MOFLO (Cytomation) cell sorter. RNA was TRIzol extracted and reverse transcribed. RT-QPCR was performed, probing for the SDI primer product. Samples were performed in triplicate. The Ct values generated were then analysed using the Livak Ct method for the relative quantification of SDI primer product, to the housekeeping genes β-Actin (**A**), PPIA (**B**) and GAPDH (**C**).

The PIV5 (wt) DIs primarily generated are Trailer DI copybacks, which do not contain the sequence for NP (Killip *et al.*, 2013). When performing the reverse transcription step, the reverse NP primer was used. Thus when RT-QPCR was performed, only PIV5 genomic NP, and not NP mRNA (which is the complement sequence to genomic NP), would be detected. Thus by analysing PIV5 genomic NP relative abundance, this is an indication of the abundance of non-defective wild-type virus in the cell, as only by normal viral replication would genomic NP be present at high levels in the sample.

Analysing the relative levels of genomic NP in GFP+ve and GFP-ve reporter cells when compared to all three of the housekeeping genes, several patterns can be observed (**Figure 43**). As expected, mock-infected cells did not contain any NP. For all reporter cells, GFP-ve cells contained high levels of NP when compared to GFP+ve cells. There is clear correlation between the high abundance of NP indicative of greater PIV5 (wt) non-defective virus replication and GFP-ve cells in which the IFN-β promoter has not been activated. This is unsurprising, as GFP+ve cells have activation of the IFN-β promoter induced by DI PAMPs, and the subsequent expression and secretion of IFN by the cell would then activate the JAK/STAT signalling pathway, leading to the induction of ISGs and the generation of an antiviral state. As a result viral transcription and replication in the GFP+ve cells would be inhibited, and thus contain less genomic NP when compared to GFP-ve cells. This supports the previous immunofluorescence data (**Figure 17**) and flow cytometry (**Figure 25, Figure 40**) of low MOI infections of PIV5 (wt), where there are a subset of GFP+ve cells that are strongly positive for GFP expression and weakly positive for NP expression.

A

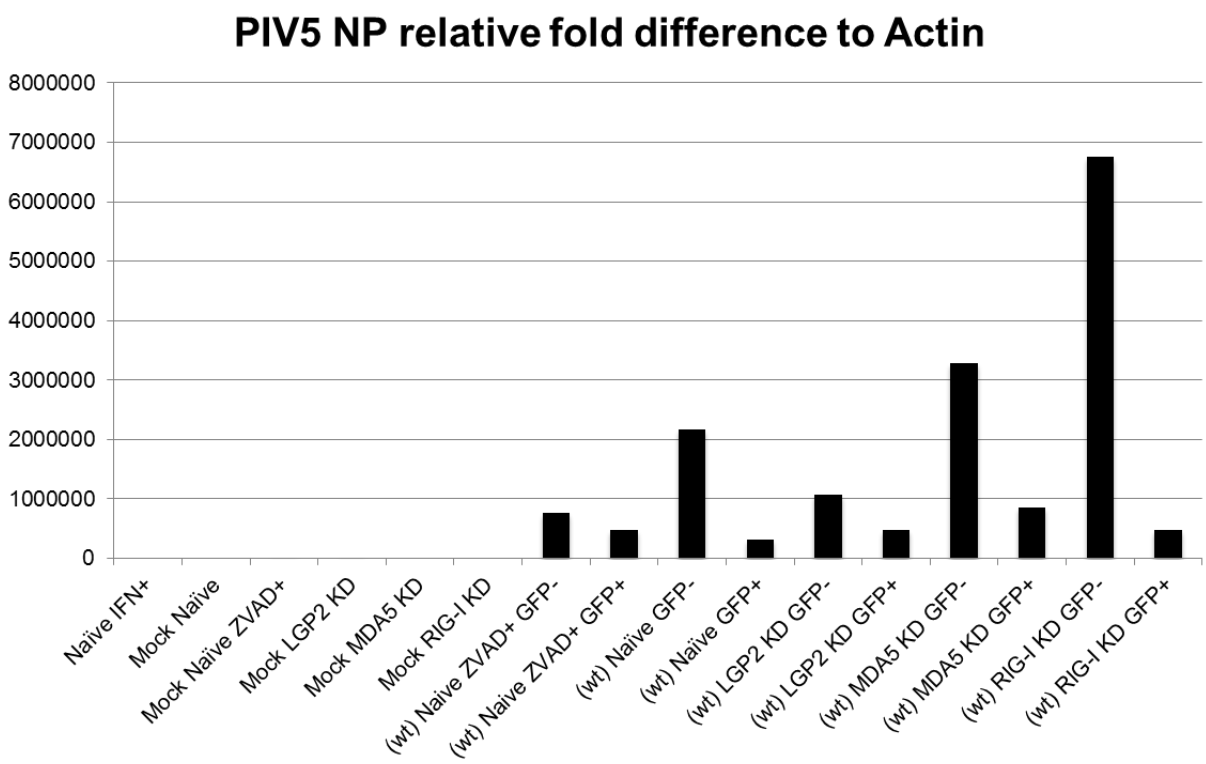
PIV5 NP relative fold difference to Actin
8000000
7000000
6000000
5000000
4000000
3000000
2000000
1000000
0
Naïve IFN+
Mock Naïve
Mock Naïve ZVAD+
Mock LGP2 KD
Mock MDA5 KD
Mock RIG-I KD
(wt) Naive ZVAD+ GFP-
(wt) Naive ZVAD+ GFP+
(wt) Naïve GFP-
(wt) Naïve GFP+
(wt) LGP2 KD GFP-
(wt) LGP2 KD GFP+
(wt) MDA5 KD GFP-
(wt) MDA5 KD GFP+
(wt) RIG-I KD GFP-
(wt) RIG-I KD GFP+

B

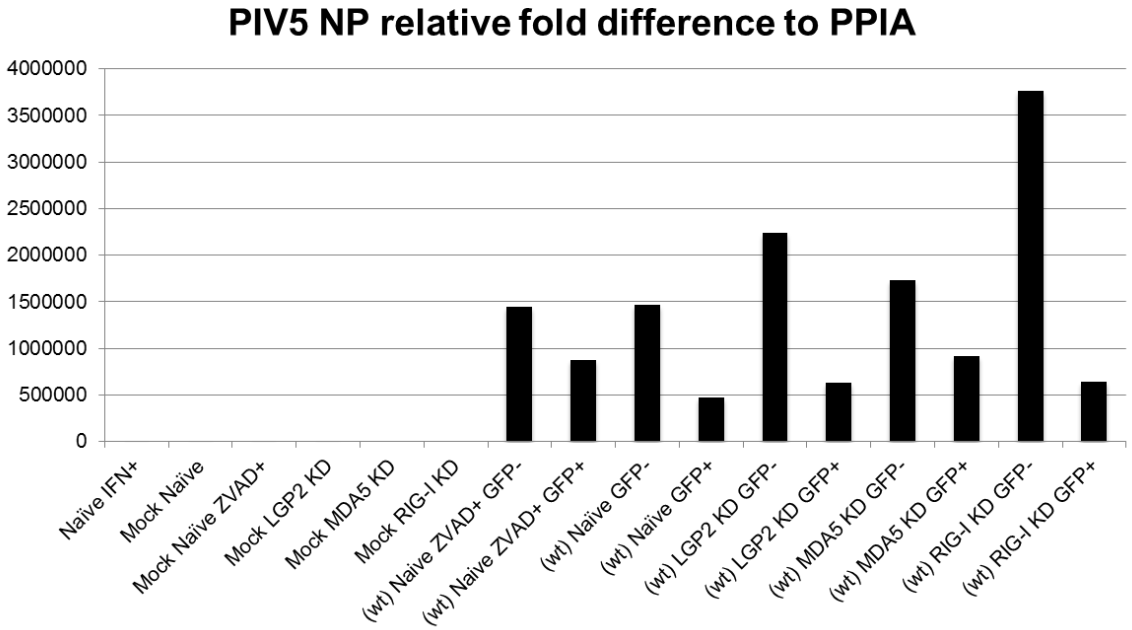
PIV5 NP relative fold difference to PPIA
4000000
3500000
3000000
2500000
2000000
1500000
1000000
500000
0
Naïve IFN+
Mock Naïve
Mock Naïve ZVAD+
Mock LGP2 KD
Mock MDA5 KD
Mock RIG-I KD
(wt) Naive ZVAD+ GFP-
(wt) Naive ZVAD+ GFP+
(wt) Naïve GFP-
(wt) Naïve GFP+
(wt) LGP2 KD GFP-
(wt) LGP2 KD GFP+
(wt) MDA5 KD GFP-
(wt) MDA5 KD GFP+
(wt) RIG-I KD GFP-
(wt) RIG-I KD GFP+

C

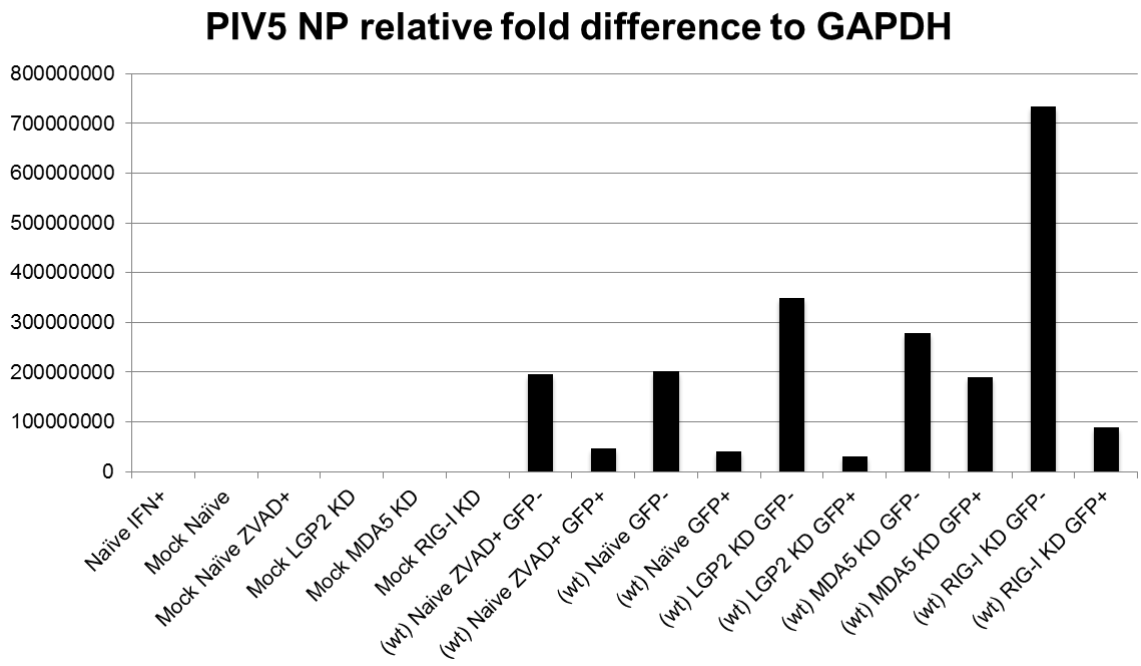

Figure 43. Relative quantification of PIV5 NP to housekeeping genes following cell sorting of GFP+ve and GFP-ve cells.

Reporter cells had previously been infected with PIV5 (wt) at a low MOI of 0.0001pfu/cell for 4 days. Following incubation, GFP+ve and GFP-ve cells were cell sorted using the Beckman Coutoure MOFLO (Cytomation) cell sorter. RNA was TRIzol extracted and reverse transcribed. RT-QPCR was performed, probing for PIV5 NP. Samples were performed in triplicate. The Ct values generated were then analysed using the Livak Ct method for the relative quantification of PIV5 genomic NP, to the housekeeping genes β-Actin (**A**), PPIA (**B**) and GAPDH (**C**).

It can be observed that for all three sets of NP relative fold differences to housekeeping genes, the absence of the RIG-I PRR increased the relative abundance of NP in GFP-ve RIG-I KD reporter cells when compared to genomic NP levels found in GFP-ve cells of Naïve, MDA5 KD and LGP2 KD reporter cells. The NP relative fold difference between GFP-ve RIG-I KD reporter cells and GFP-ve Naïve reporter cells is far greater than the difference between GFP-ve MDA5/LGP2 KD reporter cells and GFP-ve Naive reporter cells. This is due to in the absence of RIG-I sensor, the RIG-I KD reporter cells are unable to recognise the DI viral PAMPs generated during viral plaque development that activate RIG-I, reflected in the flow cytometry data (**Figure 25**, **Figure 40)** whereby far fewer GFP+ve cells were detected in RIG-I KD cells when compared to Naïve, MDA5 KD and LGP2 KD reporter cells. Thus in GFP-ve RIG-I KD reporter cells PIV5 is able to have a higher rate of replication and hence increased genomic NP expression detected, as there are fewer GFP+ve cells present in the cell population and thus fewer cells in which IFN is induced. A majority of the DI populations generated during viral plaque development and virus replication are thus primarily sensed by RIG-I.

Some DIs generated during viral plaque development are PAMPs that are recognised by MDA5, and this supported where GFP-ve MDA5 KD reporter cells have a slightly higher abundance of genomic NP, indicative of increase non-defective wild-type virus replication compared to GFP-ve Naïve reporter cells (**Figure 42**). This pattern is observed when analysing the relative abundances of genomic NP for all three housekeeping genes. The DIs that activate MDA5 are generated at a far slower rate than those that activate RIG-I, as the genomic NP expression levels in GFP+ve MDA5 KD reporter cells are far lower than that of GFP-ve RIG-I KD reporter cells. The reason for this may be due to selection pressure on the generation of MDA5 activating DIs by the PIV5 V protein that directly inhibits MDA5.

3.3.12. Further analysing the relationship between the DI mediated activation of the IFN-β promoter on non-defective viral transcription and IFN antagonism by the V protein

It was observed that during the flow cytometry analysis of reporter cells infected at an MOI of 0.0001pfu/cell with PIV5 (wt) over 2 days, that three populations with positive signals were measured following staining for NP (**Figure 25**, **3.2.5. Flow cytometry analysis of virus infected reporter cells).** As reporter cells were infected at a low MOI, only the DIs generated during viral plaque development that could mediate the activation of the IFN-β promoter. Firstly, there were reporter cells that were GFP+ve/NP-ve. This indicates that a Trailer copyback DI was produced during virus replication in a neighbouring wild-type virus infected cell. The DI egressed and infected the GFP+ve/NP-ve cell n, and the DI PAMP was recognized by the appropriate PRR, subsequently inducing the activation of the IFN-β promoter.

A second population was observed that was GFP-ve/NP+ve. This suggests that this cell population has been infected with a non-defective wild-type virus, and virus transcription has taken place without the co-infection of a DI or the generation of a DI during virus replication that is capable of being recognized by the PRRs. Hence, this cell population is GFP-ve, and NP+ve. Interestingly, a third population was observed that was strongly GFP+ve and strongly NP+ve. During the development of the viral plaque, these cells could have been co-infected with a wild-type virus and DIs generated during virus replication. This DI would have been sensed by the PRRs, leading to the activation of the IFN-β promoter and hence GFP expression. However, this raises the question of the effect of co-infecting DIs on the IFN antagonist properties of non-defective, wild-type PIV5, i.e. the ability of the V protein of PIV5 (wt) to block the DI mediated activation of the IFN-β promoter. To further examine

the relationship between the ratio of DIs to wild-type virus and the ability of PIV5 V protein to inhibit the IFN induction signalling cascade a co-infection between PIV5 wild-type virus and a DI rich PIV5 VΔC VM2 virus preparation was performed (**Figure 44**). Naïve reporter cells were infected for 18hrs with either PIV5 (wt) or PIV5 VΔC VM2 at 10 fold dilutions from a $1x10^{-8}$ pfu/ml virus stock. Cells were also co-infected with PIV5 (wt) and PIV5 VΔC VM2 (**Figure 44 I-L**). These cells were infected with PIV5 (wt) at 10^{-1} from the virus stock, and co-infected with PIV5 VΔC VM2 at 10 fold dilutions at 10^{-1}, 10^{-2}, 10^{-3}, 10^{-4}. Cells were initially infected at high MOIs in order to ensure that there was a co-infection of a DI and wild-type virus. Cells were then fixed and immunostained for NP and analysed by flow cytometry.

Flow cytometry analysis revealed, as expected, that by decreasing the concentration of PIV5 (wt) from 10^{-1} to 10^{-4} when exclusively infecting Naive reporter cells with PIV5 (wt), fewer Naïve reporter cells are thus infected with PIV5 (wt) and thus fewer GFP-ve/NP+ve cells are detected as a proportion of total cells (**Figure 44 A-D**). When the concentration of the DI rich PIV5 VΔC VM2 virus is decreased in Naive reporter cells infected exclusively with PIV5 VΔC VM2, as expected the % of GFP+ve/NP-ve cells detected is reduced, as fewer cells have activation of the IFN-β promoter as fewer cells are infected with a DI (**Figure 44 E-H**). The data presented above clearly demonstrate that high-multiplicity passage of PIV5 VΔC VM2 generates virus preparations that are efficient at activating the IFN response and that this ability correlates with an accumulation of DI genomes.

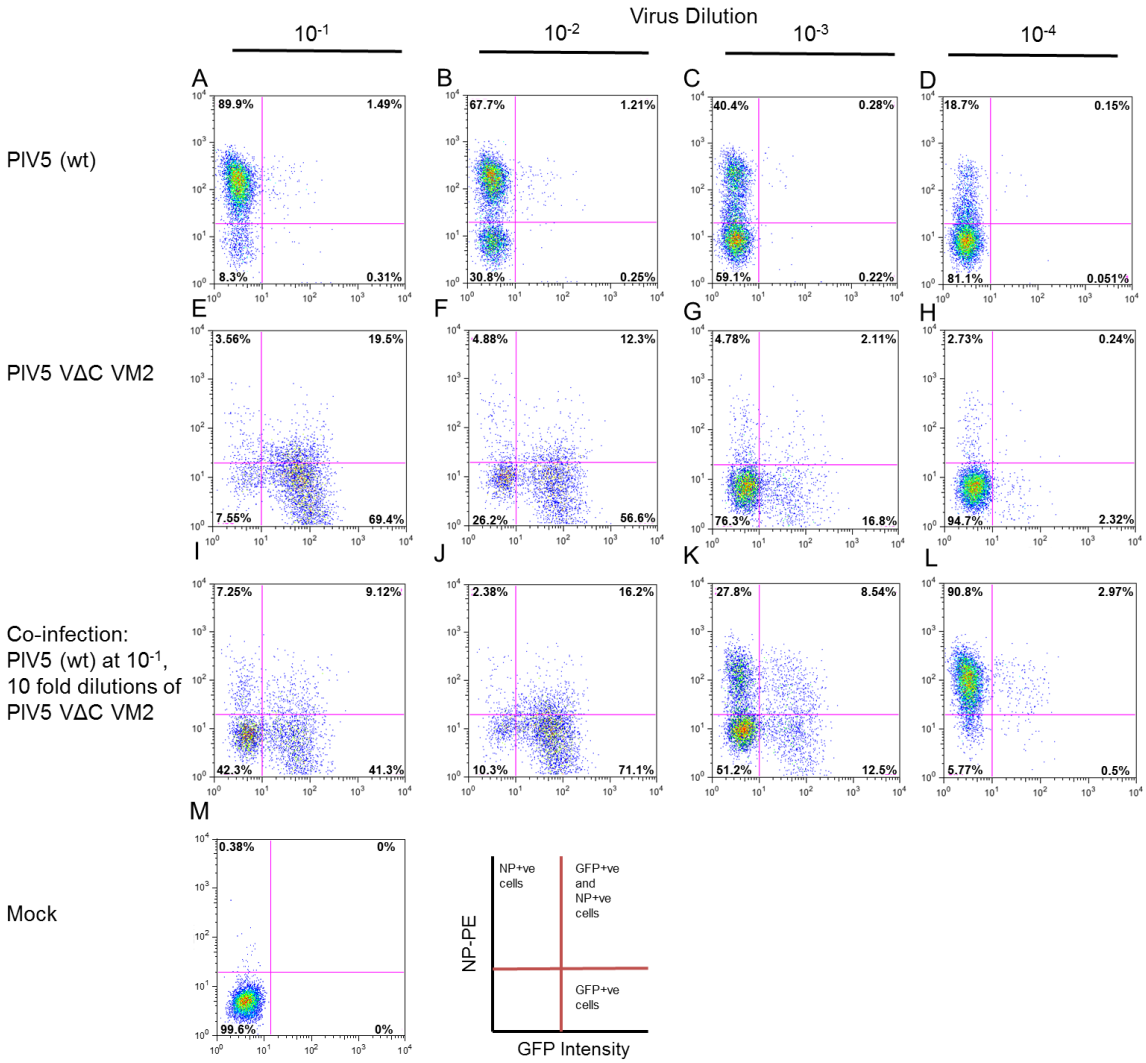

Figure 44. Flow Cytometry analysis of Co-infection of Naïve reporter cells by PIV5 (wt) and PIV5 VΔC VM2

Naïve reporter cells were infected for 18hrs with either PIV5 (wt) or PIV5 VΔC VM2 at 10 fold dilutions from a $1x10^8$ pfu/ml virus stock. Cells were infected with PIV5 (wt) at 10^{-1}, 10^{-2}, 10^{-3}, 10^{-4} (**A-D**); PIV5 VΔC VM2 at dilution 10^{-1}, 10^{-2}, 10^{-3}, 10^{-4} (**E-H**). Cells were also co-infected with PIV5 (wt) and PIV5 VΔC VM2: PIV5 (wt) at 10^{-1} dilution from stock, PIV5 VΔC VM2 at 10 fold dilutions at 10^{-1}, 10^{-2}, 10^{-3}, 10^{-4} (**I-L**). Cells were then fixed and stained for NP, and then secondary stained with PE. GFP intensity is measured on the x-axis, NP-PE is measured on the y-axis. Samples were analysed by flow cytometry on a Becton Dickinson FACSCaliber flow cytometer machine.

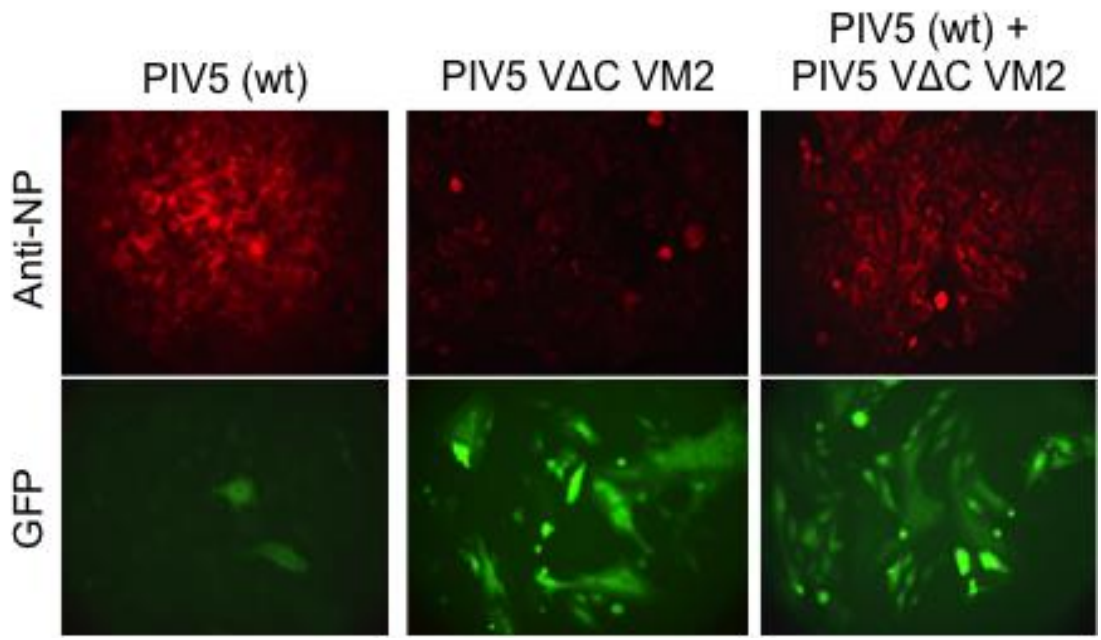

Figure 45. PIV5 (wt) does not prevent activation of the IFN-β promoter by co-infecting copyback DIs, despite encoding the V protein IFN antagonist.

Naïve reporter cells were infected at an MOI of 10pfu/cell with PIV5 (wt), PIV5 VΔC VM2, or a co-infection with a 50:50 mixture thereof. The cells were fixed at 18hr p.i., and GFP+ve cells and the distribution of NP (red), following immunostaining, were visualized by fluorescence microscopy.

When analysing the co-infection data of PIV5 (wt) co-infected with PIV5 VΔC VM2, at the highest concentration of PIV5 VΔC VM2 (**Figure 44 I**), the cell population pattern observed is similar to that when infecting cells exclusively with the highest concentration of PIV5 VΔC VM2 (**Figure 44 E**). As such, every cell in the co-infection is co-infected with non-defective virus that encodes a functional V protein, yet strikingly there was no inhibition of IFN induction signalling cascade, where the IFN-β promoter was activated in these cells (**Figure 44 I**).

In comparison, when the concentration of PIV5 VΔC VM2 is reduced to 10^{-4} in the co-infected sample (**Figure 44 L**), the cell population distribution pattern is similar to that of exclusively infecting cells with PIV5 (wt) (**Figure 44 A**). By reducing the ratio of DIs to wild-type non-defective virus in the co-infection, the % of cells that are GFP-ve/NP+ve is increases from 7.5% (**Figure 44 I)** to 90.8% (**Figure 44 L**), which is similar to cells exclusively infected with PIV5 (wt) at 89.9%. (**Figure 44 A**). In effect, by reducing the ratio of DIs to wild-type virus in the co-infection, there has been a shift in cell population distributions which can be first identified when co-infecting wild-type virus with PIV5 VΔC VM2 at 10^{-3} (**Figure 44 K**). This suggests that by reducing the ratio of DIs to wild-type virus in a co-infection to a suitable level, wild-type viral transcription is restored. The data suggests that DIs are interfering with PIV5 (wt) NP expression despite the encoding of the IFN antagonist, the V protein. This indicates that DIs inhibited the synthesis of viral proteins expressed from non-defective genomes, which would likely impact the ability of the virus to antagonize the IFN response. Consistent with this finding, non-defective PIV5 (wt) is unable to inhibit IFN induction by co-infecting DI-rich PIV5 VΔC VM2 when viewed by immunofluorescence (**Figure 45**).

Further analysing the co-infected cells, the % of GFP+ve/NP-ve cells decreases from 40.3% **(Figure 44 I)** to 0.5% **(Figure 44 L)** as the DI ratio to wild-type virus is

reduced. This suggests that the reduction of NP+ve cells observed when co-infecting with higher DI ratios to wild-type virus, is due to the DI mediated induction of IFN and the subsequent expression of ISGs hostile to viral transcription, providing further evidence that DIs are the primary inducers of IFN. Interestingly, the % of GFP+ve cells that are also NP+ve as proportion of total GFP+ve cells increases as the ratio of wild-type virus to DIs increases in the co-infected sample. When co-infecting cells with the highest ratio of DIs to wild-type virus, the proportion of total GFP+ve cells that are NP+ve is 18% (**Figure 44 I**). However, when co-infecting with the lowest ratio of DIs to wild-type virus, the proportion of total GFP+ve cells that are NP+ve is 86% (**Figure 44 L**). This suggests that co-infecting PIV5 (wt) with a DI, the non-defective virus can help DIs replicate and induce IFN. it must be emphasised that DIs do not require to replicate or be ico-infected with a non-defective virus to be recognised by the PRRs and to induce the activation of the IFN-β promoter, as evidenced by the generation of strongly GFP+ve cells weak for NP expression during a high MOI infection with DI rich PIV5 VΔC VM2 (**Figure 44 E**).

DI activation of the IFN-β promoter in the absence of viral protein synthesis

At each dilution of PIV5 (wt) (**Figure 44 A-D**) or PIV5 VΔC VM2 (**Figure 44 E-H**), cells that were strongly positive for virus NP, indicating normal virus transcription, were usually GFP-ve, whereas those that were GFP+ve were generally only very weakly NP+ve. Additionally, GFP+ve cells (weakly NP+ve) could clearly be observed even at high dilutions (10^{-4}) of PIV5 (wt) (**Figure 44 D**) and PIV5 VΔC VM2 (**Figure 44 H**) infections, where very few cells would have been infected with a non-defective virus. In cells infected at the highest concentration of PIV5 VΔC VM2 (**Figure 44 E**), whilst the majority of cells were strongly GFP+ve, the same cells were generally only NP-ve. In contrast, following infection with the highest concentration of PIV5 (wt), the

majority of reporter cells were strongly positive for NP, but were GFP-ve (**Figure 44 A**). There is a negative correlation between GFP expression and virus protein expression. Thus, for both DI-rich PIV5 VΔC VM2 and DI-poor PIV5 (wt) infections, very little (if any) virus protein synthesis and was occurring in those GFP+ve/NP-ve cells in which the IFN-β promoter had been activated. This data suggests that the DI mediated activation of the IFN-β promoter and induction of IFN is independent of viral protein synthesis.

How are the GFP+ve/NP+ve reporter cell population generated following PIV5 (wt) infection?

As mentioned previously, a DI co-infecting with a non-defective wild-type virus generates the GFP+ve/NP+ve cell populations. The wild-type non-defective virus mediates the transcription of NP where the V protein IFN antagonist is unable to inhibit the DI mediated activation of the IFN-β promoter. However, a second possible explanation for the generation of the GFP+ve/NP+ve cell populations is by infection of these cells with a Leader copyback DI that would encode NP. This Leader copyback DI could then be recognised by the PRRs, subsequently inducing the activation of the IFN-β promoter, and hence the NP+ve cells would be positive for GFP expression. This explanation is unlikely as from previous deep sequencing data of PIV5 (wt) DIs, the vast majority of DI copybacks generated during high multiplicity passaging were Trailer copyback DIs (Killip *et al.*, 2013).

In order to discount that the GFP+ve/NP+ve cell population is generated by infection with a Leader copyback DI, cells can be probed for PIV5 HN and for PIV5 NP. As HN is located at the opposite terminus to NP on the PIV5 genome (**Figure 8**), HN is encoded in Trailer copyback DIs, but not in Leader copyback DIs. Thus, if the

Leader copyback DI is the cause, then when probing co-infected cells in which the shift in cell populations is taking place in **Figure 44 K** due to the reduced ratio of DIs to wild-type virus, then there would be reduced levels of GFP+ve/HN+ve cells that would be detected in comparison to GFP+ve/NP+ve cells. The previous co-infection experiment was repeated in duplicate, whereby Naïve reporter cells were infected for 18hrs with either PIV5 (wt) or PIV5 VΔC VM2 at 10 fold dilutions from a $1x10^8$ pfu/ml virus stock. Cells were also co-infected with PIV5 (wt) and PIV5 VΔC VM2. These cells were infected with PIV5 (wt) at 10^{-1} from stock, and co-infected with PIV5 VΔC VM2 at 10 fold dilutions at 10^{-1},10^{-2},10^{-3},10^{-4}. Cells were then fixed and immunostained. One set of samples was probed for NP, and the second set were probed for HN and analysed by flow cytometry.

Analysing the flow cytometry data (**Figure 46**), it can be observed that similar patterns of cell populations are detected when probing for either for NP or HN. When probing for NP (**Figure 46 E1**) and HN (**Figure 46 E2)** of co-infected samples, at the highest co-infecting concentration of PIV5 VΔC VM2, the cell population patterns observed is similar to that when infecting cells exclusively with the highest concentration of PIV5 VΔC VM2 when probing for NP (**Figure 46 C1)** and HN **(Figure 46 C2**). When the concentration of PIV5 VΔC VM2 is reduced to 10^{-2} in the co-infected sample when probing for either NP or HN (**Figure 46 F1 and F2**), the cell population distribution pattern shifts towards the cell population distribution observed when exclusively infecting with PIV5 (wt) (**Figure 46 A-B**). The % of GFP-ve/NP+ve and GFP-ve/HN+ve cells of total cells increases as the ratio of DIs in the co-infection is reduced. The co-infecting PIV5 (wt) has its transcription levels, i.e. GFP-ve/NP+ve and GFP-ve and HN+ve cells, beginning to be restored to levels observed when exclusively infecting cells with PIV5 (wt) (**Figure 46 A-B**) as the ratio of DI to wild-type virus is reduced in the co-infection.

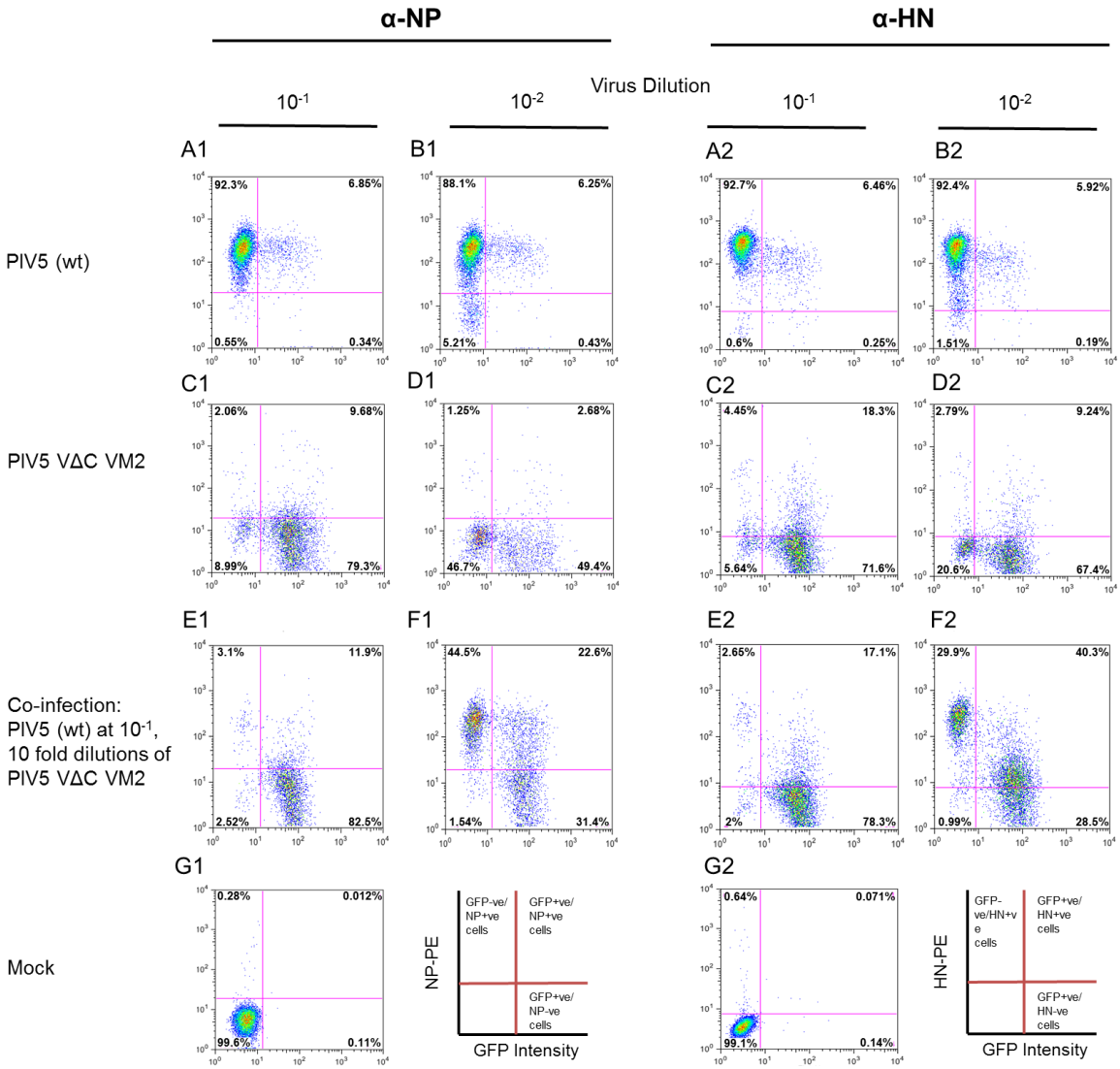

Figure 46. Flow Cytometry analysis of Co-infection of Naïve reporter cells by PIV5 (wt) and PIV5 VΔC VM2

Naïve reporter cells were for 18hrs infected with either PIV5 (wt) or PIV5 VΔC VM2 at 10 fold dilutions from a 1x10^8 pfu/ml virus stock. Cells were infected with PIV5 (wt) at 10^{-1},10^{-2}, (**A-B**); PIV5 VΔC VM2 at dilution 10^{-1},10^{-2} (**C-D**). Cells were also co-infected with PIV5 (wt) and PIV5 VΔC VM2: PIV5 (wt) at 10^{-1} dilution from stock, PIV5 VΔC VM2 at 10 fold dilutions at 10^{-1},10^{-2}, (**E-F**). Cells were then fixed and stained for NP or HN, and then secondary stained with PE. GFP intensity is measured on the x-axis, viral protein-PE is measured on the y-axis. Samples were analysed by flow cytometry on a Becton Dickinson FACSCaliber flow cytometer machine.

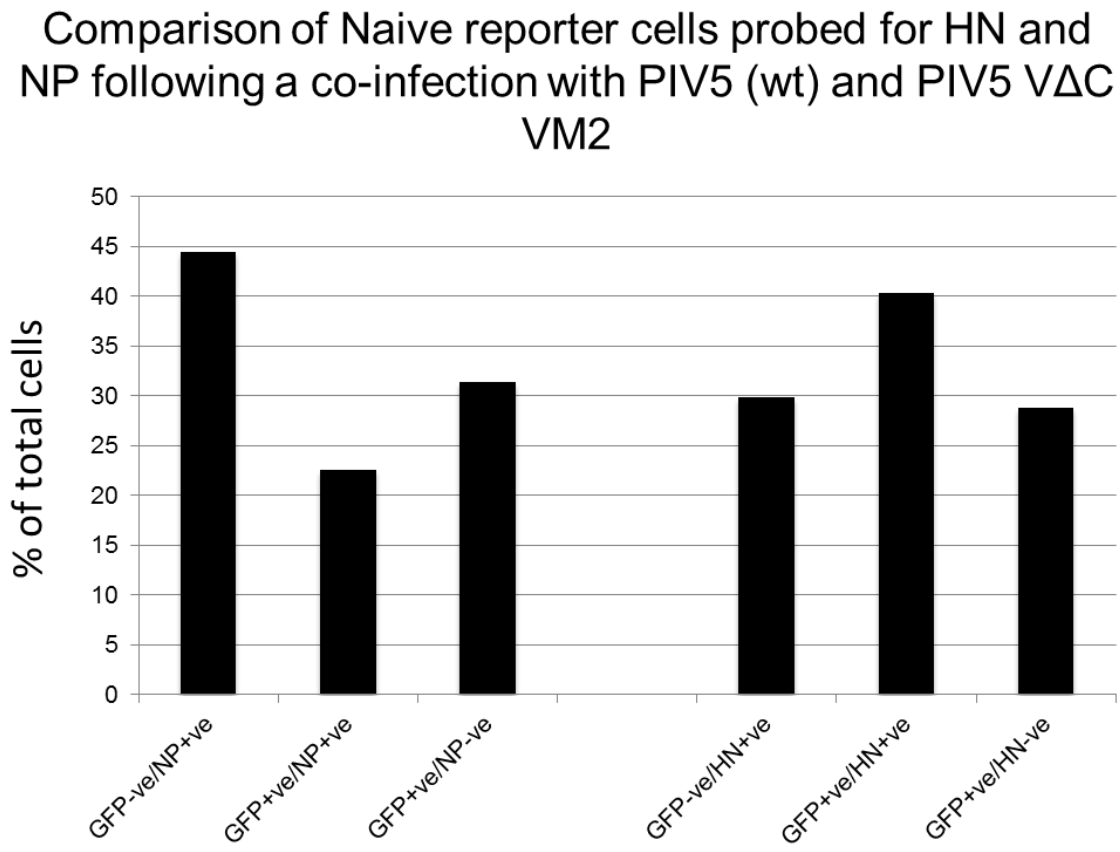

Figure 47. Comparison of Naive reporter cells probed for HN and NP following a co-infection with PIV5 (wt) and PIV5 VΔC VM2

Naïve reporter cells were for 18hrs co-infected with PIV5 (wt) or PIV5 VΔC VM2 at 10 fold dilutions from a $1x10^8$ pfu/ml virus stock. Cells were co-infected PIV5 (wt) at 10^{-1} dilution from stock, PIV5 VΔC VM2 at 10^{-2}. Cells were then fixed and stained for NP or HN, and then secondary stained with PE and analysed by flow cytometry. Values were derived from flow cytometry analysis of cells probed for NP (**Figure 46 F1)** and cells probed for HN **(Figure 46 F2).**

Further analysing the shift in co-infected cell population distributions at which the ratio of DIs to wild-type virus is reduced to an extent to allow non-defective virus transcription (**Figure 46 E1 and E2**), several patterns can be observed (**Figure 47**). Firstly, detected GFP-ve/NP+ve cells at 45% of total cells are greater than that of GFP-ve/HN+ve cells detected at 30%. This reflects the transcriptional gradient of PIV5 (wt) gene expression, in which NP is expressed at far greater quantities due to it's position as the first gene at the 3' terminus of the PIV5 genome compared to HN in which the gene coding sequence is after P/V, M, F and SH.

Secondly, the % of GFP+ve/NP-ve and GFP+ve/HN-ve cells are similar to each other at 31% and 29% respectively. This is to be expected, as both sets of samples that were probed either NP or HN were infected at the same co-infection virus concentrations and ratio of DIs to wild-type virus. Thus the % of cells that are co-infected with DIs that successfully interfere with NP or HN expression and which subsequently activate the IFN-β promoter is the same. Finally, GFP+ve/HN+ve cells can be detected in the co-infected sample. This result implicitly shows that the GFP+ve/NP+ve cell population observed in co-infected samples is not due to infection with a Leader copyback DI that does not encode HN. HN can be detected in a subset of GFP+ve cells that has been infected with wild-type virus hence leading to viral NP transcription and expression. This cell population is co-infected with a DI, hence positive GFP expression following the DI mediated activation of the IFN-β promoter. In addition, the % of GFP+ve/HN+ve cells at 40% is greater than GFP+ve/NP+ve cells at 23% of total cells. This is explained as in the GFP+ve/viral protein cell population, these cells are infected with a non-defective virus and a Trailer copyback DI which encodes HN, but not NP. Thus during viral transcription, NP is transcribed from the non-defective virus, whereas HN is transcribed from the non-defective virus and the co-infecting Trailer copyback DI.

3.3.13. Section Summary

We demonstrate that the DIs generated during PIV5 (wt) infection of reporter cells can activate the IFN induction cascade via the development of a robust method of DI detection by RT-QPCR and relative quantification of DIs via the Livak method - see the below diagram:

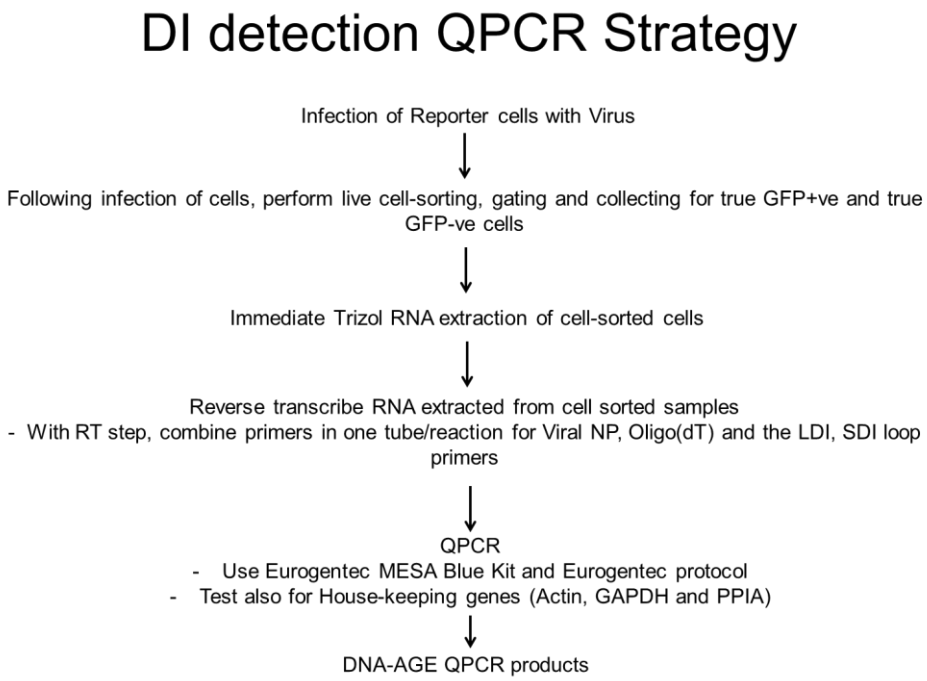

PIV5 (wt) infected GFP+ve reporter cells, which had the IFN-β promoter activated, strongly correlated with the presence of DIs. Correspondingly, DIs were minimally detected in GFP-ve reporter cells, comparative to mock cells, in which the IFN-β promoter was not activated. This is a significant result, as this further affirms the model that DIs are the primary PAMPs that induce IFN. Supporting the previous flow cytometry data, the DI populations generated are not equally recognized by the sensors as viral NP was greatly increased in PIV5 (wt) infected RIG-I KD reporter cells when compared to Naïve, MDA5 KD, LGP2 KD reporter cells, due to the RIG-I KD reporter cells being reduced in their ability to induce IFN.

4. DISCUSSION

4.1. The Heterocellular response to virus infection

We investigated the activation of the IFN-β promoter by the PAMPs generated during plaque development following a low MOI infection of reporter cells infected with negative sense RNA viruses. Infecting at a low MOI ensures that the cells at the initial site of infection are infected with wild-type virus, and not by any PAMPs present in the viral stock. It was clear from the immunofluorescence and flow cytometry of infected samples, that during plaque development only a minority of cells were positive for the expression of GFP and hence only a minority of reporter cells have activation of the IFN-β promoter and are responsible for the induction of IFN during an infection.

It has been previously reported that the IFN-β gene shows heterocellular induction in response to either the synthetic dsRNA, poly(I:C), or Sendai virus (Apostolou and Thanos, 2008; Enoch et al., 1986; Hu et al., 2007; Senger et al., 2000; Zawatzky et al., 1985). In none of these cases has the molecular basis of the restriction of induction been determined, but it has been generally assumed to be a property of the host cell, such as stage in the host cell cycle or transcription factor availability. However, in our experiments, given that GFP can be induced in at least 90% of the Naive reporter cells and even in reporter cells which have been blocked in their cell cycle (Chen *et al.*, 2010), and that the reporter gene does not compete with the endogenous IFN-β gene, it clearly indicates that induction in these cells is not restricted by transcription factor availability or signaling pathway activation. Therefore, the heterocellular induction observed in the Naïve reporter cells must be due to the property of the infecting virus, rather than the ability of the cells to respond

to virus infection. It remains possible that different cell types might show very different percentages of cells able to support IFN-β induction, with some cell lines, including A549 cells, able to induce IFN in nearly every cell in a population.

One possible explanation for the heterocellular response is that a virus infecting a cell that will go on to express GFP has been unable to block IFN induction by PAMPs that are generated during normal virus transcription or replication, either due to a defective property of the virus or a loss of expression of the IFN antagonist. If the loss of a functional V protein were the primary reason for IFN induction in infected cells, then it would be expected that with infection of reporter cells with PIV5 VΔC (VM0), which lacks a functioning V protein would activate the IFN-β promoter in all infected cells. However, we found instead that only a small minority of Naïve reporter cells expressed GFP when infected with PIV5 VΔC when analysed by flow cytometry and by immunofluorescence. The most striking result of this study was that the loss of the PIV5 IFN antagonist did not lead to IFN-β promoter activation in all PIV5 VΔC-infected cells. The data presented here, and confirmed in a subsequent study (Killip *et al.*, 2011), challenges the notion that paramyxoviruses generate PAMPs capable of activating the IFN response during their normal replication cycle, and we suggest that these PAMPs are not generated during normal non-defective PIV5 (wt) replication.

In addition to its role as an IFN antagonist, the V protein itself controls both PIV5 transcription and replication (Lin et al., 2005). In this regard it may be expected that due to the extensive deletion in V in PIV5 VΔC, this V-dependent regulation would be altered, leading to a possible increase in the generation of PAMPs capable of inducing IFN. However, our data indicate that the loss of this fine control of transcription and replication does not affect the level of activation of the IFN-β promoter during infection, since we do not see IFN-β promoter activation in the

majority of PIV5 VΔC (VM0) infected cells. Since we have shown that non-defective PIV5 VΔC (VM0) does not generate PAMPs capable of activating the IFN-β promoter during its normal replication cycle (Killip *et al.*, 2011), we suggest that, in this reporter system, DI viruses, generated due to errors in the viral polymerase, are primarily responsible for IFN induction during infection with PIV5, and will be discussed below.

4.2. The role of DIs as the primary inducers of IFN

We demonstrate that the DIs generated during PIV5 (wt) infection can activate the IFN induction cascade via the development of a robust method of DI detection by RT-QPCR and relative quantification of DIs via the Livak method between different infected cell samples. RT-QPCR conditions were optimized for reverse transcription step and housekeeping genes utilized for relative quantification of PPIA, β-actin and GAPDH. In order to test if DIs were the primary inducers of IFN, reporter cells were infected at a low MOI with PIV5 (wt) and were cell sorted into discrete GFP+ve and GFP-ve populations. PIV5 (wt) infected GFP+ve reporter cells, which had the IFN-β promoter activated, strongly correlated with the presence of DIs. Correspondingly, DIs were minimally detected in GFP-ve reporter cells, comparative to mock cells, in which the IFN-β promoter was not activated. This is a significant result, as this further affirms the model that DIs are the primary PAMPs that induce IFN.

Important features of PIV5 DIs

Flow cytometry analysis of Naïve reporter cells infected at a high MOI with either DI-poor PIV5 (wt) or DI-rich PIV5 VΔC VM2 revealed that here is a lack of correlation

between GFP and virus protein expression. For both PIV5 VΔC VM2 and PIV5 (wt) infections, very little (if any) virus protein synthesis was occurring in those cells in which the IFN-β promoter had been activated. Further studies by the Randall group confirmed that the DIs of PIV5 can activate the IFN induction cascade and the IFN-β promoter in the absence of virus protein synthesis (Killip *et al.*, 2012b). Infection of reporter cells with PIV5 VΔC VM2 DI rich virus preparations could activate the IFN induction cascade and the IFN-β promoter during treatment with cyclohexamide protein synthesis inhibitor. Activated p-IRF3 could be detected within 3hrs of infection with PIV5 VΔC VM2 and treatment with cyclohexamide. This demonstrates that the DIs are able to be sensed by the PRRs, subsequently activating IRF3 and the IFN-β promoter, leading to the induction of IFN in the absence of either cellular or viral protein synthesis. As virus protein synthesis is an absolute requirement for paramyxovirus genome replication, these results indicate that these DI viruses do not require replication to activate the IFN induction cascade.

The relationship between DIs and the V protein IFN antagonist of non-defective virus

Flow cytometry analysis of reporter cells infected with PIV5 (wt) at a low MOI revealed a cell population that was strongly positive for NP and GFP expression. These cells are infected with a non-defective virus, hence NP expression, and a DI that induces the activation of the IFN-β promoter. This indicates that V produced during non-defective wild-type virus transcription is unable to block IFN induction by PAMPs that are generated by DIs, either within cells in which the DI was initially generated, or in cells that have been co-infected with a wild-type virus and an IFN-inducing DI. By performing co-infections at high MOIs with PIV5 (wt) and PIV5 VΔC VM2, we show that non-defective PIV5 (wt) is unable to prevent activation of the IFN-β promoter by a co-infecting DI. This result is not due to an inherent inability of the V

protein to prevent IFN induction by DI-related PAMPs generated during these infections, as a related study showed that pre-infection of reporter cells with PIV5 (wt)was associated with a significant reduction in GFP expression when subsequently challenged with PIV5 VΔC VM2, compared to the level in cells that had not been pre-infected (Killip *et al.*, 2013). Although the V protein is able to inhibit IFN-β induction by PIV5 DI-derived PAMPs, it is only able to do so if present insufficiently large amounts before DI virus PAMPs are detected. Thus, the data suggests that the IFN induction cascade would normally be activated only if a non-defective virus fails to generate sufficient V protein quickly enough to block activation of the IFN induction cascade by a co-infecting DI (GFP+ve/NP+ve cells), or in cells infected with DIs in the absence of a co-infecting non-defective virus (GFP+ve/NP-ve cells).

Deep sequencing has revealed that the DIs of PIV5 that are generated during infection are primarily Trailer DI copybacks (Killip *et al.*, 2013). As mentioned previously, the GFP+ve/NP+ve reporter cell populations detected by flow cytometry would thus be generated by a co-infecting non-defective virus and a Trailer copyback DI. However, the GFP+ve/NP+ve cell population could have been due to an infection with a Leader copyback DI that would encode NP, but not HN, that also induces IFN induction signaling cascade. Co-infected reporter cells with DI and non-defective wild-type viruses were probed for NP and HN. Co-infected cells that were HN probed displayed a similar cell distribution pattern to NP probed cells, i.e. HN could be detected in a subset of GFP+ve cells. This confirms that for both strong HN expression and for GFP expression to occur in the same reporter cell, you would need a co-infected trailer copyback DI and a non-defective virus.

The implications of DIs on virus replication and pathogenicity

As mentioned previously, the work in this thesis and related studies have identified that co-infecting DIs with non-defective virus are capable of interfering with viral protein synthesis despite the encoding of a potent IFN antagonist, the V protein. The inhibition of viral protein synthesis would thereby interfere with viral replication, which depends on viral protein synthesis. Whilst the generation of DIs during viral replication, and the induction of IFN are detrimental to the successful viral transcription and replication of non-defective viruses, this feature of DIs could have added advantages to the survival of the virus in the host.

As mentioned in the Introduction, non-defective virus and DI population dynamics are similar to that of predator prey relationships in which there are cyclical fluctuations in the ratio of DI to non-defective virions. The generation of DIs would initiate immune responses and suppress viral spread in the host, allowing the virus to transmit to another host before the virus kills the infected host via an acute infection. One study examined the relationship between DIs and highly pathogenic dengue viruses (DENV) (Li *et al.*, 2011). DENV are arboviruses in the family *Flaviviridae* and are important human pathogens responsible for disease states described as dengue fever, dengue haemorrhagic fever and dengue shock syndrome. DENV are transmitted to humans by Aedes mosquitoes, principally by Aedes aegypti. The four closely related DENV serotypes are antigenically distinct and often co-circulate in tropical regions where this disease is endemic. The nucleotide sequences of the single-stranded positive-sense RNA genomes of DENV are very diverse, and most viral genomes recovered from either of the natural hosts contain defects (e.g. intra-genic stop codons, nucleotide insertions or deletions) that would render them non-infectious. In this study, short fragments of dengue virus (DENV) RNA containing only key regulatory elements at the 3′ and 5′ ends of the genome were recovered

from the sera of patients infected with any of the four DENV serotypes. Identical RNA fragments were detected in the supernatant from cultures of *Aedes* mosquito cells that were infected by the addition of sera from dengue patients, suggesting that the sub-genomic RNA might be transmitted between human and mosquito hosts in DI viral particles. DENV preparations enriched for these putative DI particles reduced the yield of wild type dengue virus following co-infections of C6/36 mosquito cells. DENV DI particles may be a part of a broad spectrum of defects in the viral genome that attenuate disease and make these viruses very effective parasites. The studies suggest that these defective genomes impose a fitness burden on the DENV populations in which they are found that may result in attenuation of disease severity, allowing greater mobility of infected human hosts and therefore greater transmission of the virus.

Like DEV, Japanese encephalitis virus is a mosquito-borne flavivirus. The virus has a normal transmission cycle between birds and mosquitoes but also a zoonotic transmission cycle with pigs serving as amplifier hosts from which infected mosquitoes transmit the virus to humans. However, the mechanism of virus survival in various hosts is unclear, but is thought to involve DIs. *Tsai et al* identified the generation of DI RNAs of Japanese encephalitis virus in C6/36 mosquito cells (Tsai *et al.*, 2007). DI RNA-containing virions in supernatant fluids from persistently infected mosquito cells could be used to establish persistent infection in BHK-21 cells. The correlation of DI RNA presence with cell survival, in comparison to acute infections, suggests that DI RNAs are contributing mechanistically to the establishment of persistent infection in both the mosquito and mammalian cells.

Thus, future studies could examine the role of DIs in establishing persistent infections. For example, a comparison of how easily persistent infections are established in cells that can produce and respond to IFN with those in which the IFN

response has been knocked out. This could lead to the development of animal models for paramyxovirus infections in which DIs could have a key role in suppressing an acute infection, and the establishment of a persistent infection that would lead to increased virus transmission between hosts.

4.3. The role of RIG-I as the primary sensor of PIV5

It has been demonstrated in this thesis via immunofluorescence, plaque assays, flow cytometry and RT-QPCR of cell sorted infected reporter cells that RIG-I is the primary sensor for the detection of the DI PAMPs generated during PIV5 replication. Reporter cells that are knocked down for RIG-I have larger plaques developed over the course of infection. Furthermore, far fewer GFP+ve RIG-I KD reporter cells are detected compared to Naïve, MDA5 and LGP2 KD reporter cells following infection with PIV5 (wt). By removing the RIG-I sensor, reporter cells are significantly reduced in their ability to recognize the DI PAMPs generated during PIV5 infection, and consequently far fewer cells do not have activation of the IFN-β promoter when compared to Naïve, MDA5 KD and LGP2 KD cells.

It can also be concluded that the majority of the DI species generated during PIV5 (wt) replication activate RIG-I, as the % of GFP+ve MDA5 KD reporter cells was not reduced to the extent of RIG-I KD GFP+ve reporter cells when compared to the relatively high levels observed for Naïve reporter cells. The knock down of RIG-I has a severe detrimental effect on the ability of reporter cells to recognize the DI PAMPs that generated during plaque development. The DI populations generated are not equally recognized by MDA5, rather, the data appears to show that the majority of the DI PAMPs generated are “tailored” for recognition by RIG-I, i.e. they contain RIG-

I specific ligands. Supporting this, viral NP was greatly increased in PIV5 (wt) infected RIG-I KD reporter cells when compared to Naïve, MDA5 KD, LGP2 KD reporter cells, due to the RIG-I KD reporter cells being reduced in their ability to induce IFN. Thus PIV5 (wt) is further able to replicate at an increased rate in RIG-I KD reporter cells when compared to Naïve, MDA5 and LGP2 KD reporter cells. This is supported by the plaque assay data where RIG-I KD reporter cell plaques were far larger than those observed for Naive and MDA5 KD reporter cells following infection with PIV5 (wt).

It is intriguing that many paramyxoviruses do not appear to inhibit RIG-I, at least through their V proteins. There are a number of potential explanations for these observations. Firstly, paramyxoviruses may have other as yet uncharacterized mechanisms to limit the production of IFN. Secondly, paramyxoviruses may be able to survive and propagate in an environment in which limited amounts of IFN are made in a RIG-I-dependent manner. The limited induction of IFN via RIG-I may be necessary to prevent the unwarranted replication of the virus and subsequent pathogenicity in the host before the virus has had a chance to be transmitted to another host. Thirdly, most paramyxoviruses encode mechanisms to disable IFN signaling, and in the case of PIV5 can even dismantle a pre-established IFN-dependent anti-viral state (Didcock et al., 1999; Carlos et al., 2005). Both MDA5 and RIG-I are IFN inducible genes (Kang et al., 2002; Berghall et al., 2006; Matikainen et al., 2006; Siren et al., 2006; Veckman et al., 2006) and thus by blocking IFN signaling, paramyxoviruses will prevent the IFN dependent upregulation of both RIG-I and MDA5 (as well as other members of the IFN induction cascade) and will severely limit the eventual production of IFN by an infected cell.

The role of MDA5 and LGP2 in the induction of IFN following PIV5 (wt) infection

Whilst the role of RIG-I as the primary sensor that detects the DI PAMPs generated during PIV5 (wt) infection, the data also points to a role of MDA5 and LGP2 in the induction of IFN. Firstly, viral plaques in MDA5 KD reporter cells infected with PIV5 (wt) were not the same size, but were smaller than those found for Naïve reporter cells. Furthermore, flow cytometry analysis of PIV5 (wt) infected MDA5 KD reporter cells showed decreased numbers of GFP+ve cells when compared to Naïve reporter cells. This demonstrates that DI PAMPs containing ligands unique to detection by MDA5 are being generated, as removal of the MDA5 sensor does reduce the % of total cells that are GFP+ve when compared to Naïve reporter cells. Indeed, analysing the flow RT-QPCR data of cell sorted GFP+ve and GFP-ve cells, DIs were present in high abundance in GFP+ve RIG-I KD reporter cells. These DIs are recognised by MDA5 and which subsequently induce the activation of the IFN-β promoter. The DIs that activate MDA5 are generated at a far slower rate than those that activate RIG-I, as the genomic NP expression levels in GFP+ve MDA5 KD reporter cells are far lower than that of GFP-ve RIG-I KD reporter cells. The reason for this may be due to selection pressure on the generation of MDA5 activating DIs by the PIV5 V protein which directly inhibits MDA5.

The role of LGP2 as an enhancer of MDA5 is supported by the flow cytometry and RT-QPCR data. The % of cells that are GFP+ve is reduced when LGP2 is knocked down in reporter cells infected with PIV5 (wt). Indeed by knocking down LGP2, viral NP expression is increased compared to Naive reporter cells. Thus MDA5 functional ability to sense DIs and subsequently activate the IFN-β promoter is reduced when LGP2 is knocked down.

Future work on DIs and their role as PAMPs and the induction of IFN

It is unclear whether it is the DI genomes themselves, RNA products made from these DI genomes, the exposure of DI virus genome to RIG-I during RNA synthesis or dsRNA formed by base-pairing of the RNA products with the DI genome template that is responsible for activating the IFN induction cascade. Further work needs to be performed to elucidate the precise nature of the PIV5 DI PAMPs that activate RIG-I.

The development of a robust detection method for DIs by RT-QPCR in reporter cells that have been cell sorted into GFP+ve and GFP-ve cells, opens up the avenue for future studies in examining the specific trailer copyback DIs that are the PAMPs of the PRRs. The DIs generated during infection are a mixed population of primarily different trailer copybacks DI species, and a small proportion of Leader copyback DIs (Killip *et al.*, 2013). By scaling up the low MOI infection of PRR KD reporter cells from 25cm^2 flask to 300cm^2 flasks, and by deep sequencing from CsCl purified nucleocapsids, the DI species/ sequences that activate either RIG-I or MDA5 could be determined following cell sorting of GFP+ve and GFP-ve cells. Furthermore, by cloning a sequence encoding for a short RNA structure called PP7 recognition sequence (PRS) into PRR activating DIs, co-immunoprecipitation studies can be performed on the complexes formed upon RIG-I and MDA5 activation. The cellular proteins involved in PRR recognition of DIs could then be identified. An additional question is whether the PAMPs produced by DIs are the most important inducers of IFN in immune cells. Immune cell reporter lines where the PRRs are knocked down could be generated, and tested for DI mediated IFN induction.

A further aim would be to identify the host cell and viral factors that influence the evolution/generation of DIs. We have already observed that the DIs generated during

PIV5 (wt) infection are able to overcome initial IFN antagonism of the V protein and inhibit viral transcription. However, the influence of host cell factors such as the ISGs, and the V protein on DI evolution over the entire course of an infection has yet to be characterized, and this could have implications on DIs as antiviral agents.

4.4. DIs and their potential as antiviral agents

DIs can detected from Naïve reporter cells infected with PIV5 (wt), and their positive impact on the activation of the IFN-β promoter following PRR recognition, and their negative impact on PIV5 (wt) transcription and virus spread has been examined in this thesis. However, questions that need to be answered are the biological and clinical relevance of DIs in disease. Future studies could focus on whether DIs can be detected *in vivo* in animal models of infection by negative sense RNA viruses, and whether DIs can be detected in clinical samples from infected patients. Further to this, Dis could have role to play in inducing the cytokine storm immune response phenomenon in which the immune system goes into overdrive in response to viral PAMPs, damaging or killing the host.

The IFN inducing properties of DIs and DI sequences could be used to induce IFN *in vivo* for enhancing the immunogenicity of vaccines, prophylactic treatment, treatment of acute and chronic viral and bacterial infections and possibly cancer therapy DIs could be an important factor in inducing an immune response for live attenuated vaccines. Shingai *et al* investigated the mechanism for differential type I IFN induction in monocyte-derived dendritic cells infected with representative MeV laboratory adapted and vaccine strains (Shingai *et al.*, 2007). Laboratory adapted and vaccine strains induced type I IFN in infected cells. The wild-type strains in

contrast induced it to a far lesser extent. It was found that most of the IFN-inducing strains possessed DI RNAs of varying sizes.

New vaccine designs are needed to control diseases associated with antigenically variable viruses, where the classical viral vaccine approaches using inactivated virus or live-attenuated virus have not been successful for some viruses, such as human immunodeficiency virus or herpes simplex virus. Therefore, new types of vaccines are needed to combat these infections such as utilizing the immunity inducing properties of DI viruses. As vaccines, DIs potentially have advantages of both classical types of viral vaccines in being as safe as inactivated virus, as they are unable to replicate by themselves, but expressing viral antigens inside infected cells so that MHC class I and class II presentation can occur efficiently.

Extensive *in vivo* studies have been performed on evaluating DIs as potential vaccines against influenza A virus, reviewed in (Dimmock & Easton, 2014). Influenza A virus has a segmented genome comprising eight molecules of single-stranded, negative sense RNA. DI RNAs can arise from deletions in any segment, but originate most often from the three largest genomic RNAs. Thus, influenza DI RNAs isolated *in vitro* or *in vivo* have a single, central deletion with a highly variable breakpoint, and maintain the $3'$ and $5'$ termini. DIs averaging 440 nucleotides in length have been found isolated *in vivo* from infected mice and sequenced. Complete protection of mice from disease caused by a lethal influenza A virus challenge has been reproducibly achieved following immunization with a DI influenza virus (Dimmock, 1996). The authors further characterized this DI induced immunity whereby defective interfering virus protects better against virulent Influenza A virus than avirulent virus strains (Dimmock & Marriott, 2006). Using reverse genetics, they made virus preparations that contain a single defective RNA, 244 DI RNA (244/PR8).

When inoculated intranasally in mice, it has the ability to protect animals from serious infection with several different influenza A virus subtypes (Dimmock *et al.*, 2008), and also of heterologous influenza B virus (Scott *et al.*, 2011). They also found that this DI induced immunity was found during *in vivo* experiments in the commonly used ferret model (Dimmock *et al.*, 2012; Mann *et al.*, 2006).

In addition, the DIs of certain viruses could promote immunity against non-related viruses. In the course of the study of DI influenza A virus 244/PR8, it was found that it also protected mice from infection with a genetically unrelated heterologous virus, pneumonia virus of mice, a member of the *Paramyxoviridae* family (Easton *et al.*, 2011). It was determined that this mechanism is dependent on type I IFN mediated responses.

4.5. Concluding Remarks

The arms race between our ability to generate novel antivirals and vaccines to the ever-changing viral threat continues in the 21st century despite the advent of advanced molecular and cellular techniques and technology. The information age has only highlighted how vulnerable our antiviral drugs and vaccines are to genetic recombination events generating new viral strains such as with seasonal influenza, or by the antiviral drug mutations caused by the high error rate in virus replication by the viral replication machinery, such as with HIV and highly active antiretroviral therapy. Novel threats continue to emerge such as Nipah virus and increased transmissible strains of Ebola virus. The IFN inducing properties of DIs may offer an important addition to our arsenal in the generation of vaccines and antivirals against these evasive and potent pathogens.

5. PUBLISHED MANUSCRIPTS

Heterocellular induction of interferon by negative-sense RNA viruses.

Chen S, **Short JA**, Young DF, Killip MJ, Schneider M, Goodbourn S, Randall RE.

(2010). **Virology 407:247–255**

Deep sequencing analysis of defective genomes of parainfluenza virus 5 and their role in interferon induction.

Killip MJ, Young DF, Gatherer D, Ross CS, **Short JA**, Davison AJ., Goodbourn S, Randall RE.

(2013). **J Virol 87: 4798–4807**

6. REFERENCES

Abramovich, C., Shulman, L. M., Ratovitski, E., Harroch, S., Tovey, M., Eid, P. & Revel, M. (1994). Differential tyrosine phosphorylation of the IFNAR chain of the type I interferon receptor and of an associated surface protein in response to IFN-alpha and IFN-beta. *EMBO J* **13**, 5871–5877.

Adelson, M. E., Martinand-Mari, C., Iacono, K. T., Muto, N. F. & Suhadolnik, R. J. (1999). Inhibition of human immunodeficiency virus (HIV-1) replication in SupT1 cells transduced with an HIV-1 LTR-driven PKR cDNA construct. *Eur J Biochem* **264**, 806–815.

Akira, S., Uematsu, S. & Takeuchi, O. (2006). Pathogen recognition and innate immunity. *Cell* **124**, 783–801.

Aljofan, M. (2013). Hendra and Nipah infection: emerging paramyxoviruses. *Virus research* **177**, 119–126.

Andersson, I., Bladh, L. & Mousavi-Jazi, M. (2004). Human MxA Protein Inhibits the Replication of Crimean-Congo Hemorrhagic Fever Virus. *Journal of …* –.

Andrejeva, J., Childs, K. S., Young, D. F., Carlos, T. S., Stock, N., Goodbourn, S. & Randall, R. E. (2004). The V proteins of paramyxoviruses bind the IFN-inducible RNA helicase, mda-5, and inhibit its activation of the IFN-beta promoter. *PNAS* **101**, 17264–17269. National Acad Sciences.

Andrejeva, J., Young, D. F., Goodbourn, S. & Randall, R. E. (2002). Degradation of STAT1 and STAT2 by the V proteins of simian virus 5 and human parainfluenza virus type 2, respectively: consequences for virus replication in the presence of alpha/beta and gamma interferons. *J Virol* **76**, 2159–2167.

Arimilli, S., Alexander-Miller, M. A. & Parks, G. D. (2006). A simian virus 5 (SV5) P/V mutant is less cytopathic than wild-type SV5 in human dendritic cells and is a more effective activator of dendritic cell maturation and function. *J Virol* **80**, 3416–3427. American Society for Microbiology.

Au, W. C., Moore, P. A., Lowther, W., Juang, Y. T. & Pitha, P. M. (1995). Identification of a member of the interferon regulatory factor family that binds to the interferon-stimulated response element and activates expression of interferon-induced genes. *Proc Natl Acad Sci U S A* **92**, 11657–11661.

Balachandran, S., Kim, C., Yeh, W. & Mak, T. (1998). Activation of the dsRNA-dependent protein kinase, PKR, induces apoptosis through FADD-mediated death signaling. *The EMBO …* –.

Balachandran, S., Roberts, P. C., Brown, L. E., Truong, H., Pattnaik, A. K., Archer, D. R. & Barber, G. N. (2000). Essential role for the dsRNA-dependent protein kinase PKR in innate immunity to viral infection. *Immunity* **13**, 129–141.

Balachandran, S., Thomas, E. & Barber, G. N. (2004). A FADD-dependent innate immune mechanism in mammalian cells. *Nature* **432**, 401–405.

Balkwill, F. & Taylor-Papadimitriou, J. (1978). Interferon affects both G1 and S+G2 in cells stimulated from quiescence to growth. *Nature* **274**, 798–800.

Banerjee, A. K. (1980). 5'-terminal cap structure in eucaryotic messenger ribonucleic acids. *Microbiol Rev* **44**, 175–205.

Bangham, C. (1990). Defective interfering particles: Effects in modulating virus growth and persistence. *Virology* **179**, 821–826.

Banninger, G. (2004). STAT2 nuclear trafficking. *Journal of Biological Chemistry* –.

Baum, A., Sachidanandam, R. & García-Sastre, A. (2010). Preference of RIG-I for short viral RNA molecules in infected cells revealed by next-generation sequencing. *Proc Natl Acad Sci U S A* **107**, 16303–16308. National Acad Sciences.

Berke, I. C., Berke, I. C., Li, Y., Li, Y., Modis, Y. & Modis, Y. (2013). Structural basis of innate immune recognition of viral RNA. *Cellular Microbiology* **15**, 386–394.

Berke, I. C., Berke, I. C., Modis, Y. & Modis, Y. (2012). MDA5 cooperatively forms dimers and ATP-sensitive filaments upon binding double-stranded RNA. *EMBO J* **31**, 1714–1726. John Wiley & Sons, Ltd.

Black, F. L. (1991). Epidemiology of Paramyxoviridae. In *The Paramyxoviruses*, pp. 509–536. Boston, MA: Springer US.

Boga, J. A., de Ona, M. & Melon, S. (2013). MAVS: A new Weapon in the fight against viral infections. *Recent patents on …* –.

Brennan, K. & Bowie, A. G. (2010). Activation of host pattern recognition receptors by viruses. *Curr Opin Microbiol* **13**, 503–507.

BROEK, M., Muller, U. & Huang, S. (1995). Immune defence in mice lacking type I and/or type II interferon receptors. *Immunological …*.

Broquet, A., Hirata, Y. & McAllister, C. (2011). RIG-I/MDA5/MAVS are required to signal a protective IFN response in rotavirus-infected intestinal epithelium. *The Journal of …*.

Calain, P. & Roux, L. (1993). The rule of six, a basic feature for efficient replication of Sendai virus defective interfering RNA. *J Virol* **67**, 4822–4830. American Society for Microbiology.

Carlos, T. S., Fearns, R. & Randall, R. E. (2005). Interferon-induced alterations in the pattern of parainfluenza virus 5 transcription and protein synthesis and the induction of virus inclusion bodies. *J Virol* **79**, 14112–14121. American Society for Microbiology.

Carlos, T. S., Young, D. F., Schneider, M., Simas, J. P. & Randall, R. E. (2009). Parainfluenza virus 5 genomes are located in viral cytoplasmic bodies whilst the virus dismantles the interferon-induced antiviral state of cells. *J Gen Virol* **90**, 2147–2156. Society for General Microbiology.

Chan, A. Y., Vreede, F. T., Smith, M., Engelhardt, O. G. & Fodor, E. (2006). Influenza virus inhibits RNA polymerase II elongation. *Virology* **351**, 210–217.

Chanock, R. M. (1956). ASSOCIATION OF A NEW TYPE OF CYTOPATHOGENIC MYXOVIRUS WITH INFANTILE CROUP. *J Exp Med* **104**, 555–576. Rockefeller Univ Press.

Chatziandreou, N., Stock, N., Young, D., Andrejeva, J., Hagmaier, K., McGeoch, D. J. & Randall, R. E. (2004). Relationships and host range of human, canine, simian and porcine isolates of simian virus 5 (parainfluenza virus 5). *J Gen Virol* **85**, 3007–3016. Society for General Microbiology.

Chen, L. & Li, S. (2011). The ISG15/USP18 ubiquitin-like pathway (ISGylation system) in Hepatitis C Virus infection and resistance to interferon therapy. *The International Journal of Biochemistry & Cell …*.

Chen, S., Short, J., Young, D. F., Killip, M. J., Schneider, M., Goodbourn, S. & Randall, R. E. (2010). Heterocellular induction of interferon by negative-sense RNA viruses. *Virology* **407**, 247–255.

Chen, Z. J. (2005). Ubiquitin signalling in the NF-|[kappa]|B pathway. *Nature cell biology* **7**, 758–765. Nature Publishing Group.

Chieux, V., Chehadeh, W., Harvey, J., Haller, O., Wattré, P. & Hober, D. (2001). Inhibition of coxsackievirus B4 replication in stably transfected cells expressing human MxA protein. *Virology* **283**, 84–92.

Childs, K. S., Andrejeva, J., Randall, R. E. & Goodbourn, S. (2009). Mechanism of mda-5 Inhibition by Paramyxovirus V Proteins. *J Virol* **83**, 1465–1473. American Society for Microbiology.

Childs, K. S., Randall, R. E. & Goodbourn, S. (2013). LGP2 Plays a Critical Role in Sensitizing mda-5 to Activation by Double-Stranded RNA. *PLoS ONE* **8** (K. L. Mossman, Ed.). Public Library of Science.

Childs, K., Randall, R. & Goodbourn, S. (2012a). Paramyxovirus V proteins interact with the RNA Helicase LGP2 to inhibit RIG-I-dependent interferon induction. *J Virol* **86**, 3411–3421.

Childs, K., Randall, R. & Goodbourn, S. (2012b). Paramyxovirus V proteins interact with the RNA Helicase LGP2 to inhibit RIG-I-dependent interferon induction. *J Virol* **86**, 3411–3421. American Society for Microbiology.

Childs, K., Stock, N., Ross, C., Andrejeva, J., Hilton, L., Skinner, M., Randall, R. & Goodbourn, S. (2007). mda-5, but not RIG-I, is a common target for paramyxovirus V proteins. *Virology* **359**, 190–200.

Chin, K. C. & Cresswell, P. (2001). Viperin (cig5), an IFN-inducible antiviral protein directly induced by human cytomegalovirus. *Proc Natl Acad Sci U S A* **98**, 15125–15130.

Choppin, P. W. (1964). Multiplication of Myxovirus (Sv5) with Minimal Cytopathic Effects + Without Interference. *Virology* **23**, 224–&.

Choppin, P. W. & Stoeckenius, W. (1964). The morphology of SV5 virus. *Virology* **23**, 195–202.

Chua, K. B., Bellini, W. J., Rota, P. A., Harcourt, B. H. & Tamin, A. (2000). Nipah virus: a recently emergent deadly paramyxovirus. *Science*.

Civril, F., Bennett, M., Moldt, M., Deimling, T., Witte, G., Schiesser, S., Carell, T. & Hopfner, K.-P. (2011). The RIG-I ATPase domain structure reveals insights into ATP-dependent antiviral signalling. *EMBO Rep* **12**, 1127–1134. Nature Publishing Group.

Clemens, M. J. (2003). Interferons and apoptosis. *J Interferon Cytokine Res* **23**, 277–292.

Colamonici, O., Yan, H., Domanski, P., Handa, R., Smalley, D., Mullersman, J., Witte, M., Krishnan, K. & Krolewski, J. (1994). Direct binding to and tyrosine phosphorylation of the alpha subunit of the type I interferon receptor by p135tyk2 tyrosine kinase. *Mol Cell Biol* **14**, 8133–8142.

Cui, S., Eisenächer, K., Kirchhofer, A., Brzózka, K., Lammens, A., Lammens, K., Fujita, T., Conzelmann, K.-K., Krug, A. & Hopfner, K.-P. (2008). The C-terminal regulatory domain is the RNA 5'-triphosphate sensor of RIG-I. *Mol Cell* **29**, 169–179.

Cusson-Hermance, N., Khurana, S. & Lee, T. (2005). Rip1 mediates the Trif-dependent Toll-like receptor 3-and 4-induced NF-κB activation but does not contribute to interferon regulatory factor 3 activation. *Journal of Biological …*.

D'Andrea, L. (2003). TPR proteins: the versatile helix. *Trends in Biochemical Sciences* **28**, 655–662.

Dalpke, A., Dalpke, A., Heeg, K., Heeg, K., Bartz, H., Bartz, H., Baetz, A. & Baetz, A. (2008). Regulation of innate immunity by suppressor of cytokine signaling (SOCS) proteins. *Immunobiology* **213**, 225–235.

Darnell, J. E., Jr. **(1997).** STATs and Gene Regulation **277**, 1630–1635.

Deng, L., Wang, C., Spencer, E., Yang, L., Braun, A., You, J., Slaughter, C., Pickart, C. & Chen, Z. J. (2000). Activation of the IkappaB kinase complex by TRAF6 requires a dimeric ubiquitin-conjugating enzyme complex and a unique polyubiquitin chain. *Cell* **103**, 351–361.

Der, S. D., Zhou, A., Williams, B. R. & Silverman, R. H. (1998). Identification of genes differentially regulated by interferon alpha, beta, or gamma using oligonucleotide arrays. *Proc Natl Acad Sci U S A* **95**, 15623–15628.

Didcock, L., Young, D. F., Goodbourn, S. & Randall, R. E. (1999). Sendai virus and simian virus 5 block activation of interferon-responsive genes: importance for virus pathogenesis. *J Virol* **73**, 3125–3133. American Society for Microbiology.

Dimmock, N. J. (1996). Antiviral Activity of Defective Interfering Influenza Virus in vivo. In *Viral and Other Infections of the Human Respiratory Tract*, pp. 421–445. Dordrecht: Springer Netherlands.

Dimmock, N. J., Dove, B. K., Scott, P. D., Meng, B., Taylor, I., Cheung, L., Hallis, B., Marriott, A. C., Carroll, M. W. & Easton, A. J. (2012). Cloned Defective Interfering Influenza Virus Protects Ferrets from Pandemic 2009 Influenza A Virus and Allows Protective Immunity to Be Established. *PLoS ONE* **7** (P. L. Ho, Ed.). Public Library of Science.

Dimmock, N. J. & Easton, A. J. (2014). Defective interfering influenza virus RNAs: time to reevaluate their clinical potential as broad-spectrum antivirals? *J Virol* **88**, 5217–5227.

Dimmock, N. J. & Marriott, A. C. (2006). In vivo antiviral activity: defective interfering virus protects better against virulent Influenza A virus than avirulent virus. *J Gen Virol* **87**, 1259–1265. Society for General Microbiology.

Dimmock, N. J., Rainsford, E. W., Scott, P. D. & Marriott, A. C. (2008). Influenza virus protecting RNA: an effective prophylactic and therapeutic antiviral. *J Virol* **82**, 8570–8578. American Society for Microbiology.

Drexler, J. F., Corman, V. M., Muller, M. A. & Maganga, G. D. (2012). *Bats host major mammalian paramyxoviruses. Nat. Commun. 3: 796*.

Easton, A. J., Scott, P. D., Edworthy, N. L., Meng, B., Marriott, A. C. & Dimmock, N. J. (2011). A novel broad-spectrum treatment for respiratory virus infections: Influenza-based defective interfering virus provides protection against pneumovirus infection in vivo. *Vaccine* **29**, 2777–2784.

Eaton, B. T., Broder, C. C., Middleton, D. & Wang, L.-F. (2006). Hendra and Nipah viruses: different and dangerous. *Nat Rev Micro* **4**, 23–35.

Erlandsson, L., Blumenthal, R., Eloranta, M. L., Engel, H., Alm, G., Weiss, S. & Leanderson, T. (1998). Interferon-beta is required for interferon-alpha production in mouse fibroblasts. *Curr Biol* **8**, 223–226.

Fagerlund, R., Melen, K., Kinnunen, L. & Julkunen, I. (2002). Arginine/lysine-rich nuclear localization signals mediate interactions between dimeric STATs and importin alpha 5. *J Biol Chem* **277**, 30072–30078.

Fairman-Williams, M. E., Guenther, U.-P. & Jankowsky, E. (2010). SF1 and SF2 helicases: family matters. *Curr Opin Struct Biol* **20**, 313–324.

Feng, Q., Hato, S. V., Langereis, M. A., Zoll, J., Virgen-Slane, R., Peisley, A., Hur, S., Semler, B. L., van Rij, R. P. & van Kuppeveld, F. J. M. (2012). MDA5 Detects the Double-Stranded RNA Replicative Form in Picornavirus-Infected Cells. *Cell Reports* **2**, 1187–1196.

Fensterl, V. & Sen, G. C. (2011). The ISG56/IFIT1 gene family. *J Interferon Cytokine Res* **31**, 71–78.

Fitzgerald, K., McWhirter, S. & Faia, K. (2003). IKKε and TBK1 are essential components of the IRF3 signaling pathway. *Nature*.

Fontana, J. & Bankamp, B. (2008). Inhibition of interferon induction and signaling by paramyxoviruses. *Immunol Rev*.

FRANK, S. A. (2000). Within-host Spatial Dynamics of Viruses and Defective Interfering Particles. *Journal of Theoretical Biology* **206**, 279–290.

Frensing, T., Heldt, F. S., Pflugmacher, A., Behrendt, I., Jordan, I., Flockerzi, D., Genzel, Y. & Reichl, U. (2013). Continuous Influenza Virus Production in Cell Culture Shows a Periodic Accumulation of Defective Interfering Particles. *PLoS ONE* **8** (S. Pöhlmann, Ed.). Public Library of Science.

Gack, M. U., Shin, Y. C., Joo, C.-H., Urano, T., Liang, C., Sun, L., Takeuchi, O., Akira, S., Chen, Z. & other authors. **(2007).** TRIM25 RING-finger E3 ubiquitin ligase is essential for RIG-I-mediated antiviral activity. *Nature* **446**, 916–920.

Gainey, M. D., Dillon, P. J., Clark, K. M., Manuse, M. J. & Parks, G. D. (2008). Paramyxovirus-Induced Shutoff of Host and Viral Protein Synthesis: Role of the P and V Proteins in Limiting PKR Activation. *J Virol* **82**, 828–839. American Society for Microbiology.

Gale, M., Blakely, C. M., Hopkins, D. A., Melville, M. W., Wambach, M., Romano, P. R. & Katze, M. G. (1998). Regulation of interferon-induced protein kinase PKR: modulation of P58IPK inhibitory function by a novel protein, P52rIPK. *Mol Cell Biol* **18**, 859–871.

Gao, S. (n.d.). *Gao: Malsburg von der A, Dick A, Faelber K, Schröder... - Google Scholar*. *Immunity*

.

García-Sastre, A. (2011). 2 methylate or not 2 methylate: viral evasion of the type I interferon response. *Nat Immunol* **12**, 114–115.

Gee, P., Chua, P. K., Gevorkyan, J., Klumpp, K., Najera, I., Swinney, D. C. & Deval, J. (2008). Essential role of the N-terminal domain in the regulation of RIG-I ATPase activity. *J Biol Chem* **283**, 9488–9496.

Gerlier, D. & Lyles, D. S. (2011). Interplay between Innate Immunity and Negative-Strand RNA Viruses: towards a Rational Model. *Microbiol Mol Biol Rev* **75**, 468–490.

Génin, P., Vaccaro, A. & Civas, A. (2009). The role of differential expression of human interferon--a genes in antiviral immunity. *Cytokine Growth Factor Rev* **20**, 283–295.

Gitlin, L., Barchet, W., Gilfillan, S., Cella, M., Beutler, B., Flavell, R. A., Diamond, M. S. & Colonna, M. (2006). Essential role of mda-5 in type I IFN responses to polyriboinosinic:polyribocytidylic acid and encephalomyocarditis picornavirus. **103**, 8459–8464.

Gitlin, L., Benoit, L., Song, C., Cella, M., Gilfillan, S., Holtzman, M. J. & Colonna, M. (2010). Melanoma Differentiation-Associated Gene 5 (MDA5) Is Involved in the Innate Immune Response to Paramyxoviridae Infection In Vivo. *PLoS Pathog* **6**, e1000734 (R. S. Baric, Ed.). Public Library of Science.

Gordien, E., Rosmorduc, O., Peltekian, C., Garreau, F., Bréchot, C. & Kremsdorf, D. (2001). Inhibition of hepatitis B virus replication by the interferon-inducible MxA protein. *J Virol* **75**, 2684–2691.

Goswami, K. K., Lange, L. S., Mitchell, D. N., Cameron, K. R. & Russell, W. C. (1984). Does simian virus 5 infect humans? *J Gen Virol* **65 (Pt 8)**, 1295–1303.

Grandvaux, N., Servant, M. J., tenOever, B., Sen, G. C., Balachandran, S., Barber, G. N., Lin, R. & Hiscott, J. (2002). Transcriptional profiling of interferon regulatory factor 3 target genes: direct involvement in the regulation of interferon-stimulated genes. *J Virol* **76**, 5532–5539.

Guo, J., Hui, D. J., Merrick, W. C. & Sen, G. C. (2000). A new pathway of translational regulation mediated by eukaryotic initiation factor 3. *EMBO J* **19**, 6891–6899.

Gutierrez, O., Pipaon, C., Inohara, N., Fontalba, A., Ogura, Y., Prosper, F., Nunez, G. & Fernandez-Luna, J. L. (2002). Induction of Nod2 in myelomonocytic and intestinal epithelial cells via nuclear factor-kappa B activation. *J Biol Chem* **277**, 41701–41705.

GÜR, S. & ACAR, A. (n.d.). Kangal Irkı Türk Çoban Köpeklerinde Canine Parainfluenzavirus Tip5 (CPIV5) Enfeksiyonunun Serolojik Olarak Araştırılması. *firatedutr*

.

Haller, O., Stertz, S. & Kochs, G. (2007). The Mx GTPase family of interferon-induced antiviral proteins. *Microbes and Infection* **9**, 1636–1643.

HAQUE, S. & SHARMA, P. (2006). *Vitamins & Hormones*. Elsevier.

Häcker, H., Redecke, V., Blagoev, B., Kratchmarova, I., Hsu, L.-C., Wang, G. G., Kamps, M. P., Raz, E., Wagner, H. & other authors. (2006). Specificity in Toll-like receptor signalling through distinct effector functions of TRAF3 and TRAF6. *Nature* **439**, 204–207.

He, B., Lin, G. Y., Durbin, J. E. & Durbin, R. K. (2001). The SH integral membrane protein of the paramyxovirus simian virus 5 is required to block apoptosis in MDBK cells. *J Virol*.

He, B., Paterson, R. G., Stock, N., Durbin, J. E., Durbin, R. K., Goodbourn, S., Randall, R. E. & Lamb, R. A. (2002). Recovery of Paramyxovirus Simian Virus 5 with a V Protein Lacking the Conserved Cysteine-rich Domain: The Multifunctional V Protein Blocks both Interferon-β Induction and Interferon Signaling. *Virology* **303**, 15–32.

Hiebert, S. W., Paterson, R. G. & Lamb, R. A. (1985). Identification and predicted sequence of a previously unrecognized small hydrophobic protein, SH, of the paramyxovirus simian virus 5. *J Virol*.

Hinnebusch, A. (2006). eIF3: a versatile scaffold for translation initiation complexes. *Trends in Biochemical Sciences*.

Hoebe, K. (2006). ScienceDirect - Trends in Molecular Medicine : TRAF3: a new component of the TLR-signaling apparatus. *Trends in molecular medicine* –.

Hornung, V., Barchet, W., Schlee, M. & Hartmann, G. (2008). RNA recognition via TLR7 and TLR8. *Handb Exp Pharmacol* 71–86.

Hornung, V., Ellegast, J., Kim, S., Brzózka, K., Jung, A., Kato, H., Poeck, H., Akira, S., Conzelmann, K.-K. & other authors. **(2006).** 5'-Triphosphate RNA is the ligand for RIG-I. *Science* **314**, 994–997.

Hovanessian, A. G. (2007). On the discovery of interferon-inducible, double-stranded RNA activated enzymes: the 2'-5'oligoadenylate synthetases and the protein kinase PKR. *Cytokine Growth Factor Rev* **18**, 351–361.

Hsiung, G. D. (1972). *Parainfluenza-5 virus. Infection of man and animal.* Progress in medical virology. Fortschritte der ….

Hsu, C. H., Re, G. G., Gupta, K. C., Portner, A. & Kingsbury, D. W. (1985). Expression of sendai virus defective-interfering genomes with internal deletions. *Virology* **146**, 38–49.

Hui, D., Bhasker, C. & Merrick, W. (2003). Viral stress-inducible protein p56 inhibits translation by blocking the interaction of eIF3 with the ternary complex eIF2· GTP· Met-tRNAi. *Journal of Biological … –*.

Hull, R. N. & Minner, J. R. (1957). NEW VIRAL AGENTS RECOVERED FROM TISSUE CULTURES OF MONKEY KIDNEY CELLS. II. PROBLEMS OF ISOLATION AND IDENTIFICATION. *Annals of the New York Academy of Sciences* **67**, 413–423. Blackwell Publishing Ltd.

Hwang, S. Y., Hertzog, P. J., Holland, K. A., Sumarsono, S. H., Tymms, M. J., Hamilton, J. A., Whitty, G., Bertoncello, I. & Kola, I. (1995). A null mutation in the gene encoding a type I interferon receptor component eliminates antiproliferative and antiviral responses to interferons alpha and beta and alters macrophage responses. *Proc Natl Acad Sci U S A* **92**, 11284–11288.

Isaacs, A. & Lindenmann, J. (1957). Virus interference. I. The interferon. *… of the Royal … –*.

Ishikawa, H. & Barber, G. N. (2008). STING is an endoplasmic reticulum adaptor that facilitates innate immune signalling. *Nature* **455**, 674–678.

Jacobs, J. L. & Coyne, C. B. (2013). Mechanisms of MAVS Regulation at the Mitochondrial Membrane. *J Mol Biol* **425**, 5009–5019.

Janeway, C. A. (1989). Approaching the asymptote? Evolution and revolution in immunology. *Cold Spring Harb Symp Quant Biol* **54 Pt 1**, 1–13.

Jensen, S. & Thomsen, A. R. (2012). Sensing of RNA Viruses: a Review of Innate Immune Receptors Involved in Recognizing RNA Virus Invasion. *J Virol* **86**, 2900–2910. American Society for Microbiology.

Jiang, D., Guo, H., Xu, C., Chang, J., Gu, B., Wang, L., Block, T. M. & Guo, J.-T. (2008). Identification of three interferon-inducible cellular enzymes that inhibit the replication of hepatitis C virus. *J Virol* **82**, 1665–1678.

Jiang, F., Ramanathan, A., Miller, M. T., Tang, G.-Q., Gale, M., Patel, S. S. & Marcotrigiano, J. (2011). Structural basis of RNA recognition and activation by innate immune receptor RIG-I. *Nature* **479**, 423–427. Nature Publishing Group.

Jiang, Q.-X. & Chen, Z. J. (2012). Structural insights into the activation of RIG-I, a nanosensor for viral RNAs. *EMBO Rep* **13**, 7–8.

Jiang, X., Kinch, L. N., Brautigam, C. A., Chen, X. & Du, F. (2012). Ubiquitin-induced oligomerization of the RNA sensors RIG-I and MDA5 activates antiviral innate immune response. *Immunity*.

Jiang, Z., Mak, T. W., Sen, G. & Li, X. (2004). Toll-like receptor 3-mediated activation of NF-kappaB and IRF3 diverges at Toll-IL-1 receptor domain-containing adapter inducing IFN-beta. *Proc Natl Acad Sci U S A* **101**, 3533–3538.

Kamijo, R., Le, J., Shapiro, D., Havell, E. A., Huang, S., Aguet, M., Bosland, M. & Vilcek, J. (1993). Mice that lack the interferon-gamma receptor have profoundly altered responses to infection with Bacillus Calmette-Guérin and subsequent challenge with lipopolysaccharide. *J Exp Med* **178**, 1435–1440.

Kanayama, A., Seth, R. B., Sun, L., Ea, C.-K., Hong, M., Shaito, A., Chiu, Y.-H., Deng, L. & Chen, Z. J. (2004). TAB2 and TAB3 activate the NF-kappaB pathway through binding to polyubiquitin chains. *Mol Cell* **15**, 535–548.

Kang, D.-C., Gopalkrishnan, R. V., Lin, L., Randolph, A., Valerie, K., Pestka, S. & Fisher, P. B. (2004). Expression analysis and genomic characterization of human melanoma differentiation associated gene-5, mda-5: a novel type I interferon-responsive apoptosis-inducing gene. *Oncogene* **23**, 1789–1800.

Kato, H., Takeuchi, O., Sato, S., Yoneyama, M., Yamamoto, M., Matsui, K., Uematsu, S., Jung, A., Kawai, T. & other authors. **(2006).** Differential roles of MDA5 and RIG-I helicases in the recognition of RNA viruses. *Nature* **441**, 101–105.

Kato, H., Takeuchi, O., Mikamo-Satoh, E., Hirai, R., Kawai, T., Matsushita, K., Hiiragi, A., Dermody, T. S., Fujita, T. & Akira, S. (2008). Length-dependent recognition of double-stranded ribonucleic acids by retinoic acid-inducible gene-I and melanoma differentiation-associated gene 5. *J Exp Med* **205**, 1601–1610.

Kawai, T., Takahashi, K., Sato, S., Coban, C., Kumar, H., Kato, H., Ishii, K. J., Takeuchi, O. & Akira, S. (2005). IPS-1, an adaptor triggering RIG-I- and Mda5-mediated type I interferon induction **6**, 981–988.

Kawai, T. & Akira, S. (2011). Toll-like Receptors and Their Crosstalk with Other Innate Receptors in Infection and Immunity **34**, 637–650.

Killip, M. J., Young, D. F., Gatherer, D., Ross, C. S., Short, J., Davison, A. J., Goodbourn, S. & Randall, R. E. (2013). Deep Sequencing Analysis of Defective Genomes of Parainfluenza Virus 5 and Their Role in Interferon Induction. *J Virol* **87**, 4798–4807. American Society for Microbiology.

Killip, M. J., Young, D. F., Precious, B. L., Goodbourn, S. & Randall, R. E. (2012a). Activation of the beta interferon promoter by paramyxoviruses in the absence of virus protein synthesis. *J Gen Virol* **93**, 299–307.

Killip, M. J., Young, D. F., Precious, B. L., Goodbourn, S. & Randall, R. E. (2012b). Activation of the beta interferon promoter by paramyxoviruses in the absence of virus protein synthesis. *J Gen Virol* **93**, 299–307. Society for General Microbiology.

Killip, M. J., Young, D. F., Ross, C. S., Chen, S., Goodbourn, S. & Randall, R. E. (2011). Failure to activate the IFN-β promoter by a paramyxovirus lacking an interferon antagonist. *Virology* **415**, 39–46.

Kirkwood, T. & BANGHAM, C. (1994). Cycles, Chaos, and Evolution in Virus Cultures - a Model of Defective Interfering Particles. *Proc Natl Acad Sci U S A* **91**, 8685–8689. National Acad Sciences.

Knipe, D. M., Howley, P., Lamb, R. A. & Parks, G. D. (2013). *Fields Virology*. Lippincott Williams & Wilkins.

Kochs, G. (1999). Interferon-induced human MxA GTPase blocks nuclear import of Thogoto virus nucleocapsids. *… of the National Academy of Sciences* –.

Kochs, G., Janzen, C., Hohenberg, H. & Haller, O. (2002). Antivirally active MxA protein sequesters La Crosse virus nucleocapsid protein into perinuclear complexes. *Proc Natl Acad Sci U S A* **99**, 3153–3158.

Kohanbash, G. & Okada, H. (2012). MicroRNAs and STAT interplay. *Semin Cancer Biol* **22**, 70–75.

Kolakofsky, D. (1976). Isolation and characterization of Sendai virus DI-RNAs. *Cell* **8**, 547–555.

Kolakofsky, D. (1979). Studies on the generation and amplification of Sendai virus defective-interfering genomes. *Virology* **93**, 589–593.

Kolakofsky, D., Kowalinski, E. & Cusack, S. (2012). A structure-based model of RIG-I activation. *RNA* **18**, 2118–2127. Cold Spring Harbor Lab.

Komuro, A. & Horvath, C. M. (2006). RNA- and virus-independent inhibition of antiviral signaling by RNA helicase LGP2. **80**, 12332–12342.

Kowalinski, E., Lunardi, T., McCarthy, A. A., Louber, J., Brunel, J., Grigorov, B., Gerlier, D. & Cusack, S. (2011). Structural basis for the activation of innate immune pattern-recognition receptor RIG-I by viral RNA. *Cell* **147**, 423–435.

Krämer, O. H. & Heinzel, T. (2010). Phosphorylation-acetylation switch in the regulation of STAT1 signaling. **315**, 40–48.

Kumar, H., Kawai, T. & Akira, S. (2011). Pathogen recognition by the innate immune system. *Int Rev Immunol* **30**, 16–34.

Kurth, A., Kohl, C., Brinkmann, A., Ebinger, A. & Harper, J. A. (2012). Novel paramyxoviruses in free-ranging European bats. *PLoS ONE*.

Kusari, J. & Sen, G. C. (1986). Regulation of synthesis and turnover of an interferon-inducible mRNA. *Mol Cell Biol* **6**, 2062–2067.

Lamb, J. R., Tugendreich, S. & Hieter, P. (1995). Tetratrico peptide repeat interactions: to TPR or not to TPR? *Trends in Biochemical Sciences*.

Landis, H., Simon-Jödicke, A., Klöti, A., Di Paolo, C., Schnorr, J.-J., Schneider-Schaulies, S., Hefti, H. P. & Pavlovic, J. (1998). Human MxA Protein Confers Resistance to Semliki Forest Virus and Inhibits the Amplification of a Semliki Forest Virus-Based Replicon in the Absence of Viral Structural Proteins. *J Virol* **72**, 1516–1522. American Society for Microbiology.

Lazzarini, R. A., Keene, J. D. & Schubert, M. (1981). The origins of defective interfering particles of the negative-strand RNA viruses. *Cell* **26**, 145–154.

Le Mercier, P., Garcin, D., Hausmann, S. & Kolakofsky, D. (2002). Ambisense sendai viruses are inherently unstable but are useful to study viral RNA synthesis. *J Virol* **76**, 5492–5502.

Lee, S. B. & Esteban, M. (1993). The interferon-induced double-stranded RNA-activated human p68 protein kinase inhibits the replication of vaccinia virus. *Virology* **193**, 1037–1041.

Lee, Y. F., Nomoto, A., Detjen, B. M. & Wimmer, E. (1977). A protein covalently linked to poliovirus genome RNA. *PNAS* **74**, 59–63. National Acad Sciences.

Lengyel, P. (2008). From RNase L to the Multitalented p200 Family Proteins: An Exploration of the Modes of Interferon Action. *J Interferon Cytokine Res* **28**, 273–281.

Lenschow, D. J., Giannakopoulos, N. V., Gunn, L. J., Johnston, C., O'Guin, A. K., Schmidt, R. E., Levine, B. & Virgin, H. W. (2005). Identification of interferon-stimulated gene 15 as an antiviral molecule during Sindbis virus infection in vivo. *J Virol* **79**, 13974–13983.

Lenschow, D. J., Lai, C., Frias-Staheli, N., Giannakopoulos, N. V., Lutz, A., Wolff, T., Osiak, A., Levine, B., Schmidt, R. E. & other authors. (2007). IFN-stimulated gene 15 functions as a critical antiviral molecule against influenza, herpes, and Sindbis viruses. *Proc Natl Acad Sci U S A* **104**, 1371–1376.

Leppert, M. (1977). Further characterization of sendai virus DI-RNAs: A model for their generation. *Cell* **12**, 539–552.

Lester, S. N. & Li, K. (2014). Toll-like receptors in antiviral innate immunity. *J Mol Biol* **426**, 1246–1264.

Leung, D. W. & Amarasinghe, G. K. (2012). Structural insights into RNA recognition and activation of RIG-I-like receptors. *Curr Opin Struct Biol* **22**, 297–303.

Leung, S., Qureshi, S. A., Kerr, I. M., Darnell, J. E. & Stark, G. R. (1995). Role of STAT2 in the alpha interferon signaling pathway. *Mol Cell Biol* **15**, 1312–1317.

Levy, D. E. & Darnell, J. E. (2002). Stats: transcriptional control and biological impact. *Nat Rev Mol Cell Biol* –.

Li, C., Ni, C.-Z., Havert, M. L., Cabezas, E., He, J., Kaiser, D., Reed, J. C., Satterthwait, A. C., Cheng, G. & Ely, K. R. (2002). Downstream regulator TANK binds to the CD40 recognition site on TRAF3. *Structure* **10**, 403–411.

Li, D., Lott, W. B., Lowry, K., Jones, A., Thu, H. M. & Aaskov, J. (2011). Defective Interfering Viral Particles in Acute Dengue Infections. *PLoS ONE* **6**, e19447 (L. L. Coffey, Ed.). Public Library of Science.

Li, X., Ranjith-Kumar, C. T., Brooks, M. T., Dharmaiah, S., Herr, A. B., Kao, C. & Li, P. (2009a). The RIG-I-like Receptor LGP2 Recognizes the Termini of Double-stranded RNA. *Journal of Biological Chemistry* **284**, 13881–13891.

Li, X., Lu, C., Stewart, M., Xu, H., Strong, R. K., Igumenova, T. & Li, P. (2009b). Structural basis of double-stranded RNA recognition by the RIG-I like receptor MDA5. *Arch Biochem Biophys* **488**, 23–33.

Li, Y., Li, C., Xue, P., Zhong, B., Mao, A.-P., Ran, Y., Chen, H., Wang, Y.-Y., Yang, F. & Shu, H.-B. (2009c). ISG56 is a negative-feedback regulator of virus-triggered signaling and cellular antiviral response. *Proc Natl Acad Sci U S A* **106**, 7945–7950.

Lin, G. Y. & Lamb, R. A. (2000). The paramyxovirus simian virus 5 V protein slows progression of the cell cycle. *J Virol* **74**, 9152–9166.

Lin, R., Yu, H., Chang, B. & Tang, W. (2009). Distinct antiviral roles for human 2′, 5′-oligoadenylate synthetase family members against dengue virus infection. *The Journal of …* –.

Lin, Y., Bright, A. C., Rothermel, T. A. & He, B. (2003). Induction of apoptosis by paramyxovirus simian virus 5 lacking a small hydrophobic gene. *J Virol*.

Lin, Y., Horvath, F., Aligo, J. A., Wilson, R. & He, B. (2005). The role of simian virus 5 V protein on viral RNA synthesis. *Virology* **338**, 270–280.

Liu, S.-Y., Sanchez, D. J. & Cheng, G. (2011). New developments in the induction and antiviral effectors of type I interferon. *Curr Opin Immunol* **23**, 57–64.

Loeb, K. R. & Haas, A. L. (1992). The interferon-inducible 15-kDa ubiquitin homolog conjugates to intracellular proteins. *J Biol Chem* **267**, 7806–7813.

Loeb, K. R. & Haas, A. L. (1994). Conjugates of ubiquitin cross-reactive protein distribute in a cytoskeletal pattern. *Mol Cell Biol* **14**, 8408–8419.

Loo, Y.-M., Fornek, J., Crochet, N., Bajwa, G., Perwitasari, O., Martinez-Sobrido, L., Akira, S., Gill, M. A., García-Sastre, A. & other authors. **(2008).** Distinct RIG-I and MDA5 signaling by RNA viruses in innate immunity. *J Virol* **82**, 335–345. American Society for Microbiology.

López, C. B. (2014). Defective Viral Genomes: Critical Danger Signals of Viral Infections. *J Virol* **88**, 8720–8723. American Society for Microbiology.

Lu, C., Xu, H., Ranjith-Kumar, C. T., Brooks, M. T., Hou, T. Y., Hu, F., Herr, A. B., Strong, R. K., Kao, C. C. & Li, P. (2010). The structural basis of 5' triphosphate double-stranded RNA recognition by RIG-I C-terminal domain. *Structure* **18**, 1032–1043.

Lu, G., Reinert, J. T., Pitha-Rowe, I., Okumura, A., Kellum, M., Knobeloch, K. P., Hassel, B. & Pitha, P. M. (2006). ISG15 enhances the innate antiviral response by inhibition of IRF-3 degradation. *Cell Mol Biol (Noisy-le-grand)* **52**, 29–41.

Lu, L. L., Puri, M., Horvath, C. M. & Sen, G. C. (2008). Select paramyxoviral V proteins inhibit IRF3 activation by acting as alternative substrates for inhibitor of kappaB kinase epsilon (IKKe)/TBK1. *J Biol Chem* **283**, 14269–14276. American Society for Biochemistry and Molecular Biology.

Luo, D., Kohlway, A. & Pyle, A. M. (2013). Duplex RNA activated ATPases (DRAs). *RNA biology* –.

Luo, D., Ding, S. C., Vela, A., Kohlway, A., Lindenbach, B. D. & Pyle, A. M. (2011). Structural insights into RNA recognition by RIG-I. *Cell* **147**, 409–422.

Luthra, P., Sun, D., Silverman, R. H. & He, B. (2011). Activation of IFN-β expression by a viral mRNA through RNase L and MDA5. *Proc Natl Acad Sci U S A* **108**, 2118–2123. National Acad Sciences.

Magnus, P. (1947). *Magnus: Studies on interference in experimental influenza - Google Scholar*. Ark. Kemi.

Malakhova, O. A., Yan, M., Malakhov, M. P., Yuan, Y., Ritchie, K. J., Kim, K. I., Peterson, L. F., Shuai, K. & Zhang, D.-E. (2003). Protein ISGylation modulates the JAK-STAT signaling pathway. *Genes Dev* **17**, 455–460.

Malathi, K., Dong, B., Gale, M. & Silverman, R. H. (2007). Small self-RNA generated by RNase L amplifies antiviral innate immunity. *Nature* **448**, 816–819.

Malathi, K., Saito, T., Crochet, N., Barton, D. J., Gale, M. & Silverman, R. H. (2010). RNase L releases a small RNA from HCV RNA that refolds into a potent PAMP. *RNA* **16**, 2108–2119.

Malsburg, von der, A., Malsburg, von der, A., Abutbul-Ionita, I., Abutbul-Ionita, I., Haller, O., Haller, O., Kochs, G. & Danino, D. (2011). Stalk Domain of the Dynamin-like MxA GTPase Protein Mediates Membrane Binding and Liposome Tubulation via the Unstructured L4 Loop. *Journal of Biological Chemistry* **286**, 37858–37865. American Society for Biochemistry and Molecular Biology.

Mann, A., Marriott, A. C., Balasingam, S., Lambkin, R., Oxford, J. S. & Dimmock, N. J. (2006). Interfering vaccine (defective interfering influenza A virus) protects ferrets from influenza, and allows them to develop solid immunity to reinfection. *Vaccine* **24**, 4290–4296.

Marcus, P. I. & Sekellick, M. J. (1977). Defective interfering particles with covalently linked [±]RNA induce interferon. *Nature* **266**, 815–819.

Marié, I., Durbin, J. E. & Levy, D. E. (1998). Differential viral induction of distinct interferon-alpha genes by positive feedback through interferon regulatory factor-7. *EMBO J* **17**, 6660–6669.

Marques, J. T., Devosse, T., Wang, D., Zamanian-Daryoush, M., Serbinowski, P., Hartmann, R., Fujita, T., Behlke, M. A. & Williams, B. R. G. (2006). A structural basis for discriminating between self and nonself double-stranded RNAs in mammalian cells. *Nat Biotechnol* **24**, 559–565.

Matsumiya, T., Imaizumi, T., Yoshida, H. & Satoh, K. (2011). Antiviral signaling through retinoic acid-inducible gene-I-like receptors. *Arch Immunol Ther Exp (Warsz)* **59**, 41–48.

McBride, K. & McDonald, C. (2000). Nuclear export signal located within the DNA-binding domain of the STAT1transcription factor. *EMBO J*.

McCandlish, I. A., Thompson, H., Cornwell, H. J. & Wright, N. G. (1978). A study of dogs with kennel cough. *Vet Rec* **102**, 293–301.

Melen, K., Fagerlund, R., Franke, J., Kohler, M., Kinnunen, L. & Julkunen, I. (2003). Importin alpha nuclear localization signal binding sites for STAT1, STAT2, and influenza A virus nucleoprotein. *J Biol Chem* **278**, 28193–28200.

Meurs, E. F., Watanabe, Y., Kadereit, S., Barber, G. N., Katze, M. G., Chong, K., Williams, B. R. & Hovanessian, A. G. (1992). Constitutive expression of human double-stranded RNA-activated p68 kinase in murine cells mediates phosphorylation of eukaryotic initiation factor 2 and partial resistance to encephalomyocarditis virus growth. *J Virol* **66**, 5805–5814.

Meylan, E., Burns, K. & Hofmann, K. (2004). RIP1 is an essential mediator of Toll-like receptor 3–induced NF-κB activation. *Nature*.

Meylan, E., Curran, J., Hofmann, K., Moradpour, D., Binder, M., Bartenschlager, R. & Tschopp, J. (2005). Cardif is an adaptor protein in the RIG-I antiviral pathway and is targeted by hepatitis C virus. *Nature* **437**, 1167–1172.

Michallet, M.-C., Meylan, E., Ermolaeva, M. A., Vazquez, J., Rebsamen, M., Curran, J., Poeck, H., Bscheider, M., Hartmann, G. & other authors. **(2008).** TRADD protein is an essential component of the RIG-like helicase antiviral pathway. *Immunity* **28**, 651–661.

Mikula, I. & Pastoreková, S. (2010). Toll-like receptors in immune response to the viral infections. *Acta Virol* **54**, 231–245.

Miyanari, Y., Atsuzawa, K., Usuda, N. & Watashi, K. (2007). The lipid droplet is an important organelle for hepatitis C virus production. *Nature cell …*.

Mogensen, T. (2009). Pathogen Recognition and Inflammatory Signaling in Innate Immune Defenses. *Clinical microbiology reviews* –.

Munshi, N., Merika, M., Yie, J., Senger, K., Chen, G. & Thanos, D. (1998). Acetylation of HMG I(Y) by CBP turns off IFN beta expression by disrupting the enhanceosome. *Mol Cell* **2**, 457–467.

Murali, A., Li, X., Ranjith-Kumar, C. T., Bhardwaj, K., Holzenburg, A., Li, P. & Kao, C. C. (2008). Structure and function of LGP2, a DEX(D/H) helicase that regulates the innate immunity response. **283**, 15825–15833.

Murphy, S. K. & Parks, G. D. (1997). Genome Nucleotide Lengths That Are Divisible by Six Are Not Essential but Enhance Replication of Defective Interfering RNAs of the Paramyxovirus Simian Virus 5. *Virology* **232**, 145–157.

Müller, M., Briscoe, J., Laxton, C., Guschin, D., Ziemiecki, A., Silvennoinen, O., Harpur, A. G., Barbieri, G., Witthuhn, B. A. & Schindler, C. (1993). The protein tyrosine kinase JAK1 complements defects in interferon-alpha/beta and -gamma signal transduction. *Nature* **366**, 129–135.

Nair, H., Simões, E. A., Rudan, I., Gessner, B. D., Azziz-Baumgartner, E., Zhang, J. S. F., Feikin, D. R., Mackenzie, G. A., Moïïsi, J. C. & other authors. **(2013).** Global and regional burden of hospital admissions for severe acute lower respiratory infections in young children in 2010: a systematic analysis. *The Lancet* **381**, 1380–1390.

Najjar, I. & Fagard, R. (2010). STAT1 and pathogens, not a friendly relationship. *Biochimie* **92**, 425–444.

Nakaya, T., Sato, M., Hata, N., Asagiri, M., Suemori, H., Noguchi, S., Tanaka, N. & Taniguchi, T. (2001). Gene induction pathways mediated by distinct IRFs during viral infection. *Biochem Biophys Res Commun* **283**, 1150–1156.

Nanduri, S., Rahman, F., Williams, B. R. & Qin, J. (2000). A dynamically tuned double-stranded RNA binding mechanism for the activation of antiviral kinase PKR. *EMBO J* **19**, 5567–5574.

NELSON, G. W. & PERELSON, A. S. (1995). Modeling Defective Interfering Virus Therapy for Aids - Conditions for Div Survival. *Math Biosci* **125**, 127–153.

Novick, D., Cohen, B. & Rubinstein, M. (1994). The human interferon alpha/beta receptor: characterization and molecular cloning. *Cell* **77**, 391–400.

O'Neill, L. A. J. & Bowie, A. G. (2010). Sensing and signaling in antiviral innate immunity. *Curr Biol* **20**, R328–33.

Oganesyan, G., Saha, S. K., Guo, B., He, J. Q., Shahangian, A., Zarnegar, B., Perry, A. & Cheng, G. (2006). Critical role of TRAF3 in the Toll-like receptor-dependent and -independent antiviral response. *Nature* **439**, 208–211.

Ogura, Y., Inohara, N., Benito, A., Chen, F. F., Yamaoka, S. & Nunez, G. (2001). Nod2, a Nod1/Apaf-1 family member that is restricted to monocytes and activates NF-kappaB. *J Biol Chem* **276**, 4812–4818.

Ogura, Y., Lala, S., Xin, W., Smith, E., Dowds, T. A., Chen, F. F., Zimmermann, E., Tretiakova, M., Cho, J. H. & other authors. **(2003).** Expression of NOD2 in Paneth cells: a possible link to Crohn's ileitis. *Gut* **52**, 1591–1597.

Okumura, A., Lu, G., Pitha-Rowe, I. & Pitha, P. M. (2006). Innate antiviral response targets HIV-1 release by the induction of ubiquitin-like protein ISG15. *Proc Natl Acad Sci U S A* **103**, 1440–1445.

Onomoto, K., Onoguchi, K., Takahasi, K. & Fujita, T. (2010). Type I interferon production induced by RIG-I-like receptors. *J Interferon Cytokine Res* **30**, 875–881.

Panda, D., Dinh, P. X., Beura, L. K. & Pattnaik, A. K. (2010). Induction of interferon and interferon signaling pathways by replication of defective interfering particle RNA in cells constitutively expressing vesicular stomatitis virus replication proteins. **84**, 4826–4831.

Parisien, J.-P., Bamming, D., Komuro, A., Ramachandran, A., Rodriguez, J. J., Barber, G., Wojahn, R. D. & Horvath, C. M. (2009). A shared interface mediates paramyxovirus interference with antiviral RNA helicases MDA5 and LGP2. *J Virol* **83**, 7252–7260. American Society for Microbiology.

Pattnaik, A. K., BALL, L. A., LEGRONE, A. W. & WERTZ, G. W. (1992). Infectious Defective Interfering Particles of Vsv From Transcripts of a Cdna Clone. *Cell* **69**, 1011–1020.

Peisley, A., Jo, M. H., Lin, C., Wu, B., Orme-Johnson, M., Walz, T., Hohng, S. & Hur, S. (2012). Kinetic mechanism for viral dsRNA length discrimination by MDA5 filaments. *Proc Natl Acad Sci U S A* **109**, E3340–9. National Acad Sciences.

Peisley, A., Lin, C., Wu, B., Orme-Johnson, M., Liu, M., Walz, T. & Hur, S. (2011). Cooperative assembly and dynamic disassembly of MDA5 filaments for viral dsRNA recognition. *Proc Natl Acad Sci U S A* **108**, 21010–21015. National Acad Sciences.

Perrault, J. (1981). Origin and replication of defective interfering particles. *Curr Top Microbiol Immunol* **93**, 151–207.

Pestka, S. & Krause, C. (2004). Interferons, interferon-like cytokines, and their receptors. *Immunol Rev*.

Peters, K. L., Smith, H. L., Stark, G. R. & Sen, G. C. (2002). IRF-3-dependent, NFkappa B- and JNK-independent activation of the 561 and IFN-beta genes in response to double-stranded RNA. *Proc Natl Acad Sci U S A* **99**, 6322–6327.

Pichlmair, A., Schulz, O., Tan, C. P., Näslund, T. I., Liljeström, P., Weber, F. & Reis e Sousa, C. (2006). RIG-I-mediated antiviral responses to single-stranded RNA bearing 5'-phosphates. *Science* **314**, 997–1001.

Pichlmair, A., Schulz, O., Tan, C. P., Rehwinkel, J., Kato, H., Takeuchi, O., Akira, S., Way, M., Schiavo, G. & Reis e Sousa, C. (2009). Activation of MDA5 requires higher-order RNA structures generated during virus infection. *J Virol* **83**, 10761–10769.

Pincetic, A., Kuang, Z., Seo, E. J. & Leis, J. (2010). The interferon-induced gene ISG15 blocks retrovirus release from cells late in the budding process. *J Virol* **84**, 4725–4736.

Pippig, D. A., Hellmuth, J. C., Cui, S., Kirchhofer, A., Lammens, K., Lammens, A., Schmidt, A., Rothenfusser, S. & Hopfner, K.-P. (2009). The regulatory domain of the RIG-I family ATPase LGP2 senses double-stranded RNA. *Nucleic Acids Res* **37**, 2014–2025.

Platanias, L. C. (2005). Mechanisms of type-I- and type-II-interferon-mediated signalling. *Nat Rev Immunol* **5**, 375–386.

Pomerantz, J. L. & Baltimore, D. (1999). *NF-kappaB activation by a signaling 667 complex containing TRAF2*. TANK and TBK1.

Poole, E., He, B., Lamb, R. A., Randall, R. E. & Goodbourn, S. (2002). The V Proteins of Simian Virus 5 and Other Paramyxoviruses Inhibit Induction of Interferon-β. *Virology* **303**, 33–46.

Prakash, A. (2005). Tissue-specific Positive Feedback Requirements for Production of Type I Interferon following Virus Infection. *Journal of Biological Chemistry* **280**, 18651–18657.

Precious, B. L., Carlos, T. S., Goodbourn, S. & Randall, R. E. (2007). Catalytic turnover of STAT1 allows PIV5 to dismantle the interferon-induced anti-viral state of cells. *Virology* **368**, 114–121.

Precious, B., Childs, K., Fitzpatrick-Swallow, V., Goodbourn, S. & Randall, R. E. (2005). Simian virus 5 V protein acts as an adaptor, linking DDB1 to STAT2, to facilitate the ubiquitination of STAT1. *J Virol* **79**, 13434–13441.

Precious, B., Young, D. F., Bermingham, A., Fearns, R., Ryan, M. & Randall, R. E. (1995). Inducible expression of the P, V, and NP genes of the paramyxovirus simian virus 5 in cell lines and an examination of NP-P and NP-V interactions. **69**, 8001–8010.

Raftopoulou, M. (2005, May). IRF-7 triggers the interferon alarm. *Nature cell biology* **7**, 459–459.

Randall, R. E. & Bermingham, A. (1996). NP:P and NP:V Interactions of the Paramyxovirus Simian Virus 5 Examined Using a Novel Protein:Protein Capture Assay. *Virology* **224**, 121–129.

Randall, R. E. & Goodbourn, S. (2008). Interferons and viruses: an interplay between induction, signalling, antiviral responses and virus countermeasures. *J Gen Virol* **89**, 1–47. Society for General Microbiology.

Re, G. G. & Kingsbury, D. W. (1986). Nucleotide sequences that affect replicative and transcriptional efficiencies of Sendai virus deletion mutants. *J Virol*.

Ritchie, K. J., Hahn, C. S., Kim, K. I., Yan, M., Rosario, D., Li, L., la Torre, de, J. C. & Zhang, D.-E. (2004). Role of ISG15 protease UBP43 (USP18) in innate immunity to viral infection. *Nat Med* **10**, 1374–1378.

Rothenfusser, S., Rothenfusser, S., Goutagny, N., Goutagny, N., DiPerna, G., DiPerna, G., Gong, M., Monks, B. G., Schoenemeyer, A. & other authors. **(2005).** The RNA Helicase Lgp2 Inhibits TLR-Independent Sensing of Viral Replication by Retinoic Acid-Inducible Gene-I **175**, 5260–5268.

Sabbah, A., Chang, T. H., Harnack, R., Frohlich, V., Tominaga, K., Dube, P. H., Xiang, Y. & Bose, S. (2009). Activation of innate immune antiviral responses by Nod2. *Nat Immunol* **10**, 1073–1080.

Sadler, A. J. & Williams, B. R. G. (2008). Interferon-inducible antiviral effectors. *Nat Rev Immunol* **8**, 559–568. Nature Publishing Group.

Sadler, A. J. & Williams, B. R. G. (2011). Dynamiting Viruses with MxA. *Immunity* **35**, 491–493.

Saito, T., Hirai, R., Loo, Y.-M., Owen, D., Johnson, C. L., Sinha, S. C., Akira, S., Fujita, T. & Gale, M. (2007). Regulation of innate antiviral defenses through a shared repressor domain in RIG-I and LGP2. *Proc Natl Acad Sci U S A* **104**, 582–587.

Samal, S. K. (2011). *The Biology of Paramyxoviruses*. Horizon Scientific Press.

Sato, M., Hata, N., Asagiri, M., Nakaya, T., Taniguchi, T. & Tanaka, N. (1998). Positive feedback regulation of type I IFN genes by the IFN-inducible transcription factor IRF-7. *FEBS Lett* **441**, 106–110.

Satoh, T., Kato, H., Kumagai, Y., Yoneyama, M., Sato, S., Matsushita, K., Tsujimura, T., Fujita, T., Akira, S. & Takeuchi, O. (2010). LGP2 is a positive regulator of RIG-I- and MDA5-mediated antiviral responses. *Proc Natl Acad Sci U S A* **107**, 1512–1517.

Schlee, M. (2013). Master sensors of pathogenic RNA - RIG-I like receptors **218**, 1322–1335.

Schlee, M., Roth, A., Hornung, V., Hagmann, C. A., Wimmenauer, V., Barchet, W., Coch, C., Janke, M., Mihailovic, A. & other authors. **(2009).** Recognition of 5' triphosphate by RIG-I helicase requires short blunt double-stranded RNA as contained in panhandle of negative-strand virus. *Immunity* **31**, 25–34.

Schmidt, A., Endres, S. & Rothenfusser, S. (2011). Pattern recognition of viral nucleic acids by RIG-I-like helicases. *J Mol Med* **89**, 5–12.

Schmidt, A., Schwerd, T., Hamm, W., Hellmuth, J. C., Cui, S., Wenzel, M., Hoffmann, F. S., Michallet, M.-C., Besch, R. & other authors. **(2009).** 5'-triphosphate RNA requires base-paired structures to activate antiviral signaling via RIG-I. *Proc Natl Acad Sci U S A* **106**, 12067–12072.

Schoenborn, J. R. & Wilson, C. B. (2007). Regulation of interferon-gamma during innate and adaptive immune responses. *Adv Immunol* **96**, 41–101.

Schoggins, J. W., Wilson, S. J., Panis, M., Murphy, M. Y., Jones, C. T., Bieniasz, P. & Rice, C. M. (2011). A diverse range of gene products are effectors of the type I interferon antiviral response. *Nature* **472**, 481–485.

Scott, P. D., Meng, B., Marriott, A. C., Easton, A. J. & Dimmock, N. J. (2011). Defective interfering influenza A virus protects in vivo against disease caused by a heterologous influenza B virus. *J Gen Virol* **92**, 2122–2132. Society for General Microbiology.

Sekellick, M. J. & Marcus, P. I. (1985). Interferon Induction by Viruses. XIV. Development of Interferon Inducibility and Its Inhibition in Chick Embryo Cells ‘Aged’ In Vitro. *Journal of Interferon Research* **5**, 651–667.

Seth, R. B., Sun, L., Ea, C.-K. & Chen, Z. J. (2005). Identification and characterization of MAVS, a mitochondrial antiviral signaling protein that activates NF-kappaB and IRF 3. *Cell* **122**, 669–682.

Sharma, S., tenOever, B. R., Grandvaux, N., Zhou, G.-P., Lin, R. & Hiscott, J. (2003). Triggering the interferon antiviral response through an IKK-related pathway. *Science* **300**, 1148–1151.

Shi, H.-X., Yang, K., Liu, X., Liu, X.-Y., Wei, B., Shan, Y.-F., Zhu, L.-H. & Wang, C. (2010). Positive regulation of interferon regulatory factor 3 activation by Herc5 via ISG15 modification. *Mol Cell Biol* **30**, 2424–2436.

Shingai, M., Ebihara, T., Begum, N. A., Kato, A., Honma, T., Matsumoto, K., Saito, H., Ogura, H., Matsumoto, M. & Seya, T. (2007). Differential type IIFN-Inducing abilities of wild-type versus vaccine strains of measles virus. *J Immunol* **179**, 6123–6133.

Silverman, R. H. (2007). Viral encounters with 2‘,5’-oligoadenylate synthetase and RNase L during the interferon antiviral response. *J Virol* **81**, 12720–12729.

Slattery, E. & Ghosh, N. (1979). Interferon, double-stranded RNA, and RNA degradation: activation of an endonuclease by (2‘-5’) An. In *Proceedings of the …*, pp. –. Presented at the Proceedings of the ….

Stahl, N., Farruggella, T. J., Boulton, T. G., Zhong, Z., Darnell, J. E. & Yancopoulos, G. D. (1995). Choice of STATs and other substrates specified by modular tyrosine-based motifs in cytokine receptors. *Science* **267**, 1349–1353.

Stancato, L. F., David, M., Carter-Su, C., Larner, A. C. & Pratt, W. B. (1996). Preassociation of STAT1 with STAT2 and STAT3 in separate signalling complexes prior to cytokine stimulation. *J Biol Chem* **271**, 4134–4137.

Strahle, L., Garcin, D. & Kolakofsky, D. (2006). Sendai virus defective-interfering genomes and the activation of interferon-beta. *Virology* **351**, 101–111.

Strahle, L., Marq, J.-B., Brini, A., Hausmann, S., Kolakofsky, D. & Garcin, D. (2007). Activation of the beta interferon promoter by unnatural Sendai virus infection requires RIG-I and is inhibited by viral C proteins. *J Virol* **81**, 12227–12237. American Society for Microbiology.

Szathmáry, E. (1992). Natural selection and dynamical coexistence of defective and complementing virus segments. *Journal of Theoretical Biology* **157**, 383–406.

Szathmáry, E. (1993). Co-operation and defection: playing the field in virus dynamics. *Journal of Theoretical Biology* **165**, 341–356.

Szretter, K. J., Daniels, B. P., Cho, H., Gainey, M. D., Yokoyama, W. M., Gale, M., Jr, Virgin, H. W., Klein, R. S., Sen, G. C. & Diamond, M. S. (2012). 2′-O Methylation of the Viral mRNA Cap by West Nile Virus Evades Ifit1-Dependent and -Independent Mechanisms of Host Restriction In Vivo. *PLoS Pathog* **8**, e1002698 (M. U. Gack, Ed.). Public Library of Science.

Takeda, K. & Akira, S. (2004). TLR signaling pathways. *Semin Immunol* **16**, 3–9.

Tallóczy, Z., Jiang, W., Virgin, H. W., Leib, D. A., Scheuner, D., Kaufman, R. J., Eskelinen, E.-L. & Levine, B. (2002). Regulation of starvation- and virus-induced autophagy by the eIF2alpha kinase signaling pathway. *Proc Natl Acad Sci U S A* **99**, 190–195.

Tallóczy, Z., Virgin, H. W. & Levine, B. (2006). PKR-dependent autophagic degradation of herpes simplex virus type 1. *Autophagy* **2**, 24–29.

Taylor, D. R., Lee, S. B., Romano, P. R., Marshak, D. R., Hinnebusch, A. G., Esteban, M. & Mathews, M. B. (1996). Autophosphorylation sites participate in the activation of the double-stranded-RNA-activated protein kinase PKR. *Mol Cell Biol* **16**, 6295–6302.

Terenzi, F., Hui, D. J., Merrick, W. C. & Sen, G. C. (2006). Distinct induction patterns and functions of two closely related interferon-inducible human genes, ISG54 and ISG56. *J Biol Chem* **281**, 34064–34071.

Terenzi, F., Saikia, P. & Sen, G. C. (2008). Interferon-inducible protein, P56, inhibits HPV DNA replication by binding to the viral protein E1. *EMBO J* **27**, 3311–3321.

Thomas, S. M., Lamb, R. A. & Paterson, R. G. (1988). Two mRNAs that differ by two nontemplated nucleotides encode the amino coterminal proteins P and V of the paramyxovirus SV5. *Cell* **54**, 891–902.

Thompson, K. A. & Yin, J. (2010). Population dynamics of an RNA virus and its defective interfering particles in passage cultures. *Virol J*.

Tsai, K.-N., Tsang, S.-F., Huang, C.-H. & Chang, R.-Y. (2007). Defective interfering RNAs of Japanese encephalitis virus found in mosquito cells and correlation with persistent infection. *Virus research* **124**, 139–150.

Van den Broek, M., Muller, U. & Huang, S. (1995). Antiviral defense in mice lacking both alpha/beta and gamma interferon receptors. *Journal of …* –.

Venkataraman, T., Valdes, M., Elsby, R., Kakuta, S., Caceres, G., Saijo, S., Iwakura, Y. & Barber, G. N. (2007). Loss of DExD/H box RNA helicase LGP2 manifests disparate antiviral responses. *J Immunol* **178**, 6444–6455.

Verhelst, J., Hulpiau, P. & Saelens, X. (2013). Mx proteins: antiviral gatekeepers that restrain the uninvited. *Microbiol Mol Biol Rev* **77**, 551–566.

Vigant, F. & Lee, B. (2011). Hendra and nipah infection: pathology, models and potential therapies. *Infectious disorders drug targets*.

Virtue, E. R., Marsh, G. A. & Wang, L.-F. (2009). Paramyxoviruses infecting humans: the old, the new and the unknown. *Future Microbiol* **4**, 537–554.

Wang, C., Deng, L., Hong, M., Akkaraju, G. R., Inoue, J. & Chen, Z. J. (2001). TAK1 is a ubiquitin-dependent kinase of MKK and IKK. *Nature* **412**, 346–351.

Wang, X., Hinson, E. R. & Cresswell, P. (2007). The interferon-inducible protein viperin inhibits influenza virus release by perturbing lipid rafts. *Cell Host Microbe* **2**, 96–105.

Wang, Y., Ludwig, J., Schuberth, C., Goldeck, M., Schlee, M., Li, H., Juranek, S., Sheng, G., Micura, R. & other authors. **(2010).** Structural and functional insights into 5'-ppp RNA pattern recognition by the innate immune receptor RIG-I. *Nat Struct Mol Biol* **17**, 781–787.

Wansley, E. K. & Parks, G. D. (2002). Naturally occurring substitutions in the P/V gene convert the noncytopathic paramyxovirus simian virus 5 into a virus that induces alpha/beta interferon synthesis and cell death. *J Virol* **76**, 10109–10121. American Society for Microbiology.

Wathelet, M. G., Lin, C. H., Parekh, B. S., Ronco, L. V., Howley, P. M. & Maniatis, T. (1998). Virus infection induces the assembly of coordinately activated transcription factors on the IFN-beta enhancer in vivo. *Mol Cell* **1**, 507–518.

Weber, F. & Haller, O. (2000). MxA GTPase blocks reporter gene expression of reconstituted Thogoto virus ribonucleoprotein complexes. *J Virol*.

Werneke, S. W., Schilte, C., Rohatgi, A., Monte, K. J., Michault, A., Arenzana-Seisdedos, F., Vanlandingham, D. L., Higgs, S., Fontanet, A. & other authors. **(2011).** ISG15 Is Critical in the Control of Chikungunya Virus Infection Independent of UbE1L Mediated Conjugation. *PLoS Pathog* **7**, e1002322.

Whelan, S. P. J., Barr, J. N. & WERTZ, G. W. (2004). Transcription and Replication of Nonsegmented Negative-Strand RNA Viruses. In *Biology of Negative Strand RNA Viruses: The Power of Reverse Genetics*, Current Topics in Microbiology and Immunology, pp. 61–119. Berlin, Heidelberg: Springer Berlin Heidelberg.

Wilkins, C. & Gale, M. (2010). Recognition of viruses by cytoplasmic sensors. *Curr Opin Immunol* **22**, 41–47.

Wilson, R. L., Fuentes, S. M., Wang, P. & Taddeo, E. C. (2006). Function of small hydrophobic proteins of paramyxovirus. *Journal of …*.

Wu, B., Peisley, A., Richards, C., Yao, H., Zeng, X., Lin, C., Chu, F., Walz, T. & Hur, S. (2013). Structural Basis for dsRNA Recognition, Filament Formation, and Antiviral Signal Activation by MDA5. *Cell* **152**, 276–289.

Wu, C. A., Harper, L. & Ben-Porat, T. (1986). Molecular basis for interference of defective interfering particles of pseudorabies virus with replication of standard virus. *J Virol* **59**, 308–317.

Xiao, H., Killip, M. J., Staeheli, P., Randall, R. E. & Jackson, D. (2013). The human interferon-induced MxA protein inhibits early stages of influenza A virus infection by retaining the incoming viral genome in the cytoplasm. *J Virol* **87**, JVI.02220–13–13058. American Society for Microbiology.

Xing-Xing, Y. & Kai, W. (2013). *Functions and regulation of MAVS, the mitochondrial antiviral signaling protein in innate immunity*. PROGRESS ….

Xu, L.-G., Wang, Y.-Y., Han, K.-J., Li, L.-Y., Zhai, Z. & Shu, H.-B. (2005). VISA is an adapter protein required for virus-triggered IFN-beta signaling. *Mol Cell* **19**, 727–740.

Yamamoto, M., Sato, S., Hemmi, H., Hoshino, K., Kaisho, T., Sanjo, H., Takeuchi, O., Sugiyama, M., Okabe, M. & other authors. **(2003).** Role of adaptor TRIF in the MyD88-independent toll-like receptor signaling pathway. *Science* **301**, 640–643.

Yamamoto, M. & Takeda, K. (2010). Current views of toll-like receptor signaling pathways. *Gastroenterol Res Pract* **2010**, 240365.

Yang, H., Ma, G., Lin, C. H., Orr, M. & Wathelet, M. G. (2004). Mechanism for transcriptional synergy between interferon regulatory factor (IRF)-3 and IRF-7 in activation of the interferon-beta gene promoter. *Eur J Biochem* **271**, 3693–3703. Blackwell Science Ltd.

Yeow, W. S., Au, W. C., Juang, Y. T., Fields, C. D., Dent, C. L., Gewert, D. R. & Pitha, P. M. (2000). Reconstitution of virus-mediated expression of interferon alpha genes in human fibroblast cells by ectopic interferon regulatory factor-7. *J Biol Chem* **275**, 6313–6320.

Yoneyama, M., Kikuchi, M., Matsumoto, K., Imaizumi, T., Miyagishi, M., Taira, K., Foy, E., Loo, Y.-M., Gale, M. & other authors. **(2005).** Shared and unique functions of the DExD/H-box helicases RIG-I, MDA5, and LGP2 in antiviral innate immunity. *J Immunol* **175**, 2851–2858. American Association of Immunologists.

Yoneyama, M., Kikuchi, M., Natsukawa, T., Shinobu, N., Imaizumi, T., Miyagishi, M., Taira, K., Akira, S. & Fujita, T. (2004). The RNA helicase RIG-I has an essential function in double-stranded RNA-induced innate antiviral responses. *Nat Immunol* **5**, 730–737.

Yoneyama, M., Onomoto, K. & Fujita, T. (2008). Cytoplasmic recognition of RNA. *Adv Drug Deliv Rev* **60**, 841–846.

Young, D. F., Andrejeva, L., Livingstone, A., Goodbourn, S., Lamb, R. A., Collins, P. L., Elliott, R. M. & Randall, R. E. (2003). Virus replication in engineered human cells that do not respond to interferons. *J Virol* **77**, 2174–2181. American Society for Microbiology.

Young, D. F., Carlos, T. S., Hagmaier, K., Fan, L. & Randall, R. E. (2007). AGS and other tissue culture cells can unknowingly be persistently infected with PIV5; A virus that blocks interferon signalling by degrading STAT1. *Virology* **365**, 238–240.

Young, D. F., Didcock, L., Goodbourn, S. & Randall, R. E. (2000). Paramyxoviridae use distinct virus-specific mechanisms to circumvent the interferon response **269**, 383–390.

Young, V. A. & Parks, G. D. (2003). Simian virus 5 is a poor inducer of chemokine secretion from human lung epithelial cells: Identification of viral mutants that activate interleukin-8 secretion by distinct mechanisms. *J Virol* **77**, 7124–7130. American Society for Microbiology.

Zeng, W., Sun, L., Jiang, X., Chen, X., Hou, F., Adhikari, A., Xu, M. & Chen, Z. J. (2010). Reconstitution of the RIG-I pathway reveals a signaling role of unanchored polyubiquitin chains in innate immunity. *Cell* **141**, 315–330.

Zhao, C., Denison, C., Huibregtse, J. M., Gygi, S. & Krug, R. M. (2005). Human ISG15 conjugation targets both IFN-induced and constitutively expressed proteins functioning in diverse cellular pathways. *Proc Natl Acad Sci U S A* **102**, 10200–10205.

Zhao, T., Yang, L., Sun, Q., Arguello, M., Ballard, D. W., Hiscott, J. & Lin, R. (2007). The NEMO adaptor bridges the nuclear factor-κB and interferon regulatory factor signaling pathways. *Nat Immunol* **8**, 592–600.

Zhong, B., Yang, Y., Li, S., Wang, Y.-Y., Li, Y., Diao, F., Lei, C., He, X., Zhang, L. & other authors. **(2008).** The adaptor protein MITA links virus-sensing receptors to IRF3 transcription factor activation. *Immunity* **29**, 538–550.

Zhou, A., Hassel, B. A. & Silverman, R. H. (1993). Expression cloning of 2-5A-dependent RNAase: a uniquely regulated mediator of interferon action. *Cell* **72**, 753–765.

Zhou, A., Paranjape, J. M., Hassel, B. A., Nie, H., Shah, S., Galinski, B. & Silverman, R. H. (1998). Impact of RNase L overexpression on viral and cellular growth and death. *J Interferon Cytokine Res* **18**, 953–961.

Zhu, Z., Zhang, X., Wang, G. & Zheng, H. (2014). The Laboratory of Genetics and Physiology 2: Emerging Insights into the Controversial Functions of This RIG-I-Like Receptor. *BioMed Research International* **2014**, 1–7. Hindawi Publishing Corporation.

Züst, R., Cervantes-Barragan, L., Habjan, M., Maier, R., Neuman, B. W., Ziebuhr, J., Szretter, K. J., Baker, S. C., Barchet, W. & other authors. **(2011a).** Ribose 2'-O-methylation provides a molecular signature for the distinction of self and non-self mRNA dependent on the RNA sensor Mda5. *Nat Immunol* **12**, 137–143.

Züst, R., Cervantes-Barragan, L., Habjan, M., Maier, R., Neuman, B. W., Ziebuhr, J., Szretter, K. J., Baker, S. C., Barchet, W. & other authors. **(2011b).** Ribose 2′-O-methylation provides a molecular signature for the distinction of self and non-self mRNA dependent on the RNA sensor Mda5. *Nat Immunol* **12**, 137–143.

ISG56/IFIT1 is primarily responsible for interferon-induced changes to patterns of parainfluenza virus type 5 transcription and protein synthesis. **(2013).** ISG56/IFIT1 is primarily responsible for interferon-induced changes to patterns of parainfluenza virus type 5 transcription and protein synthesis **94**, 59–68. Society for General Microbiology.